

ACADEMIA

Accelerating the world's research.

PDF methods for turbulent reactive flows

Driss Lazar

Progress in Energy and Combustion Science

Cite this paper

Downloaded from [Academia.edu](#) ↗

[Get the citation in MLA, APA, or Chicago styles](#)

Related papers

[Download a PDF Pack](#) of the best related papers ↗



[PDF modeling and simulations of pulverized coal combustion – Part 1: Theory and modeling](#)

Bertrand Naud, Dirk Roekaerts

[Modeling near-wall effects in second-moment closures by elliptic relaxation](#)

Mohamed Kanniche

[Eulerian and Lagrangian Pictures of Non-equilibrium Diffusions](#)

Raphaël Chetrite

PDF METHODS FOR TURBULENT REACTIVE FLOWS

S. B. POPE

Sibley School of Mechanical and Aerospace Engineering, Cornell University, Ithaca, NY 14853, U.S.A.

Abstract—The aim of the methods described is to calculate the properties of turbulent reactive flow fields. At each point in the flow field, a complete statistical description of the state of the fluid is provided by the velocity-composition joint pdf. This is the joint probability density function (pdf) of the three components of velocity and of the composition variables (species mass fractions and enthalpy). The principal method described is to solve a modelled transport equation for the velocity-composition joint pdf. For a variable-density flow with arbitrarily complex and nonlinear reactions, it is remarkable that in this equation the effects of convection, reaction, body forces and the mean pressure gradient appear exactly and so do not have to be modelled. Even though the joint pdf is a function of many independent variables, its transport equation can be solved by a Monte Carlo method for the inhomogeneous flows of practical interest. A second method that is described briefly is to solve a modelled transport equation for the composition joint pdf.

The objective of the paper is to provide a comprehensive and understandable account of the theoretical foundations of the pdf approach.

CONTENTS

1. Introduction	120
1.1. Introduction and objectives	120
1.2. Pdf methods	121
1.3. Outline	122
2. Probability Functions	122
2.1. Turbulent mixing layer	122
2.2. Random variables	123
2.3. Distribution function	123
2.4. Probability density function	124
2.5. Expectation	126
2.6. Measurements	128
2.7. Joint pdf's	129
2.8. Conditional probabilities	132
2.9. Limitations of one-point pdf's	133
3. Velocity-Composition Joint Pdf	134
3.1. Conservation equations	134
3.2. Velocity and composition spaces	136
3.3. Velocity-composition joint pdf	136
3.4. Discrete representation	138
3.5. Joint pdf transport equation	141
3.5.1. Evaluation of the integral I	142
4. Lagrangian Description	143
4.1. Equivalent systems	143
4.2. Lagrangian equations	144
4.3. Lagrangian pdf	145
4.4. Relationship between Lagrangian and Eulerian pdf's	146
4.5. Deterministic system	147
4.6. Stochastic systems	150
4.7. Normalization, mean continuity and pressure	153
4.8. Summary	156
5. Modelling	156
5.1. Guiding principles	157
5.2. Scalar dissipation	158
5.2.1. Exact equations	158
5.2.2. Deterministic model	159
5.2.3. Particle-interaction model	159
5.2.4. Langevin model	162
5.2.5. Conclusion	163
5.3. Energy decay and the return-to-isotropy	163
5.3.1. Analysis of the stochastic reorientation model	166
5.4. Rapid pressure	166
5.4.1. Solution of the Poisson equation	168

5.5. Langevin model	169
5.6. Joint pdf models	171
5.7. General flows	173
5.7.1. Inhomogeneity	173
5.7.2. Intermittency	174
5.7.3. Dissipation rates	175
5.7.4. Variable density	176
5.7.5. Laminar flamelets	176
6. Solution Algorithm	178
6.1. Introduction	178
6.2. Discrete representation	178
6.3. Fractional steps	178
6.4. First fractional step	179
6.5. Second fractional step: stochastic mixing model	180
6.6. Third fractional step: convection and mean pressure gradient	180
6.7. Determination of means	182
6.8. Variants	185
7. Composition Joint Pdf	186
7.1. Composition joint pdf equation	187
7.2. Solution algorithm	187
8. Conclusions	188
8.1. Summary	188
8.2. Discussion	190
8.2.1. Limitations of one-point closures	190
8.2.2. Advantages of the pdf approach	190
8.2.3. Model improvements	190
8.2.4. Computational considerations	190
Acknowledgements	191
References	191

1. INTRODUCTION

1.1. *Introduction and Objectives*

This paper describes the use of evolution equations for probability density functions (pdf's) to calculate the properties of turbulent reactive flows.

Most flows in the environment, in process industry, and in engineering equipment are turbulent. When these flows involve heat transfer, mass transfer or reaction, turbulence usually plays a dominant role in determining the rates of these processes. The evident importance of turbulent flows involving mixing and reaction has stimulated a wide variety of theoretical approaches, as revealed in a number of reviews, collective works, and specialist meetings.¹⁻⁸ The aim of these approaches is to calculate the important properties of the flow field. For inert flows, the turbulence closure problem⁹ makes this a difficult task and, for reactive flows, the difficulty is compounded by non-linear reaction rates and large density variations. The pdf methods described here are remarkably successful in alleviating these difficulties: in a variable-density flow, the effects of convection, reaction, body forces and the mean pressure gradient can be treated without approximation. The only remaining closure problems are due to the fluctuating pressure gradient and to molecular transport.

A cursory examination of the work on pdf methods over the past fifteen years may leave the following three impressions:

- (i) pdf methods have great potential, since (as mentioned above) they overcome the most important closure problems;

- (ii) because joint pdf's are functions of many (maybe 8) independent variables, numerical solutions to their evolution equations would be extremely difficult and costly, if not impossible; and
- (iii) the mathematical formalism associated with the pdf equations makes them inaccessible to all but a handful of specialists, and has added little to our understanding of the physical processes.

The objectives of this work are:

- (i) to make pdf methods understandable from both mathematical and physical viewpoints;
- (ii) to show that the methods overcome the most important closure problems;
- (iii) to present models for the processes that cannot be treated exactly;
- (iv) to describe a computationally-efficient solution algorithm for the modelled pdf equation that makes it feasible to calculate the properties of turbulent reactive flows of practical interest; and
- (v) to show that considerable insight is gained by describing physical processes in the multidimensional state space in which the pdf's are defined.

In comparison to conventional turbulence models,^{10,11} pdf methods derive their advantage from their more complete representation of the turbulent flow field. Consider a flow involving three scalars $\phi_1(\mathbf{x}, t)$, $\phi_2(\mathbf{x}, t)$ and $\phi_3(\mathbf{x}, t)$ —these could be fuel mass fraction, oxidant mass fraction and enthalpy. With a two-equation turbulence model (e.g. the $k-\varepsilon$ model), at each point the turbulent reactive flow is represented by eight quantities—the means of the three velocity components, the means of the three scalars, k and ε . In the pdf method, on the other hand, the flow is represented by the joint pdf of the three velocities and

the three scalars. At each point this is a function of six independent variables. Clearly, the six-dimensional joint pdf contains much more information than the eight quantities considered in the conventional turbulence-model approach.

Probability density functions have been used in the study of turbulent reactive flows for at least 35 years.¹² In the last ten years, several models have been developed in which pdf's play a central role.^{13,14} In these models, a parametric form for the pdf is assumed¹⁵⁻¹⁸ in terms of its first and second moments, for which transport equations are solved. The methods described here are distinctly different in that the shape of the pdf is not assumed, but it is calculated from a modelled evolution equation for the pdf.

The pdf methods are applicable to a wide class of flows. While we restrict our attention to single-phase, low-Mach number flows, no restrictions are placed on the complexity of the thermochemistry—there can be large density variations, and there can be nonlinear reactions involving many species. Pdf methods are well-suited to flows with complex thermochemistry, and most of the work on pdf's in the last ten years has been applied to reactive flows. This work, too, is concerned with reactive flow: but this should not hide the fact that (compared to conventional turbulence models) pdf methods have many advantages for inert and constant-density flows.

1.2. Pdf Methods

The method of solving a modelled pdf equation started in 1969. Lundgren¹⁹ derived, modelled, and solved a transport equation for the joint pdf of velocity. In this equation, convective transport appears in closed form. In mean-flow closures¹⁰ a model is needed for the Reynolds stresses (which transport momentum), and in Reynolds-stress closures^{11,20} a model is needed for the triple velocity correlations (which transport the Reynolds stresses). These transport processes are usually modelled by gradient diffusion. But in the velocity pdf equation these processes do not have to be modelled and so the gradient-diffusion assumption is avoided. Lundgren proposed simple relaxation models for the unknown terms, and obtained analytic solutions to the modelled pdf equation for simple flows.

Dopazo and O'Brien²¹⁻²³ and Pope²⁴ derived, modelled, and solved the transport equation for the composition joint pdf—that is, the joint pdf of a set of scalars (e.g. mass fractions and enthalpy) that describe the thermochemical state of the fluid. This equation is remarkable in that arbitrarily complicated reactions can be treated without approximation. This is in marked contrast to conventional turbulence models in which the mean reaction rate can be determined only in special circumstances—when the reaction rate is linear or when it is either very fast or very slow compared with the turbulent time scales. For a

general, nonlinear, finite-rate reaction, conventional turbulence models reach an impasse.

The modelled composition joint pdf equation has been solved for a variety of flows, demonstrating its ability to handle nonlinear reactions. Janicka *et al.*^{25,26} and Nguyen and Pope²⁷ studied hydrogen-air turbulent diffusion flames; Pope²⁸ and McNutt²⁹ studied turbulent premixed flames; and Sherikar and Chevray³⁰ and Givi *et al.*³¹ studied the NO-O₃ reaction in turbulent shear flows. There have also been several solutions of the transport equation for the pdf of a conserved scalar.³²⁻³⁶

While the composition-pdf equation overcomes the closure problem associated with nonlinear reaction rates, it does not address the problem of determining the turbulent flow field. In most of the composition pdf calculations referenced above, the standard $k-\epsilon$ turbulence model was used to determine the mean velocity and turbulence fields. The mean velocity and the turbulent diffusivity and frequency were then used as inputs to the modelled transport equation for the composition joint pdf. In this equation, turbulent transport is generally modelled by gradient diffusion.

For the inhomogeneous flows of practical interest, analytical solutions to the pdf transport equations are out of the question, and numerical methods are required. Standard techniques such as finite-differences are severely limited because of the large dimensionality of joint pdf's. For example in a statistically two-dimensional flow, the velocity joint pdf and the joint pdf of three compositions are each a function of five independent variables and time. It can be estimated³² that each time step in a finite-difference solution to these joint pdf equations requires of the order 10^{11} computer operations (additions or multiplications). With current computing rates of order 10^6 operations per second, such requirements are excessive if not prohibitive. Further, the computer requirements rise exponentially with the dimensionality of the pdf.

For problems with a large number of independent variables, Monte Carlo methods^{37,38} usually provide a feasible alternative means of obtaining numerical solutions. In 1980, Pope³⁹ devised a Monte Carlo method to solve the composition joint pdf equation. This can be viewed as an extension to the inhomogeneous case of the stochastic mixing models of Spielman and Levenspiel⁴⁰ and Flagan and Appleton.⁴¹ In this case the computer requirements rise only linearly with the dimensionality of the pdf—the best that can be achieved. The Monte Carlo method has been used to solve the equation for the joint pdf of three compositions in a one-dimensional flow²⁸ and that of two compositions in a two-dimensional flow.^{30,31}

The ability of the Monte Carlo method to handle joint pdf's of large dimensionality opened the way to combining the velocity and composition pdf methods to obtain the advantages of both. This is achieved by considering the transport equation for the joint pdf of the velocities and compositions. In this equation, con-

vection appears in closed form (as it does in the velocity-pdf equation) and reaction appears in closed form (as it does in the composition-pdf equation). Even though the velocity-composition joint pdf is a function of many independent variables, its evolution equation can be solved by a Monte Carlo method.⁴² The joint pdf equation has been solved for a plane jet,^{42,43} for a thermal wake,⁴⁴ for a premixed flame,⁴⁵ and for a diffusion flame.⁴⁶

The pdf's considered here are Eulerian—that is, they are the pdf's of fluid properties at a fixed spatial location. But the pdf equations can be derived, modelled and solved by either Eulerian or Lagrangian methods. In the works cited above, the Eulerian view is generally adopted. Here we make use of both approaches.

Frost^{47,48} and Chung^{49,50} have obtained pdf equations from a Lagrangian formulation by using the Langevin equation to model the fluid particle motion. (The Langevin equation⁵¹ was originally devised to describe Brownian motion.) Calculations of turbulent diffusion flames using these pdf equations have been performed by Frost⁴⁸ and by Bywater.⁵²

1.3. Outline

This paper is primarily concerned with the evolution equation for the velocity-composition joint pdf—its derivation, interpretations, modelling, and solution. The objective is to provide a comprehensive and understandable account of the theoretical foundations of the approach.

The next section contains a review of the definition and properties of the probability functions used in subsequent sections. In Section 3, the governing conservation equations of turbulent reactive flow are presented: the properties of the velocity-composition joint pdf are examined, and its evolution equation is derived. In Section 4 this equation is studied from a Lagrangian viewpoint. This Lagrangian description affords a clear physical interpretation of the equation and provides the framework for the modelling (Section 5) and for the solution algorithm (Section 6). Three types of models are described: linear deterministic models; stochastic particle-interaction models; and, models based on the Langevin equation. In Section 7 the composition joint pdf equation is examined. The final section contains a summary of the most important points, and a discussion on the attributes and limitations of the pdf approach.

2. PROBABILITY FUNCTIONS

Considering the stochastic nature of turbulence, it is remarkable how little probability theory is used in most theoretical approaches to the subject (see, for example, Hinze⁵³). In this section various probability functions are defined and their properties outlined in order to provide the theoretical foundation on which the rest of the paper is built. The texts on probability theory by Drake⁵⁴ and Gnedenko⁵⁵ and those more

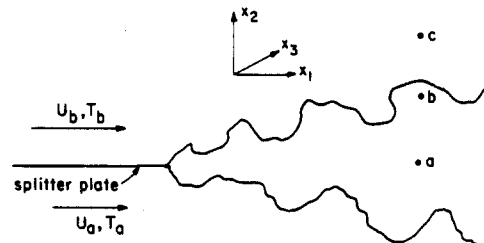


FIG. 2.1. Sketch of a turbulent mixing layer showing locations of (a) fully turbulent flow, (b) intermittent flow, (c) non-turbulent flow.

closely related to turbulence by Lumley⁵⁶ and Panchev⁵⁷ can be used as general references, but these do not contain all the necessary results.

The reader familiar with probability theory may wish just to examine the use of delta functions (most importantly in Eqs (2.67) and (2.150)) before passing on to Section 3.

In the following development, the concepts of probability are linked to turbulence by reference to measurements in a hypothetical experiment involving a turbulent flow.

2.1. Turbulent Mixing Layer

Figure 2.1 is a sketch of the turbulent mixing layer formed between two parallel streams of air. The axial and lateral coordinates are x_1 and x_2 , and the width of the apparatus is assumed to be infinite in the spanwise, x_3 , direction. The lower air stream has an axial velocity U_a and absolute temperature T_a , while the upper stream has a higher velocity U_b and a higher temperature T_b . The figure shows the flow a long time after its initiation, when the free stream properties (U_a , T_a , U_b and T_b) no longer vary with time. However, we are also interested in the temporal development of the flow from a uniform, quiescent initial condition. This initial state exists before the time $t = 0$ when the flow is started in a repeatable way.

It is assumed that the temperature $T(\underline{x}, t)$ is always in the range,

$$T_a \leq T \leq T_b. \quad (2.1)$$

This assumption is valid if the initial and boundary conditions satisfy Eq. (2.1), and if the Mach number Ma is small. Specifically, we require

$$Ma^2 \ll \frac{T_b - T_a}{T_b + T_a}. \quad (2.2)$$

The normalized temperature $\phi(\underline{x}, t)$ is defined by

$$\phi(\underline{x}, t) \equiv (T(\underline{x}, t) - T_a)/(T_b - T_a), \quad (2.3)$$

and, in view of Eq. (2.1), ϕ adopts values between zero and unity:

$$0 \leq \phi \leq 1. \quad (2.4)$$

In referring to measurements of the normalized temperature $\phi(\underline{x}, t)$ and of the velocity $\underline{U}(\underline{x}, t)$, we

assume that the measurements are free from error, and that the measurement process does not affect the flow.

2.2. Random Variables

In the mixing-layer experiment, at a particular time $t = t_0$ and at a particular location within the turbulent flow $\underline{x} = \underline{x}_0$, the value of $\phi(\underline{x}_0, t_0)$ is measured. The experiment is then repeated and a second measured value of $\phi(\underline{x}_0, t_0)$ is obtained. (Recall that the time t is measured from the initiation of the flow.) Almost certainly, the two measured values of ϕ will be different. This is the nature of turbulent flows and the result may not be surprising. But, the source of the difference between the two realizations of the flow needs careful consideration.

In both cases the flow is governed by the same deterministic equations with the same initial and boundary conditions. Why then is the flow not uniquely determined as the solution of these equations? The answer is that the initial and boundary conditions, though nominally the same, are not identical. Small air movements before the start of the experiment lead to slightly different initial conditions. Mechanical disturbances to the apparatus (such as vibrations) lead to slightly different boundary conditions. Even the governing equations may be slightly different because impurities in the air lead to different fluid properties. These differences, however small, are amplified by the turbulence so that after some time the temperature and velocity fields in the two experiments are completely different.

We conclude, then, that in any turbulent flow experiment, the boundary and initial conditions cannot be controlled (or even known) sufficiently for the evolution of the flow to be determined. Consequently, it is appropriate to treat any flow property as a random variable. The temperature $\phi(\underline{x}_0, t_0)$ and the axial velocity $U_1(\underline{x}_0, t_0)$ are simple examples of flow properties that can be treated as random variables.

A probabilistic theory makes no attempt to predict the value of a random variable ($\phi(\underline{x}_0, t_0)$, for example) in a particular experiment, since this value is indeterminate. Instead, the aim of the theory is to determine the probabilities of the random variables adopting specified values. The relationship between these probabilities and measured values is discussed in Section 2.6.

2.3. Distribution Function

We take as an example of a random variable the normalized temperature at $(\underline{x}, t) = (\underline{x}_0, t_0)$ which is denoted simply by ϕ , rather than by $\phi(\underline{x}_0, t_0)$. When the experiment is performed and the temperature is measured, the value of ϕ can be plotted as a point on

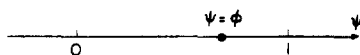


FIG. 2.2. Sample space (ψ -space) for the random variable ϕ , showing the sample point $\psi = \phi$.

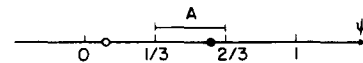


FIG. 2.3. Sample space showing the region corresponding to the event $A \equiv 1/3 \leq \phi < 2/3$: ● sample point for which A occurs; ○ sample point for which A does not occur.

the real line. Figure 2.2 shows the real line as the axis of the independent variable ψ , with the experimental point (or sample point) plotted at $\psi = \phi$. The ψ axis (or ψ -space) is called the sample space of the random variable ϕ . Since ϕ is a normalized temperature, ψ is an independent temperature variable, and so ψ -space is also called temperature space.

The significance of the sample space is that any event determined by the random variable corresponds to a region of the sample space. For example, let the event A be

$$A \equiv (1/3 \leq \phi < 2/3). \quad (2.5)$$

The region of ψ -space corresponding to this event is, simply, $1/3 \leq \psi < 2/3$, see Fig. 2.3. If the sample point $\psi = \phi$ falls within this region, then the event A occurred; if not, A did not occur.

The probability of the occurrence of the event A (or simply, the probability of A) is denoted by $P(A)$. The probability of an event is a real number between zero and unity. If an event cannot occur (i.e. it is impossible) then its probability is zero. If an event must occur (i.e. it is certain) then its probability is one. For example, consider the events

$$B \equiv \phi > 2, \quad (2.6)$$

$$C \equiv \sin \phi \geq 0. \quad (2.7)$$

Now, since ϕ can only take values in the range $0 \leq \phi \leq 1$ (Eq. 2.4), it is clear that B is impossible and that C is certain:

$$P(B) = 0, \quad (2.8)$$

$$P(C) = 1. \quad (2.9)$$

These events are sketched on Fig. 2.4.

Since every event can be associated with a region of the sample space, the probability of the event is equal to the probability of the random variable being within that region. The probability for any region can be determined from the distribution function: for the random variable ϕ , the distribution function $F_\phi(\psi)$ is defined by

$$F_\phi(\psi) \equiv P(\phi < \psi). \quad (2.10)$$

Thus, for example, for the event

$$D \equiv \phi < 1/4, \quad (2.11)$$

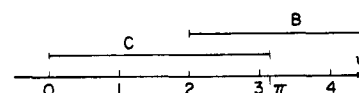


FIG. 2.4. Sample space showing the regions corresponding to the events $B \equiv \phi > 2$ and $C \equiv \sin \phi \geq 0$.

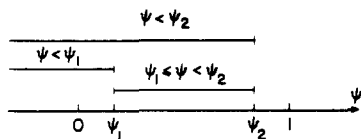


FIG. 2.5. Sample space showing the region $\psi_1 \leq \psi < \psi_2$ as the difference between the regions $\psi < \psi_2$ and $\psi < \psi_1$.

its probability is

$$P(D) = F_\phi(1/4). \quad (2.12)$$

Consider the event E

$$E \equiv \psi_1 \leq \phi < \psi_2, \quad (2.13)$$

where $\psi_2 > \psi_1$. The probability of E can be determined by noting that the region $\psi_1 \leq \psi < \psi_2$ is equal to the (infinite) region $\psi < \psi_2$ minus the (infinite) region $\psi < \psi_1$, see Fig. 2.5. Thus,

$$\begin{aligned} P(E) &= P(\psi_1 \leq \phi < \psi_2) \\ &= P(\psi < \psi_2) - P(\psi < \psi_1) \\ &= F_\phi(\psi_2) - F_\phi(\psi_1). \end{aligned} \quad (2.14)$$

The fundamental properties of the distribution function are readily deduced. Since the event $(-\infty < \phi < \infty)$ is certain, we obtain

$$P(\phi < -\infty) = F_\phi(-\infty) = 0, \quad (2.15)$$

and

$$P(\phi < \infty) = F_\phi(\infty) = 1. \quad (2.16)$$

(These properties hold for any random variable and do not depend upon our knowledge of ϕ , e.g. Eq. (2.4)). The probability of the event E , Eqs (2.13)–(2.14), is

$$P(E) = F_\phi(\psi_2) - F_\phi(\psi_1) \geq 0, \quad (2.17)$$

and hence

$$F_\phi(\psi_2) \geq F_\phi(\psi_1), \text{ for } \psi_2 > \psi_1. \quad (2.18)$$

Thus $F_\phi(\psi)$ is a non-decreasing function of ψ that increases from zero to one as ψ varies from $-\infty$ to ∞ .

An example of $F_\phi(\psi)$ for the mixing-layer experiment is sketched on Fig. 2.6. It may be noted that in this case $F_\phi(0) = 0$ and $F_\phi(1) = 1$, by virtue of Eq. (2.4).

2.4. Probability Density Function

The probability density function (pdf) $f_\phi(\psi)$ of the random variable ϕ is the derivative of the distribution

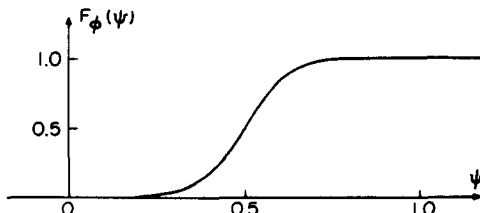


FIG. 2.6. Distribution function $F_\phi(\psi)$ against ψ .

function $F_\phi(\psi)$:

$$f_\phi(\psi) \equiv \frac{d}{d\psi} F_\phi(\psi). \quad (2.19)$$

By integrating this equation between ψ_1 and ψ_2 ($\psi_2 > \psi_1$) and comparing the result with Eq. (2.14), we find that

$$\begin{aligned} \int_{\psi_1}^{\psi_2} f_\phi(\psi) d\psi &= F_\phi(\psi_2) - F_\phi(\psi_1) \\ &= P(\psi_1 \leq \phi < \psi_2). \end{aligned} \quad (2.20)$$

That is, the probability of ϕ in a given region is equal to the integral of the pdf over that region. In particular, for an infinitesimal region,

$$P(\psi \leq \phi < \psi + d\psi) = f_\phi(\psi) d\psi. \quad (2.21)$$

A probability density function has three fundamental properties. Since $F_\phi(\psi)$ is a non-decreasing function of ψ , its derivative $f_\phi(\psi)$ cannot be negative:

$$f_\phi(\psi) \geq 0. \quad (2.22)$$

The event $-\infty \leq \phi < \infty$ is certain, and so from Eq. (2.20), we obtain

$$\int_{-\infty}^{\infty} f_\phi(\psi) d\psi = 1. \quad (2.23)$$

As $|\psi|$ tends to infinity, $F_\phi(\psi)$ tends monotonically to a constant (0 or 1), and so its derivative $f_\phi(\psi)$ tends to zero:

$$f_\phi(-\infty) = f_\phi(\infty) = 0. \quad (2.24)$$

Figure 2.7 shows the pdf $f_\phi(\psi)$ corresponding to the distribution function of Fig. 2.6.

In some treatments of probability theory, the pdf is defined only if the distribution function is continuous. In the present context, this restriction is unnecessary, but clearly the definition of the pdf as the derivative of a discontinuous function requires further comment. A simple example of a discontinuous distribution function arises when the random variable ϕ always adopts the constant value $\phi = \phi_*$. Then,

$$\begin{aligned} P(\phi < \phi_*) &= 0, \\ P(\phi = \phi_*) &= 1, \\ P(\phi > \phi_*) &= 0, \end{aligned} \quad (2.25)$$

and the corresponding distribution function is

$$\begin{aligned} F_\phi(\psi) &= 0, \psi \leq \phi_*, \\ &= 1, \psi > \phi_*. \end{aligned} \quad (2.26)$$

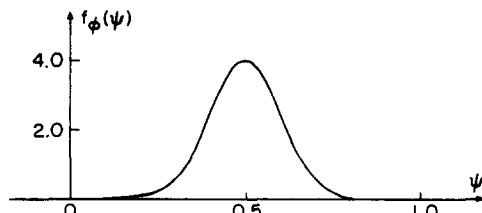


FIG. 2.7. Probability density function $f_\phi(\psi)$ against ψ .

Discontinuous distribution functions such as Eq. (2.26) can be expressed as Heaviside functions, and then the corresponding pdf's are composed of Dirac delta functions. The definitions and properties of these generalized functions are given briefly here: a more detailed and rigorous treatment can be found in Refs 58 and 59.

The Heaviside function (or unit step function) $H(y)$ is given by

$$\begin{aligned} H(y) &= 0, y \leq 0, \\ &= 1, y > 0. \end{aligned} \quad (2.27)$$

A better definition of $H(y)$ is that, for any function $g(y)$ (that is integrable and continuous at the origin)

$$\int_{-\infty}^{\infty} H(y)g(y)dy = \int_0^{\infty} g(y)dy. \quad (2.28)$$

The Dirac delta function (or unit impulse function) $\delta(y)$ is the derivative of the Heaviside function:

$$\delta(y) = \frac{dH(y)}{dy}. \quad (2.29)$$

It is zero everywhere except at $y = 0$ where it is infinite. The area under the delta function is unity since for any positive number a ,

$$\int_{-a}^a \delta(y)dy = H(a) - H(-a) = 1. \quad (2.30)$$

The delta function is best defined by its fundamental (sifting) property:

$$\int_{-\infty}^{\infty} \delta(y)g(y)dy = g(0). \quad (2.31)$$

The quantity $bH(y-c)$ is a step at $y = c$ of

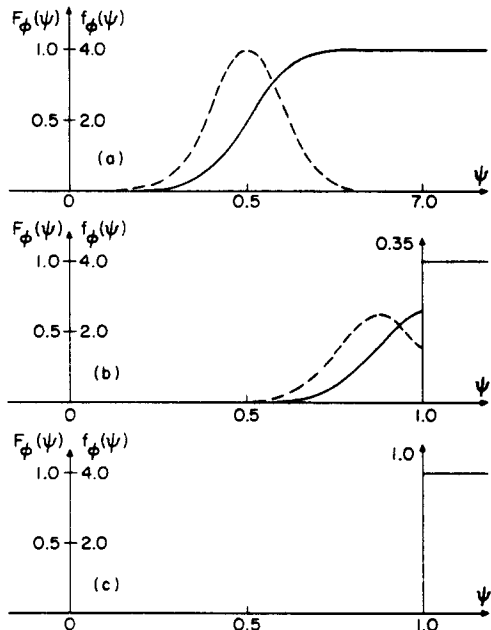


FIG. 2.8. Distribution functions and pdf's in a turbulent flow: (a) fully turbulent region; (b) intermittent region; (c) non-turbulent region.

magnitude b , and its derivative $b\delta(y-c)$ is a delta function at $y = c$ of magnitude b . (By "delta function of magnitude b " we mean a delta function multiplied by a constant of magnitude b .) From Eq. (2.31) we obtain,

$$\int_{-\infty}^{\infty} b\delta(y-c)g(y)dy = bg(c). \quad (2.32)$$

The discontinuous distribution function Eq. (2.26) can now be written as

$$F_{\phi}(\psi) = H(\psi - \phi^*), \quad (2.33)$$

and the corresponding pdf is obtained by differentiating both sides,

$$f_{\phi}(\psi) = \delta(\psi - \phi^*). \quad (2.34)$$

In turbulent flows, distribution functions are encountered that are sometimes continuous, and sometimes discontinuous. For example, Fig. 2.8(a) shows the continuous distribution function and pdf of ϕ when the measuring location x_0 is chosen in the center of the turbulent flow (see Fig. 2.1). If, on the other hand, x_0 had been located away from the turbulent flow in the high temperature free stream (where $\phi = 1$), then the distribution function would have been,

$$F_{\phi}(\psi) = H(\psi - 1). \quad (2.35)$$

This is shown on Fig. 2.8(c) with the corresponding pdf which is a delta function at $\psi = 1$. At the edge of the mixing layer the flow is intermittent—sometimes turbulent, sometimes non-turbulent with $\phi = 1$. The corresponding distribution, sketched on Fig. 2.8(b), is continuous up to $\psi = 1$, where there is a jump of magnitude 0.35. The pdf is also continuous up to $\psi = 1$ where there is a delta function of magnitude 0.35.

The probability of ϕ adopting the particular value ϕ_* can be deduced from Eq. (2.17):

$$\begin{aligned} P(\phi = \phi_*) &= \lim_{\Delta\psi \rightarrow 0} P(\phi_* \leq \phi < \phi_* + \Delta\psi) \\ &= \lim_{\Delta\psi \rightarrow 0} \{F_{\phi}(\phi_* + \Delta\psi) - F_{\phi}(\phi_*)\}. \end{aligned} \quad (2.36)$$

If the distribution function $F_{\phi}(\psi)$ has a step of magnitude b at $\psi = \phi_*$ and, consequently, the pdf $f_{\phi}(\psi)$ has a delta function of magnitude b at $\psi = \phi_*$, then we obtain

$$P(\phi = \phi_*) = b. \quad (2.37)$$

If, on the other hand, $F_{\phi}(\psi)$ is continuous in the neighborhood of ϕ_* , then $P(\phi = \phi_*)$ is zero. The event $\phi = \phi_*$ is not impossible, but it has probability zero since it is just one of an infinite number of possible events. Similarly, the event $\phi \neq \phi_*$ has probability one, but it is not certain.

We have taken as our example of a random variable the normalized temperature ϕ . Consider now the temperature T measured in degrees Kelvin and the same temperature θ measured in degrees Rankine.

With \hat{T} and $\hat{\theta}$ being the sample space variables corresponding to T and θ we have

$$\theta = \frac{9}{5} T, \quad (2.38)$$

and

$$\hat{\theta} = \frac{9}{5} \hat{T}. \quad (2.39)$$

The event $T < \hat{T}$ is identical to the event $\theta < \hat{\theta}$ and so (in an obvious notation) the distribution functions are equal:

$$F_T(\hat{T}) = F_\theta(\hat{\theta}). \quad (2.40)$$

Differentiating both sides with respect to \hat{T} we obtain

$$\frac{dF_T(\hat{T})}{d\hat{T}} = f_T(\hat{T}) = \frac{d\hat{\theta}}{d\hat{T}} \frac{dF_\theta(\hat{\theta})}{d\hat{\theta}} = \frac{9}{5} f_\theta(\hat{\theta}). \quad (2.41)$$

Since 1 degree Kelvin corresponds to $9/5$ degrees Rankine, the probability per degree Kelvin, $f_T(\hat{T})$, is $9/5$ times the probability per degree Rankine, $f_\theta(\hat{\theta})$. Note that f_T and f_θ have dimensions of $(K)^{-1}$ and $(R)^{-1}$ respectively. (It is because of these observations that pdf's earn the designation "density".)

For the more general change of variables

$$\theta = \Theta(T) \text{ and } \hat{\theta} = \Theta(\hat{T}), \quad (2.42)$$

where Θ is a monotonically increasing function, we obtain similar results:

$$F_T(\hat{T}) = F_\theta(\hat{\theta}), \quad (2.43)$$

and

$$f_T(\hat{T}) = \frac{d\Theta(\hat{T})}{d\hat{T}} f_\theta(\hat{\theta}). \quad (2.44)$$

For $\Theta(T)$, being a monotonically decreasing function of T , the event $T < \hat{T}$ is identical to the event $\theta \geq \hat{\theta} = \Theta(\hat{T})$. Thus

$$P(T < \hat{T}) = P(\theta \geq \hat{\theta}) = 1 - P(\theta < \hat{\theta}), \quad (2.45)$$

and so

$$F_T(\hat{T}) = 1 - F_\theta(\hat{\theta}). \quad (2.46)$$

Differentiating both sides with respect to \hat{T} yields

$$f_T(\hat{T}) = - \frac{d\Theta(\hat{T})}{d\hat{T}} f_\theta(\hat{\theta}). \quad (2.47)$$

Since, in this case $d\Theta(\hat{T})/d\hat{T}$ is negative, Eqs (2.44) and (2.47) can be rewritten in the common form

$$f_T(\hat{T}) = \left| \frac{d\Theta(\hat{T})}{d\hat{T}} \right| f_\theta(\hat{\theta}). \quad (2.48)$$

The random variable ϕ that we have been considering is the normalized temperature at the particular location $(\underline{x}, t) = (\underline{x}_0, t_0)$. The distribution function of ϕ is $F_\phi(\psi)$, and its pdf is $f_\phi(\psi)$. Clearly, the normalized temperature at any location is a random variable, and consequently the distribution function and pdf are defined for all \underline{x} and t :

$$F_\phi(\psi, \underline{x}, t) \equiv P(\phi(\underline{x}, t) < \psi), \quad (2.49)$$

and

$$f_\phi(\psi; \underline{x}, t) \equiv \frac{\partial F_\phi(\psi, \underline{x}, t)}{\partial \psi}. \quad (2.50)$$

A semi-colon is used to indicate that f_ϕ is a density with respect to ψ (to the left of the semi-colon).

A flow is said to be *statistically stationary* if all probabilities are independent of time. Thus for a statistically stationary flow,

$$\frac{\partial F_\phi(\psi, \underline{x}, t)}{\partial t} = 0, \quad (2.51)$$

and

$$\frac{\partial f_\phi(\psi; \underline{x}, t)}{\partial t} = 0. \quad (2.52)$$

If there is a coordinate system $(\bar{x}_1, \bar{x}_2, \bar{x}_3)$ in which all probabilities are independent of \bar{x}_3 , then the flow is said to be *statistically two-dimensional*. For such a flow,

$$\frac{\partial F_\phi(\psi, \bar{x}_1, \bar{x}_2, \bar{x}_3, t)}{\partial \bar{x}_3} = 0, \quad (2.53)$$

and

$$\frac{\partial f_\phi(\psi; \bar{x}_1, \bar{x}_2, \bar{x}_3, t)}{\partial \bar{x}_3} = 0. \quad (2.54)$$

Similarly, if all probabilities are independent of \bar{x}_2 and \bar{x}_3 , the flow is statistically *one-dimensional*. If all probabilities are independent of position (\bar{x}_1, \bar{x}_2 and \bar{x}_3) then the flow is *statistically homogeneous*.

By most definitions, all turbulent flows are three-dimensional and time dependent. But many flows of interest are statistically stationary and many are statistically one- or two-dimensional. The turbulent mixing layer sketched in Fig. 2.1 is statistically two-dimensional and, for large times, it can be expected to be statistically stationary.

2.5. Expectation

Most readers will be familiar with time averaging, a procedure that is useful only in statistically-stationary flows. For the normalized temperature $\phi(\underline{x}, t)$, the time average $\langle \phi(\underline{x}, t) \rangle_{\Delta t}$ is defined by

$$\langle \phi(\underline{x}, t) \rangle_{\Delta t} \equiv \frac{1}{\Delta t} \int_t^{t+\Delta t} \phi(\underline{x}, \tau) d\tau, \quad (2.55)$$

where Δt is a specified time interval. The time average is itself a random variable. But if the time interval Δt is sufficiently large, the measured value of $\langle \phi(\underline{x}, t) \rangle_{\Delta t}$ may vary little in successive repetitions of the experiment. In that case the measured time average is an approximation to a far more fundamental quantity — the expectation of $\phi(\underline{x}, t)$.

In this sub-section the definition and properties of the expectation of a random variable are described. In the next sub-section the relationship between expectations and measurable quantities (such as time averages) is examined.

The *mathematical expectation* of the random variable ϕ is denoted by $E(\phi)$ or $\langle \phi \rangle$ and is defined

by,

$$E(\phi) = \langle \phi \rangle \equiv \int_{-\infty}^{\infty} \psi f_{\phi}(\psi) d\psi. \quad (2.56)$$

The terms *mathematical expectation*, *expectation*, *expected value*, *mean value* and *mean*, are all synonymous. The mean $\langle \phi \rangle$ is the center of the pdf, in that the first moment about $\langle \phi \rangle$ is zero,

$$\int_{-\infty}^{\infty} (\psi - \langle \phi \rangle) f_{\phi}(\psi) d\psi = 0. \quad (2.57)$$

A function of a random variable is itself a random variable. For example, in the mixing layer between two air streams of different temperatures, the density $\rho(\phi)$ is a function of the normalized temperature. In general, let $Q(\phi)$ be a function* of the random variable ϕ : then the expectation of Q is defined by

$$\langle Q(\phi) \rangle = \int_{-\infty}^{\infty} Q(\psi) f_{\phi}(\psi) d\psi. \quad (2.58)$$

(It may be seen that the definition of $\langle \phi \rangle$, Eq. (2.56), is a particular case of this more general definition.) In the infinitesimal region $\psi \leq \phi < \psi + d\psi$, the value of $Q(\phi)$ is $Q(\psi)$ and the probability is $f_{\phi}(\psi) d\psi$. Thus the mean $\langle Q \rangle$ is the probability-weighted integral of all possible values of Q .

After the mean, the second most important numerical characteristic of a random variable is its variance. The variance of ϕ is denoted by $D(\phi)$ and is defined by

$$D(\phi) \equiv E([\phi - \langle \phi \rangle]^2) = \int_{-\infty}^{\infty} (\psi - \langle \phi \rangle)^2 f_{\phi}(\psi) d\psi. \quad (2.59)$$

The random variable ϕ can be decomposed into its mean $\langle \phi \rangle$ and the fluctuation ϕ' ,

$$\phi = \langle \phi \rangle + \phi', \quad (2.60)$$

where,

$$\phi' \equiv \phi - \langle \phi \rangle. \quad (2.61)$$

The variance is the mean of the square of the fluctuation

$$D(\phi) = \langle \phi'^2 \rangle. \quad (2.62)$$

The standard deviation, which is the square root of the variance, is a measure of the width of the probability density function.

The variance is the second central moment of ϕ . The m th central moment is defined by

$$\mu_m = \langle \phi'^m \rangle = \int_{-\infty}^{\infty} (\psi - \langle \phi \rangle)^m f_{\phi}(\psi) d\psi. \quad (2.63)$$

It is evident from Eq. (2.63) that all the moments of ϕ can be determined from the pdf: but, in general, the

* Here and henceforth, we assume that functions such as $Q(\psi)$ have whatever properties are required for the integrals such as Eq. (2.58) to exist. In general these properties are difficult to specify. If the pdf is continuous it is sufficient that $Q(\psi)$ be integrable. If the distribution function $F_{\phi}(\psi)$ contains discontinuities, then $Q(\psi)$ must be continuous at all points of discontinuity of $F_{\phi}(\psi)$.

pdf cannot be determined from a finite number of moments.

The expectation $\langle Q \rangle$ of the random variable $Q(\phi)$ is defined only if the integral

$$\int_{-\infty}^{\infty} |Q(\psi)| f_{\phi}(\psi) d\psi$$

exists. For the pdf's considered here, it is certain that the means and variances exist, and it is highly likely that all the central moments exist. It is equally likely that the expectation of rapidly increasing functions—such as $\exp(\exp(\phi))$ —do not exist (for unbounded random variables).

It proves to be very useful to identify $F_{\phi}(\psi)$ and $f_{\phi}(\psi)$ as the expectations of $H(\psi - \phi)$ and $\delta(\psi - \phi)$. Let G be the event

$$G \equiv \phi < \psi. \quad (2.64)$$

The probability of G is, simply,

$$P(G) = P(\phi < \psi) = F_{\phi}(\psi). \quad (2.65)$$

If the event G occurs, then the Heaviside function $H(\psi - \phi)$ is unity, and if G does not occur, $H(\psi - \phi)$ is zero. Thus the expected value of $H(\psi - \phi)$ is

$$\begin{aligned} \langle H(\psi - \phi) \rangle &= 1 \cdot P(G) + 0 \cdot (1 - P(G)) \\ &= F_{\phi}(\psi). \end{aligned} \quad (2.66)$$

Differentiating both sides with respect to ψ we obtain

$$\langle \delta(\psi - \phi) \rangle = f_{\phi}(\psi). \quad (2.67)$$

This property—that the pdf is the expected value of the delta function—is of paramount importance in pdf methods. Indeed in some treatments of the subject (e.g. Ref. 60) it is taken as the starting point: $\delta(\psi - \phi)$ is defined as the “fine grained” pdf (i.e. the pdf in one realization of the flow), and then the pdf $f_{\phi}(\psi)$ is defined as $\langle \delta(\psi - \phi) \rangle$. Both approaches or viewpoints lead to the same results. (It may also be noted that Eqs (2.66) and (2.67) could also be obtained by substituting $H(\psi - \phi)$ and $\delta(\psi - \phi)$ for $Q(\psi)$ in Eq. (2.58)—provided that $f_{\phi}(\psi)$ is continuous. The above development is to be preferred since it places no restrictions on the pdf.)

An important result is that differentiation (with respect to x or t) and taking the mean, commute: that is,

$$\left\langle \frac{\partial \phi}{\partial x_i} \right\rangle = \frac{\partial \langle \phi \rangle}{\partial x_i}, \quad (2.68)$$

and

$$\left\langle \frac{\partial \phi}{\partial t} \right\rangle = \frac{\partial \langle \phi \rangle}{\partial t}. \quad (2.69)$$

These properties follow trivially from the definition of a derivative:

$$\begin{aligned} \left\langle \frac{\partial \phi}{\partial t} \right\rangle &= \left\langle \lim_{\delta t \rightarrow 0} \{ \phi(t + \delta t) - \phi(t) \} \right\rangle \\ &= \lim_{\delta t \rightarrow 0} \{ \langle \phi(t + \delta t) \rangle - \langle \phi(t) \rangle \} = \frac{\hat{\partial} \langle \phi \rangle}{\hat{\partial} t}. \end{aligned} \quad (2.70)$$

2.6. Measurements

From a theoretical viewpoint, the definition of the mean $\langle \phi \rangle$ as the mathematical expectation $E(\phi)$ is, without doubt, superior to other possible choices. Other possible definitions of the mean are: the ensemble average (for flows that can be duplicated); the realization average (for flows that can be repeated); the time average (for statistically-stationary flows); the spatial average (for flows that are statistically homogeneous in one or more coordinate directions); and the phase average (for flows that are statistically periodic). Of all the possible choices, only the mathematical expectation is defined for all flows. Consequently, only a theory based on this definition is generally applicable. However, unlike the other averages, the mathematical expectation cannot be measured. We need, therefore, to consider the relationship between measurable quantities and the mathematical expectation.

Consider the ensemble average of the random variable $\phi = \phi(\mathbf{x}_0, t_0)$ for the turbulent mixing-layer experiment. A large number N of (nominally) identical apparatus are constructed, and the experiment is performed on each one with (nominally) the same initial and boundary conditions. For the n th apparatus, the measured value of ϕ is denoted by $\phi^{(n)}$. Then the ensemble average $\langle \phi \rangle_N$ of ϕ is defined by

$$\langle \phi \rangle_N \equiv \frac{1}{N} \sum_{n=1}^N \phi^{(n)}. \quad (2.71)$$

The ensemble average $\langle \phi \rangle_N$ is clearly an estimate of the mean $\langle \phi \rangle$ since, for any N ,

$$E(\langle \phi \rangle_N) = \langle \phi \rangle. \quad (2.72)$$

For large N , the Central Limit Theorem reveals the relationship between $\langle \phi \rangle_N$ and $\langle \phi \rangle$. We define the normalized error ε by

$$\varepsilon \equiv (\langle \phi \rangle_N - \langle \phi \rangle) / \varepsilon_N, \quad (2.73)$$

where the standard error ε_N is defined by

$$\varepsilon_N \equiv \sigma / \sqrt{N}, \quad (2.74)$$

and σ is the standard deviation of ϕ , $\langle \phi'^2 \rangle^{1/2}$. Then as N tends to infinity, according to the Central Limit Theorem,⁵⁵ the pdf of ε , $f_\varepsilon(\xi)$, tends to the standardized normal distribution

$$f_\varepsilon(\xi) = (2\pi)^{-1/2} \exp\left(-\frac{1}{2}\xi^2\right). \quad (2.75)$$

The following three results are readily deduced from Eq. (2.75):

- Almost certainly (i.e. with probability one), as N tends to infinity, $\langle \phi \rangle_N$ tends to $\langle \phi \rangle$.
- A finite N suffices to reduce the error $|\langle \phi \rangle_N - \langle \phi \rangle|$ below any specified positive limit with any required probability (less than unity). That is, for any $a > 0$ and $p < 1$, there is a finite M such that

$$P(|\langle \phi \rangle_N - \langle \phi \rangle| < a) \geq p, \quad (2.76)$$

for $N > M$.

- For large N , with probability 0.68, the error $|\langle \phi \rangle_N - \langle \phi \rangle|$ is less than the standard error ε_N .

$$\varepsilon_N \equiv (\langle \phi'^2 \rangle / N)^{1/2}. \quad (2.77)$$

Thus, although $\langle \phi \rangle$ cannot be measured with absolute certainty, for sufficiently large N , the ensemble average $\langle \phi \rangle_N$ provides as good an approximation as may be required. It may be noted from (iii) that the likely error is proportional to the standard deviation $\sqrt{\langle \phi'^2 \rangle}$ and decreases with the square root of N . In order to halve the error, N must be increased by a factor of four.

Similar results are obtained for the realization average and, with some additional assumptions, for the time, spatial and periodic averages. In practice, then, the theory predicts values of the mathematical expectation which can legitimately be compared with experimentally determined averages. The ensemble average of $Q(\phi)$, a function of ϕ , is defined by,

$$\langle Q(\phi) \rangle_N \equiv \frac{1}{N} \sum_{n=1}^N Q(\phi^{(n)}). \quad (2.78)$$

The relationship between $\langle Q \rangle_N$ and $\langle Q \rangle$ is precisely the same as that between $\langle \phi \rangle_N$ and $\langle \phi \rangle$. In particular,

$$E(\langle Q \rangle_N) = \langle Q \rangle, \quad (2.79)$$

for any $N \geq 1$.

By analogy to Eqs (2.66) and (2.67) the ensemble-averaged distribution function $F_{\phi N}(\psi)$ and pdf $f_{\phi N}(\psi)$ are defined by

$$F_{\phi N}(\psi) \equiv \langle H(\psi - \phi) \rangle_N = \frac{1}{N} \sum_{n=1}^N H(\psi - \phi^{(n)}), \quad (2.80)$$

and

$$f_{\phi N}(\psi) \equiv \langle \delta(\psi - \phi) \rangle_N = \frac{1}{N} \sum_{n=1}^N \delta(\psi - \phi^{(n)}). \quad (2.81)$$

Again, for any $N \geq 1$, the expectations of these ensemble averages are

$$E\{F_{\phi N}(\psi)\} = F_\phi(\psi), \quad (2.82)$$

and

$$E\{f_{\phi N}(\psi)\} = f_\phi(\psi). \quad (2.83)$$

These definitions are consistent since the ensemble average of any function of ϕ can be recovered without error:

$$\begin{aligned} \int_{-\infty}^{\infty} Q(\psi) f_{\phi N}(\psi) d\psi &= \frac{1}{N} \sum_{n=1}^N \int_{-\infty}^{\infty} Q(\psi) \delta(\psi - \phi^{(n)}) d\psi \\ &= \frac{1}{N} \sum_{n=1}^N Q(\phi^{(n)}) = \langle Q(\phi) \rangle_N. \end{aligned} \quad (2.84)$$

To illustrate the difference between ensemble-averaged distributions and their continuous counterparts, Fig. 2.9 shows distributions for the Gaussian or normal pdf.

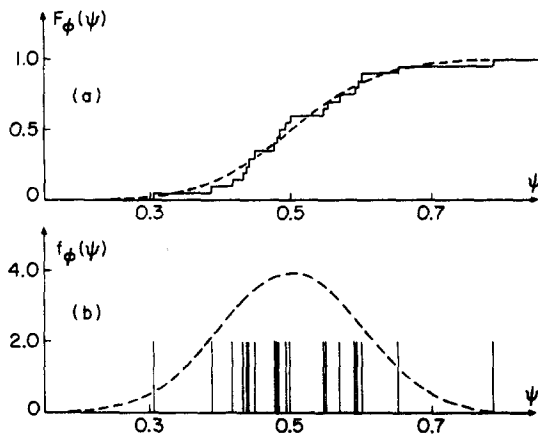


FIG. 2.9. (a) Distribution functions against ψ : dashed line $F_\phi(\psi)$; solid line $F_{\phi N}(\psi)$. (b) PDF's against ψ : dashed line $f_\phi(\psi)$; vertical lines (representing delta functions of magnitude 0.05) $f_{\phi N}(\psi)$.

$$f_\phi(\psi) = (2\pi\langle\phi'^2\rangle)^{-1/2} \exp(-\frac{1}{2}(\psi - \langle\phi\rangle)^2/\langle\phi'^2\rangle), \quad (2.85)$$

with $\langle\phi\rangle = 0.5$ and $\langle\phi'^2\rangle = 0.01$. On Fig. 2.9a, the dashed line is the distribution function $F_\phi(\psi)$ (obtained by integrating Eq. (2.85)), and the solid line is $F_{\phi N}(\psi)$ for $N = 20$. (The 20 samples $\phi^{(n)}$ are normally-distributed random numbers with mean 0.5 and variance 0.01.) It may be seen that while $F_\phi(\psi)$ is continuous, $F_{\phi N}(\psi)$ is a piece-wise constant with N points of discontinuity. On Fig. 2.9b, the dashed line is the pdf $f_\phi(\psi)$, Eq. (2.85), and the delta functions (each of magnitude $1/N = 1/20$) form the ensemble-averaged pdf $f_{\phi N}(\psi)$.

The definition of the ensemble-averaged pdf is satisfactory since it possesses the required mathematical properties, Eqs (2.83–84). But its relationship to the pdf requires further comment: they are distinctly different quantities in that $f_{\phi N}(\psi)$ is composed of delta functions whereas $f_\phi(\psi)$ may be continuous. The relationship between $f_{\phi N}(\psi)$ and $f_\phi(\psi)$ can be understood as follows.

Each value $\phi^{(n)}$ is a sample of the random variable ϕ , and each location $\psi = \phi^{(n)}$ is a sample point in ψ -space. Let $m(\psi, \Delta\psi)$ denote the number of sample points in the region $\psi \leq \phi < \psi + \Delta\psi$. The normalized sample point number density is defined by

$$f_{\phi N}^*(\psi) \equiv \lim_{\Delta\psi \rightarrow 0} \left\{ \frac{m(\psi, \Delta\psi)}{N\Delta\psi} \right\}, \quad (2.86)$$

and is the fraction of sample points per unit distance along the ψ -axis. Clearly, $f_{\phi N}^*(\psi)$ is zero except at the sample points where there is a delta function of magnitude $1/N$. In other words, it is equal to the ensemble-averaged pdf:

$$f_{\phi N}^*(\psi) = f_{\phi N}(\psi). \quad (2.87)$$

Thus the ensemble-averaged pdf is the normalized sample point number density in ψ -space.

As N tends to infinity, the ensemble-averaged pdf $f_{\phi N}$ does not converge to f_ϕ , since $f_{\phi N}$ is still composed

of delta functions. The ensemble-averaged distribution function $F_{\phi N}$ is composed of steps and, even as N tends to infinity, it does not become differentiable. Nonetheless, for any continuous function $Q(\phi)$, the ensemble-average $\langle Q(\phi) \rangle_N$ almost certainly converges to $\langle Q(\phi) \rangle$; and, for any $N \geq 1$, the expectation of $f_{\phi N}$ is f_ϕ .

It may be noted that the expectation of Eq. (2.87)

$$\mathbf{E}\{f_{\phi N}^*(\psi)\} = f_\phi(\psi), \quad (2.88)$$

shows that the pdf is the expectation of the normalized sample point number density.

These considerations are important for the theory developed below, where pdf's are represented indirectly by ensembles of sample points. The principal conclusions are that the pdf can be regarded as the expectation of the normalized sample point density, which is equal to the ensemble-averaged pdf. As the size of the ensemble N tends to infinity, all ensemble averages $\langle Q \rangle_N$ almost certainly tend to the means $\langle Q \rangle$.

2.7. Joint Pdf's

For the mixing-layer experiment, the random variable that we have been considering is the normalized temperature at a particular location, $\phi = \phi(\mathbf{x}_0, t_0)$. We now consider a second random variable U , which is the normalized axial velocity at the same location:

$$U \equiv (U_1(\mathbf{x}_0, t_0) - U_a)/(U_b - U_a). \quad (2.89)$$

When the steady state is reached, in the low-speed free stream U and ϕ are zero, and in the high-speed stream U and ϕ are unity; but the same is not the case for the velocity, since pressure fluctuations can cause U to exceed these bounds. (Experimental data⁶¹ show that U does indeed exceed these bounds.)

A sample space (temperature space, or ψ -space) has been associated with the random variable ϕ , so that any value of ϕ can be plotted as a sample point $\psi = \phi$. Similarly, velocity space of V -space is introduced so that any value of U can be plotted as the sample point $V = U$.

The distribution function $F_u(V)$ and the pdf $f_u(V)$ are defined by,

$$F_u(V) \equiv \mathbf{P}(U < V), \quad (2.90)$$

and

$$f_u(V) = \frac{dF_u(V)}{dV}. \quad (2.91)$$

These definitions and the properties of the functions are exactly analogous to those for ϕ . The mean (mathematical expectation) of U is

$$\langle U \rangle = \int_{-\infty}^{\infty} V f_u(V) dV, \quad (2.92)$$

and the mean of a function† of U , $Q(U)$ is

† See previous footnote.

$$\langle Q(U) \rangle = \int_{-\infty}^{\infty} Q(V) f_u(V) dV. \quad (2.93)$$

The variance of U is

$$D(U) = \langle u^2 \rangle = \int_{-\infty}^{\infty} (V - \langle U \rangle)^2 f_u(V) dV, \quad (2.94)$$

where u is the fluctuation

$$u \equiv U - \langle U \rangle. \quad (2.95)$$

The distribution functions $F_\phi(\psi)$ and $F_u(V)$ contain all the information about ϕ and U separately, but they do not contain joint information. That is, if ϕ and U are measured, the probability of $\phi < \psi$ is given by $F_\phi(\psi)$ and the probability of $U < V$ is given by $F_u(V)$. But $F_\phi(\psi)$ and $F_u(V)$ do not contain sufficient information to determine the probability of the joint (simultaneous) event $\phi < \psi$ and $U < V$. This information is provided by the joint distribution function $F_{u\phi}(V, \psi)$ which is defined by

$$F_{u\phi}(V, \psi) \equiv P(U < V, \phi < \psi). \quad (2.96)$$

It is emphasized that the event $(U < V, \phi < \psi)$ refers to simultaneous values of U and ϕ .

The following properties of the joint distribution function are readily deduced:

$$0 \leq F_{u\phi}(V, \psi) \leq 1, \quad (2.97)$$

$$F_{u\phi}(-\infty, \psi) = F_{u\phi}(V, -\infty) = 0, \quad (2.98)$$

$$F_{u\phi}(\infty, \psi) = F_\phi(\psi), \quad (2.99)$$

$$F_{u\phi}(V, \infty) = F_u(V), \quad (2.100)$$

and, $F_{u\phi}(V, \psi)$ is a non-decreasing function of both V and ψ .

The joint pdf of U and ϕ , $f_{u\phi}(V, \psi)$, is defined by

$$f_{u\phi}(V, \psi) \equiv \frac{\partial^2}{\partial V \partial \psi} F_{u\phi}(V, \psi). \quad (2.101)$$

Both $F_{u\phi}(V, \psi)$ and $f_{u\phi}(V, \psi)$ are defined in the two-dimensional V - ψ sample space. By integrating Eq. (2.101) over an infinitesimal area in this velocity-temperature space, we obtain

$$f_{u\phi}(V, \psi) dV d\psi = P(V \leq U < V + dV, \psi \leq \phi < \psi + d\psi). \quad (2.102)$$

Other properties of the joint pdf are:

$$f_{u\phi}(V, \psi) \geq 0, \quad (2.103)$$

$$\int_{-\infty}^{\infty} \int_{-\infty}^{\infty} f_{u\phi}(V, \psi) dV d\psi = 1, \quad (2.104)$$

$$\int_{-\infty}^{\infty} f_{u\phi}(V, \psi) dV = f_\phi(\psi), \quad (2.105)$$

and

$$\int_{-\infty}^{\infty} f_{u\phi}(V, \psi) d\psi = f_u(V). \quad (2.106)$$

The pdf's $f_\phi(\psi)$ and $f_u(V)$ are called marginal pdf's, and the last two equations show that these marginal pdf's can be recovered from the joint pdf. But, as has

already been noted, the joint pdf cannot (in general) be determined from the marginal pdf's.

If $Q(U, \phi)$ is a function of U and ϕ , then its mean (mathematical expectation) is

$$\langle Q(U, \phi) \rangle = \int_{-\infty}^{\infty} \int_{-\infty}^{\infty} Q(V, \psi) f_{u\phi}(V, \psi) dV d\psi. \quad (2.107)$$

If Q is a function only of U , then this formula yields

$$\begin{aligned} \langle Q(U) \rangle &= \int_{-\infty}^{\infty} Q(V) \left\{ \int_{-\infty}^{\infty} f_{u\phi}(V, \psi) d\psi \right\} dV \\ &= \int_{-\infty}^{\infty} Q(V) f_u(V) dV, \end{aligned} \quad (2.108)$$

which is consistent with the earlier definition, Eq. (2.93).

The marginal pdf's $f_u(V)$ and $f_\phi(\psi)$ have means $\langle U \rangle$ and $\langle \phi \rangle$ and variances $\langle u^2 \rangle$ and $\langle \phi'^2 \rangle$. For the joint pdf $f_{u\phi}(V, \psi)$ another important characteristic is the covariance $\langle u\phi' \rangle$,

$$\langle u\phi' \rangle \equiv \int_{-\infty}^{\infty} \int_{-\infty}^{\infty} (V - \langle U \rangle)(\psi - \langle \phi \rangle) f_{u\phi}(V, \psi) dV d\psi. \quad (2.109)$$

The normalized covariance r is called the *correlation coefficient*:

$$r \equiv \langle u\phi' \rangle / \langle u^2 \rangle \langle \phi'^2 \rangle^{1/2}. \quad (2.110)$$

If r is zero, then U and ϕ are said to be uncorrelated. If $|r| = 1$, then U and ϕ are perfectly correlated. In general, r lies between minus one and one,

$$-1 \leq r \leq 1. \quad (2.111)$$

Perfect correlation occurs when U and ϕ are linearly related,

$$\phi = \alpha + \beta U, \quad (2.112)$$

where α and β are constants. If β is positive, then $r = 1$ and U and ϕ are perfectly positively correlated: if β is negative, $r = -1$ and U and ϕ are perfectly negatively correlated.

In nearly-homogeneous turbulence, experiments⁶² show that $f_{u\phi}(V, \psi)$ is a joint normal distribution:

$$f_{u\phi}(V, \psi) = c^{-1/2} \exp(-\lambda(V, \psi)), \quad (2.113)$$

where the constant c is

$$c = 4\pi^2 \langle u^2 \rangle \langle \phi'^2 \rangle (1 - r^2), \quad (2.114)$$

and $\lambda(V, \psi)$ is the positive definite quadratic function

$$\begin{aligned} \lambda(V, \psi) &= \frac{1}{2} \{ (V - \langle U \rangle)^2 / \langle u^2 \rangle \} \\ &\quad - 2r(V - \langle U \rangle)(\psi - \langle \phi \rangle) / \langle u^2 \rangle \langle \phi'^2 \rangle^{1/2} \\ &\quad + (\psi - \langle \phi \rangle)^2 / \langle \phi'^2 \rangle / (1 - r^2). \end{aligned} \quad (2.115)$$

The marginal pdf's $f_u(V)$ and $f_\phi(\psi)$ can be obtained by integrating Eq. (2.113) over ψ and V respectively. Both are normal distributions,

$$f_u(V) = (2\pi \langle u^2 \rangle)^{-1/2} \exp(-\frac{1}{2}(V - \langle U \rangle)^2 / \langle u^2 \rangle). \quad (2.116)$$

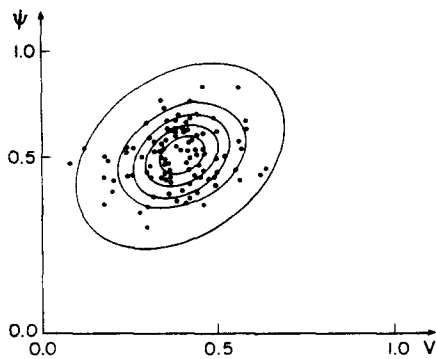


FIG. 2.10. Joint-normal pdf, and 100 sample points. The probability of a sample point being inside each ellipse is (from the inside outward) 0.2, 0.4, 0.6, 0.8 and 0.99.

and

$$f_\phi(\psi) = (2\pi\langle\phi'^2\rangle)^{-1/2} \exp(-\frac{1}{2}(\psi - \langle\phi\rangle)^2/\langle\phi'^2\rangle). \quad (2.117)$$

The joint-normal pdf is maximum at $(V, \psi) = (\langle U \rangle, \langle \phi \rangle)$ where λ , Eq. (2.115), is zero. Lines of constant (positive) λ are ellipses in the V - ψ sample space, and on these ellipses the probability density is constant, Eq. (2.113). From Eqs (2.113-2.115) it can be shown⁵⁵ that the probability $P(\lambda_*)$ of a sample point $(V, \psi) = (U, \phi)$ lying within the ellipse given by $\lambda = \lambda_*$ is

$$P(\lambda_*) = 1 - \exp(-\lambda_*). \quad (2.118)$$

Figure 2.10 shows the joint-normal pdf corresponding to $\langle U \rangle = 0.4$, $\langle \phi \rangle = 0.5$, $\langle u^2 \rangle = 0.01$, $\langle \phi'^2 \rangle = 0.00696$ and $r = 0.3$. The maximum probability density (at $(V, \psi) = (\langle U \rangle, \langle \phi \rangle)$) is 20. Five ellipses are shown on which the probability densities are (from the inside outward) 16, 12, 8, 4 and 0.2. The probability of a sample point being within each ellipse is 0.2, 0.4, 0.6, 0.8 and 0.99. Also shown are 100 sample points which were obtained from an appropriate

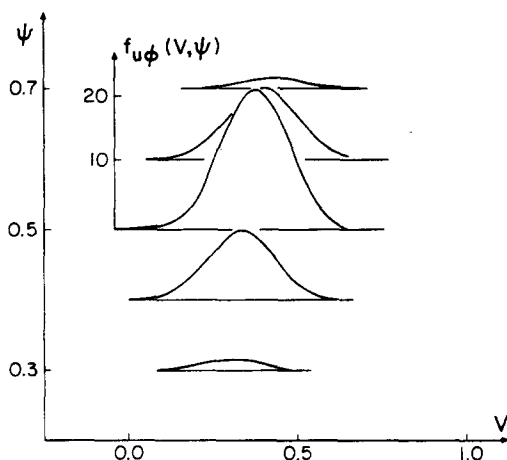


FIG. 2.11. Joint-normal pdf: $f_{u\phi}(V, \psi)$ against V for $\psi = 0.3, 0.4, 0.5, 0.6$ and 0.7 .

random number generator. It may be seen that the sample-point density approximates the probability density.

Figure 2.10 shows $f_{u\phi}(V, \psi)$ as a contour plot. Alternatively, $f_{u\phi}(V, \psi)$ can be plotted against V for different values of ψ . This representation is shown on Fig. 2.11.

The joint normal distribution is defined by the means, variances and covariances of the random variables. It is emphasized, however, that in general a pdf or a joint pdf cannot be determined from a finite number of moments. Because of their occurrence in nearly-homogeneous turbulence, joint normal pdf's have an important place in pdf methods. But in inhomogeneous flows, especially turbulent reactive flow, pdf's can be far from normal.⁶³

At a given location in sample space, the distribution function $F_{u\phi}(V, \psi)$ can be continuous or it can be discontinuous in either or both of V and ψ . For example, if ϕ adopts the constant value $\phi = \phi_*$, then $F_{u\phi}$ is discontinuous in ϕ :

$$F_{u\phi}(V, \psi) = F_u(V)H(\psi - \phi_*). \quad (2.119)$$

The corresponding pdf is

$$f_{u\phi}(V, \psi) = f_u(V)\delta(\psi - \phi_*). \quad (2.120)$$

If U also adopts a constant value $U = U_*$, then $F_{u\phi}$ is discontinuous in both V and ψ :

$$F_{u\phi}(V, \psi) = H(V - U_*)H(\psi - \phi_*), \quad (2.121)$$

and the joint pdf is,

$$f_{u\phi}(V, \psi) = \delta(V - U_*)\delta(\psi - \phi_*). \quad (2.122)$$

The delta function product, or two-dimensional delta function, in Eq. (2.122) represents a unit spike at location (U_*, ϕ_*) in the V - ψ sample space.

We now consider the transformation of the joint pdf under a change of variables. (Equation 2.48 is the transformation for a marginal pdf.) Let g and h be random variables (with corresponding sample-space variables \hat{g} and \hat{h}) defined by

$$g = G(U, \phi), \quad \hat{g} = G(V, \psi), \quad (2.123)$$

and

$$h = H(U, \phi), \quad \hat{h} = H(V, \psi). \quad (2.124)$$

We require that the functions G and H be such that there is a one-to-one correspondence between points in V - ψ space and those in \hat{g} - \hat{h} space. This requirement is met if the Jacobian

$$\frac{\partial(\hat{g}, \hat{h})}{\partial(V, \psi)} = \begin{vmatrix} \frac{\partial \hat{g}}{\partial V} & \frac{\partial \hat{g}}{\partial \psi} \\ \frac{\partial \hat{h}}{\partial V} & \frac{\partial \hat{h}}{\partial \psi} \end{vmatrix}, \quad (2.125)$$

has the same sign everywhere.

A given event corresponds to a region of V - ψ space which, in turn, corresponds to a region of \hat{g} - \hat{h} space. As an example, the event

$$A \equiv (V_a \leq U \leq V_b, \psi_a \leq \phi \leq \psi_b), \quad (2.126)$$

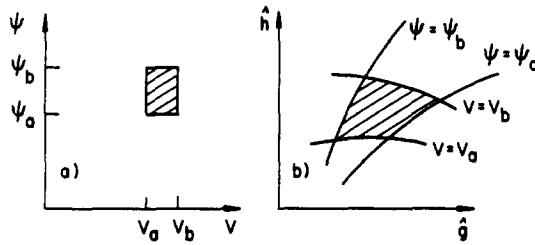


FIG. 2.12. The event A (Eq. 2.126) in: (a) V - ψ space, (b) \hat{g} - \hat{h} space.

is sketched as a region of V - ψ space on Fig. 2.12a and as a region of \hat{g} - \hat{h} space in Fig. 2.12b. With $f_{gh}(\hat{g}, \hat{h})$ being the joint pdf of g and h , the probability of the event A is

$$\begin{aligned} \mathbf{P}(A) &= \int_{V_a}^{V_b} \int_{\psi_a}^{\psi_b} f_{u\phi}(V, \psi) dV d\psi \\ &= \int_A \int f_{u\phi}(V, \psi) dV d\psi \\ &= \int_A \int f_{gh}(\hat{g}, \hat{h}) d\hat{g} d\hat{h}. \end{aligned} \quad (2.127)$$

Now since there is a one-to-one correspondence between points in the two spaces, the last integral can be rewritten⁶⁴

$$\int_A \int f_{gh}(\hat{g}, \hat{h}) d\hat{g} d\hat{h} = \int_A \int f_{gh}(\hat{g}, \hat{h}) \left| \frac{\partial(\hat{g}, \hat{h})}{\partial(V, \psi)} \right| dV d\psi. \quad (2.128)$$

Since the event A can be chosen arbitrarily, comparing the last two equations we obtain the transformation rule

$$f_{u\phi}(V, \psi) = f_{gh}(\hat{g}, \hat{h}) \left| \frac{\partial(\hat{g}, \hat{h})}{\partial(V, \psi)} \right|. \quad (2.129)$$

The absolute value of the Jacobian represents the volume ratio between the two spaces. The probability in an infinitesimal volume $dV d\psi$ at (V, ψ) is $f_{u\phi}(V, \psi) dV d\psi$. In \hat{g} - \hat{h} space, the corresponding volume is $|\partial(\hat{g}, \hat{h})/\partial(V, \psi)| dV d\psi$ and hence the corresponding probability is

$$f_{gh}(\hat{g}, \hat{h}) \left| \frac{\partial(\hat{g}, \hat{h})}{\partial(V, \psi)} \right| dV d\psi.$$

As Eq. (2.129) states, these two probabilities are equal.

The joint distribution function and pdf have been defined for the random variables U and ϕ measured at the particular location \underline{x}_0, t_0 . As with the marginal pdf's, this definition can be generalized to make $F_{u\phi}$ and $f_{u\phi}$ functions of \underline{x} and t :

$$F_{u\phi}(V, \psi, \underline{x}, t) \equiv \mathbf{P}(U(\underline{x}, t) < V, \phi(\underline{x}, t) < \psi), \quad (2.130)$$

and

$$f_{u\phi}(V, \psi; \underline{x}, t) \equiv \frac{\partial^2}{\partial V \partial \psi} F_{u\phi}(V, \psi, \underline{x}, t). \quad (2.131)$$

As before, the semicolon is used to separate the variables (V, ψ) with respect to which $f_{u\phi}$ is a density.

2.8. Conditional Probabilities

Conditional expectations play a central role in pdf methods. Before examining their properties we need to define conditional probability and conditional pdf's.

Let A and B be two events with positive probabilities $\mathbf{P}(A)$ and $\mathbf{P}(B)$. The probability of the joint event AB is $\mathbf{P}(AB)$. Since the joint event AB can only occur if both A and B occur, it is clear that,

$$\mathbf{P}(AB) \leq \mathbf{P}(A), \quad (2.132)$$

and

$$\mathbf{P}(AB) \leq \mathbf{P}(B). \quad (2.133)$$

The conditional probability of A and B is defined by

$$\mathbf{P}(A|B) \equiv \mathbf{P}(AB)/\mathbf{P}(B). \quad (2.134)$$

This is the probability of the event A , given that the event B occurs. It is obvious from Eqs (2.132–2.134) that $\mathbf{P}(A|B)$ conforms with the requirements on probabilities, namely

$$0 \leq \mathbf{P}(A|B) \leq 1. \quad (2.135)$$

The meaning of conditional probabilities is illustrated in the following example. Let n denote the outcome of the throw of a fair die (i.e. $n = 1, 2, 3, 4, 5$ or 6 with equal probability). If A is the event “ $n = 2$ ”, and B is the event “ n is even (2, 4 or 6)” then,

$$\mathbf{P}(A) = 1/6 \quad (2.136)$$

$$\mathbf{P}(B) = 1/2 \quad (2.137)$$

and

$$\mathbf{P}(AB) = 1/6. \quad (2.138)$$

From the definition of conditional probabilities, Eq. (2.134),

$$\mathbf{P}(A|B) = (1/6)/(1/2) = 1/3, \quad (2.139)$$

and

$$\mathbf{P}(B|A) = (1/6)/(1/6) = 1. \quad (2.140)$$

That is, if n is even (event B), then the probability of $n = 2$ (event A) is $1/3$, Eq. (2.139); if $n = 2$, n is certainly even, Eq. (2.140).

For the random variables U and ϕ , consider the events

$$A \equiv U < V, \quad (2.141)$$

and

$$B \equiv \psi \leq \phi < \psi + \Delta\psi. \quad (2.142)$$

The probabilities $\mathbf{P}(A)$, $\mathbf{P}(B)$ and $\mathbf{P}(AB)$ can be determined from the joint pdf $f_{u\phi}(V, \psi)$. Hence, using the definition of conditional probabilities, we obtain,

$$\mathbf{P}(A|B) = \mathbf{P}(U < V | \psi \leq \phi < \psi + \Delta\psi)$$

$$= \int_{-\infty}^V \int_{\psi}^{\psi + \Delta\psi} f_{u\phi}(\hat{V}, \hat{\psi}) d\hat{\psi} d\hat{V} / \int_{\psi}^{\psi + \Delta\psi} f_{\phi}(\hat{\psi}) d\hat{\psi}. \quad (2.143)$$

The conditional distribution function $F_{u|\phi}(V|\psi)$ is defined as the limit of this conditional probability as

$\Delta\psi$ tends to zero*:

$$\begin{aligned} F_{u|\phi}(V|\psi) &\equiv \mathbf{P}(U < V|\phi = \psi) \\ &= \int_{-\infty}^V f_{u|\phi}(\hat{V}, \psi) d\hat{V} / f_{\phi}(\psi). \end{aligned} \quad (2.144)$$

The conditional pdf $f_{u|\phi}$ is the derivative (with respect to V) of the conditional distribution function,

$$f_{u|\phi}(V|\psi) \equiv f_{u\phi}(V, \psi) / f_{\phi}(\psi). \quad (2.145)$$

It is simple to verify that $F_{u|\phi}$ and $f_{u|\phi}$ have all the properties of a distribution function and a pdf, respectively. The significance of the conditional pdf is that

$$f_{u|\phi}(V|\psi) dV$$

is the probability that U is in the infinitesimal range $V \leq U < V + dV$, given that ϕ is equal to ψ . It is also evident from Eq. (2.145) that the joint pdf can be recovered from the conditional pdf by

$$f_{u\phi} = f_{\phi} f_{u|\phi} = f_u f_{\phi|u}. \quad (2.146)$$

If $Q(U, \phi)$ is a function of U and ϕ , the *conditional expectation* of Q , given $\phi = \psi$, is

$$\begin{aligned} \mathbf{E}(Q(U, \phi)|\phi = \psi) &= \langle Q(U, \phi)|\phi = \psi \rangle \\ &= \int_{-\infty}^{\infty} f_{u|\phi}(V|\psi) Q(V, \psi) dV. \end{aligned} \quad (2.147)$$

The unconditional mean of Q can then be obtained by

$$\begin{aligned} \langle Q(U, \phi) \rangle &= \int_{-\infty}^{\infty} \int_{-\infty}^{\infty} f_{u\phi}(V, \psi) Q(V, \psi) dV d\psi \\ &= \int_{-\infty}^{\infty} f_{\phi}(\psi) \left\{ \int_{-\infty}^{\infty} f_{u|\phi}(V|\psi) Q(V, \psi) dV \right\} d\psi \\ &= \int_{-\infty}^{\infty} f_{\phi}(\psi) \langle Q(U, \phi)|\phi = \psi \rangle d\psi. \end{aligned} \quad (2.148)$$

In particular, the unconditional expectation of U is

$$\langle U \rangle = \int_{-\infty}^{\infty} f_{\phi}(\psi) \langle U|\phi = \psi \rangle d\psi. \quad (2.149)$$

In the subsequent derivation and examination of pdf equations, terms of the form $\langle U \delta(\phi - \psi) \rangle$ are frequently encountered. Substituting $U \delta(\phi - \psi)$ for $Q(U, \phi)$ in Eq. (2.148) we obtain:

$$\begin{aligned} \langle U \delta(\phi - \psi) \rangle &= \int_{-\infty}^{\infty} f_{\phi}(\psi') \langle U \delta(\phi - \psi')|\phi = \psi' \rangle d\psi' \\ &= \int_{-\infty}^{\infty} f_{\phi}(\psi') \langle U \delta(\psi' - \psi)|\phi = \psi' \rangle d\psi' \\ &= \int_{-\infty}^{\infty} f_{\phi}(\psi') \delta(\psi' - \psi) \langle U|\phi = \psi' \rangle d\psi' \\ &= f_{\phi}(\psi) \langle U|\phi = \psi \rangle. \end{aligned} \quad (2.150)$$

This important result is used extensively below.

For the joint-normal distribution, the conditional

* If $F_{\phi}(\psi)$ is discontinuous, $F_{u|\phi}$ and $f_{u|\phi}$ can still be defined but not by Eqs (2.144) and (2.145).

pdf $f_{u|\phi}$ is obtained by dividing $f_{u\phi}$, Eq. (2.113), by f_{ϕ} , Eq. (2.117):

$$\begin{aligned} f_{u|\phi}(V|\psi) &= [2\pi \langle u^2 \rangle (1-r)]^{-1/2} \\ &\times \exp \left\{ -\frac{1}{2} (V - \langle U|\phi = \psi \rangle)^2 / \langle u^2 \rangle (1-r^2) \right\}, \end{aligned}$$

where the conditional mean of U is

$$\langle U|\phi = \psi \rangle = \langle U \rangle + \langle u\phi' \rangle (\psi - \langle \phi \rangle) / \langle \phi'^2 \rangle. \quad (2.151)$$

Thus the conditional pdf $f_{u|\phi}$ may be seen to be a normal distribution with mean $\langle U|\phi = \psi \rangle$ and variance $\langle u^2 \rangle (1-r^2)$. Similarly, $f_{\phi|u}$ is a normal distribution with mean

$$\langle \phi|U = V \rangle = \langle \phi \rangle + \langle u\phi' \rangle (V - \langle U \rangle) / \langle u^2 \rangle \quad (2.152)$$

and variance $\langle \phi'^2 \rangle (1-r^2)$.

By definition, the random variables U and ϕ are *independent* if their joint pdf is the product of their marginal pdf's:

$$f_{u\phi}(V, \psi) = f_u(V) f_{\phi}(\psi). \quad (2.153)$$

It then follows from Eq. (2.145) that the conditional pdf's are equal to the unconditional pdf's,

$$f_{u|\phi}(V|\psi) = f_u(V), \quad (2.154)$$

and

$$f_{\phi|u}(\psi|V) = f_{\phi}(\psi). \quad (2.155)$$

Equation (2.154) shows that, if U and ϕ are independent, a knowledge of ϕ provides no information about U . In particular, the conditional expectation of U is the same as the unconditional expectation.

Independent random variables are uncorrelated since

$$\begin{aligned} \langle u\phi' \rangle &= \int_{-\infty}^{\infty} \int_{-\infty}^{\infty} (V - \langle U \rangle) (\psi - \langle \phi \rangle) f_{u\phi}(V, \psi) dV d\psi \\ &= \int_{-\infty}^{\infty} (V - \langle U \rangle) f_u(V) dV \int_{-\infty}^{\infty} (\psi - \langle \phi \rangle) f_{\phi}(\psi) d\psi \\ &= 0. \end{aligned} \quad (2.156)$$

But a lack of correlation does not, in general, imply independence. For example, with ξ being a uniformly distributed random variable between zero and one, the random variables $g \equiv \cos(2\pi\xi)$ and $h \equiv \sin(2\pi\xi)$ are uncorrelated, but they are obviously not independent.

2.9. Limitations of One-Point Pdf's

All the pdf's considered in this paper are one-point pdf's—pdf's of random variables at the same location and time. An example of a two-point pdf, is the joint pdf $f_{2\phi}$ of the random variables $\phi(\underline{x}, t)$ and $\phi(\underline{x}_*, t_*)$. The two-point distribution function $F_{2\phi}$ is defined by

$$F_{2\phi}(\psi, \psi_*, \underline{x}, t, \underline{x}_*, t_*) \equiv \mathbf{P}(\phi(\underline{x}, t) < \psi, \phi(\underline{x}_*, t_*) < \psi_*), \quad (2.157)$$

and the two-point joint pdf is

$$f_{2\phi}(\psi, \psi_*; \underline{x}, t, \underline{x}_*, t_*) \equiv \frac{\partial^2}{\partial \psi \partial \psi_*} F_{2\phi}(\psi, \psi_*, \underline{x}, t, \underline{x}_*, t_*). \quad (2.158)$$

The one-point pdf can be recovered by

$$f_\phi(\psi; \underline{x}, t) = \int_{-\infty}^{\infty} f_{2\phi}(\psi, \psi_*; \underline{x}, t, \underline{x}_*, t_*) d\psi_*, \quad (2.159)$$

but, in general, the two-point pdf cannot be determined from $f_\phi(\psi; \underline{x}, t)$ and $f_\phi(\psi_*; \underline{x}_*, t_*)$.

It is clear, then, that one-point pdf's do not provide a complete description of random fields. They provide information at each point separately, but no joint information at two or more points. As a consequence, one-point pdf's contain no information about the frequency or length scale of the fluctuations.

To illustrate this observation, suppose that $\phi(\underline{x}, t)$ is a travelling sine wave of frequency ω , wave length L , and random phase,

$$\phi(\underline{x}, t) = \frac{1}{2} + \frac{1}{2} \sin \{2\pi(\omega t + x_1/L + \xi)\}, \quad (2.160)$$

where ξ is a random variable, uniformly distributed between zero and one. The corresponding pdf is

$$f_\phi(\psi; \underline{x}, t) = \frac{1}{\pi} \{1 - (2\psi - 1)^2\}^{-1/2}. \quad (2.161)$$

The pdf, it may be seen, is independent of both the frequency ω and the wave length L . Consequently the one-point pdf contains insufficient information to determine a quantity such as $\langle (\partial\phi/\partial x_1)^2 \rangle$ which clearly depends upon the wave length L . (It follows from Eq. (2.160) that this quantity is given by,

$$\left\langle \left(\frac{\partial \phi}{\partial x_1} \right)^2 \right\rangle = \frac{1}{2} \pi^2 / L^2. \quad (2.162)$$

3. VELOCITY-COMPOSITION JOINT PDF

In a low Mach number gaseous flow, the state of the fluid at any location is fully described by the three components of velocity ($\underline{U} = U_1, U_2, U_3$) and by a set of σ scalars ($\underline{\phi} = \phi_1, \phi_2, \dots, \phi_\sigma$). The set of scalars $\underline{\phi}$ comprises the species mass fractions and the enthalpy. In section 3.1 the transport equations for \underline{U} and $\underline{\phi}$ are presented.

A complete one-point statistical description of a turbulent reactive flow is provided by $f(\underline{V}, \underline{\psi}; \underline{x}, t)$ —the joint pdf of \underline{U} and $\underline{\phi}$. At a given location in physical space and time (\underline{x}, t), the joint pdf $f(\underline{V}, \underline{\psi})$ is the probability density in the combined three-dimensional velocity space (\underline{V} -space) and the σ -dimensional composition space ($\underline{\psi}$ -space). The properties of the velocity-composition space and of the pdf are outlined in Sections 3.2 and 3.3. The joint pdf can be represented by an ensemble of delta functions (cf. Eq. 2.81). This discrete representation, which plays a central role in the pdf approach, is described in section

3.4. In Section 3.5 the transport equation for $f(\underline{V}, \underline{\psi}; \underline{x}, t)$ is derived from the transport equations for \underline{U} and $\underline{\phi}$.

3.1. Conservation Equations

The state of a reacting gas mixture composed of s species is fully described by the species mass fractions $m_\alpha(\underline{x}, t)$ ($\alpha = 1, 2, \dots, s$), the specific enthalpy $h(\underline{x}, t)$, the pressure $p(\underline{x}, t)$, and the velocity $\underline{U}(\underline{x}, t)$. An equation of state determines the density ρ as a function of \underline{m} , h and p :

$$\rho = \rho(\underline{m}, h, p), \quad (3.1)$$

where \underline{m} denotes the set of species mass fractions.

The evolution of the reactive flow field is governed by the conservation equations of mass, momentum, chemical species and enthalpy^{65,66}:

$$\frac{\partial \rho}{\partial t} + \frac{\partial}{\partial x_i} (\rho U_i) = 0, \quad (3.2)$$

$$\rho \frac{D \underline{U}_j}{D t} = \frac{\partial \tau_{ij}}{\partial x_i} - \frac{\partial p}{\partial x_j} + \rho g_j, \quad (3.3)$$

$$\rho \frac{D m_\alpha}{D t} = - \frac{\partial J_i^\alpha}{\partial x_i} + \rho S_\alpha, \quad (3.4)$$

and

$$\rho \frac{D h}{D t} = - \frac{\partial J_i^h}{\partial x_i} + \rho S_h, \quad (3.5)$$

where the material derivative (the rate of change following the fluid) is

$$\frac{D}{D t} = \frac{\partial}{\partial t} + U_i \frac{\partial}{\partial x_i}. \quad (3.6)$$

In these equations, g_j is the body force (per unit mass) in the x_j -direction; τ_{ij} is the sum of the viscous and viscous-diffusive stress tensors⁶⁶; S_α is the mass rate of addition (per unit mass) of species α due to reaction; J_i^α is the diffusive mass flux vector of species α ; S_h is the source of specific enthalpy due to compressibility, viscous dissipation and radiation; and J^h is the specific energy flux vector due to molecular transport. The molecular transport quantities τ_{ij} , J^α and J^h are complicated functions of the local properties and their gradients.⁶⁶

The source of m_α , S_α , is a combination of reaction rates and stoichiometric coefficients. The reaction rates depend upon the mass fractions, the pressure, and the temperature $T(\underline{x}, t)$. Since the temperature can be determined from \underline{m} , h and p ,

$$T = T(\underline{m}, h, p), \quad (3.7)$$

so also can the source S_α :

$$S_\alpha = S_\alpha(\underline{m}, h, p). \quad (3.8)$$

The fluid mechanical equations (Eqs 3.2–3.3) are coupled to the thermochemical equations (Eqs 3.1, 3.4, 3.5, 3.8) principally by the pressure and density. It proves to be extremely useful to invoke the low Mach number assumption to remove the coupling through the pressure. Let \underline{x}_0 be a reference location and let the

reference pressure p_0 be

$$p_0(t) = \langle p(\underline{x}_0, t) \rangle. \quad (3.9)$$

The pressure can then be written as

$$p(\underline{x}, t) = p_0(t) + \Delta p(\underline{x}, t), \quad (3.10)$$

where the pressure variation Δp is defined by

$$\Delta p(\underline{x}, t) \equiv p(\underline{x}, t) - p_0(t). \quad (3.11)$$

The pressure-gradient term in the momentum equation can be rewritten as

$$\frac{\partial p}{\partial x_j} = \frac{\partial}{\partial x_j} (\Delta p(\underline{x}, t) + p_0(t)) = \frac{\partial \Delta p}{\partial x_j}, \quad (3.12)$$

showing that the uniform reference pressure p_0 has no effect.

The density and the reaction rates (and hence S_α) depend upon the magnitude of the pressure, not upon the pressure gradient. The equation of state (Eq. 3.1) can be expanded in a Taylor series in p around p_0 to yield,

$$\rho(\underline{m}, h, p) = \rho(\underline{m}, h, p_0) \left\{ 1 + \frac{p_0}{\rho} \frac{\partial \rho}{\partial p} \frac{\Delta p}{p_0} + \dots \right\}. \quad (3.13)$$

Now, since $\Delta p/p_0$ can be estimated to be of the order of the Mach number squared,¹⁷ only the first term in the expansion need be retained. Thus, to a good approximation,

$$\rho = \rho(\underline{m}, h, p_0), \quad (3.14)$$

and similarly, the sources S_α can be evaluated by

$$S_\alpha = S_\alpha(\underline{m}, h, p_0). \quad (3.15)$$

The source in the enthalpy equation is⁶⁵

$$\rho S_h = \tau_{ij} \frac{\partial U_i}{\partial x_j} + \frac{Dp}{Dt} + (A - \varepsilon), \quad (3.16)$$

where A and ε are the rates of absorption and emission of radiant energy (per unit volume). At low Mach number, the viscous dissipation term is negligible and the pressure term is well approximated by

$$\frac{Dp}{Dt} = \frac{dp_0}{dt}. \quad (3.17)$$

In non-sooting gaseous flames, radiative heat transfer can usually be neglected in the enthalpy equation. It is assumed that the rate of absorption A is negligible, but the rate of emission can be retained in the equation since it is a function of \underline{m} , T and p_0 . Thus, with the assumption of low Mach number and the neglect of radiation absorption we obtain

$$S_h = S_h(\underline{m}, h, p_0, dp_0/dt). \quad (3.18)$$

It may be seen that with the low Mach number assumption, the pressure variations Δp do not affect the thermochemical equations while the reference pressure p_0 does not affect the momentum equations directly. The equations are still coupled through the density which depends upon p_0 . (Strahle⁶⁷ and others

have also determined that Δp does not affect the thermochemical equations at low Mach number.)

In some applications (notably internal combustion engines) the reference pressure $p_0(t)$ varies significantly with time. In other applications (open flames, furnaces, and gas turbine combustors in the steady state) the reference pressure is constant. For simplicity, we consider the case of constant reference pressure, but the extension to the variable case is straightforward.

The mass fraction and enthalpy equations can be written in a common form by defining the set of $\sigma = s + 1$ scalars $\underline{\phi}(\underline{x}, t)$ by:

$$\phi_\alpha = m_\alpha, \quad \alpha = 1, 2, \dots, s = \sigma - 1,$$

and

$$\phi_\sigma = h. \quad (3.19)$$

Then, with $J_i^\alpha \equiv J_i^h$ and $S_\alpha \equiv S_h$, the general scalar transport equation is,

$$\rho \frac{D\phi_\alpha}{Dt} = -\frac{\partial J_i^\alpha}{\partial x_i} + \rho S_\alpha, \quad \alpha = 1, 2, \dots, \sigma. \quad (3.20)$$

For a given reference pressure p_0 (assumed constant), the density and sources depend only on the set of scalars $\underline{\phi}$:

$$\rho = \rho(\underline{\phi}), \quad (3.21)$$

and

$$S_\alpha = S_\alpha(\underline{\phi}). \quad (3.22)$$

The set of σ scalars $\underline{\phi}$ defined by Eq. (3.19) provides a complete description of the thermochemical properties of the gas mixture. Many combustion problems involve a large number of species, and consequently σ is large. (For example, the combustion of methanol may involve 26 species.⁶⁸) In turbulent combustion calculations, simplifying assumptions are usually made in order to reduce the number of scalars needed to describe the gas composition. Extreme examples are the idealized premixed and diffusion flames, in each of which the gas composition is (by assumption) determined by a single scalar. For the idealized premixed flame⁶⁹ the single scalar is the *progress variable* (or the normalized product concentration): for the idealized diffusion flame⁷⁰ the single scalar is the *mixture fraction* (or the nozzle-fluid concentration).

In order to exploit such simplifying assumptions, we redefine the set of scalars considered as follows:

$\underline{\phi}$ is a set of σ scalars ($\underline{\phi} = \phi_1, \phi_2, \dots, \phi_\sigma$), governed by the general transport equation Eq. (3.20), which, in conjunction with the simplifying assumptions (if any), is sufficient to determine the density ρ , the source terms S_α ($\alpha = 1, 2, \dots, \sigma$) and any other thermochemical property of interest.

The scalars $\underline{\phi}$ are called the *composition variables* since they determine the composition of the gas mixture. Their definition ensures that Eqs (3.20–3.22) hold, and that (at least by assumption) the mass fractions and enthalpy are known functions:

$$m_x = m_x(\underline{\phi}), \quad (3.23)$$

and

$$h = h(\underline{\phi}). \quad (3.24)$$

In summary, the equations governing the evolution of the turbulent reactive flow field are the mass conservation equation, Eq. (3.2), the momentum conservation equation, Eq. (3.3), the composition equations, Eq. (3.20) and the equation of state, Eq. (3.21). No assumptions have been made about the reaction rates S_x or the molecular transport terms τ_{ij} , \mathbf{J}^x and \mathbf{J}^h .

3.2. Velocity and Composition Spaces

At a given position and time $(\underline{x}, t) = (\underline{x}_0, t_0)$ in a turbulent flow, each component of the velocity $(U_i = U_i(\underline{x}, t), i = 1, 2, 3)$ is a random variable. Together, the three components form the *random vector* \underline{U} . Let (V_1, V_2, V_3) be the coordinates of the point \underline{V} in a three-dimensional Euclidean space that we call the *velocity space*. Then the simultaneously-measured values U_1 , U_2 and U_3 can be plotted as the sample point $\underline{V} = \underline{U}$ in the velocity space. The velocity space (or \underline{V} -space) is the sample space of the random vector \underline{U} .

Similarly, each of the composition variables $(\phi_\alpha = \phi_\alpha(\underline{x}_0, t_0), \alpha = 1, 2, \dots, \sigma)$ is a random variable: taken together they form a σ -dimensional random vector $\underline{\phi}$. Let $(\psi_1, \psi_2, \dots, \psi_\sigma)$ be the coordinates of the point $\underline{\psi}$ in a σ -dimensional Euclidean space that we call the *composition space*. This is the sample space of the composition variables, since a simultaneous measurement of $(\phi_1, \phi_2, \dots, \phi_\sigma)$ can be plotted as the sample point $\underline{\psi} = \underline{\phi}$.

If the composition variable ϕ_α is a mass fraction— m_α , say—then (from the definition of mass fractions) ϕ_α must lie between zero and unity:

$$0 \leq \phi_\alpha \leq 1. \quad (3.25)$$

A value of ϕ_α exceeding these bounds cannot occur. In general, there is a region in composition space ($\underline{\psi}$ -space) called the *allowed region* within which any point $\underline{\psi}$ corresponds to a possible composition $\underline{\phi} = \underline{\psi}$. Outside the allowed region, a point $\underline{\psi}$ corresponds to a composition $\underline{\phi} = \underline{\psi}$ that cannot occur—possibly because a negative mass fraction is implied.

Equations (3.21–3.24) show that properties such as ρ , S_x , m_x and h are known in terms of the composition variables $\underline{\phi}$. Since every point $\underline{\psi}$ in the allowed region of the composition space corresponds to a possible composition $\underline{\phi} = \underline{\psi}$, the corresponding properties at the point are $\rho(\underline{\psi})$, $S_x(\underline{\psi})$, $m_x(\underline{\psi})$, $h(\underline{\psi})$, and so on. In this way, any property of $\underline{\phi}$ can be regarded as a function in composition space. The density ρ is a scalar, while quantities which have σ components can be regarded as vectors in $\underline{\psi}$ -space. In particular, $\underline{\phi} = (\phi_1, \phi_2, \dots, \phi_\sigma)$ and $\underline{S} = (S_1, S_2, \dots, S_\sigma)$ are vectors.

Processes, as well as properties, can be represented in composition space. Consider a homogeneous,

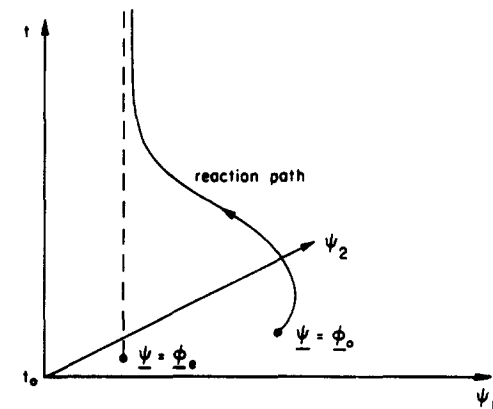


FIG. 3.1. Reaction path in augmented composition space.

quiescent, reactive gas mixture, which at time t_0 has the composition $\underline{\phi}(t_0) = \underline{\phi}_0$. According to Eq. (3.20), as reaction takes place, the composition evolves by

$$\frac{d\phi_\alpha}{dt} = S_x(\underline{\phi}), \quad (3.26)$$

or, in terms of the vectors $\underline{\phi}$ and \underline{S} ,

$$\frac{d\underline{\phi}}{dt} = \underline{S}(\underline{\phi}). \quad (3.27)$$

(Because of the assumed homogeneity, $\underline{\phi}$ depends only upon t , and the other terms in Eq. (3.20) are zero.) The solution to Eq. (3.27) can be written

$$\underline{\phi}(t) = \underline{\Phi}(\underline{\phi}_0, t), \quad (3.28)$$

to show, explicitly the dependence of $\underline{\phi}(t)$ upon the initial condition $\underline{\phi}_0$.

At any time, the composition can be represented by a point in $\underline{\psi}$ -space. Initially the point is $\underline{\psi} = \underline{\Phi}(\underline{\phi}_0, t)$. Such a trajectory—or reaction path—is sketched on Fig. 3.1 in the augmented composition space ($\underline{\psi}$ - t space). The composition is shown approaching the value $\underline{\psi} = \underline{\phi}_e$ corresponding to chemical equilibrium. It is evident from Eq. (3.27) that \underline{S} represents the velocity of the point in composition space, and consequently reaction paths are everywhere tangential to \underline{S} .

The velocity vector \underline{U} is a three-dimensional random vector and $\underline{\phi}$ is a σ -dimensional random vector. Taken together, the $(3 + \sigma)$ quantities $(\underline{U}, \underline{\phi}) = (U_1, U_2, U_3, \phi_1, \phi_2, \dots, \phi_\sigma)$ form a $(3 + \sigma)$ -dimensional random vector. The appropriate sample space for this random vector is the $(3 + \sigma)$ -dimensional Euclidean space in which the coordinates of the point $(\underline{V}, \underline{\psi})$ are $(V_1, V_2, V_3, \psi_1, \psi_2, \dots, \psi_\sigma)$. This is called the *velocity-composition space* or *\underline{V} - $\underline{\psi}$ space*. The experimental techniques of laser-Doppler-anemometry and Raman spectroscopy are approaching the stage where simultaneous measurements of \underline{U} and $\underline{\phi}$ are possible.⁷¹ A simultaneous measurement of these $(3 + \sigma)$ quantities could be plotted as a point in \underline{V} - $\underline{\psi}$ space.

3.3. Velocity-Composition Joint Pdf

At the particular location and time $(\underline{x}, t) = (\underline{x}_0, t_0)$, the three components of velocity and the σ com-

position variables, form the $(3+\sigma)$ -dimensional random vector $(\underline{U}, \underline{\phi})$. The $(3+\sigma)$ -dimensional distribution function of $(\underline{U}, \underline{\phi})$ is defined by

$$F_{\underline{u}\underline{\phi}}(\underline{V}, \underline{\psi}) \equiv \mathbf{P}(U_1 < V_1, U_2 < V_2, U_3 < V_3, \phi_1 < \psi_1, \phi_2 < \psi_2, \dots, \phi_\sigma < \psi_\sigma). \quad (3.29)$$

At every point in the velocity-composition space (\underline{V} - $\underline{\psi}$ space), this distribution function has a value between zero and one. The joint pdf of $(\underline{U}, \underline{\phi})$ is defined by,

$$f_{\underline{u}\underline{\phi}}(\underline{V}, \underline{\psi}) = \frac{\partial^{3+\sigma}}{\partial V_1 \partial V_2 \partial V_3 \partial \psi_1 \partial \psi_2 \dots \partial \psi_\sigma} F_{\underline{u}\underline{\phi}}(\underline{V}, \underline{\psi}). \quad (3.30)$$

Before outlining the properties of $f_{\underline{u}\underline{\phi}}$, we introduce some abbreviated notation. First, f (without subscripts) is written for $f_{\underline{u}\underline{\phi}}$:

$$f(\underline{V}, \underline{\psi}) = f_{\underline{u}\underline{\phi}}(\underline{V}, \underline{\psi}). \quad (3.31)$$

An infinitesimal volume in \underline{V} -space is written $d\underline{V}$,

$$d\underline{V} = dV_1 dV_2 dV_3, \quad (3.32)$$

and an infinitesimal volume in $\underline{\psi}$ -space is $d\underline{\psi}$,

$$d\underline{\psi} = d\psi_1 d\psi_2 \dots d\psi_\sigma. \quad (3.33)$$

Thus $d\underline{V} d\underline{\psi}$ is an infinitesimal $(3+\sigma)$ -dimensional volume in velocity-composition space. Integration over the whole of \underline{V} -space or $\underline{\psi}$ -space is indicated by a single integral sign:

$$\int (\dots) d\underline{V} = \int_{-\infty}^{\infty} \int_{-\infty}^{\infty} \int_{-\infty}^{\infty} (\dots) dV_1 dV_2 dV_3, \quad (3.34)$$

and

$$\int (\dots) d\underline{\psi} = \int_{-\infty}^{\infty} \int_{-\infty}^{\infty} \dots \int_{-\infty}^{\infty} (\dots) d\psi_1 d\psi_2 \dots d\psi_\sigma. \quad (3.35)$$

Integration over the whole of \underline{V} - $\underline{\psi}$ space is written as

$$\int \int (\dots) d\underline{V} d\underline{\psi}.$$

The joint pdf of the three velocity components $f_u(\underline{V})$ is obtained from $f(\underline{V}, \underline{\psi})$ by integrating over $\underline{\psi}$ -space:

$$f_u(\underline{V}) = \int f(\underline{V}, \underline{\psi}) d\underline{\psi}. \quad (3.36)$$

And the marginal pdf of a single velocity component— U_1 , say—is obtained by integrating f_u over the other two velocities:

$$f_{u_1}(V_1) = \int_{-\infty}^{\infty} \int_{-\infty}^{\infty} f_u(\underline{V}) dV_2 dV_3. \quad (3.37)$$

Similarly the joint pdf of the compositions, $f_\phi(\underline{\psi})$ is obtained by integrating $f(\underline{V}, \underline{\psi})$ over velocity space

$$f_\phi(\underline{\psi}) = \int f(\underline{V}, \underline{\psi}) d\underline{V}. \quad (3.38)$$

The probability that \underline{U} is in the infinitesimal volume $d\underline{V}$ at \underline{V} is $f_u(\underline{V}) d\underline{V}$: the probability that $\underline{\phi}$ is in the

infinitesimal volume $d\underline{\psi}$ at $\underline{\psi}$ is $f_\phi(\underline{\psi}) d\underline{\psi}$. Similarly, for the $(3+\sigma)$ -dimensional random vector $(\underline{U}, \underline{\phi})$, the probability of its being in the infinitesimal volume $d\underline{V} d\underline{\psi}$ at $(\underline{V}, \underline{\psi})$ is $f(\underline{V}, \underline{\psi}) d\underline{V} d\underline{\psi}$. (These properties of the pdf's follow from the definition of the distribution function, Eq. (3.29).)

The sample point corresponding to a value of the random vector $(\underline{U}, \underline{\phi})$ is sure to lie somewhere in the \underline{V} - $\underline{\psi}$ sample space. Thus the probability of this event (which is given by the integral of $f(\underline{V}, \underline{\psi})$ over the whole space) is one:

$$\int \int f(\underline{V}, \underline{\psi}) d\underline{V} d\underline{\psi} = 1. \quad (3.39)$$

Similarly,

$$\int f_u(\underline{V}) d\underline{V} = 1, \quad (3.40)$$

and

$$\int f_\phi(\underline{\psi}) d\underline{\psi} = 1. \quad (3.41)$$

Let $Q(\underline{U}, \underline{\phi})$ be a function* of \underline{U} and $\underline{\phi}$. Correspondingly, $Q(\underline{V}, \underline{\psi})$ is a function defined everywhere in velocity-composition space. The mean, or expectation, of Q is

$$\langle Q(\underline{U}, \underline{\phi}) \rangle = \int \int Q(\underline{V}, \underline{\psi}) f(\underline{V}, \underline{\psi}) d\underline{V} d\underline{\psi}. \quad (3.42)$$

If Q is a function of \underline{U} only, then its mean is

$$\begin{aligned} \langle Q(\underline{U}) \rangle &= \int \int Q(\underline{V}) f(\underline{V}, \underline{\psi}) d\underline{V} d\underline{\psi} \\ &= \int Q(\underline{V}) \left\{ \int f(\underline{V}, \underline{\psi}) d\underline{\psi} \right\} d\underline{V} \\ &= \int Q(\underline{V}) f_u(\underline{V}) d\underline{V}. \end{aligned} \quad (3.43)$$

Similarly, if Q is a function of $\underline{\phi}$ only,

$$\langle Q(\underline{\phi}) \rangle = \int Q(\underline{\psi}) f_\phi(\underline{\psi}) d\underline{\psi}. \quad (3.44)$$

It may be recalled that $\underline{\phi}$ is always within the allowed region of $\underline{\psi}$ -space. Physical properties such as the density ρ have no physical meaning outside the allowed region. However, it aids both the notation and the analysis to regard $\rho(\underline{\psi})$ as a finite continuous function defined everywhere in $\underline{\psi}$ -space. The definition of $\rho(\underline{\psi})$ outside the allowed region is arbitrary (except that $\rho(\underline{\psi})$ should be finite and continuous) since $\rho(\underline{\psi}) f_\phi(\underline{\psi})$ is non-zero only in the allowed region. Thus, the mean density can be determined from

$$\langle \rho(\underline{\phi}) \rangle = \int \rho(\underline{\psi}) f_\phi(\underline{\psi}) d\underline{\psi}, \quad (3.45)$$

and is independent of the definition of $\rho(\underline{\psi})$ outside the allowed region. Similarly, all other functions (e.g. $\underline{S}(\underline{\psi})$) are regarded as being defined everywhere in composition space.

* See footnote in Section 2.5.

In Section 2.5 it was shown that the pdf of a single scalar $f_\phi(\psi)$ is equal to the expectation of a delta function $\langle \delta(\psi - \phi) \rangle$, Eq. (2.67). Similarly, for the joint pdf we have

$$f(\underline{V}, \underline{\psi}) = \langle \delta(\underline{V} - \underline{U}) \delta(\underline{\psi} - \underline{\phi}) \rangle, \quad (3.46)$$

where $\delta(\underline{V} - \underline{U})$ is written for the three-dimensional delta function at $\underline{V} = \underline{U}$,

$$\delta(\underline{V} - \underline{U}) \equiv \delta(V_1 - U_1) \delta(V_2 - U_2) \delta(V_3 - U_3), \quad (3.47)$$

and, similarly, $\delta(\underline{\psi} - \underline{\phi})$ is the σ -dimensional delta function at $\underline{\psi} = \underline{\phi}$,

$$\delta(\underline{\psi} - \underline{\phi}) = \prod_{\alpha=1}^{\sigma} \delta(\psi_\alpha - \phi_\alpha). \quad (3.48)$$

If R is any random variable, its mean can be determined by

$$\langle R \rangle = \iint \langle R | \underline{U} = \underline{V}, \underline{\phi} = \underline{\psi} \rangle f(\underline{V}, \underline{\psi}) d\underline{V} d\underline{\psi}, \quad (3.49)$$

where $\langle R | \underline{U} = \underline{V}, \underline{\phi} = \underline{\psi} \rangle$ is the conditional expectation of R , given that $\underline{U} = \underline{V}$ and $\underline{\phi} = \underline{\psi}$ (cf. Eq. 2.149). If R is independent of \underline{U} and $\underline{\phi}$, then the conditional expectation is equal to the mean,

$$\langle R | \underline{U} = \underline{V}, \underline{\phi} = \underline{\psi} \rangle = \langle R \rangle, \quad (3.50)$$

in which case Eq. (3.49) is not useful. At the opposite extreme, if R is completely determined by \underline{U} and $\underline{\phi}$ (i.e. $R = R(\underline{U}, \underline{\phi})$), then

$$\langle R(\underline{U}, \underline{\phi}) | \underline{U} = \underline{V}, \underline{\phi} = \underline{\psi} \rangle = R(\underline{V}, \underline{\psi}), \quad (3.51)$$

and Eq. (3.49) reduces to the definition of the unconditional mean. Henceforth, conditional expectations are written $\langle R | \underline{V}, \underline{\psi} \rangle$, it being implied that \underline{V} is the value of \underline{U} , and $\underline{\psi}$ is the value of $\underline{\phi}$.

An important result embracing conditional expectations and delta functions is

$$\langle R \delta(\underline{V} - \underline{U}) \delta(\underline{\psi} - \underline{\phi}) \rangle = \langle R | \underline{V}, \underline{\psi} \rangle f(\underline{V}, \underline{\psi}). \quad (3.52)$$

This result, which is used extensively below, can be deduced from Eq. (3.42), (cf. Eq. 2.150).

For variable-density flows, there can be an advantage¹⁷ in considering density-weighted means (or Favre averages⁷⁰). For the random variable R , the density-weighted mean \tilde{R} is defined by

$$\tilde{R} \equiv \langle \rho R \rangle / \langle \rho \rangle, \quad (3.53)$$

and the fluctuation about this mean is

$$R'' \equiv R - \tilde{R}. \quad (3.54)$$

From Eqs (3.49) and (3.53) we obtain

$$\begin{aligned} \tilde{R} &= \iint \langle \rho(\underline{\phi}) R | \underline{V}, \underline{\psi} \rangle f(\underline{V}, \underline{\psi}) d\underline{V} d\underline{\psi} / \langle \rho \rangle \\ &= \iint \rho(\underline{\psi}) \langle R | \underline{V}, \underline{\psi} \rangle f(\underline{V}, \underline{\psi}) d\underline{V} d\underline{\psi} / \langle \rho \rangle \\ &= \iint \langle R | \underline{V}, \underline{\psi} \rangle \tilde{f}(\underline{V}, \underline{\psi}) d\underline{V} d\underline{\psi}, \end{aligned} \quad (3.55)$$

where the density-weighted joint pdf \tilde{f} is defined⁷⁰ by

$$\tilde{f}(\underline{V}, \underline{\psi}) \equiv f(\underline{V}, \underline{\psi}) \rho(\underline{\psi}) / \langle \rho \rangle. \quad (3.56)$$

With this definition of \tilde{f} , Eq. (3.55) for the density-weighted mean, \tilde{R} is directly analogous to Eq. (3.49) for the mean $\langle R \rangle$.

The random vector $(\underline{U}, \underline{\phi})$ has been defined as the velocity and composition at the particular location and time $(\underline{x}, t) = (\underline{x}_0, t_0)$. Clearly, the random vector (and hence the distribution function and pdf) can be defined at any (\underline{x}, t) . In general, then, the joint distribution function is defined by,

$$\begin{aligned} F_{\underline{u}\underline{\phi}}(\underline{V}, \underline{\psi}, \underline{x}, t) &\equiv \mathbf{P}(U_1(\underline{x}, t) < V_1, U_2(\underline{x}, t) \\ &< V_2, U_3(\underline{x}, t) < V_3, \phi_1(\underline{x}, t) \\ &< \psi_1, \phi_2(\underline{x}, t) < \psi_2, \dots, \phi_\sigma(\underline{x}, t) < \psi_\sigma), \end{aligned} \quad (3.57)$$

and the joint pdf is defined by,

$$\begin{aligned} f(\underline{V}, \underline{\psi}; \underline{x}, t) &\equiv \frac{\partial^{3+\sigma}}{\partial V_1 \partial V_2 \partial V_3 \partial \psi_1 \partial \psi_2 \dots \partial \psi_\sigma} \\ &\quad \times F_{\underline{u}\underline{\phi}}(\underline{V}, \underline{\psi}, \underline{x}, t). \end{aligned} \quad (3.58)$$

It is emphasized that $f(\underline{V}, \underline{\psi}; \underline{x}, t)$ contains information about every point (\underline{x}, t) separately: it contains no two-point information in physical space or time.

In applying the pdf equation to inhomogeneous, variable-density flows, the natural dependent variable is neither f nor \tilde{f} but it is the *mass density function* (mdf)

$$\begin{aligned} \mathcal{F}(\underline{V}, \underline{\psi}, \underline{x}; t) &\equiv \rho(\underline{\psi}) f(\underline{V}, \underline{\psi}; \underline{x}, t) \\ &= \langle \rho \rangle \tilde{f}(\underline{V}, \underline{\psi}; \underline{x}, t). \end{aligned} \quad (3.59)$$

As is explained in the next subsection, the mass density function \mathcal{F} is the expected mass density in $\underline{V} - \underline{\psi} - \underline{x}$ space.

The important properties of \mathcal{F} follow immediately from its definition and from the properties of f :

$$\iint \mathcal{F}(\underline{V}, \underline{\psi}, \underline{x}; t) d\underline{V} d\underline{\psi} = \langle \rho \rangle, \quad (3.60)$$

$$\iint \mathcal{F}(\underline{V}, \underline{\psi}, \underline{x}; t) [\rho(\underline{\psi})]^{-1} d\underline{V} d\underline{\psi} = 1, \quad (3.61)$$

$$\iint \mathcal{F}(\underline{V}, \underline{\psi}, \underline{x}; t) Q(\underline{V}, \underline{\psi}) d\underline{V} d\underline{\psi} = \langle \rho Q \rangle = \langle \rho \rangle \tilde{Q}, \quad (3.62)$$

and

$$\iint \mathcal{F}(\underline{V}, \underline{\psi}, \underline{x}; t) \langle R | \underline{V}, \underline{\psi} \rangle d\underline{V} d\underline{\psi} = \langle \rho R \rangle = \langle \rho \rangle \tilde{R}. \quad (3.63)$$

In these equations, the means are functions of \underline{x} and t and $\langle R | \underline{V}, \underline{\psi} \rangle$ is written for

$$\langle R(\underline{x}, t) | \underline{U}(\underline{x}, t) = \underline{V}, \underline{\phi}(\underline{x}, t) = \underline{\psi} \rangle.$$

3.4. Discrete Representation

In Section 2.6 the ensemble-averaged pdf $f_{\phi N}$ was defined by (Eq. 2.81)

$$f_{\phi N}(\psi) \equiv \frac{1}{N} \sum_{n=1}^N \delta(\psi - \phi^{(n)}), \quad (3.64)$$

where $\phi^{(n)}$ is the n th measured value of $\phi(\underline{x}_0, t_0)$. The pdf $f_\phi(\psi)$ and the ensemble-averaged pdf $f_{\phi N}(\psi)$ are related in two ways. First, for any N ($N \geq 1$), f_ϕ is the expected value of $f_{\phi N}$ (Eq. 2.83):

$$\langle f_{\phi N}(\psi) \rangle = f_\phi(\psi). \quad (3.65)$$

Second, for large N , the ensemble average of any function $Q(\phi)$,

$$\langle Q(\phi) \rangle_N \equiv \int Q(\psi) f_{\phi N}(\psi) d\psi, \quad (3.66)$$

approximates the mean $\langle Q(\phi) \rangle$. The statistical error in this approximation is of order $N^{-1/2}$.

In this section the discrete representation of pdf's as ensembles of delta functions is extended and generalized. This discrete representation is central to the whole approach. First, for homogeneous constant-density flows, a discrete representation for the joint pdf $f(\underline{V}, \underline{\psi})$ is obtained: then, for the general case, a discrete representation for the mass density function $\mathcal{F}(\underline{V}, \underline{\psi}, \underline{x})$ is given.

The discrete pdf $f_{\phi N}(\psi)$ (Eq. 3.64) is defined in terms of N sample values $\phi^{(n)}$, $n = 1, 2, \dots, N$. In order to represent the joint pdf $f(\underline{V}, \underline{\psi})$, N samples are needed of the $(3 + \sigma)$ -dimensional random vector $(\underline{U}, \underline{\phi})$. Then the discrete pdf $f_N(\underline{V}, \underline{\psi})$ is

$$f_N(\underline{V}, \underline{\psi}) \equiv \frac{1}{N} \sum_{n=1}^N \delta(\underline{V} - \underline{U}^{(n)}) \delta(\underline{\psi} - \underline{\phi}^{(n)}). \quad (3.67)$$

This is an ensemble of N $(3 + \sigma)$ -dimensional delta functions in velocity-composition space.

While it is natural to think of $(\underline{U}^{(n)}, \underline{\phi}^{(n)})$ as simultaneously-measured values of the velocity and composition, the discrete representation (Eq. 3.67) is valid for any random variables $(\underline{U}^{(n)}, \underline{\phi}^{(n)})$ with pdf $f(\underline{V}, \underline{\psi})$. For then, the expectation of Eq. (3.67) is

$$\langle f_N(\underline{V}, \underline{\psi}) \rangle = f(\underline{V}, \underline{\psi}). \quad (3.68)$$

The ensemble-average $\langle Q(\underline{U}, \underline{\phi}) \rangle_N$ of any function $Q(\underline{U}, \underline{\phi})$ can be obtained consistently from the discrete representation by

$$\begin{aligned} \langle Q(\underline{U}, \underline{\phi}) \rangle_N &= \int \int Q(\underline{V}, \underline{\psi}) f_N(\underline{V}, \underline{\psi}) d\underline{V} d\underline{\psi} \\ &= \frac{1}{N} \sum_{n=1}^N Q(\underline{U}^{(n)}, \underline{\phi}^{(n)}). \end{aligned} \quad (3.69)$$

The ensemble average $\langle Q \rangle_N$ approximates the mean $\langle Q \rangle$ with a statistical error ε_{QN} :

$$\langle Q \rangle_N = \langle Q \rangle + \varepsilon_{QN}. \quad (3.70)$$

The expected error $E(\varepsilon_{QN})$ is zero, and the standard deviation ε'_{QN} is

$$\varepsilon'_{QN} = \sqrt{\mathbf{D}(\varepsilon_{QN})} = N^{-1/2} \sqrt{\mathbf{D}(Q)}. \quad (3.71)$$

This formula (Eq. 3.71) for the standard error reveals the strength and weakness of the discrete representation. The weakness is that the statistical error decreases slowly with increasing N : if 100 samples ($N = 100$)

produce 10% accuracy, then 10,000 samples are needed for 1% accuracy and 1,000,000 samples are needed for 0.1% accuracy. The over-riding strength of the representation is its ability to handle pdf's of large dimensionality. The discrete pdf is defined by N $(3 + \sigma)$ -vectors, that is, by $(3 + \sigma)N$ numbers. Thus for given N , the number of numbers required to represent the pdf rises only linearly with the dimensionality of the sample space. And Eq. (3.71) shows that the statistical error is independent of the dimensionality of the sample space. Thus, if a three-dimensional pdf can be adequately represented by 1,000 samples (3,000 numbers) then a ten-dimensional pdf can be represented to the same accuracy by just 10,000 numbers.

The ability to treat the problems of large dimensionality and the slow convergence ($\varepsilon'_{QN} \propto N^{-1/2}$) are characteristics of all Monte Carlo methods.³⁷

Each of the N vectors $(\underline{U}^{(n)}, \underline{\phi}^{(n)})$ defines a sample point in velocity-composition space. These points can be thought of as the locations $(\underline{V}, \underline{\psi}) = (\underline{U}^{(n)}, \underline{\phi}^{(n)})$ of N notational particles in \underline{V} - $\underline{\psi}$ space. The normalized particle number density (in \underline{V} - $\underline{\psi}$ space) is

$$\frac{1}{N} \sum_{n=1}^N \delta(\underline{V} - \underline{U}^{(n)}) \delta(\underline{\psi} - \underline{\phi}^{(n)}) = f_N(\underline{V}, \underline{\psi}), \quad (3.72)$$

and Eq. (3.68) shows that the pdf $f(\underline{V}, \underline{\psi})$ is the expectation of this normalized particle number density.

This discrete representation of $f(\underline{V}, \underline{\psi})$ (Eq. 3.67) is used to study homogeneous flows. But for the general variable-density inhomogeneous case, a discrete representation of the mass density function $\mathcal{F}(\underline{V}, \underline{\psi}, \underline{x})$ is required.

Consider the turbulent flow within a volume \mathbb{V} of physical space (\underline{x} -space). The expected mass of fluid within this volume is M ,

$$M = \int \langle \rho(\underline{x}) \rangle d\underline{x}, \quad (3.73)$$

where $\int d\underline{x}$ is written for the integral over \mathbb{V} ,

$$\int (\dots) d\underline{x} \equiv \int \int \int_{\mathbb{V}} (\dots) d\underline{x}_1 d\underline{x}_2 d\underline{x}_3. \quad (3.74)$$

Within the volume \mathbb{V} , the mass density function $\mathcal{F}(\underline{V}, \underline{\psi}, \underline{x})$ is represented by N notional particles, each representing a mass Δm ,

$$\Delta m \equiv M/N. \quad (3.75)$$

The n th particle has velocity $\underline{U}^{(n)}$, composition $\underline{\phi}^{(n)}$ and position $\underline{x}^{(n)}$. The $(6 + \sigma)$ -dimensional vector $(\underline{U}^{(n)}, \underline{\phi}^{(n)}, \underline{x}^{(n)})$ defines the state of the particle and is called the state vector. This state corresponds to the point $(\underline{V}, \underline{\psi}, \underline{x}) = (\underline{U}^{(n)}, \underline{\phi}^{(n)}, \underline{x}^{(n)})$ in the $(6 + \sigma)$ -dimensional state space— $(\underline{V}$ - $\underline{\psi}$ - \underline{x}) space. The discrete mass density function $\mathcal{F}_N(\underline{V}, \underline{\psi}, \underline{x})$ is defined by

$$\mathcal{F}_N(\underline{V}, \underline{\psi}, \underline{x}) \equiv \Delta m \sum_{n=1}^N \delta(\underline{V} - \underline{U}^{(n)}) \delta(\underline{\psi} - \underline{\phi}^{(n)}) \delta(\underline{x} - \underline{x}^{(n)}). \quad (3.76)$$

The numbering of the particles is arbitrary. In other words the random vectors $(\underline{U}^{(n)}, \underline{\phi}^{(n)}, \underline{x}^{(n)})$, $n = 1, 2, \dots, N$, are identically distributed. Con-

sequently, the expectation of Eq. (3.76) can be written

$$\langle \mathcal{F}_N(\underline{V}, \underline{\psi}, \underline{x}) \rangle = \Delta m \sum_{n=1}^N \langle \delta(\underline{V} - \underline{U}^{(n)}) \delta(\underline{\psi} - \underline{\phi}^{(n)}) \times \delta(\underline{x} - \underline{x}^{(n)}) \rangle, \quad (3.77)$$

or, alternatively,

$$\langle \mathcal{F}_N(\underline{V}, \underline{\psi}, \underline{x}) \rangle = M \langle \delta(\underline{V} - \underline{U}^{(n)}) \delta(\underline{\psi} - \underline{\phi}^{(n)}) \delta(\underline{x} - \underline{x}^{(n)}) \rangle, \quad (3.78)$$

for any n ($1 \leq n \leq N$).

The discrete mass density function \mathcal{F}_N has been defined (Eq. 3.76) in terms of the state vectors of the N notional particles, but the properties of these random vectors have yet to be defined. Their properties are now deduced from the requirement that the expectation of \mathcal{F}_N is the mass density function \mathcal{F} :

$$\langle \mathcal{F}_N(\underline{V}, \underline{\psi}, \underline{x}) \rangle = \mathcal{F}(\underline{V}, \underline{\psi}, \underline{x}). \quad (3.79)$$

Let $h(\underline{x})$ be the pdf of particle positions—that is, $h(\underline{x})$ is the probability density of $\underline{x}^{(n)} = \underline{x}$. Then integrating Eq. (3.78) over velocity–composition space yields

$$\begin{aligned} \iint \langle \mathcal{F}_N \rangle d\underline{V} d\underline{\psi} &= M \langle \delta(\underline{x} - \underline{x}^{(n)}) \rangle \\ &= M h(\underline{x}), \end{aligned} \quad (3.80)$$

and integrating Eq. (3.79) yields

$$\iint \langle \mathcal{F}_N \rangle d\underline{V} d\underline{\psi} = \langle \rho(\underline{x}) \rangle. \quad (3.81)$$

A comparison of these results shows that the particle position pdf is

$$h(\underline{x}) = \langle \rho(\underline{x}) \rangle / M. \quad (3.82)$$

Thus the number density of notional particles in physical space is proportional to the mean fluid density. (It may be noted that the integral over \mathbb{V} of each side of Eq. (3.82) is unity.)

Let $f^*(\underline{V}, \underline{\psi} | \underline{x})$ denote the joint pdf of $\underline{U}^{(n)}$ and $\underline{\phi}^{(n)}$ conditional upon $\underline{x}^{(n)} = \underline{x}$. This is the joint pdf of $\underline{U}^{(n)}$ and $\underline{\phi}^{(n)}$ for a notional particle located at \underline{x} . In terms of delta functions, this conditional pdf is

$$\begin{aligned} f^*(\underline{V}, \underline{\psi} | \underline{x}) &= \langle \delta(\underline{V} - \underline{U}^{(n)}) \delta(\underline{\psi} - \underline{\phi}^{(n)}) \\ &\quad \times \delta(\underline{x} - \underline{x}^{(n)}) \rangle / \langle \delta(\underline{x} - \underline{x}^{(n)}) \rangle. \end{aligned} \quad (3.83)$$

The numerator is $\langle \mathcal{F}_N \rangle / M$ (Eq. 3.78) while the denominator is $\langle \rho \rangle / M$ (Eq. 3.82). Thus invoking Eqs. (3.79) and (3.59) we obtain

$$\begin{aligned} f^*(\underline{V}, \underline{\psi} | \underline{x}) &= \mathcal{F}(\underline{V}, \underline{\psi}, \underline{x}) / \langle \rho(\underline{x}) \rangle \\ &= \tilde{f}(\underline{V}, \underline{\psi}; \underline{x}). \end{aligned} \quad (3.84)$$

This equation shows that, in order to satisfy the requirement $\langle \mathcal{F}_N \rangle = \mathcal{F}$, the pdf of notional particle properties at a given location must be equal to the density-weighted pdf of the fluid properties.

To summarize the properties of the discrete representation for variable-density inhomogeneous flows: the mass density function $\mathcal{F}(\underline{V}, \underline{\psi}, \underline{x})$ is represented by N notional particles, each representing a mass Δm (Eq.

3.76). In physical space, the expected particle number density is proportional to the mean fluid density (Eq. 3.82). At a given location in physical space, the expected particle number density in velocity–composition space is proportional to the density-weighted joint pdf \tilde{f} (Eq. 3.84). In state space (\underline{V} – $\underline{\psi}$ – \underline{x} space) the expected particle number density is proportional to the mass density function \mathcal{F} (Eqs 3.78 and 3.79).

For constant-density homogeneous flows, the expected particle number density is uniform in physical space and the statistics of $\underline{U}^{(n)}$ and $\underline{\phi}^{(n)}$ are independent of $\underline{x}^{(n)}$. The volume average of the discrete representation of $\mathcal{F}(\underline{V}, \underline{\psi}, \underline{x})$ (Eq. 3.76) is then the same as the discrete representation of $f(\underline{V}, \underline{\psi})$ (Eq. 3.67), thus establishing the consistency of the two representations.

We have obtained a prescription for determining the discrete representation $\mathcal{F}_N(\underline{V}, \underline{\psi}, \underline{x})$ from the mass density function $\mathcal{F}(\underline{V}, \underline{\psi}, \underline{x})$. In the solution procedure described in Section 6, the discrete representation is used, and consequently we need to consider the inverse problem—to determine (or, rather, to approximate) expectations from $\mathcal{F}_N(\underline{V}, \underline{\psi}, \underline{x})$.

To this end, let the volume \mathbb{V} be divided into K cells, the k th being centered at $\underline{x}_{(k)}$ and having volume \mathbb{V}_k . These cells are sufficiently small that within each one statistical homogeneity can be assumed, and the total number of particles N is sufficiently large that the number of particles N_k in the k th cell is large.

The volume average of Eq. (3.82) over the k th cell is

$$\langle N_k \rangle / (N \mathbb{V}_k) = \langle \rho(\underline{x}_{(k)}) \rangle / M \quad (3.85)$$

where $\underline{x}_{(k)}$ is a location within the cell. Consequently, an approximation to the mean density is

$$\langle \rho(\underline{x}_{(k)}) \rangle \approx \Delta m N_k / \mathbb{V}_k. \quad (3.86)$$

This is simply the mass of particles in the cell divided by the cell volume. There are two approximations in Eq. (3.86): first $\langle N_k \rangle$ has been replaced by N_k , resulting in a statistical error of relative magnitude $N_k^{-1/2}$; second, because of the assumed homogeneity with the cell, $\underline{x}_{(k)}$ has been replaced by $\underline{x}_{(k)}$.

A similar approximation is obtained for the density-weighted mean of any function $Q(\underline{U}, \underline{\phi})$. Multiplying Eq. (3.79) by $Q(\underline{V}, \underline{\psi})$, integrating over \underline{V} – $\underline{\psi}$ space, and taking the volume average over cell k we obtain

$$\langle \rho(\underline{x}_{(k)}) Q(\underline{x}_{(k)}) \rangle = \frac{\Delta m}{\mathbb{V}_k} \left\langle \sum_{N_k} Q(\underline{U}^{(n)}, \underline{\phi}^{(n)}) \right\rangle, \quad (3.87)$$

where $\underline{x}_{(k)}$ is a location within the cell, and summation is over all the particles in the cell. Consequently an approximation to \tilde{Q} is

$$\langle \rho(\underline{x}_{(k)}) \rangle \tilde{Q}(\underline{x}_{(k)}) \approx \left\{ \frac{\Delta m N_k}{\mathbb{V}_k} \right\} \frac{1}{N_k} \sum_{N_k} Q(\underline{U}^{(n)}, \underline{\phi}^{(n)}), \quad (3.88)$$

or, recognizing that the term in braces is an approximation to $\langle \rho(\underline{x}_{(k)}) \rangle$ (Eq. 3.86),

$$\tilde{Q}(\underline{x}_{(k)}) \approx \frac{1}{N_k} \sum_{N_k} Q(\underline{U}^{(n)}, \underline{\phi}^{(n)}). \quad (3.89)$$

Thus, the ensemble average over the particles in the cell approximates the density-weighted mean.

3.5. Joint Pdf Transport Equation

A transport equation for the velocity-composition joint pdf can be derived from the transport equations for \underline{U} and $\underline{\phi}$, Eqs (3.3) and (3.20). These equations can be rewritten as

$$\frac{DU_j}{Dt} = A_j, \quad (3.90)$$

and

$$\frac{D\phi_\alpha}{Dt} = \Theta_\alpha, \quad (3.91)$$

where \underline{A} is the force per unit mass,

$$\rho A_j(\underline{x}, t) \equiv \frac{\partial \tau_{ij}}{\partial x_i} - \frac{\partial p}{\partial x_j} + \rho g_j, \quad (3.92)$$

and $\underline{\Theta}$ is the net source of $\underline{\phi}$,

$$\rho \Theta_\alpha(\underline{x}, t) \equiv -\frac{\partial J_\alpha^i}{\partial x_i} + \rho S_\alpha. \quad (3.93)$$

There are several different methods of deriving pdf transport equations. A useful method (originated by Lundgren¹⁹ and subsequently used by several researchers^{24,25,17,60}) starts from the expression for the pdf as the expectation of a delta function. Starting from the expression

$$f(\underline{V}, \underline{\psi}; \underline{x}, t) = \langle \delta(\underline{V} - \underline{U}(\underline{x}, t)) \delta(\underline{\psi} - \underline{\phi}(\underline{x}, t)) \rangle, \quad (3.94)$$

Pope⁷² used this method to derive the transport equation for f . A different method that does not involve delta functions is used here. The method is to equate two independent expressions for $\langle \rho DQ/Dt \rangle$, where $Q(\underline{U}, \underline{\phi})$ is (almost) any function. (The choice of Q is discussed in Section 3.5.1.) With the aid of the continuity equation, Eq. (3.2), we obtain

$$\begin{aligned} \left\langle \rho \frac{DQ}{Dt} \right\rangle &= \frac{\partial}{\partial t} \iint \rho(\underline{\psi}) Q(\underline{V}, \underline{\psi}) f d\underline{V} d\underline{\psi} \\ &+ \frac{\partial}{\partial x_j} \iint \rho(\underline{\psi}) V_j Q(\underline{V}, \underline{\psi}) f d\underline{V} d\underline{\psi} \\ &= \iint Q(\underline{V}, \underline{\psi}) \left\{ \rho(\underline{\psi}) \frac{\partial f}{\partial t} + \rho(\underline{\psi}) V_j \frac{\partial f}{\partial x_j} \right\} d\underline{V} d\underline{\psi}. \end{aligned} \quad (3.95)$$

This is the first expression for $\langle \rho DQ/Dt \rangle$.

A second expression is obtained by relating changes in Q to changes in \underline{U} and $\underline{\phi}$,

$$\frac{DQ(\underline{U}, \underline{\phi})}{Dt} = \frac{\partial Q}{\partial U_j} \frac{DU_j}{Dt} + \frac{\partial Q}{\partial \phi_\alpha} \frac{D\phi_\alpha}{Dt}. \quad (3.96)$$

Note that summation is implied over repeated suffices (j and α). The material derivatives can be replaced by A_j and Θ_α (Eqs 3.90 and 3.91) to yield

$$\left\langle \rho \frac{DQ}{Dt} \right\rangle = \left\langle \rho \frac{\partial Q}{\partial U_j} A_j \right\rangle + \left\langle \rho \frac{\partial Q}{\partial \phi_\alpha} \Theta_\alpha \right\rangle. \quad (3.97)$$

The first term on the right-hand side can be re-

expressed in terms of a conditional expectation,

$$\begin{aligned} \left\langle \rho \frac{\partial Q(\underline{U}, \underline{\phi})}{\partial U_j} A_j \right\rangle &= \iint \left\langle \rho \frac{\partial Q(\underline{U}, \underline{\phi})}{\partial U_j} A_j | \underline{V}, \underline{\psi} \right\rangle f d\underline{V} d\underline{\psi} \\ &= \iint \rho(\underline{\psi}) \frac{\partial Q(\underline{V}, \underline{\psi})}{\partial V_j} \langle A_j | \underline{V}, \underline{\psi} \rangle f d\underline{V} d\underline{\psi} \\ &\quad \times f d\underline{V} d\underline{\psi}. \end{aligned} \quad (3.98)$$

The second step follows since, for $\underline{U} = \underline{V}$ and $\underline{\phi} = \underline{\psi}$, $\rho \partial Q / \partial U_j$ is a known function of \underline{V} and $\underline{\psi}$. Integration by parts yields,

$$\begin{aligned} \left\langle \rho \frac{\partial Q}{\partial U_j} A_j \right\rangle &= I - \iint Q(\underline{V}, \underline{\psi}) \frac{\partial}{\partial V_j} \\ &\quad \times [\rho(\underline{\psi}) \langle A_j | \underline{V}, \underline{\psi} \rangle f] d\underline{V} d\underline{\psi}, \end{aligned} \quad (3.99)$$

where

$$I = \iint \frac{\partial}{\partial V_j} [\rho(\underline{\psi}) Q(\underline{V}, \underline{\psi}) \langle A_j | \underline{V}, \underline{\psi} \rangle f] d\underline{V} d\underline{\psi}. \quad (3.100)$$

In Section 3.5.1 it is shown that for the wide class of functions Q considered, the integral I is zero.

Following the same procedure for the final term in Eq. (3.97) we obtain

$$\begin{aligned} \left\langle \rho \frac{\partial Q}{\partial \phi_\alpha} \Theta_\alpha \right\rangle &= - \iint Q(\underline{V}, \underline{\psi}) \frac{\partial}{\partial \psi_\alpha} \\ &\quad \times [\rho(\underline{\psi}) \langle \Theta_\alpha | \underline{V}, \underline{\psi} \rangle f] d\underline{V} d\underline{\psi}, \end{aligned} \quad (3.101)$$

and combining Eqs (3.99) and (3.101) (with $I = 0$), the second expression for $\langle \rho DQ/Dt \rangle$ is obtained,

$$\begin{aligned} \left\langle \rho \frac{DQ}{Dt} \right\rangle &= - \iint Q(\underline{V}, \underline{\psi}) \left\{ \frac{\partial}{\partial V_j} [\rho(\underline{\psi}) \langle A_j | \underline{V}, \underline{\psi} \rangle f] \right. \\ &\quad \left. + \frac{\partial}{\partial \psi_\alpha} [\rho(\underline{\psi}) \langle \Theta_\alpha | \underline{V}, \underline{\psi} \rangle f] \right\} d\underline{V} d\underline{\psi}. \end{aligned} \quad (3.102)$$

By subtracting the second expression for $\langle \rho DQ/Dt \rangle$, Eq. (3.102), from the first expression, Eq. (3.95), we obtain,

$$\begin{aligned} \iint Q(\underline{V}, \underline{\psi}) \left\{ \rho(\underline{\psi}) \frac{\partial f}{\partial t} + \rho(\underline{\psi}) V_j \frac{\partial f}{\partial x_j} \right. \\ &\quad \left. + \frac{\partial}{\partial V_j} [\rho(\underline{\psi}) \langle A_j | \underline{V}, \underline{\psi} \rangle f] \right. \\ &\quad \left. + \frac{\partial}{\partial \psi_\alpha} [\rho(\underline{\psi}) \langle \Theta_\alpha | \underline{V}, \underline{\psi} \rangle f] \right\} d\underline{V} d\underline{\psi} = 0. \end{aligned} \quad (3.103)$$

The terms within the braces are independent of Q . Consequently, a sufficient condition for the satisfaction of Eq. (3.103) (for any Q) is that the terms within braces sum to zero: but since Q can be chosen arbitrarily from a wide class of functions, this is also a necessary condition.

Hence we obtain the transport equation for the velocity-scalar joint pdf $f(\underline{V}, \underline{\psi}; \underline{x}, t)$:

$$\begin{aligned} \rho(\underline{\psi}) \frac{\partial f}{\partial t} + \rho(\underline{\psi}) V_j \frac{\partial f}{\partial x_j} &= - \frac{\partial}{\partial V_j} [\rho(\underline{\psi}) \langle A_j | \underline{V}, \underline{\psi} \rangle f] \\ &\quad - \frac{\partial}{\partial \psi_\alpha} [\rho(\underline{\psi}) \langle \Theta_\alpha | \underline{V}, \underline{\psi} \rangle f]. \end{aligned} \quad (3.104)$$

Equivalently, the transport equation for the mass density function ($\mathcal{F} = \rho f$) is

$$\begin{aligned} \frac{\partial \mathcal{F}}{\partial t} + \frac{\partial}{\partial x_j} [V_j \mathcal{F}] + \frac{\partial}{\partial V_j} [\langle A_j | \underline{V}, \underline{\psi} \rangle \mathcal{F}] \\ + \frac{\partial}{\partial \underline{\psi}_a} [\langle \Theta_a | \underline{V}, \underline{\psi} \rangle \mathcal{F}] = 0. \end{aligned} \quad (3.105)$$

It may be seen that the change of \mathcal{F} with time is caused by transport in \underline{x} -space (due to the velocity), transport in \underline{V} -space (due to A), and transport in $\underline{\psi}$ -space (due to Θ). A complete discussion of this fundamental equation is provided in the next section.

Expressions for the conditional expectations of A and Θ are obtained from their defining equations. From Eq. (3.93) we obtain

$$\begin{aligned} \rho(\underline{\psi}) \langle \Theta_a | \underline{V}, \underline{\psi} \rangle &= \left\langle -\frac{\partial J_i^a}{\partial x_i} + \rho S_a | \underline{V}, \underline{\psi} \right\rangle \\ &= -\left\langle \frac{\partial J_i^a}{\partial x_i} | \underline{V}, \underline{\psi} \right\rangle + \rho(\underline{\psi}) S_a(\underline{\psi}). \end{aligned} \quad (3.106)$$

By decomposing the pressure p into its mean $\langle p \rangle$ and fluctuation p'

$$p' \equiv p - \langle p \rangle, \quad (3.107)$$

from Eq. (3.92) we obtain

$$\begin{aligned} \rho(\underline{\psi}) \langle A_j | \underline{V}, \underline{\psi} \rangle &= \left\langle \frac{\partial \tau_{ij}}{\partial x_i} - \frac{\partial \langle p \rangle}{\partial x_j} - \frac{\partial p'}{\partial x_j} + \rho g_j | \underline{V}, \underline{\psi} \right\rangle \\ &= \left\langle \frac{\partial \tau_{ij}}{\partial x_i} | \underline{V}, \underline{\psi} \right\rangle - \frac{\partial \langle p \rangle}{\partial x_j} - \left\langle \frac{\partial p'}{\partial x_j} | \underline{V}, \underline{\psi} \right\rangle \\ &\quad + \rho(\underline{\psi}) g_j. \end{aligned} \quad (3.108)$$

With these expressions for the conditional expectations, the joint pdf transport equation, Eq. (3.104) can be written as,

$$\begin{aligned} \rho(\underline{\psi}) \frac{\partial f}{\partial t} + \rho(\underline{\psi}) V_j \frac{\partial f}{\partial x_j} + \left(\rho(\underline{\psi}) g_j \right. \\ \left. - \frac{\partial \langle p \rangle}{\partial x_j} \right) \frac{\partial f}{\partial V_j} + \frac{\partial}{\partial \underline{\psi}_a} [\rho(\underline{\psi}) S_a(\underline{\psi}) f] \\ = \frac{\partial}{\partial V_j} \left[\left\langle -\frac{\partial \tau_{ij}}{\partial x_i} + \frac{\partial p'}{\partial x_j} \right| \underline{V}, \underline{\psi} \right\rangle f \\ + \frac{\partial}{\partial \underline{\psi}_a} \left[\left\langle \frac{\partial J_i^a}{\partial x_i} \right| \underline{V}, \underline{\psi} \right\rangle f \right]. \end{aligned} \quad (3.109)$$

If the conditional expectations appearing on the right-hand side were known, this equation could be solved for f (ρ and S are known functions in $\underline{\psi}$ -space and $\langle p \rangle$ can be determined from f , see Section 4.7). Thus, the processes represented by the terms on the left-hand side are accounted for exactly, without any approximation. These processes are: transport in physical space; transport in velocity space by gravity and by the mean pressure gradient; and, transport in composition space by reaction. It is remarkable that in a variable-density flow with arbitrarily complicated reactions, all these processes can be treated without approximation.

The terms on the right-hand side of Eq. (3.109) represent transport in velocity space by the viscous stresses and by the fluctuating pressure gradient, and transport in composition space by the molecular fluxes. Before the equation can be solved for f , the conditional expectations appearing in these terms must be determined or approximated. In Section 5 models are presented that approximate the conditional expectations as functions of the joint pdf and of a specified turbulent time scale $\tau(\underline{x}, t)$.

3.5.1. Evaluation of the integral I

It is shown that the integral

$$I \equiv \int \int \frac{\partial}{\partial V_j} [\rho(\underline{\psi}) Q(\underline{V}, \underline{\psi}) \langle A_j | \underline{V}, \underline{\psi} \rangle f] d\underline{V} d\underline{\psi}, \quad (3.110)$$

is zero for a wide class of functions Q . It is simply shown that I is zero if Q has bounded support. In addition, with very reasonable physical assumptions, it is shown that I is zero if Q is monotonic as $|\underline{V}|$ tends to infinity and the expectation $\langle \rho A_j Q \rangle$ exists.

Let $S(v)$ denote the surface of the sphere in \underline{V} -space, centered at the origin, and with radius v ,

$$v^2 = \underline{V} \cdot \underline{V}, \quad (3.111)$$

and let $g(v)$ be the probability density of $[\underline{U} \cdot \underline{U}]^{1/2} = v$. By first integrating over composition space, the integral I becomes

$$I = \int \frac{\partial}{\partial V_j} [\langle \rho A_j Q | \underline{V} \rangle f_u(\underline{V})] d\underline{V}. \quad (3.112)$$

This is the integral of a divergence in \underline{V} -space, and hence using the divergence theorem, it can be rewritten as the surface integral,

$$I = \lim_{v \rightarrow \infty} \int_{S(v)} \langle \rho A_j Q | \underline{V} \rangle n_j f_u(\underline{V}) dS(v) \quad (3.113)$$

$$= \lim_{v \rightarrow \infty} \langle \rho A_j n_j Q | v \rangle g(v), \quad (3.114)$$

where \underline{n} is the outward-pointing normal vector.

It is obvious from Eq. (3.114) that if Q has bounded support then I is zero.

We now consider less stringent conditions on Q . The mean $\langle \rho A_j Q \rangle$ can be expressed as

$$\langle \rho A_j Q \rangle = \int \langle \rho A_j Q | \underline{V} \rangle f_u(\underline{V}) d\underline{V}, \quad (3.115)$$

and its existence implies the absolute convergence of this integral. That is, it implies the convergence of the integral,

$$\begin{aligned} &\int | \langle \rho A_j Q | \underline{V} \rangle | f_u(\underline{V}) d\underline{V} \\ &= \int_0^\infty \left\{ \int_{S(v)} | \langle \rho A_j Q | \underline{V} \rangle | f_u(\underline{V}) dS(v) \right\} dv. \end{aligned} \quad (3.116)$$

Now if Q is monotonic as $v \rightarrow \infty$, since ρ and A_j are physical quantities it is reasonable to assume that $|\langle \rho A_j Q | v \rangle|$ is also monotonic. Then, the convergence of the integral (3.116) implies

$$\lim_{v \rightarrow \infty} \langle \rho A_j Q | v \rangle | g(v) = 0. \quad (3.117)$$

Now from Eq. (3.114),

$$\begin{aligned} |I| &= \lim_{v \rightarrow \infty} \langle \rho A_j n_j Q | v \rangle | g(v) \\ &\leq \lim_{v \rightarrow \infty} \sum_{j=1}^3 \langle \rho A_j Q | v \rangle | g(v) = 0. \end{aligned} \quad (3.118)$$

Thus the monotonicity of Q at infinity and the existence of $\langle \rho A_j Q \rangle$ are sufficient to ensure that I is zero.

4. LAGRANGIAN DESCRIPTION

The velocity–composition pdf equation derived in the previous section is clearly useful, since the major processes (convection and reaction) can be treated without approximation. Before calculations can be made using the equation, the conditional expectations must be modelled, and a method of solving the equation must be devised. With simple models and for extremely simple flows, analytic solutions can be obtained. But, in general, a numerical technique is required. A standard technique—such as finite-differences—is bound to be impracticable,³² because $f(\underline{V}, \underline{\psi}; \underline{x}, t)$ is a function of $(6 + \sigma)$ variables and time.

The modelling and the numerical solution procedure are strongly interconnected. The purpose of this section is to show this interconnection by considering both topics in general terms. In the following two sections, modelling (Section 5) and the solution procedure (Section 6) are examined more specifically.

In Section 4.1 the observation is made that many different systems evolve with the same pdf. In Sections 4.5 and 4.6 deterministic and stochastic systems evolving with the same pdf are described. These systems are used to interpret the pdf equation and to model it, respectively. All the systems considered consist of particles. Hence a Lagrangian viewpoint—developed in Sections 4.2–4—is adopted. This Lagrangian formulation provides a close link between the pdf equation and the physical processes of turbulent reactive flows.

There are subtle questions concerning the mean pressure field, the mean continuity equation, and the normalization of the mass density function. These questions are addressed in Section 4.7.

This section may be the most difficult to comprehend: several different pdf's are introduced, and (as usual with Lagrangian formulations) the notation is involved. So that the important conclusions are not obscured by these difficulties, a summary is provided in Section 4.8. The reader may find it useful to refer to this summary after reading each sub-section.

4.1. Equivalent Systems

In Section 3, the joint pdf transport equation was derived from the conservation equations,

$$\frac{\partial \rho}{\partial t} + \frac{\partial}{\partial x_i} (\rho U_i) = 0, \quad (4.1)$$

$$\left(\frac{\partial}{\partial t} + U_i \frac{\partial}{\partial x_i} \right) U_j = A_j(\underline{x}, t), \quad (4.2)$$

and

$$\left(\frac{\partial}{\partial t} + U_i \frac{\partial}{\partial x_i} \right) \phi_a = \Theta_a(\underline{x}, t), \quad (4.3)$$

where \underline{A} and $\underline{\Theta}$ are given by Eqs (3.92) and (3.93). In a turbulent flow, these rates of change (\underline{A} and $\underline{\Theta}$) are random variables. Their conditional expectations are, of course, not random variables, but are (unknown) functions that are determined by the initial and boundary conditions. Thus, for a given turbulent flow, denoting these conditional expectations by \underline{a} and $\underline{\theta}$, we have

$$\langle A_j(\underline{x}, t) | \underline{V}, \underline{\psi} \rangle = a_j(\underline{V}, \underline{\psi}, \underline{x}, t), \quad (4.4)$$

and

$$\langle \Theta_a(\underline{x}, t) | \underline{V}, \underline{\psi} \rangle = \theta_a(\underline{V}, \underline{\psi}, \underline{x}, t). \quad (4.5)$$

In order to stress that \underline{a} and $\underline{\theta}$ are not random variables, we note that

$$\langle a_j(\underline{V}, \underline{\psi}, \underline{x}, t) \rangle = a_j(\underline{V}, \underline{\psi}, \underline{x}, t), \quad (4.6)$$

and that

$$\langle \theta_a(\underline{V}, \underline{\psi}, \underline{x}, t) | \underline{V} = \underline{V}', \underline{\psi} = \underline{\psi}' \rangle = \theta_a(\underline{V}', \underline{\psi}', \underline{x}, t). \quad (4.7)$$

The transport equations for the joint pdf f (Eq. 3.104) and for the mass density function \mathcal{F} (Eq. 3.105) were derived from the conservation equations Eqs (4.1–4.3). In terms of $\underline{a}(\underline{V}, \underline{\psi}, \underline{x}, t)$ and $\underline{\theta}(\underline{V}, \underline{\psi}, \underline{x}, t)$, the transport equation for $\mathcal{F}(\underline{V}, \underline{\psi}, \underline{x}; t)$ is,

$$\frac{\partial \mathcal{F}}{\partial t} = - \frac{\partial}{\partial x_i} [\mathcal{F} V_i] - \frac{\partial}{\partial V_i} [\mathcal{F} a_i] - \frac{\partial}{\partial \psi_a} [\mathcal{F} \theta_a]. \quad (4.8)$$

This is a deterministic equation. Although \mathcal{F} is the mass density function of random variables, and a_i and θ_a are conditional expectations of random variables, nevertheless, for a given flow, $\mathcal{F}(\underline{V}, \underline{\psi}, \underline{x}; t)$, $a_i(\underline{V}, \underline{\psi}, \underline{x}, t)$ and $\theta_a(\underline{V}, \underline{\psi}, \underline{x}, t)$ are functions determined by the initial and boundary conditions. This equation (Eq. 4.8) shows how these deterministic functions are related.

A second important observation is that the dynamics of the velocity and composition fields enter the conservation equations (Eqs 4.1–4.3) through the random variables $\underline{A}(\underline{x}, t)$ and $\underline{\Theta}(\underline{x}, t)$. But, in the equation for \mathcal{F} (Eq. 4.8), the dynamics enter only through the conditional expectations \underline{a} and $\underline{\theta}$. This is significant because many different random variables can have the same expectations, and consequently, the same mass-density-function equation can describe the evolution of many different stochastic systems. Two systems that evolve with the same pdf or mass density function are said to be *stochastically equivalent*.

Stochastically equivalent systems are used in two ways: to interpret the equation for the mass density function, and to provide a method for its solution. In both cases, a Lagrangian view is adopted.

4.2. Lagrangian Equations

In presenting transport equations, we have adopted the Eulerian view—we have considered the fluid properties at a fixed location \underline{x} . The starting point for the alternative—Lagrangian—view is the concept of a *fluid particle*. Let $\underline{x}^+(\underline{x}_0, t)$ be the location (at time t) of the fluid particle that at time t_0 ($t_0 \leq t$) was located at $\underline{x} = \underline{x}_0$. The fluid particle has velocity $\underline{U}^+(\underline{x}_0, t)$ and composition $\underline{\phi}^+(\underline{x}_0, t)$: these are just the velocity and composition at $\underline{x}^+(\underline{x}_0, t)$,

$$\underline{U}^+(\underline{x}_0, t) = \underline{U}[\underline{x}^+(\underline{x}_0, t), t], \quad (4.9)$$

and

$$\underline{\phi}^+(\underline{x}_0, t) = \underline{\phi}[\underline{x}^+(\underline{x}_0, t), t]. \quad (4.10)$$

By definition, the fluid particle moves with the fluid velocity,

$$\frac{\partial \underline{x}^+(\underline{x}_0, t)}{\partial t} = \underline{U}^+(\underline{x}_0, t). \quad (4.11)$$

Differentiating Eq. (4.9) with respect to time we obtain

$$\begin{aligned} \frac{\partial U_j^+(\underline{x}_0, t)}{\partial t} &= \left(\frac{\partial U_j}{\partial t} + \frac{\partial x_i^+}{\partial t} \frac{\partial U_j}{\partial x_i} \right)_{\underline{x} = \underline{x}^+} \\ &= \left(\frac{DU_j}{Dt} \right)_{\underline{x} = \underline{x}^+}, \end{aligned} \quad (4.12)$$

since $\partial x_i^+/\partial t$ is just the velocity U_i . This confirms the interpretation of the material derivative D/Dt as the rate of change following the fluid. Thus, (from Eqs 4.2–4.3) the Lagrangian equations for \underline{U}^+ and $\underline{\phi}^+$ are

$$\frac{\partial}{\partial t} U_j^+(\underline{x}_0, t) = A_j[\underline{x}^+(\underline{x}_0, t), t], \quad (4.13)$$

and

$$\frac{\partial}{\partial t} \phi_a^+(\underline{x}_0, t) = \Theta_a[\underline{x}^+(\underline{x}_0, t), t], \quad (4.14)$$

where \underline{A} and $\underline{\Theta}$ are given by Eqs (3.92–3.93).

Consider an infinitesimal material element of fluid that at time t_0 occupies the volume $dV(t_0) = d\underline{V}_0$ at \underline{x}_0 . The mass of this element is

$$dm = \rho(\underline{x}_0, t_0) dV(t_0). \quad (4.15)$$

At a later time $t > t_0$, the material element occupies the volume $dV(t)$ at $\underline{x}^+(\underline{x}_0, t)$, and its mass (which, by definition of a material element, is unchanged) is,

$$dm = \rho[\underline{x}^+(\underline{x}_0, t), t] dV(t). \quad (4.16)$$

The volume $dV(t)$ is related to $dV(t_0)$ by the Jacobian

$$\begin{aligned} dV(t) &= \frac{\partial(x_1^+, x_2^+, x_3^+)}{\partial(x_{01}, x_{02}, x_{03})} dV(t_0) \\ &= \frac{\partial(\underline{x}^+)}{\partial(\underline{x}_0)} dV(t_0). \end{aligned} \quad (4.17)$$

From these three equations we obtain the Lagrangian form of the continuity equation

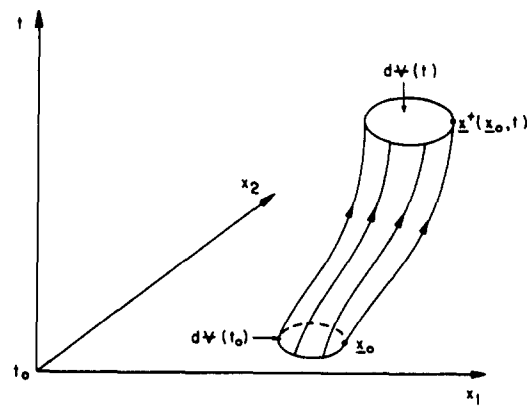


FIG. 4.1. Fluid particle paths and material element volume change in x_1-x_2-t space.

$$\rho(\underline{x}^+, t) \frac{\partial(\underline{x}^+)}{\partial(\underline{x}_0)} = \rho(\underline{x}_0, t_0). \quad (4.18)$$

Figure 4.1 is a sketch of fluid particle paths (or pathlines) in $\underline{x}-t$ space for a two-dimensional flow. The fluid particle which is initially at \underline{x}_0 follows the fluid particle path to reach $\underline{x}^+(\underline{x}_0, t)$ at time t . The fluid particles which initially occupy the (two-dimensional) volume $dV(t_0)$, at time t occupy the larger volume $dV(t)$. This volume expansion is due to a decrease in density, Eq. (4.18).

The state of a given fluid particle (i.e. given \underline{x}_0) is defined by its position \underline{x}^+ , its velocity \underline{U}^+ and its composition $\underline{\phi}^+$. At any time t , the state of the particle can be represented by a point $(\underline{V}, \underline{\psi}, \underline{x}) = (\underline{U}^+, \underline{\phi}^+, \underline{x}^+)$ in the $(6+\sigma)$ -dimensional state space or $\underline{V}-\underline{\psi}-\underline{x}$ space; and $(\underline{U}^+, \underline{\phi}^+, \underline{x}^+)$ is the *state vector*.

As time progresses, the state of the particle changes and the point defined by the state vector moves in state space. The Lagrangian equations show that the state vector evolves by,

$$\frac{\partial}{\partial t} \begin{bmatrix} \underline{U}^+ \\ \underline{\phi}^+ \\ \underline{x}^+ \end{bmatrix} = \begin{bmatrix} \underline{A} \\ \underline{\Theta} \\ \underline{U}^+ \end{bmatrix}. \quad (4.19)$$

Thus the vector $(\underline{A}, \underline{\Theta}, \underline{U}^+)$ represents the rate of change of state, or the velocity in state space. The evolution of the state of the particle can be represented by a path in the *augmented state space* or $\underline{V}-\underline{\psi}-\underline{x}-t$ space. For given \underline{x}_0 , the particle path is

$$\begin{bmatrix} \underline{V} \\ \underline{\psi} \\ \underline{x} \end{bmatrix} = \begin{bmatrix} \underline{U}^+(t) \\ \underline{\phi}^+(t) \\ \underline{x}^+(t) \end{bmatrix}. \quad (4.20)$$

If at $(\underline{x}, t) = (\underline{x}_0, t_0)$ the flow is turbulent, then the initial state

$$\begin{bmatrix} \underline{V} \\ \underline{\psi} \\ \underline{x} \end{bmatrix} = \begin{bmatrix} \underline{U}^+(t_0) \\ \underline{\phi}^+(t_0) \\ \underline{x}^+(t_0) \end{bmatrix} = \begin{bmatrix} \underline{U}(\underline{x}_0, t_0) \\ \underline{\phi}(\underline{x}_0, t_0) \\ \underline{x}_0 \end{bmatrix}, \quad (4.21)$$

is a random vector. The rates of change \underline{A} and $\underline{\Theta}$ are also random vectors. Consequently, different realizations of

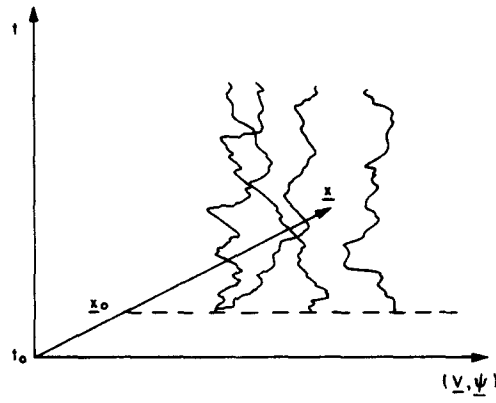


FIG. 4.2. Fluid particle paths in the augmented state space.

the same turbulent flow generate different particle paths in the augmented state space.

Figure 4.2 is a sketch of particle paths for different realizations of the same turbulent flow. This sketch can only be suggestive of the true paths, since the $(7+\sigma)$ -dimensional augmented state space is represented as a three-dimensional space. The following observations can be made:

- (i) in different realizations, the initial value of $\underline{x} = \underline{x}_0$ is the same, but the initial values of \underline{U}^+ and $\underline{\phi}^+$ are likely to be different;
- (ii) the particle paths can cross, since the state vector $(\underline{U}^+, \underline{\phi}^+, \underline{x}^+)$ does not uniquely determine the rate of change vector $(\underline{A}, \underline{\Theta}, \underline{U}^+)$; and
- (iii) the state vector changes in time and physical space on all scales, down to the smallest (Kolmogorov) scales.

4.3. Lagrangian Pdf

The Lagrangian conditional joint pdf considered— $f_L(\underline{V}, \underline{\psi}, \underline{x}; t | \underline{V}_0, \underline{\psi}_0, \underline{x}_0)$ —is the joint pdf of the fluid particle properties at time t , conditional upon the particle properties at the earlier time t_0 . More precisely, f_L is the joint probability density of the event

$$S_t \equiv \{\underline{U}^+(\underline{x}_0, t) = \underline{V}, \underline{\phi}^+(\underline{x}_0, t) = \underline{\psi}, \underline{x}^+(\underline{x}_0, t) = \underline{x}\}, \quad (4.22)$$

conditional upon the event

$$S_0 \equiv \{\underline{U}^+(\underline{x}_0, t_0) = \underline{U}(\underline{x}_0, t_0) = \underline{V}_0, \underline{\phi}^+(\underline{x}_0, t_0) = \underline{\phi}(\underline{x}_0, t_0) = \underline{\psi}_0\}. \quad (4.23)$$

This is a quantity of fundamental importance and usefulness since, as is shown below, it is the *transition density* for turbulent reactive flows. That is, the mass density function at time t can be determined from its value at t_0 by

$$\mathcal{F}(\underline{V}, \underline{\psi}, \underline{x}; t) = \int \int \int f_L(\underline{V}, \underline{\psi}, \underline{x}; t | \underline{V}_0, \underline{\psi}_0, \underline{x}_0) \times \mathcal{F}(\underline{V}_0, \underline{\psi}_0, \underline{x}_0; t_0) d\underline{V}_0 d\underline{\psi}_0 d\underline{x}_0. \quad (4.24)$$

The evolution equation for f_L is derived here using the delta-function method. First—mainly to simplify the notation—several *fine-grained* pdf's are introduced. These are just delta-function products that can be thought of as pdf's in a single realization of the flow.⁶⁰ The Eulerian fine-grained joint pdf is

$$f'(\underline{V}, \underline{\psi}; \underline{x}, t) \equiv \delta(\underline{U}(\underline{x}, t) - \underline{V}) \delta(\underline{\phi}(\underline{x}, t) - \underline{\psi}), \quad (4.25)$$

and its expectation is $f(\underline{V}, \underline{\psi}; \underline{x}, t)$ (cf. Eq. 3.46). The Lagrangian fine-grained joint pdf is

$$f'_p(\underline{V}, \underline{\psi}, \underline{x}; t | \underline{x}_0) \equiv \delta(\underline{U}^+(\underline{x}_0, t) - \underline{V}) \delta(\underline{\phi}^+(\underline{x}_0, t) - \underline{\psi}) \times \delta(\underline{x}^+(\underline{x}_0, t) - \underline{x}). \quad (4.26)$$

This pdf is conditional upon the initial particle location \underline{x}_0 , but not upon its initial properties. The conditional Lagrangian pdf f_L can be expressed as

$$f_L(\underline{V}, \underline{\psi}, \underline{x}; t | \underline{V}_0, \underline{\psi}_0, \underline{x}_0) = \langle f'_p(\underline{V}, \underline{\psi}, \underline{x}; t | \underline{x}_0) f'(\underline{V}_0, \underline{\psi}_0; \underline{x}_0, t_0) \rangle / f(\underline{V}_0, \underline{\psi}_0; \underline{x}_0, t_0), \quad (4.27)$$

(cf. Eq. 2.145).

The evolution equation for f_L is derived by differentiating Eq. (4.27) with respect to time. In order to do this we need to determine the derivatives of the delta functions. For the temporal derivative of $\delta(\underline{U}^+(\underline{x}_0, t) - \underline{V})$ we have

$$\begin{aligned} \frac{\partial \delta(\underline{U}^+ - \underline{V})}{\partial t} &= \frac{\partial U_i^+}{\partial t} \frac{\partial \delta(\underline{U}^+ - \underline{V})}{\partial U_i^+} \\ &= \frac{-\partial U_i^+}{\partial t} \frac{\partial \delta(\underline{U}^+ - \underline{V})}{\partial V_i} \\ &= -\frac{\partial}{\partial V_i} \left\{ \frac{\partial U_i^+}{\partial t} \delta(\underline{U}^+ - \underline{V}) \right\} \\ &= -\frac{\partial}{\partial V_i} \{ A_i(\underline{x}^+, t) \delta(\underline{U}^+ - \underline{V}) \}. \end{aligned} \quad (4.28)$$

The second step follows since an infinitesimal change in \underline{U}^+ of $d\underline{U}^+$ has the same effect on the delta function as a change in \underline{V} of $d\underline{V} = -d\underline{U}^+$; the third step follows because $\partial U_i^+ / \partial t$ is not a function of \underline{V} ; and the final result is obtained by using Eq. (4.13).

Differentiating Eq. (4.27) with respect to time (noting that only f'_p is a function of t) we obtain

$$\begin{aligned} \frac{\partial f_L}{\partial t} &= \left\langle -\frac{\partial}{\partial V_i} \{ A_i(\underline{x}^+, t) f'_p f' \} \right\rangle / f \\ &\quad + \left\langle -\frac{\partial}{\partial \psi_a} \{ \Theta_a(\underline{x}^+, t) f'_p f' \} \right\rangle / f \\ &\quad + \left\langle -\frac{\partial}{\partial x_i} \{ U_i^+(\underline{x}_0, t) f'_p f' \} \right\rangle / f, \end{aligned} \quad (4.29)$$

where f_L, f'_p, f' and f have the same arguments as in Eq. (4.27), and Eqs (4.11) and (4.14) have been used to eliminate $\partial \underline{x}^+ / \partial t$ and $\partial \underline{\phi}^+ / \partial t$. Now for the term in A_i we have (see Eq. 2.150)

$$\begin{aligned} \langle A_i(\underline{x}^+, t) f'_p f' \rangle / f &= \langle A_i(\underline{x}^+, t) | S_i, S_0 \rangle \langle f'_p f' \rangle / f \\ &= \langle A_i(\underline{x}, t) | S_i, S_0 \rangle f_L, \end{aligned} \quad (4.30)$$

where the conditions S_i and S_0 are defined by Eqs (4.22–23). In the final step, \underline{x}^+ can be replaced by \underline{x} since $\underline{x}^+ = \underline{x}$ is one of the conditions in S_i . By applying the same treatment to the other terms, we obtain the evolution equation for f_L :

$$\begin{aligned} \frac{\partial f_L}{\partial t} + \frac{\partial}{\partial \underline{x}_i} [f_L V_i] + \frac{\partial}{\partial V_i} [f_L \langle A_i | S_i, S_0 \rangle] \\ + \frac{\partial}{\partial \underline{\psi}_a} [f_L \langle \Theta_a | S_i, S_0 \rangle] = 0. \end{aligned} \quad (4.31)$$

The evolution equation for f_L has a similar form to that for \mathcal{F} , Eq. (4.8). There are two important differences: f_L is a pdf rather than a mass density function; and in Eq. (4.31) A and Θ are conditioned on S_0 as well as on S_i .

(It is interesting to note that the form of Eq. (4.31) does not change if additional fixed conditions are applied to (or removed from) f_L . [By definition a fixed condition is independent of t .] Let C denote a set of fixed conditions and let $f_c(\underline{V}, \underline{\psi}, \underline{x}; t | C, \underline{x}_0)$ be the corresponding Lagrangian conditional pdf. Then the evolution equation for f_c is the same as Eq. (4.31) with f_c replacing f_L and C replacing S_0 .)

4.4. Relationship between Lagrangian and Eulerian Pdf's

In this subsection f_L is shown to be the transition density (by establishing Eq. 4.24, and then further relationships between f_L and \mathcal{F} are demonstrated.

Consider the quantity

$$\mathcal{F}'(\underline{V}, \underline{\psi}, \underline{x}; t) \equiv \int \int \int \rho(\underline{\psi}_0) f'_p f' d\underline{V}_0 d\underline{\psi}_0 d\underline{x}_0, \quad (4.32)$$

where f'_p and f' have the same arguments as in Eq. (4.27). It is now shown that the expectation of \mathcal{F}' is equal to each side of Eq. (4.24), thus establishing the equation's validity.

Simply taking the expectation of Eq. (4.32) yields

$$\begin{aligned} \langle \mathcal{F}'(\underline{V}, \underline{\psi}, \underline{x}; t) \rangle &= \int \int \int \rho(\underline{\psi}_0) f_L(\underline{V}, \underline{\psi}, \underline{x}; t | \underline{V}_0, \underline{\psi}_0, \underline{x}_0) \\ &\quad \times f(\underline{V}_0, \underline{\psi}_0; \underline{x}_0, t_0) d\underline{V}_0 d\underline{\psi}_0 d\underline{x}_0 \\ &= \int \int \int f_L(\underline{V}, \underline{\psi}, \underline{x}; t | \underline{V}_0, \underline{\psi}_0, \underline{x}_0) \\ &\quad \times \mathcal{F}(\underline{V}_0, \underline{\psi}_0, \underline{x}_0; t_0) d\underline{V}_0 d\underline{\psi}_0 d\underline{x}_0, \end{aligned} \quad (4.33)$$

which is the same as the right-hand side of Eq. (4.24).

To establish that \mathcal{F}' is the fine-grained mass density function (as is implied by the notation) is less simple. In Eq. (4.32), the integral over the particle positions at time t_0 ($\int d\underline{x}_0$) can be replaced by the integral over their positions at time t

$$\int \frac{\hat{c}(\underline{x}_0)}{\hat{c}(\underline{x}_+)} d\underline{x}^+.$$

Now, the Jacobian is known from the Lagrangian continuity equation Eq. (4.18) in terms of the densities. Thus, Eq. (4.32) can be rewritten

$$\begin{aligned} \mathcal{F}'(\underline{V}, \underline{\psi}, \underline{x}; t) &= \int \int \int \rho(\underline{\psi}_0) \rho(\underline{\phi}^+) / \rho(\underline{\phi}[\underline{x}_0, t]) \\ &\quad \times \delta(\underline{U}^+ - \underline{V}) \delta(\underline{\phi}^+ - \underline{\psi}) \\ &\quad \times \delta(\underline{U}[\underline{x}_0, t_0] - \underline{V}_0) \\ &\quad \times \delta(\underline{\phi}[\underline{x}_0, t_0] - \underline{\psi}_0) \\ &\quad \times \delta(\underline{x}^+ - \underline{x}) d\underline{V}_0 d\underline{\psi}_0 d\underline{x}^+. \end{aligned} \quad (4.34)$$

The right-hand side of this equation can be determined by integrating over \underline{V}_0 , $\underline{\psi}_0$ and \underline{x}^+ in turn. Only $\delta(\underline{U}[\underline{x}_0, t] - \underline{V}_0)$ depends upon \underline{V}_0 and its integral over the whole of \underline{V}_0 -space is unity. Only $\rho(\underline{\psi}_0)$ and $\delta(\underline{\phi}[\underline{x}_0, t_0] - \underline{\psi}_0)$ depend upon $\underline{\psi}_0$, and in view of the sifting property of the delta function (Eq. 2.32) we have

$$\int \rho(\underline{\psi}_0) \{ \rho(\underline{\phi}[\underline{x}_0, t]) \}^{-1} \delta(\underline{\phi}[\underline{x}_0, t] - \underline{\psi}_0) d\underline{\psi}_0 = 1. \quad (4.35)$$

Thus, Eq. (4.34) reduces to

$$\begin{aligned} \mathcal{F}'(\underline{V}, \underline{\psi}, \underline{x}; t) &= \int \rho(\underline{\phi}^+) \delta(\underline{U}^+ - \underline{V}) \delta(\underline{\phi}^+ - \underline{\psi}) \\ &\quad \times \delta(\underline{x}^+ - \underline{x}) d\underline{x}^+. \end{aligned} \quad (4.36)$$

Again in view of the sifting property, the only contribution to this integral is from fluid particles located at $\underline{x}^+ = \underline{x}$. And at this location, the Lagrangian properties (e.g. $\underline{U}^+(\underline{x}_0, t)$) can be written as Eulerian variables (i.e. $\underline{U}(\underline{x}, t)$). We thus obtain

$$\mathcal{F}'(\underline{V}, \underline{\psi}, \underline{x}; t) = \rho(\underline{\psi}) \delta(\underline{U}(\underline{x}, t) - \underline{V}) \delta(\underline{\phi}(\underline{x}, t) - \underline{\psi}), \quad (4.37)$$

and taking the mean

$$\langle \mathcal{F}'(\underline{V}, \underline{\psi}, \underline{x}; t) \rangle = \rho(\underline{\psi}) f(\underline{V}, \underline{\psi}; \underline{x}, t) = \mathcal{F}(\underline{V}, \underline{\psi}, \underline{x}; t). \quad (4.38)$$

Equating the two different expressions for $\langle \mathcal{F}' \rangle$ (Eqs 4.33 and 4.38) yields the required result

$$\begin{aligned} \mathcal{F}(\underline{V}, \underline{\psi}, \underline{x}; t) &= \int \int \int f_L(\underline{V}, \underline{\psi}, \underline{x}; t | \underline{V}_0, \underline{\psi}_0, \underline{x}_0) \\ &\quad \times \mathcal{F}(\underline{V}_0, \underline{\psi}_0, \underline{x}_0; t_0) d\underline{V}_0 d\underline{\psi}_0 d\underline{x}_0. \end{aligned} \quad (4.39)$$

This identifies f_L as the relevant transition pdf: it is the probability density of the fluid particle's transition from the initial state $(\underline{V}_0, \underline{\psi}_0, \underline{x}_0)$ at time t_0 to the state $(\underline{V}, \underline{\psi}, \underline{x})$ at time t . The mass density at time t is (according to Eq. 4.39) the mass-probability-weighted integral of this transition pdf over all initial states.

The Lagrangian pdf f_L has been conditioned on $\underline{V}_0, \underline{\psi}_0$ and \underline{x}_0 . In fact, the conditioning on \underline{V}_0 is not needed in order to obtain a relation similar to Eq. (4.39).

The conditioning on $\underline{\psi}_0$ is needed in order to relate the Jacobian $\partial(\underline{x}^+)/\partial(\underline{x}_0)$ to densities. But in constant-density flows (in which the Jacobian is unity) only the conditioning on \underline{x}_0 is needed. In this (constant-density) case Eq. (4.39) reduces to

$$f(\underline{V}, \underline{\psi}; \underline{x}, t) = \int f_L(\underline{V}, \underline{\psi}, \underline{x}; t|\underline{x}_0) d\underline{x}_0. \quad (4.40)$$

It is useful to be able to derive Eulerian pdf evolution equations from Lagrangian equations. This can be done by differentiating Eq. (4.39) and substituting for $\partial f_L/\partial t$ from Eq. (4.31):

$$\begin{aligned} \frac{\partial \mathcal{F}(\underline{V}, \underline{\psi}, \underline{x}; t)}{\partial t} &= - \int \int \int \left\{ \frac{\partial}{\partial \underline{x}_i} [f_L V_i] + \frac{\partial}{\partial V_i} [f_L \langle A_i | S_i, S_0 \rangle] \right. \\ &\quad \left. + \frac{\partial}{\partial \psi_a} [f_L \langle \Theta_a | S_i, S_0 \rangle] \right\} \\ &\quad \times \mathcal{F}(\underline{V}_0, \underline{\psi}_0, \underline{x}_0; t_0) d\underline{V}_0 d\underline{\psi}_0 d\underline{x}_0. \quad (4.42) \end{aligned}$$

It may be noted that, for each of the three terms, the derivative ($\partial/\partial \underline{x}_i$, $\partial/\partial V_i$ or $\partial/\partial \psi_a$) can be removed from the integral, since $\mathcal{F}(\underline{V}_0, \underline{\psi}_0, \underline{x}_0; t_0) d\underline{V}_0 d\underline{\psi}_0 d\underline{x}_0$ does not depend upon the state variables $(\underline{V}, \underline{\psi}, \underline{x})$. The resulting integrals are then of the form

$$\int \int \int f_L \langle Q | S_i, S_0 \rangle \mathcal{F}(\underline{V}_0, \underline{\psi}_0, \underline{x}_0; t_0) d\underline{V}_0 d\underline{\psi}_0 d\underline{x}_0.$$

We now show that this integral is equal to

$$\langle Q(\underline{x}, t) | \underline{V}, \underline{\psi} \rangle \mathcal{F}(\underline{V}, \underline{\psi}, \underline{x}; t).$$

Multiplying Eq. (4.32) by an arbitrary function $Q(\underline{x}, t)$ and taking the mean we obtain

$$\langle Q \mathcal{F}'(\underline{V}, \underline{\psi}, \underline{x}; t) \rangle = \int \int \int \rho(\underline{\psi}_0) \langle Q f_p' f' \rangle d\underline{V}_0 d\underline{\psi}_0 d\underline{x}_0. \quad (4.43)$$

Having identified \mathcal{F}' as the fine-grained mass density function, the left-hand side can be re-expressed as

$$\begin{aligned} \langle Q \mathcal{F}' \rangle &= \langle Q \rho f' \rangle = \langle Q(\underline{x}, t) | \underline{V}, \underline{\psi} \rangle \rho(\underline{\psi}) f(\underline{V}, \underline{\psi}, \underline{x}, t) \\ &= \langle Q(\underline{x}, t) | \underline{V}, \underline{\psi} \rangle \mathcal{F}(\underline{V}, \underline{\psi}, \underline{x}; t). \quad (4.44) \end{aligned}$$

(The second step is analogous to Eq. 2.150.) Similarly, the right-hand side of Eq. (4.43) is

$$\begin{aligned} &\int \int \int \rho(\underline{\psi}_0) \langle Q f_p' f' \rangle d\underline{V}_0 d\underline{\psi}_0 d\underline{x}_0 \\ &= \int \int \int \rho(\underline{\psi}_0) \langle Q | S_i, S_0 \rangle \langle f_p' f' \rangle d\underline{V}_0 d\underline{\psi}_0 d\underline{x}_0 \\ &= \int \int \int \langle Q | S_i, S_0 \rangle f_L(\underline{V}, \underline{\psi}, \underline{x}; t | \underline{V}_0, \underline{\psi}_0, \underline{x}_0) \\ &\quad \times \mathcal{F}(\underline{V}_0, \underline{\psi}_0, \underline{x}_0; t_0) d\underline{V}_0 d\underline{\psi}_0 d\underline{x}_0. \quad (4.45) \end{aligned}$$

Thus, combining the last three equations we obtain the required result:

$$\begin{aligned} &\int \int \int \langle Q | S_i, S_0 \rangle f_L \mathcal{F}(\underline{V}_0, \underline{\psi}_0, \underline{x}_0; t_0) d\underline{V}_0 d\underline{\psi}_0 d\underline{x}_0 \\ &= \langle Q(\underline{x}, t) | \underline{V}, \underline{\psi} \rangle \mathcal{F}(\underline{V}, \underline{\psi}, \underline{x}; t). \quad (4.46) \end{aligned}$$

With this result, Eq. (4.42) becomes

$$\begin{aligned} \frac{\partial \mathcal{F}}{\partial t} &= - \frac{\partial}{\partial \underline{x}_i} [\mathcal{F} V_i] - \frac{\partial}{\partial V_i} [\mathcal{F} \langle A_i | \underline{V}, \underline{\psi} \rangle] \\ &\quad - \frac{\partial}{\partial \psi_a} [\mathcal{F} \langle \Theta_a | \underline{V}, \underline{\psi} \rangle]. \quad (4.47) \end{aligned}$$

This is the evolution equation for the Eulerian mass density function \mathcal{F} derived from the Lagrangian equations for the evolution of fluid particle properties $(\underline{U}^+, \underline{\phi}^+, \underline{x}^+)$. Inevitably the result is the same as Eq. (4.8) which is derived from the evolution equations for the Eulerian properties \underline{U} and $\underline{\phi}$.

4.5. Deterministic System

It has already been noted that the joint pdf transport equation, Eq. (4.8), is deterministic. In this subsection the equation is interpreted in terms of a deterministic Lagrangian system.

In the joint pdf equation, the rates of change $\underline{A}(\underline{x}, t)$, $\underline{\Theta}(\underline{x}, t)$ and $\underline{U}(\underline{x}, t)$ appear as their conditionally expected values:

$$\begin{bmatrix} \underline{a}(\underline{V}, \underline{\psi}, \underline{x}, t) \\ \underline{\theta}(\underline{V}, \underline{\psi}, \underline{x}, t) \\ \underline{U} \end{bmatrix} \equiv \begin{bmatrix} \langle \underline{A}(\underline{x}, t) | \underline{V}, \underline{\psi} \rangle \\ \langle \underline{\Theta}(\underline{x}, t) | \underline{V}, \underline{\psi} \rangle \\ \langle \underline{U}(\underline{x}, t) | \underline{V}, \underline{\psi} \rangle \end{bmatrix}. \quad (4.48)$$

For a given flow, the conditional rate of change vector $(\underline{a}, \underline{\theta}, \underline{U})$ is an unknown but nonetheless determined vector function in state space.

Consider now the deterministic Lagrangian equation

$$\frac{\partial}{\partial t} \begin{bmatrix} \underline{U} \\ \underline{\phi} \\ \underline{x} \end{bmatrix} = \begin{bmatrix} \underline{a}(\underline{U}, \underline{\phi}, \underline{x}, t) \\ \underline{\theta}(\underline{U}, \underline{\phi}, \underline{x}, t) \\ \underline{U} \end{bmatrix}. \quad (4.49)$$

In this case the state vector $(\underline{U}, \underline{\phi}, \underline{x})$ does not pertain to a fluid particle, since fluid particles evolve by a different equation, Eq. (4.19). Equation (4.49) describes the evolution of the state of notational quantities called conditionally-expected particles, or *conditional particles*, for short.

From a given initial state $(\underline{V}_0, \underline{\psi}_0, \underline{x}_0)$ at time $t = t_0$, a conditional particle follows a path determined by Eq. (4.49). In order to show explicitly the dependence on the initial state, we write this path as,

$$\begin{bmatrix} \underline{V} \\ \underline{\psi} \\ \underline{x} \end{bmatrix} = \begin{bmatrix} \underline{U}(\underline{V}_0, \underline{\psi}_0, \underline{x}_0, t) \\ \underline{\phi}(\underline{V}_0, \underline{\psi}_0, \underline{x}_0, t) \\ \underline{x}(\underline{V}_0, \underline{\psi}_0, \underline{x}_0, t) \end{bmatrix}. \quad (4.50)$$

In the augmented state space $(\underline{V}-\underline{\psi}-\underline{x}-t\text{-space})$, this equation defines the *conditional path* from the initial state $(\underline{V}_0, \underline{\psi}_0, \underline{x}_0)$.

For the fluid particle with state $(\underline{U}^+, \underline{\phi}^+, \underline{x}^+)$, its rate of change $(\underline{A}, \underline{\Theta}, \underline{U}^+)$ is a random variable (although the \underline{x} -component \underline{U}^+ is, of course, known). Thus, in a subsequent repetition of the flow, a fluid particle may be found with the same state $(\underline{U}^+, \underline{\phi}^+, \underline{x}^+)$ but with a different rate of change $(\underline{A}, \underline{\Theta}, \underline{U}^+)$; see Fig. 4.2. For the conditional particle with state $(\underline{U}, \underline{\phi}, \underline{x})$, its rate of

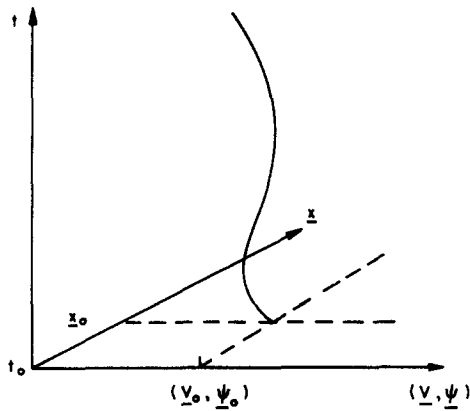


FIG. 4.3. Conditional path from (V_0, ψ_0, x_0) at $t = t_0$ in the augmented state space.

change $(\underline{a}, \underline{\theta}, \underline{U})$ is not a random variable: it is the conditional expectation of the rate of change of fluid particles with the same state.

The conditional path from the state (V_0, ψ_0, x_0) at $t = t_0$ is sketched on Fig. 4.3. Again, this sketch is only suggestive since the $(7 + \sigma)$ -dimensional augmented state space ($V - \psi - x - t$ -space) is shown as being 3-dimensional. The following observations can be made:

- the conditional path is uniquely defined by the initial state;
- since the state vector uniquely determines the rate of change vector $(\underline{a}, \underline{\theta}, \underline{U})$ conditional paths cannot cross; and
- the state vector changes in time and physical space on scales characteristic of the larger scale turbulent motions.

While the behavior of fluid particles and conditional particles are quite different, their (one-point) statistics are identical. This is simply because in each case the evolution for the mass density function \mathcal{F} is Eq. (4.8). Thus, for a given flow, if initially (at time t_0) the conditional particles are distributed in state space identically to the fluid particles, then the conditional and fluid particle distributions remain identical at future times.

For conditional particles, the transition density is

$$f_L(V, \psi, x; t | V_0, \psi_0, x_0) = \delta(V - \underline{U}) \delta(\psi - \underline{\phi}) \delta(x - \underline{x}), \quad (4.51)$$

since, by definition, $(\underline{U}, \underline{\phi}, \underline{x})$ is the state at time t of the conditional particle that had the state (V_0, ψ_0, x_0) at time t_0 . Thus, from Eq. (4.39), the mass density function at time t is determined by its value at time t_0 and by the conditional paths:

$$\mathcal{F}(V, \psi, x; t) = \iint \mathcal{F}(V_0, \psi_0, x_0; t_0) \delta(V - \underline{U}) \times \delta(\psi - \underline{\phi}) \delta(x - \underline{x}) dV_0 d\psi_0 dx_0. \quad (4.52)$$

Because of the particular nature of the transition density, Eq. (4.51), this formal solution can be expressed locally, rather than as an integral over all initial states.

The integration $dV_0 d\psi_0 dx_0$ over the initial states can be replaced by the integration $d\underline{U} d\underline{\phi} d\underline{x}$ over the final states, multiplied by the Jacobian:

$$\begin{aligned} \mathcal{F}(V, \psi, x; t) &= \iint \delta(V - \underline{U}) \delta(\psi - \underline{\phi}) \delta(x - \underline{x}) \\ &\times \left\{ \mathcal{F}(V_0, \psi_0, x_0; t_0) \right. \\ &\left. \times \frac{\partial(V_0, \psi_0, x_0)}{\partial(\underline{U}, \underline{\phi}, \underline{x})} \right\} d\underline{U} d\underline{\phi} d\underline{x}. \end{aligned} \quad (4.53)$$

The left-hand side of this equation can also be written as an integral over the final states, namely

$$\begin{aligned} \mathcal{F}(V, \psi, x; t) &= \iint \delta(V - \underline{U}) \delta(\psi - \underline{\phi}) \delta(x - \underline{x}) \\ &\times \{ \mathcal{F}(\underline{U}, \underline{\phi}, \underline{x}; t) \} d\underline{U} d\underline{\phi} d\underline{x}. \end{aligned} \quad (4.54)$$

Now, since both these equations for \mathcal{F} must hold for all states (V, ψ, x) , the two terms in braces must be equal:

$$\mathcal{F}(\underline{U}, \underline{\phi}, \underline{x}; t) = \mathcal{F}(V_0, \psi_0, x_0; t_0) \frac{\partial(V_0, \psi_0, x_0)}{\partial(\underline{U}, \underline{\phi}, \underline{x})}, \quad (4.55)$$

or, dividing by the Jacobian,

$$\mathcal{F}(\underline{U}, \underline{\phi}, \underline{x}; t) \frac{\partial(\underline{U}, \underline{\phi}, \underline{x})}{\partial(V_0, \psi_0, x_0)} = \mathcal{F}(V_0, \psi_0, x_0; t_0). \quad (4.56)$$

This formal solution, Eq. (4.56), has a simple geometric interpretation in terms of *expected mass* and *conditional tubes*. Let S_0 be the surface in state space that encloses a $(6 + \sigma)$ -dimensional volume V_0 . At the time t_0 , the quantity

$$m(t_0) \equiv \iint \int_{V_0} \mathcal{F}(V_0, \psi_0, x_0; t_0) dV_0 d\psi_0 dx_0, \quad (4.57)$$

represents the expectation of the mass within the particular region of state space V_0 : that is, $m(t_0)$ is the *expected mass* in V_0 at time t_0 .

In the augmented state space ($V - \psi - x - t$), the *conditional tube* (associated with V_0) is defined to be the surface formed by all the conditional paths that at $t = t_0$

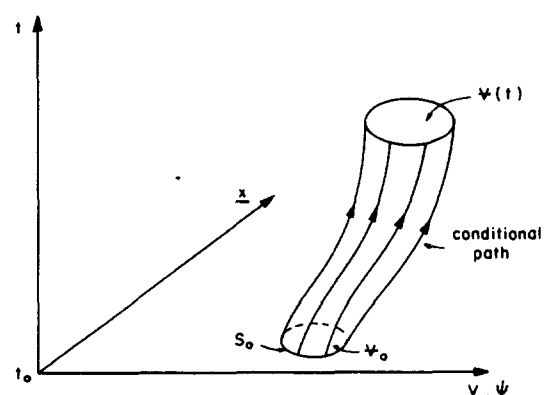


FIG. 4.4. Conditional tube in augmented state space.

pass through the surface S_0 . Since, by definition, the tube is everywhere tangential to conditional paths, a conditional particle cannot cross from inside to outside the tube or vice versa. A conditional tube is sketched on Fig. 4.4. Because \underline{x} and $(\underline{V}, \underline{\psi})$ are each represented by a single coordinate, the surface S_0 appears as a closed curve, and the volume \mathbb{V}_0 appears as a two-dimensional area.

At the later time $t > t_0$, the conditional tube occupies the volume $\mathbb{V}(t)$ in state space, see Fig. 4.4. The expected mass in $\mathbb{V}(t)$ is

$$m(t) = \iiint_{\mathbb{V}(t)} \mathcal{F}(\underline{V}, \underline{\psi}, \underline{x}; t) d\underline{V} d\underline{\psi} d\underline{x}. \quad (4.58)$$

There is a one-to-one correspondence between the points in \mathbb{V}_0 , $(\underline{V}_0, \underline{\psi}_0, \underline{x}_0)$, and points in $\mathbb{V}(t)$, $(\underline{U}, \underline{\phi}, \underline{\hat{x}})$. Consequently, the integral over $\mathbb{V}(t)$ can be replaced by an integral over \mathbb{V}_0 :

$$m(t) = \iiint_{\mathbb{V}_0} \mathcal{F}(\underline{U}, \underline{\phi}, \underline{\hat{x}}; t) \frac{\partial(\underline{U}, \underline{\phi}, \underline{\hat{x}})}{\partial(\underline{V}_0, \underline{\psi}_0, \underline{x}_0)} d\underline{V}_0 d\underline{\psi}_0 d\underline{x}_0. \quad (4.59)$$

Now the formal solution to the pdf equation, Eq. (4.56), states that the integrals in Eq. (4.57) and (4.59) are equal. Thus we obtain

$$m(t) = m(t_0). \quad (4.60)$$

Expected mass is constant along a conditional tube.

The same analysis applies to an infinitesimal conditional tube. In an obvious notation we have

$$dm(t_0) \equiv \mathcal{F}(\underline{V}_0, \underline{\psi}_0, \underline{x}_0; t_0) d\mathbb{V}_0, \quad (4.61)$$

$$\begin{aligned} dm(t) &\equiv \mathcal{F}(\underline{V}, \underline{\psi}, \underline{x}; t) d\mathbb{V}(t) \\ &= \mathcal{F}(\underline{U}, \underline{\phi}, \underline{\hat{x}}; t) \frac{\partial(\underline{U}, \underline{\phi}, \underline{\hat{x}})}{\partial(\underline{V}_0, \underline{\psi}_0, \underline{x}_0)} d\mathbb{V}_0 \\ &= dm(t_0). \end{aligned} \quad (4.62)$$

The Jacobian represents the volume ratio $d\mathbb{V}(t)/d\mathbb{V}_0$ for the infinitesimal conditional tube. If the conditional paths converge, $d\mathbb{V}(t)$ decreases and the Jacobian is less than unity. In order that the expected mass remains constant, the mass density \mathcal{F} must increase. Conversely, if the conditional paths diverge, $d\mathbb{V}(t)$ increases, the Jacobian is greater than unity, and the mass density decreases.

There is a direct analogy between Eq. (4.56) for the mass density along a conditional path, and Eq. (4.18) for the fluid density along a fluid particle path. This analogy may also be seen by comparing Figs 4.1 and 4.4. The analogy arises because expected mass is conserved along conditional tubes, and mass is conserved following a material element: mass density is expected mass per unit volume (in the state space), and the fluid density is mass per unit volume (in physical space).

These considerations of conditional paths lead to a computationally feasible method of solving the joint pdf equation. At the initial time t_0 , the mass density function is approximated by a large number N of particles in state space (see Eq. 3.76):

$$\begin{aligned} \mathcal{F}(\underline{V}_0, \underline{\psi}_0, \underline{x}_0; t_0) &\approx \mathcal{F}_N(\underline{V}_0, \underline{\psi}_0, \underline{x}_0; t_0) \\ &\equiv \Delta m \sum_{n=1}^N \delta(\underline{V}_0 - \underline{U}_0^{(n)}) \\ &\quad \times \delta(\underline{\psi}_0 - \underline{\phi}_0^{(n)}) \delta(\underline{x}_0 - \underline{x}_0^{(n)}). \end{aligned} \quad (4.63)$$

Each particle represents a mass Δm and (at time t_0) $(\underline{U}_0^{(n)}, \underline{\phi}_0^{(n)}, \underline{x}_0^{(n)})$ is the state of the n th particle. Replacing \mathcal{F} by \mathcal{F}_N on the right-hand side of Eq. (4.52) yields

$$\begin{aligned} \mathcal{F}(\underline{V}, \underline{\psi}, \underline{x}; t) &\approx \Delta m \sum_{n=1}^N \iiint \delta(\underline{V}_0 - \underline{U}_0^{(n)}) \delta(\underline{\psi}_0 - \underline{\phi}_0^{(n)}) \delta(\underline{x}_0 - \underline{x}_0^{(n)}) \\ &\quad \times \delta(\underline{V} - \underline{U}[\underline{V}_0, \underline{\psi}_0, \underline{x}_0, t]) \delta(\underline{\psi} - \underline{\phi}[\underline{V}_0, \underline{\psi}_0, \underline{x}_0, t]) \\ &\quad \times \delta(\underline{x} - \underline{x}[\underline{V}_0, \underline{\psi}_0, \underline{x}_0, t]) d\underline{V}_0 d\underline{\psi}_0 d\underline{x}_0 \\ &= \Delta m \sum_{n=1}^N \delta(\underline{V} - \underline{U}^{(n)}[t]) \delta(\underline{\psi} - \underline{\phi}^{(n)}[t]) \delta(\underline{x} - \underline{x}^{(n)}[t]), \end{aligned} \quad (4.64)$$

where

$$\begin{bmatrix} \underline{U}^{(n)}(t) \\ \underline{\phi}^{(n)}(t) \\ \underline{x}^{(n)}(t) \end{bmatrix} = \begin{bmatrix} \underline{U}(\underline{U}_0^{(n)}, \underline{\phi}_0^{(n)}, \underline{x}_0^{(n)}, t) \\ \underline{\phi}(\underline{U}_0^{(n)}, \underline{\phi}_0^{(n)}, \underline{x}_0^{(n)}, t) \\ \underline{x}(\underline{U}_0^{(n)}, \underline{\phi}_0^{(n)}, \underline{x}_0^{(n)}, t) \end{bmatrix}. \quad (4.65)$$

The state $[\underline{U}^{(n)}(t), \underline{\phi}^{(n)}(t), \underline{x}^{(n)}(t)]$ is the state at time t of the conditional particle that at time t_0 had the state $[\underline{U}_0^{(n)}, \underline{\phi}_0^{(n)}, \underline{x}_0^{(n)}]$. Thus Eq. (4.64) shows that for all time the mass density function can be approximated by a large number of conditional particles.

Through Eq. (4.64) we have reduced the problem of determining $\mathcal{F}(\underline{V}, \underline{\psi}, \underline{x}; t)$ to that of determining the states of N conditional particles. Suppose that the unknown conditional rates of change $\underline{a}(\underline{V}, \underline{\psi}, \underline{x}, t)$ and $\underline{\theta}(\underline{V}, \underline{\psi}, \underline{x}, t)$ can be modelled as simply computed functions in state space. Then the particle states can be determined by solving the equations

$$\begin{bmatrix} \frac{\partial}{\partial t} \underline{U}^{(n)} \\ \frac{\partial}{\partial t} \underline{\phi}^{(n)} \\ \frac{\partial}{\partial t} \underline{x}^{(n)} \end{bmatrix} = \begin{bmatrix} \underline{a}(\underline{U}^{(n)}, \underline{\phi}^{(n)}, \underline{x}^{(n)}, t) \\ \underline{\theta}(\underline{U}^{(n)}, \underline{\phi}^{(n)}, \underline{x}^{(n)}, t) \\ \underline{U}^{(n)} \end{bmatrix}, \quad n = 1, 2, \dots, N, \quad (4.66)$$

from the initial conditions $(\underline{U}_0^{(n)}, \underline{\phi}_0^{(n)}, \underline{x}_0^{(n)})$. For each value of n , Eq. (4.66) is a set of $(6+\sigma)$ simultaneous ordinary differential equations. To solve these equations numerically is trivially simple compared to solving directly the equation for \mathcal{F} (Eq. 4.8) which is a partial differential equation in $(7+\sigma)$ dimensions.

The conclusion that the pdf equation can be solved economically via Eq. (4.66) is based on the supposition that \underline{a} and $\underline{\theta}$ can be modelled as simply computed functions* in state space. In Section 5.2.2 such simple deterministic models are examined and it is shown that, in general, they are unsatisfactory. Satisfactory deterministic models can be constructed, but they are far

* For the present purpose, a “simply computed function” can be defined to be a function of $\underline{V}, \underline{\psi}, \underline{x}$ and t that can depend upon the first few moments of the pdf, but is otherwise independent of the pdf.

from simple, and the computational advantages of Eq. (4.66) are lost. Satisfactory modelling combined with computational economy can be obtained through stochastic models. These are discussed in the next subsection and in Sections 5.2.3-4.

4.6. Stochastic Systems

Many different systems evolve with the same pdf. Fluid particles and conditional particles behave quite differently, but nevertheless their pdf's are the same. We now consider systems of *stochastic particles* whose behavior is physically and mathematically different from that of fluid or conditional particles. The essence of the whole approach is to construct a system of stochastic particles whose evolution is simply computed and in which the pdf evolves in the same way as the pdf of fluid particles.

We consider two types of stochastic processes. *Poisson processes* form the basis of *particle interaction models* (Section 5.3); and *diffusion processes* form the basis for *Langevin models* (Section 5.5).

At time t , the state of a stochastic particle is denoted by $(U^*(t), \phi^*(t), \underline{x}^*(t))$. This is a $(6+\sigma)$ -dimensional state vector that corresponds to a point in state space. The state of the particle evolves according to a stochastic prescription, and the corresponding point moves—not necessarily continuously—in the augmented state space $(V, \underline{\psi}, \underline{x}, t)$.

In order to examine Poisson and diffusion processes it is sufficient to consider a single (scalar) state property. Let $U^*(t)$ be the state property at time t and let $f^*(V; t)$ be the corresponding pdf. The stochastic process $U^*(t)$ can be defined either in terms of the increment

$$\Delta_{\delta t} U^*(t) \equiv U^*(t + \delta t) - U^*(t), \quad (4.67)$$

or in terms of the transition density $f_{\delta t}(V; t|V_0)$. This is the probability density of the event $U^*(t + \delta t) = V$ conditional upon $U^*(t) = V_0$. In both cases we consider the limit as the (positive) time interval, δt tends to zero. (Note that $\Delta_{\delta t}$ is the forward-difference operator.)

For a Poisson process, the increment is:

with probability $1 - \delta t/\tau$: $\Delta_{\delta t} U^*(t) = 0$,

with probability $\delta t/\tau$: $\Delta_{\delta t} U^*(t) = U^0(t) - U^*(t)$, (4.68)

where $\tau(t)$ is a specified time scale and $U^0(t)$ is a random variable with a specified conditional pdf $g(V|V_0, t)$.

A sample of such a process is shown on Fig. 4.5. The conditional pdf in this example is

$$g(V|V_0, t) = \delta\left(V - \frac{9}{10}V_0\right), \quad (4.69)$$

and the time scale τ is taken to be constant. It may be seen from the figure that $U^*(t)$ is constant except at a finite number of points where it changes abruptly. In this example, the value of U^* is reduced by 10% at each such change. The time interval between abrupt changes is a random variable: the probability density of the time interval being Δt is $\tau^{-1} e^{-\Delta t/\tau}$ (see Ref. 55).

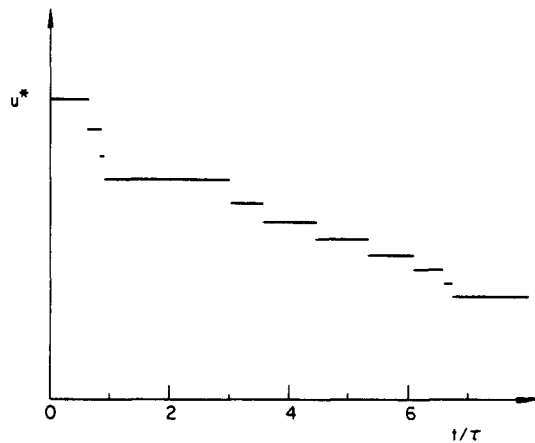


FIG. 4.5. A sample of the Poisson process $U^*(t)$.

An evolution equation for $f^*(V; t)$ —the pdf of $U^*(t)$ —is now derived. Because U^* is a discontinuous function of time, the methods of derivation used in Sections 3.5 and 4.3 cannot be employed. However the evolution equation is readily derived from the transition density through the relation

$$f^*(V; t + \delta t) = \int f^*(V_0; t) f_{\delta t}(V; t|V_0) dV_0, \quad (4.70)$$

(cf. Eq. 4.39). The transition density for the Poisson process, corresponding to Eq. (4.68), is

$$f_{\delta t}(V; t|V_0) = (1 - \delta t/\tau) \delta(V - V_0) + (\delta t/\tau) g(V|V_0, t). \quad (4.71)$$

Substituting for $f_{\delta t}$ in Eq. (4.70) yields

$$f^*(V; t + \delta t) = (1 - \delta t/\tau) f^*(V; t) + (\delta t/\tau) \times \int f^*(V_0; t) g(V|V_0, t) dV_0. \quad (4.72)$$

Hence in the limit as δt tends to zero we obtain the evolution equation

$$\frac{\partial f^*(V; t)}{\partial t} = \frac{1}{\tau} \int f^*(V_0; t) g(V|V_0, t) dV_0 - f^*(V; t)/\tau. \quad (4.73)$$

It may be seen that although $U^*(t)$ evolves stochastically and discontinuously, its pdf $f^*(V; t)$ evolves deterministically and smoothly (provided that neither $f^*(V; t_0)$ nor $g(V|V_0, t)$ is pathological).

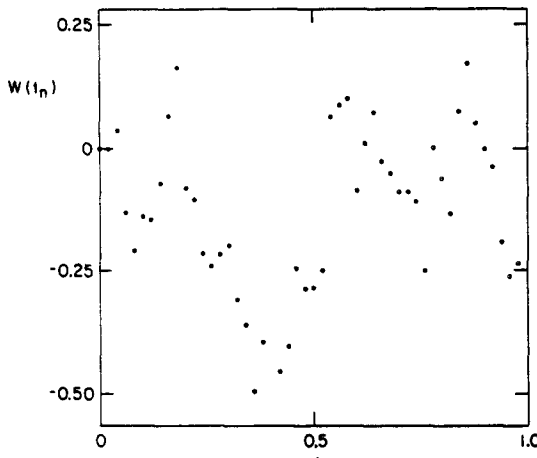
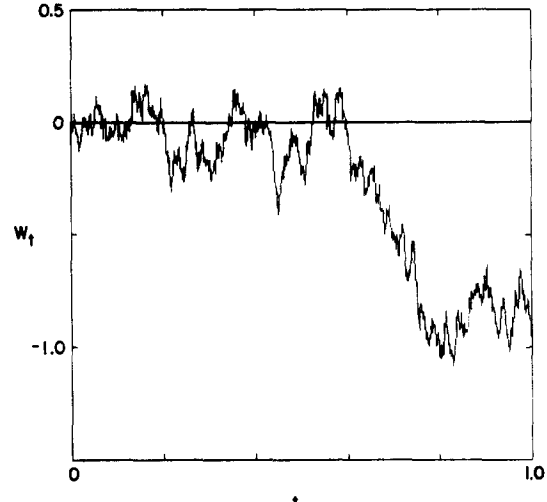
The usefulness of the Poisson process is discussed below, but now we turn our attention to diffusion processes. A necessary preliminary is to describe the Weiner process.

Let the time interval from $t = 0$ to $t = T$ be divided into N equal subintervals of duration $\delta t = T/N$, and let $\xi_{(n)}$ ($n = 1, 2, \dots, N$) denote N independent standardized normal random variables; thus

$$\langle \xi_{(n)} \rangle = 0, \quad (4.74)$$

and

$$\langle \xi_{(n)} \xi_{(m)} \rangle = \delta_{nm}. \quad (4.75)$$

FIG. 4.6. A sample of the function $W(t_n)$.FIG. 4.7. Sample of the Weiner process W_t .

Consider the quantity

$$W(t_n) \equiv (\delta t)^{1/2} \sum_{i=1}^n \xi_{(i)}, \quad (4.76)$$

where $t_n = n\Delta t$. Alternatively, $W(t_n)$ can be defined by the increment

$$\Delta_{\delta t} W(t_{n-1}) = (\delta t)^{1/2} \xi_{(n)}, \quad n = 1, 2, \dots, N, \quad (4.77)$$

with the initial condition $W(t_0) = 0$. Figure 4.6 shows $W(t_n)$ for $T = 1$ and $N = 50$.

The mean and variance of the difference $W(t_n) - W(t_m)$ ($m < n$) is readily deduced from Eqs (4.74–75):

$$\langle W(t_n) - W(t_m) \rangle = (\delta t)^{1/2} \sum_{i=m+1}^n \langle \xi_{(i)} \rangle = 0, \quad (4.78)$$

and

$$\begin{aligned} \langle [W(t_n) - W(t_m)]^2 \rangle &= \delta t \sum_{i=m+1}^n \sum_{j=m+1}^n \langle \xi_{(i)} \xi_{(j)} \rangle \\ &= \delta t \sum_{i=m+1}^n \sum_{j=m+1}^n \delta_{ij} \\ &= \delta t(n-m) = t_n - t_m. \end{aligned} \quad (4.79)$$

Thus the difference $W(t_n) - W(t_m)$ is a Gaussian random variable with zero mean, and variance equal to the time difference $t_n - t_m$. This last result, it may be noted, is independent of the choice of N . By a similar procedure it is readily shown that (for $m < n < p < q$) the random variables $[W(t_n) - W(t_m)]$ and $[W(t_q) - W(t_p)]$ are uncorrelated and hence independent (in view of their Gaussianity), with means of zero and variances $(t_n - t_m)$ and $(t_q - t_p)$ respectively.

The Weiner process, denoted by W_t , can be thought of as the discrete process described above in the limit as δt tends to zero (N tends to infinity). A sample is shown on Fig. 4.7. In fact, it is better to define the Weiner process by the properties deduced above⁷³: for $0 \leq t_1 < t_2 \leq$

$t_3 < t_4$, $[W_{t_2} - W_{t_1}]$ and $[W_{t_4} - W_{t_3}]$ are independent Gaussian random variables with zero means and variances $(t_2 - t_1)$ and $(t_4 - t_3)$ respectively.[†]

The increment

$$\Delta_{\delta t} W_t = W_{t+\delta t} - W_t, \quad (4.80)$$

is equal to $\delta t^{1/2}$ multiplied by a standardized Gaussian random variable (cf. Eq. 4.77). Consequently, as δt tends to zero, so does $\Delta_{\delta t} W_t$, showing that W_t is a continuous function. On the other hand $(\Delta_{\delta t} W_t)/\delta t$ becomes infinite and hence W_t is not differentiable.

The general diffusion process $U^*(t)$ considered has the increment (as δt tends to zero)

$$\Delta_{\delta t} U^*(t) = D(U^*[t], t) \delta t + [B(U^*[t], t)]^{1/2} \Delta_{\delta t} W_t, \quad (4.81)$$

where D and B are specified functions, B being non-negative. This increment is a Gaussian random variable with conditional mean

$$\langle \Delta_{\delta t} U^*(t) | U^*(t) = V_0 \rangle = D(V_0, t) \delta t, \quad (4.82)$$

and variance

$$\langle [\Delta_{\delta t} U^*(t) - D(V_0, t) \delta t]^2 | U^*(t) = V_0 \rangle = B(V_0, t) \delta t. \quad (4.83)$$

Consequently the transition density $f_{\delta t}(V; t | V_0)$ is a Gaussian pdf with mean $V_0 + D(V_0, t) \delta t$ and variance $B(V_0, t) \delta t$.

Since $U^*(t)$, like W_t , is not differentiable, the evolution equation for its pdf $f^*(V; t)$ cannot be derived by the methods of Sections 3.5 or 4.3. The standard method^{74,75} involves $g_{\delta t}(\Delta V | V_0, t)$ —the pdf of $\Delta_{\delta t} U^*(t)$ conditional upon $U^*(t) = V_0$. In general, $g_{\delta t}$ is simply related to the transition density by

$$g_{\delta t}(\Delta V | V_0, t) = f_{\delta t}(V_0 + \Delta V; t | V_0), \quad (4.84)$$

[†] It follows from the central limit theorem that for a finite time interval $(t_2 - t_1)$, the increment $[W_{t_2} - W_{t_1}]$ is Gaussian even if the infinitesimal increments $\xi_{(n)}$ (Eqs 4.74–4.75) are not.

and, in the case being considered, $g_{\delta t}$ is Gaussian with mean $D(V_0, t)\delta t$ and variance $B(V_0, t)\delta t$.

Either from first principles or by combining Eqs (4.70) and (4.84) (with $V_0 = V - \Delta V$) we obtain

$$f^*(V; t + \delta t) = \int f^*(V - \Delta V; t) g_{\delta t}(\Delta V | V - \Delta V, t) d(\Delta V). \quad (4.85)$$

The right-hand side can be re-expressed as a Taylor series:

$$f^*(V; t + \delta t) = \int \left\{ f^*(V; t) g_{\delta t}(\Delta V | V, t) - \Delta V \frac{\partial(f^* g_{\delta t})}{\partial V} + \frac{1}{2!} (\Delta V)^2 \frac{\partial^2(f^* g_{\delta t})}{\partial V^2} \dots \right\} d(\Delta V), \quad (4.86)$$

where $f^* g_{\delta t}$ is written for $f^*(V; t) g_{\delta t}(\Delta V | V, t)$. Now the derivatives and f^* can be removed from the integral, and the remaining terms can be identified as conditional moments of $\Delta_{\delta t} U^*(t)$:

$$\int (\Delta V)^n g_{\delta t}(\Delta V | V, t) d(\Delta V) = \langle [\Delta_{\delta t} U^*(t)]^n | V \rangle. \quad (4.87)$$

From Eqs (4.82–83) it may be seen that the first and second moments are of order δt while higher moments are of smaller order.[†] Thus, to first order in δt ,

$$f^*(V; t + \delta t) = f^*(V; t) - \frac{\partial}{\partial V} [f^*(V; t) D(V, t) \delta t] + \frac{1}{2} \frac{\partial^2}{\partial V^2} [f^*(V; t) B(V, t) \delta t],$$

and hence in the limit as δt tends to zero we obtain the evolution equation for f^* :

$$\frac{\partial f^*(V; t)}{\partial t} = -\frac{\partial}{\partial V} [f^*(V; t) D(V, t)] + \frac{1}{2} \frac{\partial^2}{\partial V^2} [f^*(V; t) B(V, t)]. \quad (4.88)$$

The evolution equation for the pdf in a diffusion process, Eq. (4.88), is called the Fokker-Planck equation and has found wide application in many fields.^{73–76} The functions $D(V, t)$ and $B(V, t)$ are called the coefficients of drift and diffusion. If D is uniform, then its effect is to cause the pdf to move in V -space at the speed D . If B is uniform (and D is zero) then Eq. (4.88) reduces to the unsteady one-dimensional heat conduction equation:

$$\frac{\partial f^*}{\partial t} = \frac{1}{2} B \frac{\partial^2 f^*}{\partial V^2}. \quad (4.89)$$

From this it may be seen that the term in B causes the pdf

[†] These conditions on the moments are sufficient for Eq. (4.88) to follow. The infinitesimal increment $\Delta_{\delta t} U^*(t)$ does not have to be Gaussian.

to diffuse in V -space. (The diffusion process Eq. (4.81) causes the pdf to diffuse in V -space. This should not be confused with gradient-diffusion models of turbulent transport which cause diffusion in physical space.)

For the particular case in which B is uniform and D is linear in V ,

$$D(V, t) = G(t)V, \quad (4.90)$$

the general diffusion process (Eq. 4.81) reduces to

$$\Delta_{\delta t} U^*(t) = G(t) U^*(t) \delta t + [B(t)]^{1/2} \Delta_{\delta t} W_t. \quad (4.91)$$

This is the Langevin equation. Originally proposed⁵¹ to model the velocity of a particle undergoing Brownian motion, the Langevin equation and its generalizations have been widely studied.^{73–75}

We now consider, in general terms, the modelling of a physical process by a stochastic process. Let $U(t)$ be a physical quantity (e.g. one component of velocity) and let $A(t)$ (a random variable) be its rate of change. The pdf of $U(t) - f_u(V; t)$ —evolves according to

$$\frac{\partial f_u(V; t)}{\partial t} \equiv -\frac{\partial}{\partial V} [a(V, t) f_u(V; t)], \quad (4.92)$$

(cf. Eq. 4.8) where

$$a(V, t) \equiv \langle A(t) | U(t) = V \rangle. \quad (4.93)$$

For a Poisson process, $U^*(t)$ is a discontinuous function of time, and for a diffusion process it is continuous but not differentiable. Clearly then, neither of these stochastic processes provides a good direct model of the physical process $U(t)$. But the pdf's of $U^*(t)$ and $U(t)$ can evolve identically and hence $f^*(V; t)$ can be a perfect model of $f_u(V; t)$. The conditions that have to be satisfied for this to be the case can be deduced by comparing Eqs (4.73), (4.88) and (4.92). For the Poisson process, the time scale τ and the pdf g must be such that

$$a(V, t) = \int_{-\infty}^V \left\{ f_u(V'; t) - \int f_u(V_0; t) \times g(V' | V_0, t) dV_0 \right\} dV' / [\tau f_u(V; t)]. \quad (4.94)$$

For the diffusion process, the functions D and B must be such that

$$a(V, t) = D(V, t) - \frac{1}{2} [f_u(V; t)]^{-1} \frac{\partial}{\partial V} [f_u(V; t) B(V, t)]. \quad (4.95)$$

And of course in both cases the initial conditions $f_u(V; t_0)$ and $f^*(V; t_0)$ must be the same.

At the end of the last sub-section a computationally feasible deterministic method of solving the joint pdf equation was outlined. In the present context the method is to approximate the initial pdf $f_u(V; t_0)$ by a large number of conditional particles in V -space:

$$f_u(V; t_0) \approx \frac{1}{N} \sum_{n=1}^N \delta(V - \hat{U}^{(n)}(t_0)). \quad (4.96)$$

It was supposed that $a(V, t)$ could be modelled as a simply computed function, and hence the evolution of

the conditional particles could be simply computed by solving the N ordinary differential equations

$$\frac{d\hat{U}^{(n)}(t)}{dt} = a(\hat{U}^{(n)}[t], t). \quad (4.97)$$

Although the selection of the initial conditions $U^{(n)}(t_0)$ may involve randomness, the subsequent evolution according to Eq. (4.97) is deterministic.

The pdf equations arising from the stochastic models, Eqs (4.73) and (4.88), can be solved either by a deterministic method or by a random—Monte Carlo—method. The deterministic method is as described above, with $a(\hat{U}^{(n)}[t], t)$ in Eq. (4.97) obtained from Eq. (4.94) for a Poisson process, or from Eq. (4.95) for a diffusion process. But this method is not computationally feasible since the integrals or differentials of f required by Eqs (4.94–95) are extremely difficult to compute from the discrete representation.

The alternative—Monte Carlo—method is straightforward and computationally efficient. The initial pdf $f^*(V; t_0)$ is represented by a large number N of stochastic particles in V -space:

$$f^*(V; t_0) \approx \frac{1}{N} \sum_{n=1}^N \delta(V - U^{(n)}(t_0)). \quad (4.98)$$

The stochastic particles then evolve according to the stochastic processes: Eq. (4.68) for a Poisson process, Eq. (4.81) for a different process. (These equations are simple to solve numerically.) Then, provided that the modelling is accurate (i.e. Eq. (4.94) or (4.95) is satisfied), $f^*(V; t)$ is equal to $f_u(V; t)$ for all time.

This algorithm is called an *indirect* Monte Carlo method³⁷—indirect because $U^*(t)$ does not model $U(t)$ directly.

We now revert to the general case in which a stochastic particle has the $(6+\sigma)$ -dimensional state vector $\underline{U}^*(t), \underline{\phi}^*(t), \underline{x}^*(t)$, with corresponding (unconditional) Lagrangian pdf $f_L^*(\underline{V}, \underline{\psi}, \underline{x}; t)$ and Eulerian mass density function $\mathcal{F}^*(\underline{V}, \underline{\psi}, \underline{x}; t)$. In order to illustrate how the equations for f_L^* and \mathcal{F}^* can be derived, we take the following process as an example:

$$\Delta_{\delta t} x_j^*(t) = U_j^*(t) \delta t, \quad (4.99)$$

$$\Delta_{\delta t} U_j^*(t) = M_j(\underline{x}^*[t], t) \delta t + G_{jk}(\underline{x}^*[t], t) U_k^*(t) \delta t + [B(\underline{x}^*[t], t)]^{1/2} \Delta_{\delta t}(W_j)_t, \quad (4.100)$$

with probability $1 - \delta t/\tau$: $\Delta_{\delta t} \phi_a^*(t) = 0$,

$$\text{with probability } \delta t/\tau : \Delta_{\delta t} \phi_a^*(t) = \phi_a^0(t) - \phi_a^*(t). \quad (4.101)$$

Here, $M_j(\underline{x}, t)$, $G_{jk}(\underline{x}, t)$ and $B(\underline{x}, t)$ are specified functions; \underline{W}_t is an isotropic Weiner process so that

$$\langle \Delta_{\delta t}(W_i)_t \Delta_{\delta t}(W_j)_t \rangle = \delta t \delta_{ij}; \quad (4.102)$$

and ϕ^0 is a random σ -vector with specified conditional joint pdf $g(\underline{\psi}|\underline{\psi}_0, \underline{x}, t)$ —conditional, that is, on $\phi^*(t) = \underline{\psi}_0$ and $\underline{x}^*(t) = \underline{x}$.

By the methods presented in this section, the evolution equation for the Lagrangian joint pdf $f_L^*(\underline{V}, \underline{\psi}, \underline{x}; t)$ can be derived from Eqs (4.99–101).

The result is:

$$\begin{aligned} \frac{\partial f_L^*}{\partial t} = & -V_j \frac{\partial f_L^*}{\partial x_j} - M_j(\underline{x}, t) \frac{\partial f_L^*}{\partial V_j} \\ & - G_{jk}(\underline{x}, t) \frac{\partial}{\partial V_j} (f_L^* V_k) + \frac{1}{2} B(\underline{x}, t) \frac{\partial^2 f_L^*}{\partial V_i \partial V_i} \\ & + \frac{1}{\tau} \left\{ \int f_L^*(\underline{V}, \underline{\psi}_0, \underline{x}; t) g(\underline{\psi}|\underline{\psi}_0, \underline{x}, t) d\underline{\psi}_0 - f_L^* \right\}. \end{aligned} \quad (4.103)$$

Both stochastic processes considered are Markov processes. That is, given the current state $U^*(t)$, the future state $U^*(t_1)$ is independent of the past $U^*(t_0)$ ($t_0 < t < t_1$). Consequently,⁷⁶ the conditional pdf $f_L^*(\underline{V}, \underline{\psi}, \underline{x}; t|\underline{V}_0, \underline{\psi}_0, \underline{x}_0)$ evolves according to the same evolution equation as the unconditional pdf, Eq. (4.103). In fact, the conditional pdf can be determined as the solution of this equation with the initial condition

$$f_L^*(\underline{V}, \underline{\psi}, \underline{x}; t_0) = \delta(\underline{V} - \underline{V}_0) \delta(\underline{\psi} - \underline{\psi}_0) \delta(\underline{x} - \underline{x}_0). \quad (4.104)$$

As before, the evolution equation for the (Eulerian) mass density function $\mathcal{F}^*(\underline{V}, \underline{\psi}, \underline{x}; t)$ can be obtained from the conditional Lagrangian pdf via Eq. (4.39). Differentiating this equation with respect to time and substituting the right-hand side of Eq. (4.103) for $\partial f_L^*/\partial t$ yields:

$$\begin{aligned} \frac{\partial \mathcal{F}^*}{\partial t} = & -\frac{\partial}{\partial x_j} [V_j \mathcal{F}^*] - \frac{\partial}{\partial V_j} [\{M_j + G_{jk} V_k\} \mathcal{F}^*] \\ & + \frac{1}{2} B \frac{\partial^2 \mathcal{F}^*}{\partial V_i \partial V_i} + \frac{1}{\tau} \\ & \times \left\{ \int \mathcal{F}^*(\underline{V}, \underline{\psi}_0, \underline{x}; t) g(\underline{\psi}|\underline{\psi}_0, \underline{x}, t) d\underline{\psi}_0 - \mathcal{F}^* \right\}. \end{aligned} \quad (4.105)$$

Although f_L^* and \mathcal{F}^* have distinctly different properties, it may be seen that their evolution equations (Eqs 4.103 and 4.105) are identical.

4.7. Normalization, Mean Continuity and Pressure

The mass density function $\mathcal{F}(\underline{V}, \underline{\psi}, \underline{x}; t)$ satisfies the following conditions:

$$\mathcal{F}(\underline{V}, \underline{\psi}, \underline{x}; t) \geq 0, \quad (4.106)$$

$$\int \int \mathcal{F}(\underline{V}, \underline{\psi}, \underline{x}; t) d\underline{V} d\underline{\psi} = \langle \rho(\underline{x}, t) \rangle, \quad (4.107)$$

and

$$\int \int \mathcal{F}(\underline{V}, \underline{\psi}, \underline{x}; t) [\rho(\underline{\psi})]^{-1} d\underline{V} d\underline{\psi} = 1, \quad (4.108)$$

(see Section 3.3). Conversely, any function $\mathcal{F}^*(\underline{V}, \underline{\psi}, \underline{x}; t)$ satisfying these conditions is a valid mass density function.[†]

[†] \mathcal{F}^* denotes any mass density function that approximates the fluid mass density function \mathcal{F} .

We now ask: starting from a consistent initial condition $\mathcal{F}^*(\underline{V}, \underline{\psi}, \underline{x}; t_0)$, what conditions must be satisfied by a modelled pdf equation in order that \mathcal{F}^* remains a valid mass density function? This question is answered by establishing the following propositions.

- (i) Any model that can be expressed in terms of the evolution of the discrete mass density function \mathcal{F}_n satisfies the realizability condition, Eq. (4.106).
- (ii) The consistency condition, Eq. (4.107), and the normalization condition, Eq. (4.108), are equivalent (one implies the other).
- (iii) The satisfaction of the mean continuity equation

$$\frac{\partial \langle \rho \rangle}{\partial t} + \frac{\partial [\langle \rho \rangle \bar{U}_i]}{\partial x_i} = 0, \quad (4.109)$$

is a necessary and sufficient condition for the satisfaction of the consistency condition.

- (iv) The mean continuity equation is satisfied for all time if, and only if, the mean pressure satisfies a Poisson equation, Eq. (4.129).

Thus, if the model can be expressed in terms of the evolution of the discrete mass density function, and if the mean pressure is correctly determined (by Eq. 4.129), then the modelled mass density function \mathcal{F}^* is valid (i.e. it satisfies Eqs 4.106–108).

The discrete representation of the mass density function, Eq. (3.76), is a positive quantity (Δm) multiplied by the sum of delta function locations moving in state space. But irrespective of the delta functions' locations (i.e. irrespective of the modelling) the delta functions are non-negative and hence proposition (i) is established. Thus in pdf methods, realizability is guaranteed in a simple, natural manner.

Rather than assuming Eq. (4.107), we define

$$q(\underline{x}, t) \equiv \int \int \mathcal{F}^*(\underline{V}, \underline{\psi}, \underline{x}; t) d\underline{V} d\underline{\psi}, \quad (4.110)$$

and then define

$$\bar{f}(\underline{V}, \underline{\psi}; \underline{x}, t) \equiv \mathcal{F}^*(\underline{V}, \underline{\psi}, \underline{x}; t) / q(\underline{x}, t). \quad (4.111)$$

Since \bar{f} is non-negative and integrates to unity, it is a joint pdf. Density weighted means are defined (at any \underline{x}, t) by

$$\bar{Q}(\underline{U}, \underline{\phi}) \equiv \int \int Q(\underline{V}, \underline{\psi}) \bar{f}(\underline{V}, \underline{\psi}) d\underline{V} d\underline{\psi}. \quad (4.112)$$

These are consistent definitions that assume Eq. (4.106) but not Eqs (4.107–108).

Now with $Q(\underline{U}, \underline{\phi}) = [\rho(\underline{\phi})]^{-1}$, Eq. (4.112) yields

$$\begin{aligned} \widetilde{[\rho(\underline{\phi})]^{-1}} &= \langle \rho(\underline{\phi}) \rangle^{-1} = \int \int [\rho(\underline{\psi})]^{-1} \bar{f}(\underline{V}, \underline{\psi}) d\underline{V} d\underline{\psi} \\ &= \int \int [\rho(\underline{\psi})]^{-1} \mathcal{F}^*(\underline{V}, \underline{\psi}) d\underline{V} d\underline{\psi} / q. \end{aligned} \quad (4.113)$$

By comparing this equation with Eqs (4.107–108), we clearly see that the consistency and normalization

conditions are satisfied if, and only if,

$$\langle \rho(\underline{\phi}[\underline{x}, t]) \rangle = q(\underline{x}, t). \quad (4.114)$$

Hence proposition (ii).

The terms to be modelled in the evolution equation for \mathcal{F}^* represent transport in \underline{V} - $\underline{\psi}$ space. Consequently, when any modelled evolution equation for \mathcal{F}^* is integrated over all \underline{V} and $\underline{\psi}$ the modelled terms vanish leaving:

$$\begin{aligned} \frac{\partial}{\partial t} \int \int \mathcal{F}^*(\underline{V}, \underline{\psi}, \underline{x}; t) d\underline{V} d\underline{\psi} \\ + \frac{\partial}{\partial x_i} \int \int \mathcal{F}^*(\underline{V}, \underline{\psi}, \underline{x}; t) V_i d\underline{V} d\underline{\psi} = 0. \end{aligned} \quad (4.115)$$

Evaluating the integrals using Eqs (4.111–112) yields

$$\frac{\partial q}{\partial t} + \frac{\partial}{\partial x_i} (q \bar{U}_i) = 0, \quad (4.116)$$

or

$$\frac{\bar{D}}{\bar{D}t} \ln q = - \frac{\partial \bar{U}_i}{\partial x_i}, \quad (4.117)$$

where

$$\frac{\bar{D}}{\bar{D}t} \equiv \frac{\partial}{\partial t} + \bar{U}_i \frac{\partial}{\partial x_i}. \quad (4.118)$$

Rather than assuming the satisfaction of the mean continuity equation (Eq. 4.109), we define the function $\chi(\underline{x}, t)$ by

$$\langle \rho \rangle \chi(\underline{x}, t) \equiv \frac{\partial \langle \rho \rangle}{\partial t} + \frac{[\langle \rho \rangle \bar{U}_i]}{\partial x_i}. \quad (4.119)$$

Then $\chi = 0$ is a necessary and sufficient condition for the continuity equation to be satisfied. Obtaining $\partial \bar{U}_i / \partial x_i$ from this equation and substituting into Eq. (4.117) yields:

$$\frac{\bar{D} \ln q}{\bar{D}t} = \frac{\bar{D} \ln \langle \rho \rangle}{\bar{D}t} - \chi. \quad (4.120)$$

Since q and $\langle \rho \rangle$ are initially equal (for all \underline{x}), then it is obvious from Eq. (4.120) that they remain equal if and only if $\chi = 0$. Thus proposition (iii) is established.

The satisfaction of the mean continuity equation for all time is equivalent to the satisfaction of

$$\frac{\partial \chi}{\partial t} = 0, \quad (4.121)$$

with the initial condition $\chi(\underline{x}, t_0) = 0$. Differentiating Eq. (4.120) with respect to time we obtain

$$\begin{aligned} \frac{\partial \chi}{\partial t} &= \frac{\partial^2}{\partial t^2} \{ \langle \rho \rangle - q \} + \bar{U}_i \frac{\partial}{\partial x_i} \frac{\partial}{\partial t} \{ \langle \rho \rangle - q \} \\ &\quad + \frac{\partial \bar{U}_i}{\partial t} \frac{\partial}{\partial x_i} \{ \langle \rho \rangle - q \}. \end{aligned} \quad (4.122)$$

Suppose that at time t the consistency condition ($\langle \rho \rangle = q$) and the continuity equation ($\chi = 0$) are satisfied. Then the last term in Eq. (4.122) is clearly zero, and so also is the next to last term. This follows since (for the case considered) Eq. (4.120) yields $\partial / \partial t (\langle \rho \rangle - q) = 0$. Thus in order to satisfy Eq. (4.121) and

hence the continuity equation we require

$$\frac{\partial^2}{\partial t^2} \{ \langle \rho \rangle - q \} = 0. \quad (4.123)$$

We now show that this equation is satisfied if, and only if, the mean pressure satisfies a Poisson equation, (Eq. 4.129).

For a fluid particle with state $\underline{U}^+(t)$, $\underline{\phi}^+(t)$, $\underline{x}^+(t)$, the velocity evolves by (see Eq. 3.3)

$$\frac{\partial U_j^+}{\partial t} = -\rho(\underline{\phi}^+)^{-1} \left\{ \frac{\partial p}{\partial x_j} - \frac{\partial \tau_{ij}}{\partial x_i} \right\}_{x^+} + g_j.$$

Thus in a small time interval δt , the velocity increment $\Delta_{\delta t} \underline{U}^+$ due to the mean pressure gradient is

$$-\delta t \rho(\underline{\phi}^+)^{-1} [\nabla \langle p \rangle]_{x^+}.$$

We consider, then, the general model for the velocity increment of a stochastic particle:

$$\Delta_{\delta t} \underline{U}^*(t) = -\delta t \rho(\underline{\phi}^*)^{-1} [\nabla \langle p \rangle]_{x^*} + \underline{\alpha}_{\delta t}. \quad (4.124)$$

The first term on the right-hand side represents the effect of the mean pressure gradient. The random function $\underline{\alpha}_{\delta t}$ can depend upon the state variables $\underline{U}^*(t)$, $\underline{\phi}^*(t)$, $\underline{x}^*(t)$ and time. The corresponding Eulerian mean momentum equation is obtained by deriving the appropriate equation for $F^*(\underline{V}, \underline{\psi}, \underline{x}; t)$, multiplying by V_j , and integrating over all \underline{V} and $\underline{\psi}$. The result is

$$\frac{\partial}{\partial t} (q \widetilde{U}_j) = -\frac{\partial}{\partial x_i} (q \widetilde{U}_i \widetilde{U}_j) - \frac{q}{\langle \rho \rangle} \frac{\partial \langle p \rangle}{\partial x_j} + q \widetilde{A}_j^0 \quad (4.125)$$

where†

$$\widetilde{A}^0(\underline{x}, t) \equiv \langle \rho \rangle^{-1} \lim_{\delta t \rightarrow 0} \{ \langle \rho \underline{\alpha}_{\delta t} \rangle / \delta t \}. \quad (4.126)$$

From Eq. (4.116) we obtain

$$-\frac{\partial q^2}{\partial t^2} = \frac{\partial}{\partial x_j} \frac{\partial}{\partial t} (q \widetilde{U}_j). \quad (4.127)$$

Adding $\partial^2 \langle \rho \rangle / \partial t^2$ to both sides and using Eq. (4.125) to substitute for $\partial / \partial t (q \widetilde{U}_j)$ yields

$$\begin{aligned} \frac{\partial^2}{\partial t^2} \{ \langle \rho \rangle - q \} &= \frac{\partial^2 \langle \rho \rangle}{\partial t^2} - \frac{\partial^2 (q \widetilde{U}_i \widetilde{U}_j)}{\partial x_i \partial x_j} \\ &\quad - \frac{\partial}{\partial x_j} \left(\frac{q}{\langle \rho \rangle} \frac{\partial \langle p \rangle}{\partial x_j} \right) + \frac{\partial}{\partial x_j} (q \widetilde{A}_j^0). \end{aligned} \quad (4.128)$$

In order to satisfy Eq. (4.123), the right-hand side of Eq. (4.128) must be zero. For the case considered (in which $[\langle \rho \rangle - q]$, but not necessarily its temporal derivatives, is zero), this condition leads to the Poisson equation

$$\frac{\partial^2 \langle p \rangle}{\partial x_j \partial x_j} = \frac{\partial^2 \langle \rho \rangle}{\partial t^2} - \frac{\partial^2 \langle \rho U_i U_j \rangle}{\partial x_i \partial x_j} + \frac{\partial \langle \rho \rangle}{\partial x_j} \widetilde{A}_j^0. \quad (4.129)$$

† It may be seen that in order for the mean momentum to evolve continuously, the limit $\lim_{\delta t \rightarrow 0} \langle \underline{\alpha}_{\delta t} \rangle / \delta t$ must exist. This does not imply that $\lim_{\delta t \rightarrow 0} \underline{\alpha}_{\delta t} / \delta t$ exists: indeed this limit exists for neither Poisson nor diffusion processes.

To summarize this development: if, and only if, the mean pressure satisfies Eq. (4.129) then, in turn, Eqs (4.123), (4.121) and the mean continuity equation, Eq. (4.109) are satisfied, thus establishing proposition (iv).

The starting point for this derivation of the Poisson equation for $\langle p \rangle$ is the general model for a stochastic particle, Eq. (4.124). The result is valid even if \underline{U}^* is not a differentiable function of time. For the more familiar but less general case of fluid particles, the same equation is readily derived. From Eq. (3.3) we have

$$\frac{\partial \rho U_j}{\partial t} + \frac{\partial}{\partial x_i} (\rho U_i U_j) = -\frac{\partial \langle p \rangle}{\partial x_j} + \rho A_j^0, \quad (4.130)$$

where

$$\rho A_j^0 \equiv \frac{\partial \tau_{ij}}{\partial x_i} - \frac{\partial p'}{\partial x_j} + \rho g_j. \quad (4.131)$$

(This redefinition of A^0 is, for the case considered, consistent with definition (4.126).) The Poisson equation, Eq. (4.129) is obtained by taking the mean of Eq. (4.130), differentiating with respect to x_j , and substituting

$$\frac{\partial}{\partial x_j} \frac{\partial}{\partial t} \langle \rho U_j \rangle = -\frac{\partial^2 \langle \rho \rangle}{\partial t^2}, \quad (4.132)$$

which is obtained from the continuity equation.

Finally, we note that the mean continuity equation, Eq. (4.109), and the Poisson equation, Eq. (4.129), are kinematic equations. That is, they hold at each time t independent of the past or future. For a constant-density Newtonian fluid this is obvious because the equations reduce to

$$\nabla \cdot \langle \underline{U} \rangle = 0, \quad (4.133)$$

and

$$\nabla^2 \langle p \rangle = -\rho \frac{\partial^2 \langle U_i U_j \rangle}{\partial x_i \partial x_j}. \quad (4.134)$$

But in variable-density flow, the occurrence of $\partial \langle \rho \rangle / \partial t$ and $\partial^2 \langle \rho \rangle / \partial t^2$ in Eqs (4.109) and (4.129) suggests the contrary. However, the time derivatives of $\langle \rho \rangle$ can be re-expressed solely in terms of the fields at time t .

From Eqs (3.20) and (3.21) we obtain

$$\begin{aligned} \frac{\partial \rho}{\partial t} &= \frac{\partial}{\partial t} \rho(\underline{\phi}[\underline{x}, t]) \\ &= L_a(\underline{\phi}) \frac{\partial \phi_a}{\partial t} \\ &= L_a(\underline{\phi}) \left\{ -U_i \frac{\partial \phi_a}{\partial x_i} - \frac{1}{\rho} \frac{\partial J_i^a}{\partial x_i} + S_a(\underline{\phi}) \right\}, \end{aligned} \quad (4.135)$$

where

$$L_a(\underline{\psi}) \equiv \frac{\partial}{\partial \psi_a} \rho(\underline{\psi}). \quad (4.136)$$

Each quantity on the right-hand-side of Eq. (4.135) can be evaluated from the fields $\underline{U}(\underline{x}, t)$ and $\underline{\phi}(\underline{x}, t)$ independent of their rates of change. By the same

method an expression for $\partial^2\rho/\partial t^2$ can be derived, and hence it may be seen that $\partial\langle\rho\rangle/\partial t$ and $\partial^2\langle\rho\rangle/\partial t^2$ can be determined from the dependent variables at a single time.

(The conclusion that the pressure is determined kinematically stems from the assumption that the density is independent of pressure. Without this assumption there would be an acoustic pressure field that is not kinematically determined.)

4.8. Summary

We have considered several different systems of particles. The *fluid particle* originating from \underline{x}_0 at time t_0 has the state $\underline{U}^+(\underline{x}_0, t)$, $\underline{\phi}^+(\underline{x}_0, t)$, $\underline{x}^+(\underline{x}_0, t)$, which evolves according to Eq. (4.19). Fluid particle paths are sketched on Fig. 4.2.

The Lagrangian conditional joint pdf $f_L(\underline{V}, \underline{\psi}, \underline{x}; t | \underline{V}_0, \underline{\psi}_0, \underline{x}_0)$ is the joint pdf of the fluid particle state $(\underline{U}^+, \underline{\phi}^+, \underline{x}^+)$ at time t , conditional upon its state being $(\underline{V}_0, \underline{\psi}_0, \underline{x}_0)$ at time t_0 . This is the transition density for turbulent reactive flows: the mass density function at time t , $\mathcal{F}(\underline{V}, \underline{\psi}, \underline{x}; t)$, is equal to the mass-probability-weighted integral of f_L over all initial states, Eq. (4.24).

Conditional particles evolve deterministically with the same pdf as fluid particles. From the initial state $(\underline{V}_0, \underline{\psi}_0, \underline{x}_0)$ at time t_0 , the state $(\underline{U}, \underline{\phi}, \underline{x})$ of a conditional particle evolves according to Eq. (4.49). The rate of change of state of a conditional particle is the conditional expectation of the rate of change of state of fluid particles with the same state. The solution to the joint pdf equation can be formally written in terms of conditional particle states, Eqs (4.52) and (4.56).

Many different systems of particles evolve with the same pdf. The essence of the whole approach is to construct a system of *stochastic particles* whose evolution is simply computed and in which the pdf evolves in the same way as the pdf of fluid particles. The stochastic particle originating from \underline{x}_0 at time t_0 has the state $(\underline{U}^*, \underline{\phi}^*, \underline{x}^*)$ with the corresponding pdf $f_L^*(\underline{V}, \underline{\psi}, \underline{x}; t)$.

In a *Poisson process*, the state of a stochastic particle is constant except at a finite number of time-points where it changes abruptly; see, for example, Fig. 4.5. For a *diffusion process*, in the small time interval δt , the change of state of a stochastic particle has two components: a deterministic component of order δt , and a random component with zero mean and standard deviation of order $(\delta t)^{1/2}$. The state variables are continuous but non-differentiable functions of time: see, for example, Fig. 4.7.

Equations (4.99–101) provide an example of a combined Poisson and diffusion process. The corresponding pdf equation for f_L^* , Eq. (4.103), shows that the Poisson process gives rise to integrals over state space, whereas the diffusion process leads to a term corresponding to diffusion of the pdf in state space.

The task of modelling is to devise a stochastic process such that the pdf f_L^* of the stochastic particles evolves in the same way as the pdf f_L of fluid particles.

Then the corresponding mass density functions \mathcal{F}^* and \mathcal{F} will also have the same evolution. To solve the evolution equation for \mathcal{F}^* directly would be a prohibitively difficult computational task. But it is straightforward to compute the evolution of a large number of stochastic particles which, through the discrete representation Eq. (4.98), approximate the mass density function \mathcal{F}^* .

The mass density function \mathcal{F} satisfies realizability, normalization and consistency conditions, Eqs (4.106–108). The modelled mass density function \mathcal{F}^* also satisfies these conditions provided that

- (i) the model can be expressed in terms of the evolution of the discrete mass density function; and
- (ii) the mean pressure is determined by the Poisson equation, Eq. (4.129).

5. MODELLING

In a turbulent reactive flow, the evolution equation for the joint pdf $f(\underline{V}, \underline{\psi}; \underline{x}, t)$ is (see Eq. 3.109):

$$\begin{aligned} \rho(\underline{\psi}) \frac{\partial f}{\partial t} + \rho(\underline{\psi}) V_j \frac{\partial f}{\partial x_j} &+ \left(\rho(\underline{\psi}) g_j - \frac{\partial \langle p \rangle}{\partial x_j} \right) \frac{\partial f}{\partial V_j} + \frac{\partial}{\partial \psi_x} [\rho(\underline{\psi}) S_x(\underline{\psi}) f] \\ &= \frac{\partial}{\partial V_j} \left[\left\langle -\frac{\partial \tau_{ij}}{\partial x_i} + \frac{\partial p'}{\partial x_j} \right| \underline{V}, \underline{\psi} \right\rangle f + \frac{\partial}{\partial \psi_x} \left[\left\langle \frac{\partial J_i^a}{\partial x_i} \right| \underline{V}, \underline{\psi} \right\rangle f \right]. \end{aligned} \quad (5.1)$$

The mean pressure $\langle p \rangle$ is obtained from the Poisson equation, (Eq. 4.129), and $\rho(\underline{\psi})$ and $S(\underline{\psi})$ are known functions. Thus all the terms on the left-hand side of Eq. (5.1) are in closed form. The three conditional expectations containing τ_{ij} , p' and J_i^a need to be modelled while the remaining terms are known. Before considering the terms to be modelled, we emphasize that no modelling is needed for the terms pertaining to reaction, the mean pressure gradient, buoyancy, or transport in physical space.

In this section, models for the three conditional expectations are presented. The emphasis is on the form of the models, their qualitative performance, and how they affect the solution procedure.

In Section 5.1, the general principles that guide the modelling are outlined. In order to demonstrate the qualitative features of different types of models, in Section 5.2, deterministic, particle-interaction, and Langevin models are presented for the effect of molecular diffusion on the pdf $f_\phi(\underline{\psi})$ of a single composition. A combined deterministic and particle-interaction model for the velocity joint pdf $f_u(\underline{V})$ is presented in Sections 5.3 and 5.4; and the generalized Langevin model for $f_u(\underline{V})$ is described in Section 5.5. In Section 5.6 the models for $f_\phi(\underline{\psi})$ and $f_u(\underline{V})$ are combined and extended to apply to the joint pdf $f(\underline{V}, \underline{\psi})$. The models presented in Sections 5.2–5.6 are for inert, constant-density, high-Reynolds-number,

homogeneous turbulence. The development of more accurate and general models is an active area of current and future research which is discussed in Section 5.7.

For the homogeneous flows considered in Sections 5.2–5.6, the joint pdf $f(\underline{V}, \underline{\psi}; \underline{x}, t)$ is found to be a joint normal distribution.⁶² The aim of the modelling is, therefore, to produce Gaussian pdf's whose first and second moments evolve correctly.

The joint pdf $f(\underline{V}, \underline{\psi}; \underline{x}, t)$ contains no information about the time or length scales of the turbulent fluctuations: such information must be supplied. All the models presented involve a turbulent time scale $\tau(\underline{x}, t)$ defined by

$$\tau = k/\varepsilon, \quad (5.2)$$

where $k(\underline{x}, t)$ is the turbulent kinetic energy

$$k = \frac{1}{2} \langle u_i u_i \rangle = \int \int \frac{1}{2} (V_i - \langle U_i \rangle) (V_i - \langle U_i \rangle) f d\underline{V} d\underline{\psi}, \quad (5.3)$$

and ε is the rate of dissipation of k ,

$$\varepsilon = \left\langle \tau'_{ij} \frac{\partial U_j}{\partial x_i} \right\rangle / \rho. \quad (5.4)$$

(Here, and until Section 5.7, constant density is assumed.) Since k is known as a function of f , the time scale τ can be obtained by solving a modelled transport equation for ε .¹⁰ Alternatively, in simple flows, τ (or the length scale $k^{1/2}\tau$) can be specified directly. There is further discussion concerning the determination of τ in Section 5.7.3.

5.1. Guiding Principles

The modelling process consists of replacing exact but unknown quantities in the joint pdf equation with approximations in terms of known quantities. For each of the exact quantities to be modelled (and for the pdf equation itself) several quite general properties can be deduced, usually by examining the effects of various transformations. The modelling is guided by the requirement that the modelled quantities have the same properties as their exact counterparts.

The six principles that have guided the modelling presented here are:

- (i) dimensional consistency,
- (ii) coordinate system independence,
- (iii) Gallilean invariance,
- (iv) realizability,
- (v) linearity and independence of conserved passive scalars, and
- (vi) boundedness of compositions.

The velocity $\underline{U}_{\text{ref}}$ (at a reference point and time) in a flow can be expressed in various units (e.g. m/sec, ft/hr etc.), and the reference point can be expressed in various coordinate systems. But the physical process (i.e. the flow), being oblivious of these human con-

structs, is invariant under a change of units and under a change of coordinate system. Principles (i) and (ii) guarantee that the model equations also have these properties. Dimensional consistency simply requires that the exact and modelled terms have the same dimensions. Coordinate system independence is guaranteed provided that the exact and modelled terms can be written as Cartesian tensors with the same suffices.

The principle of Gallilean invariance states that (in Newtonian mechanics) the equations of motion are invariant under a change of inertial frame. Consequently, under such a change, exact and modelled terms must transform in the same way.

Schumann⁷⁷ introduced the realizability principle into turbulence modelling and it has subsequently been used by several authors (e.g. Ref. 11). In fact the ideas introduced by Schumann can be made more precise by distinguishing between three different principles: *weak realizability*; *strong realizability*; and the *accessibility of extreme states*. These principles are now described and illustrated.

The weak realizability principle states that if a physical quantity (q , say) satisfies an inequality (e.g. $q > 0$), then the value of the quantity obtained from the model equations should satisfy the same inequality. Examples of such inequalities are

$$\mathcal{F}(\underline{V}, \underline{\psi}) \geq 0, \quad (5.5)$$

and

$$\langle u_1 u_1 \rangle \geq 0, \quad (5.6)$$

where $\underline{u} \equiv \underline{U} - \langle \underline{U} \rangle$.

Equation (5.5) is the principal weak realizability condition that the mass density function (or equivalently the joint pdf) has to satisfy. If Eq. (5.5) is satisfied, then all weak realizability conditions applicable to moments (e.g. Eq. 5.6) are also satisfied. As is pointed out in Section 4.7, the discrete representation of the mass density function satisfies Eq. (5.5), and hence any model that can be expressed in terms of its evolution satisfies the weak realizability condition. All the models presented below satisfy this condition. Another weak realizability condition to be satisfied by the mass density function is the boundedness of compositions, principle (vi). This is discussed separately.

The strong realizability condition is concerned with behavior of physical quantities in extreme states. If the physical quantity $q(t)$ satisfies the inequality

$$q \geq 0, \quad (5.7)$$

then, by definition, $q = 0$ is an extreme state. Now if, at some time t_1 , q attains its extreme value (i.e. $q(t_1) = 0$) then its rate of change at t_1 must also be zero—for if not, either q will be negative at the next instant of time, or, contrary to assumption, q is not a differentiable function of time. Equation (5.7) then implies

$$\left(\frac{\partial q}{\partial t} \right)_{q=0} = 0. \quad (5.8)$$

In general, the *strong realizability principle* is that the rate of change of a physical quantity in an extreme state is zero.

Suppose that the evolution of q is modelled by the equation

$$\frac{dq}{dt} = R(q[t], r[t]), \quad (5.9)$$

where r is some other physical quantity, and the specific model is defined by the choice of the function R . If $q(t) = 0$, then the strong realizability principle requires

$$R(0, r[t]) = 0. \quad (5.10)$$

But consider a model for which

$$R(0, r[t]) > 0. \quad (5.11)$$

In this case the extreme state $q(t) = 0$ cannot be reached (except as the initial condition) and so the strong realizability principle Eq. (5.8) is not violated, but it becomes mute. Thus we conclude that the strong realizability condition is not violated by a model for which

$$R(0, r[t]) \geq 0. \quad (5.12)$$

We introduce the *principle of the accessibility of extreme states*, according to which a model equation should allow the extreme states to be reached. Equation (5.10) is then a necessary condition for this principle to be satisfied. But, unlike the realizability principles, there is no fundamental reason why we should demand that the accessibility principle be satisfied.

The models presented here conform to Eq. (5.12) rather than (5.10). Thus the strong realizability condition is not violated but the extreme states may be inaccessible. The extreme states generally considered are two-dimensional turbulence,^{11,78} and the perfect correlation of the velocity and scalar fields.^{11,79} Since neither of these states is likely to exist in the turbulent reactive flows being considered, their accessibility is most likely not an important consideration.

The fifth and sixth guiding principles are concerned with the modelling of the scalars $\phi(\underline{x}, t)$. In a reactive flow each scalar may have a different source $S_a(\phi)$ and a different molecular transport term. But the modelled pdf equation should be applicable to the simpler case of ϕ being a set of conserved passive scalars with the same diffusivities: that is,

$$S(\phi) = 0, \quad (5.13)$$

$$J_i^a = -\Gamma \frac{\partial \phi_a}{\partial x_i}, \quad (5.14)$$

with the diffusivity Γ and the density ρ being constant. For this simple case, each scalar evolves independently according to the same equation that is linear in ϕ .

By considering linear transformations of the set of scalars ϕ , Pope⁸⁰ deduced constraints on the construction of consistent closure approximations. For scalar moments (e.g. for $\langle u_i \phi_a \rangle$ or $\langle \phi_a \phi_b \rangle$), the evolu-

tion equations must be homogeneous (i.e. the same scalar suffices must appear in each term, including any repeated suffices).

In pdf models, the linearity and independence conditions are simply stated in terms of the scalar increment. If the modelled mass density function $\mathcal{F}^*(\underline{V}, \underline{\psi}, \underline{x}; t)$ is represented by N stochastic particles with the n th having the composition $\phi^{*(n)}(t)$, then the increment

$$\Delta_{\delta t} \phi_x^{*(n)}(t) \equiv \phi_x^{*(n)}(t + \delta t) - \phi_x^{*(n)}(t), \quad (5.15)$$

must be a linear function of $\phi_x^{*(n)}$ ($n = 1, 2, \dots, N$), independent of any other scalar property (e.g. $\langle \phi_a \phi_b \rangle$). The models presented below satisfy this condition.

As discussed in Section 3.2, composition variables are usually bounded. For example, if ϕ_x is a species mass fraction, then

$$0 \leq \phi_x \leq 1. \quad (5.16)$$

Consequently there is an allowed region of composition space corresponding to possible values of ϕ . Outside the allowed region the joint pdf $f(\underline{V}, \underline{\psi}; \underline{x}, t)$ is zero. Clearly a modelled pdf equation should preserve this property.

5.2. Scalar Dissipation

In order to examine the qualitative performance of linear deterministic models, particle-interaction models, and Langevin models, we consider the effect of molecular diffusion on the pdf of a conserved passive scalar. This allows general conclusions to be drawn (Section 5.2.5) about the use of these models in pdf methods.

5.2.1. Exact equations

We consider the simple case of the evolution of the pdf $f_a(\psi; t)$ of a single conserved passive scalar $\phi(\underline{x}, t)$ in constant-density homogeneous turbulence. There are no mean gradients (of $\langle \underline{U} \rangle$ or $\langle \phi \rangle$) and the coordinate system is chosen so that the mean velocity is zero.

Before examining the behavior of the pdf, we consider the evolution of the mean $\langle \phi \rangle$ and the variance $\langle \phi^2 \rangle$. Assuming simple gradient diffusion, with Γ being the constant diffusion coefficient, the molecular flux of ϕ is

$$J_i = -\Gamma \frac{\partial \phi}{\partial x_i}. \quad (5.17)$$

Then, the transport equation for $\phi(\underline{x}, t)$ (Eq. 3.20) is:

$$\rho \frac{D\phi}{Dt} = \Gamma \nabla^2 \phi. \quad (5.18)$$

For the case considered, the mean of this equation is

$$\frac{d\langle \phi \rangle}{dt} = 0, \quad (5.19)$$

showing that the mean $\langle \phi \rangle$ remains constant. An equation for the variance $\langle \phi^2 \rangle$ is obtained by multi-

plying Eq. (5.18) by ϕ and taking the mean:

$$\frac{1}{2} \frac{d\langle\phi'^2\rangle}{dt} = -\varepsilon_\phi, \quad (5.20)$$

where the scalar dissipation is

$$\varepsilon_\phi = (\Gamma/\rho) \left\langle \frac{\partial\phi'}{\partial x_i} \frac{\partial\phi'}{\partial x_i} \right\rangle. \quad (5.21)$$

Since ε_ϕ is positive, it is evident that the variance $\langle\phi'^2\rangle$ decays.

Just as $\tau = k/\varepsilon$ is the decay time scale of the velocity fluctuations, $\tau_\phi \equiv \frac{1}{2}\langle\phi'^2\rangle/\varepsilon_\phi$ is the decay time scale of the scalar fluctuations. The determination of ε_ϕ is discussed in Section 5.7.3. For the moment we adopt Spalding's suggestion⁸¹ that τ and τ_ϕ are proportional:

$$\tau_\phi = \tau/C_\phi, \quad (5.22)$$

where the empirical constant C_ϕ is taken to be 2.0. Thus,

$$\varepsilon_\phi = \frac{1}{2}C_\phi\langle\phi'^2\rangle/\tau. \quad (5.23)$$

Defining the non-dimensional time t^* by

$$dt^* = dt/\tau, \quad (5.24)$$

the equation for the variance (Eq. 5.20) becomes

$$\frac{d\langle\phi'^2\rangle}{dt^*} = -C_\phi\langle\phi'^2\rangle, \quad (5.25)$$

which, with the initial condition of $\langle\phi'^2\rangle_0$ at $t^* = 0$, has the solution

$$\langle\phi'^2\rangle = \langle\phi'^2\rangle_0 \exp(-C_\phi t^*). \quad (5.26)$$

If the pdf of ϕ , $f(\psi; t)$, is Gaussian then it is completely determined by the (constant) mean $\langle\phi\rangle$ and the variance $\langle\phi'^2\rangle$:

$$f_\phi(\psi) = (2\pi\langle\phi'^2\rangle)^{-1/2} \exp(-\frac{1}{2}[\psi - \langle\phi\rangle]^2/\langle\phi'^2\rangle). \quad (5.27)$$

A satisfactory modelled pdf equation should admit this Gaussian pdf as a solution.

The evolution equation for $f_\phi(\psi; t)$ is obtained from the equation for $f(\underline{V}, \psi; \underline{x}, t)$ (Eq. 3.109) by integrating over velocity space and invoking the conditions of constant density and statistical homogeneity:

$$\rho \frac{\partial f_\phi}{\partial t} = \frac{\partial}{\partial \psi} \left[f_\phi \left\langle \frac{\partial J_i}{\partial x_i} \right| \psi \right], \quad (5.28)$$

or

$$\frac{\partial f_\phi}{\partial t} = -\frac{\partial}{\partial \psi} [f_\phi \langle (\Gamma/\rho) \nabla^2 \phi | \psi \rangle]. \quad (5.29)$$

It may be seen that the evolution of the pdf depends entirely upon the conditional expectation $\langle (\Gamma/\rho) \nabla^2 \phi | \psi \rangle$ which is to be modelled.

5.2.2. Deterministic model

Dopazo⁸³ suggested the following deterministic model:

$$\langle (\Gamma/\rho) \nabla^2 \phi | \psi \rangle = -\frac{1}{2}C_\phi(\psi - \langle\phi\rangle)/\tau. \quad (5.30)$$

The behavior of the model is best understood in terms of the corresponding equation for a conditional particle:

$$\frac{d\hat{\phi}}{dt^*} = -\frac{1}{2}C_\phi(\hat{\phi} - \langle\phi\rangle). \quad (5.31)$$

In composition space (ψ -space) the conditional particle moves towards the mean $\langle\phi\rangle$ at a rate proportional to its distance (in ψ -space) from the mean $\langle\phi\rangle$. Thus, as time proceeds, the conditional paths converge to the location $\psi = \langle\phi\rangle$. The constant of proportionality $\frac{1}{2}C_\phi$ is chosen to yield the correct decay rate of the variance.

This model is attractive in its simplicity, and it is straightforward to verify that the modelled pdf equation admits the Gaussian solution Eq. (5.27) as it should. But in general its qualitative behavior is incorrect.⁸² From the arbitrary initial condition

$$f(\psi; 0) = \langle\phi'^2\rangle_0^{-1/2} g([\psi - \langle\phi\rangle] \langle\phi'^2\rangle_0^{-1/2}), \quad (5.32)$$

(where g is an arbitrary standardized pdf) the solution to the modelled pdf equation is

$$f(\psi; t) = \langle\phi'^2\rangle^{-1/2} g([\psi - \langle\phi\rangle] \langle\phi'^2\rangle^{-1/2}). \quad (5.33)$$

(The mean $\langle\phi\rangle$ remains constant and the variance $\langle\phi'^2\rangle$ decays according to Eq. 5.26.) As is readily seen, the model predicts that the shape of the pdf remains unchanged during decay, and consequently, from an arbitrary initial pdf, there is no relaxation to a Gaussian distribution. This incorrect behaviour might be expected since the model contains no information about the shape of the distribution—only the mean $\langle\phi\rangle$ appears in Eq. (5.30).

In order for arbitrary pdf's to relax, the model must contain information about the shape of the distribution. Such models have been proposed by Pope,²⁴ Janicka *et al.*²⁶ and Dopazo.⁸³ In each case the model contains functions of the pdf integrated over composition space. The nonlinear and integral nature of the resulting pdf equation, prohibits analytical solutions. Numerical solutions can be obtained, but only for one-dimensional (and possibly, two-dimensional) composition spaces. For flows with many species, and hence a composition space of large dimension, the computational work needed to perform the integration over ψ -space is prohibitive.³² Fortunately, the same result can be obtained by computationally-efficient stochastic models.

5.2.3. Particle-interaction model

Consider the discrete representation in which the pdf $f_\phi(\psi)$ is represented by N delta functions:

$$f_{\phi N}^*(\psi; t) \equiv \frac{1}{N} \sum_{n=1}^N \delta(\psi - \phi^{*(n)}(t)). \quad (5.34)$$

The discrete pdf evolves by the N stochastic particles $\phi^{*(n)}$ moving in ψ -space.

We now describe a stochastic mixing model (similar to a Poisson process) that simulates scalar dissipation.

In a small interval of time δt , there is a small probability that a pair of stochastic particles will "mix". The time τ_N is defined by

$$\tau_N \equiv \tau/(C_\phi N). \quad (5.35)$$

Then in the time interval δt , with probability $1 - \delta t/\tau_N$, the compositions of all the stochastic particles do not change; but, with probability $\delta t/\tau_N$, the compositions of a pair of particles change. These two particles (denoted by p and q) are selected at random without replacement and their values of ϕ^* are replaced by their common mean $\frac{1}{2}(\phi^{*(p)} + \phi^{*(q)})$. (Sampling without replacement simply means that p and q may not be the same particle.) This stochastic model can be written

with probability $1 - \delta t/\tau_N$:

$$\phi^{*(n)}(t + \delta t) = \phi^{*(n)}(t), \quad n = 1, 2, \dots, N; \quad (5.36)$$

with probability $\delta t/\tau_N$:

$$\phi^{*(p)}(t + \delta t) = \phi^{*(q)}(t + \delta t) = \frac{1}{2}[\phi^{*(p)}(t) + \phi^{*(q)}(t)],$$

and

$$(5.37)$$

$$\phi^{*(n)}(t + \delta t) = \phi^{*(n)}(t), \quad n = 1, 2, \dots, N, \quad n \neq p, n \neq q.$$

It is important to realize that this stochastic process is not a direct model of the physical process—a fluid particle does not change its composition discontinuously at discrete times. Rather, Eqs (5.36–37) define a stochastic system whose *expected* state corresponds to the *expected* state of the physical system. The pdf for the stochastic system

$$f_\phi^*(\psi; t) \equiv \mathbf{E} \frac{1}{N} \sum_{n=1}^N \delta(\psi - \phi^{*(n)}(t)), \quad (5.38)$$

evolves continuously and deterministically, and models the evolution of the pdf $f_\phi(\psi)$. If the model is accurate then f_ϕ^* is equal to f_ϕ and the stochastic system is equivalent to the physical system. Then, consistent with Eq. (5.38), the mean of a function of ϕ , $\langle Q(\phi) \rangle$, is equal to the expectation of the ensemble average of $Q(\phi^{*(n)})$:

$$\langle Q(\phi) \rangle = \mathbf{E} \frac{1}{N} \sum_{n=1}^N Q(\phi^{*(n)}). \quad (5.39)$$

To every stochastic model there is a corresponding deterministic model. Using the techniques presented in Section 4.6, or by other means,^{84,85} the evolution equation for $f_\phi^*(\psi; t)$ corresponding to this model (Eqs 5.35–37) can be shown to be

$$\frac{\partial f_\phi^*(\psi; t)}{\partial t^*} = 2C_\phi \left\{ 2 \int f_\phi^*(\psi + \psi') f_\phi^*(\psi - \psi') d\psi' - f_\phi^*(\psi) \right\}. \quad (5.40)$$

(Note that the number of particles N does not appear in Eq. (5.40). It is shown below that the specification of τ_N by Eq. (5.35) produces the correct decay rate of

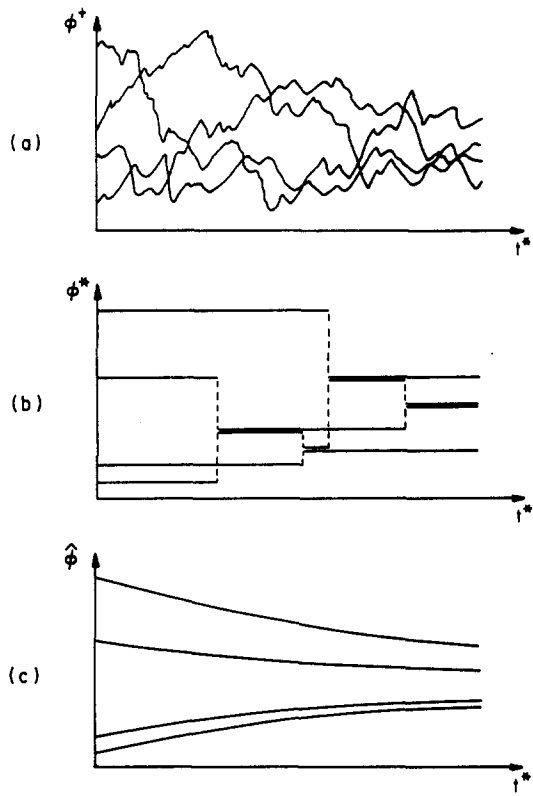


FIG. 5.1. Particle trajectories: (a) fluid particles; (b) stochastic particles; (c) conditional particles.

$\langle \phi'^2 \rangle$ independent of N .) All the well-behaved deterministic models proposed^{24,26,83–85} contain an integral over composition space such as that in Eq. (5.40). In a numerical solution, these integrals are computationally-expensive to perform, and consequently it is advantageous to use the stochastic model instead.

The distinct behaviour of fluid particles, stochastic particles and conditional particles is illustrated in Fig. 5.1. Fluid particle paths in ψ -space (Fig. 5.1a) are erratic with variations on all time scales down to the Kolmogorov scale. A stochastic particle path (Fig. 5.1b) is discontinuous since $\phi^{*(n)}$ is a piecewise constant function of t : the duration of the intervals of constancy is of order τ . Conditional paths (Fig. 5.1c) are uniquely determined, smooth and continuous. In each case the particle paths converge since the variance $\langle \phi'^2 \rangle$ decreases with time.

The preceding discussion is aimed at describing the nature of stochastic models and at establishing their connection to pdf equations. We now turn to examine the performance of the stochastic model defined by Eqs (5.35–37). This model, of which there are many variants, is variously called Curl's model, the coalescence/dispersal model, or the stochastic mixing model. The evolution of the mean $\langle \phi \rangle$ and variance $\langle \phi'^2 \rangle$ can be determined either from the pdf equation, Eq. (5.40), or by examining the model directly. It is instructive to adopt the latter approach.

The modelled mixing process does not affect the mean value of ϕ . From Eq. (5.39) we obtain

$$\langle \phi(t+\delta t) \rangle - \langle \phi(t) \rangle = E \left\{ \frac{1}{N} \sum_{n=1}^N [\phi^{*(n)}(t+\delta t) - \phi^{*(n)}(t)] \right\}. \quad (5.41)$$

If in the time interval δt there is no mixing then the sum in Eq. (5.41) is zero (see Eq. 5.36). If a pair of elements (p and q) mix, then the sum is again zero since, from Eq. (5.37), we have

$$\phi^{*(p)}(t+\delta t) + \phi^{*(q)}(t+\delta t) = \phi^{*(p)}(t) + \phi^{*(q)}(t). \quad (5.42)$$

Thus the model correctly leaves the mean $\langle \phi \rangle$ unaffected.

Since the mean is constant, a change in the variance $\langle \phi'^2 \rangle$ is the same as a change in $\langle \phi^2 \rangle$. In the time interval δt this is

$$\begin{aligned} \Delta_{\delta t} \langle \phi^2 \rangle &= \langle \phi^2(t+\delta t) \rangle - \langle \phi^2(t) \rangle \\ &= \frac{1}{N} E \left\{ \sum_{n=1}^N [\phi^{*(n)}(t+\delta t)]^2 - \sum_{n=1}^N [\phi^{*(n)}(t)]^2 \right\}. \end{aligned} \quad (5.43)$$

The only contribution to the right-hand side is from the particles p and q in the event that they mix. The probability of this event is $\delta t/\tau_N$. Thus

$$\begin{aligned} \Delta_{\delta t} \langle \phi'^2 \rangle &= \frac{\delta t}{N\tau_N} E \{ [\phi^{*(p)}(t+\delta t)]^2 + [\phi^{*(q)}(t+\delta t)]^2 \\ &\quad - [\phi^{*(p)}(t)]^2 - [\phi^{*(q)}(t)]^2 \} \\ &= \frac{C_\phi \delta t}{\tau} E \{ 2[\frac{1}{2}\phi^{*(p)}(t) + \frac{1}{2}\phi^{*(q)}(t)]^2 \\ &\quad - [\phi^{*(p)}(t)]^2 - [\phi^{*(q)}(t)]^2 \} \\ &= \frac{C_\phi \delta t}{\tau} E \{ -\frac{1}{2}[\phi^{*(p)}(t)]^2 - \frac{1}{2}[\phi^{*(q)}(t)]^2 \\ &\quad + \phi^{*(p)}(t)\phi^{*(q)}(t) \}. \end{aligned} \quad (5.44)$$

The second step follows from the definitions of τ_N and $\phi^{*(p)}(t+\delta t)$. Since $\phi^{*(p)}$ is an element selected at random from the ensemble, we have

$$E[\phi^{*(p)}]^2 = \langle \phi^2 \rangle = \langle \phi'^2 \rangle + \langle \phi \rangle^2, \quad (5.45)$$

and the same for $E[\phi^{*(q)}]^2$. On the other hand, since $\phi^{*(p)}$ and $\phi^{*(q)}$ are independent samples, we have

$$E\{\phi^{*(p)}\phi^{*(q)}\} = E\{\phi^{*(p)}\}E\{\phi^{*(q)}\} = \langle \phi \rangle^2. \quad (5.46)$$

Substituting these results in Eq. (5.44) and dividing by δt we obtain

$$\Delta_{\delta t} \langle \phi'^2 \rangle / \delta t = -C_\phi \langle \phi'^2 \rangle / \tau. \quad (5.47)$$

Hence, in the limit as δt tends to zero, the correct decay rate of $\langle \phi'^2 \rangle$ is obtained (cf. Eq. 5.25).

(In fact, rather than showing that Eq. 5.47 yields the correct decay rate, this analysis is used to determine the time τ_N (Eq. 5.35) that produces the correct result.)

As well as having the correct effect on the mean and variance, the stochastic mixing model causes arbitrary initial pdf's to relax to a bell-shaped curve. Unfortunately, this bell-shaped curve is significantly dif-

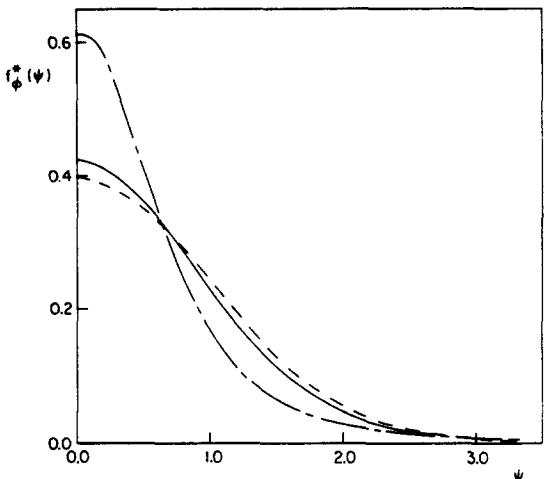


FIG. 5.2. Standardized pdf's $f_\phi^*(\psi)$ against ψ : --- Gaussian; —— standard stochastic mixing model; —— improved stochastic mixing model. ($f_\phi^*(\psi)$ is symmetric about $\psi = 0$: it is shown for $\psi \geq 0$ only.)

ferent from a Gaussian pdf. In particular the flatness factor $\langle \phi'^4 \rangle / \langle \phi'^2 \rangle^2$ for the mixing model's pdf is infinite whereas it is equal to 3 for a Gaussian. Pope⁶⁵ has developed an improved stochastic model that produces pdf's that are closer to Gaussian. Figure 5.2 shows the pdf's for the standard mixing model and for the improved model compared with a Gaussian.

Stochastic mixing models are readily extended to apply to a set of σ scalars, $\underline{\phi} = \phi_1, \phi_2, \dots, \phi_\sigma$. The joint pdf $f_{\underline{\phi}}(\underline{\psi}; t)$ is represented by N stochastic particles ($\underline{\phi}^{*(n)}$, $n = 1, 2, \dots, N$), and the mixing occurs by these particles moving in the σ -dimensional composition space. For the simple stochastic model described, two particles (p and q) are selected at random (in the same way as for a single scalar), and mixing occurs by:

$$\underline{\phi}^{*(n)}(t+\delta t) = \frac{1}{2}[\underline{\phi}^{*(p)}(t) + \underline{\phi}^{*(q)}(t)],$$

$$n = p \text{ or } n = q, \quad (5.48)$$

$$\underline{\phi}^{*(n)}(t+\delta t) = \underline{\phi}^{*(n)}(t), n \neq p \text{ and } n \neq q. \quad (5.49)$$

Figure 5.3 illustrates the mixing process given by Eq.

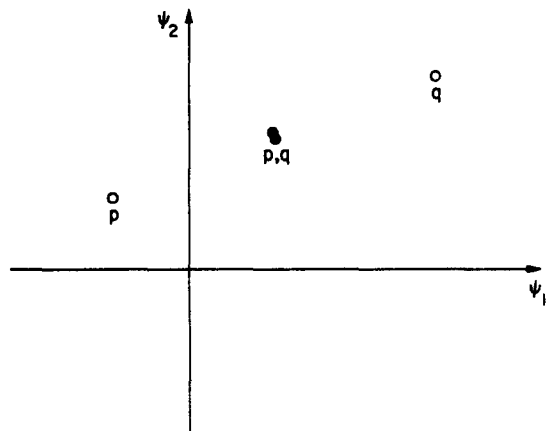


FIG. 5.3. Effect of mixing on the stochastic particles $\underline{\phi}^{*(p)}$ and $\underline{\phi}^{*(q)}$: \circ before mixing, \bullet after mixing.

(5.48) for a two-dimensional $(\psi_1 - \psi_2)$ composition space. After mixing, both the stochastic particles $\phi^{*(p)}$ and $\phi^{*(q)}$ lie half-way between their initial locations.

According to this simple mixing model the means and variances evolve by,

$$\frac{d\langle\phi_x\rangle}{dt} = 0, \quad (5.50)$$

and

$$\frac{d\langle\phi'_x\phi'_y\rangle}{dt^*} = -C_\phi\langle\phi'_x\phi'_y\rangle. \quad (5.51)$$

5.2.4. Langevin model

A model of scalar dissipation analogous to the Langevin equation is (cf. Eqs 4.81 and 4.91):

$$\Delta_{\delta t}\phi^*(t) = G[\phi^*(t) - \langle\phi(t)\rangle]\delta t/\tau + [B\langle\phi'^2\rangle/\tau]^{1/2}\Delta_{\delta t}W_t. \quad (5.52)$$

Here G and B are constants to be determined ($B > 0$), and W_t is a Weiner process. Thus the first term on the right-hand side of (5.52) represents a deterministic change in the composition of the stochastic particle; while the second term represents a random change of mean zero and variance $B\langle\phi'^2\rangle\delta t/\tau$.

Corresponding to this Langevin model, the evolution for the pdf $f_\phi^*(\psi; t)$ is (cf. Eq. 4.88)

$$\frac{\partial f_\phi^*}{\partial t^*} = -\frac{\partial}{\partial\psi}[f_\phi^*G(\psi - \langle\phi\rangle)] + \frac{1}{2}B\langle\phi'^2\rangle\frac{\partial^2 f_\phi^*}{\partial\psi^2}. \quad (5.53)$$

Multiplying this equation by $(\psi - \langle\phi\rangle)$ and integrating yields Eq. (5.19), showing that the mean $\langle\phi\rangle$ does not change. Alternatively, the same conclusion follows from the observation that the mean of Eq. (5.52) is simply

$$\Delta_{\delta t}\langle\phi^*(t)\rangle = 0. \quad (5.54)$$

The evolution of the variance $\langle\phi'^2\rangle$ can be determined either from Eq. (5.52) or by multiplying Eq. (5.53) by $(\psi - \langle\phi\rangle)^2$ and integrating. The result is

$$\frac{d\langle\phi'^2\rangle}{dt^*} = (2G + B)\langle\phi'^2\rangle. \quad (5.55)$$

By comparing this equation with the known decay rate, Eq. (5.25), we obtain a relationship between the constants:

$$G = -\frac{1}{2}(B + C_\phi). \quad (5.56)$$

Figures 5.4a and 5.4b show $\phi^*(t)$ according to the Langevin model, Eq. (5.52), for two different values of B —2.0 and 0.2 respectively. For both plots the same initial condition $\phi^*(0)$ was used and also the same sample of the Weiner process W_t , namely that shown on Fig. 4.7. A comparison of the figures illustrates the role of the constant B in determining the variance of the random fluctuations.

These plots of $\phi^*(t)$ according to the Langevin model can also be compared to the plots of $\phi^+(t)$,

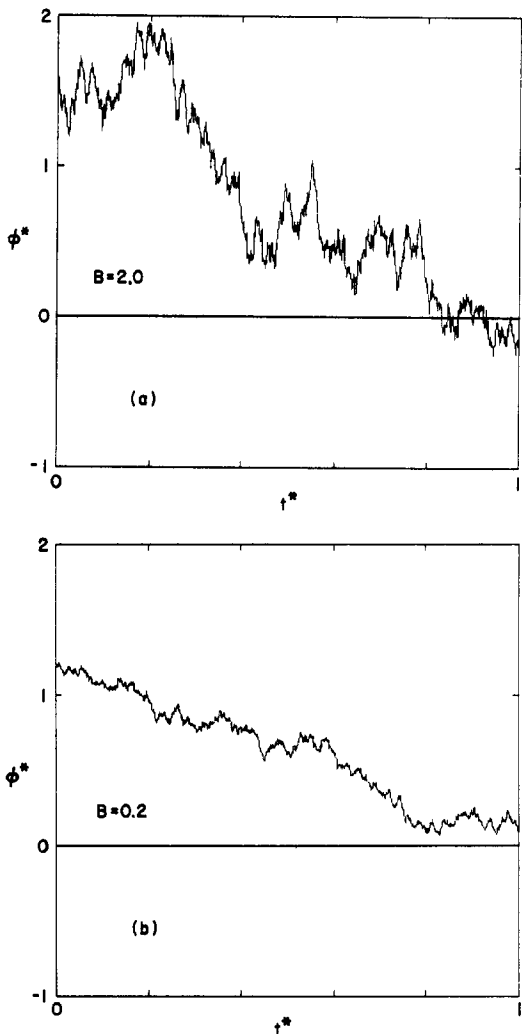


FIG. 5.4. Samples of $\phi^*(t)$ given by the Langevin model with (a) $B = 2.0$, (b) $B = 0.2$.

$\phi^*(t)$ and $\hat{\phi}(t)$ shown on Fig. 5.1. The behavior of $\phi^*(t)$ according to the Langevin model is similar to that of fluid particles. However $\phi^*(t)$ has fluctuation on all time scales whereas $\phi^+(t)$ has fluctuations only down to the Kolmogorov time scale.

The pdf admits the desired Gaussian solution, Eq. (5.27). Further it can be shown (by Fourier analysis) that from any initial condition the pdf relaxes to a Gaussian. The rate at which it relaxes depends on the value of B . (For $B = 0$, the Langevin equation, Eq. (5.52), reduces to the deterministic model Eq. (5.30) and there is no relaxation.)

The qualitative behavior of the Langevin model is satisfactory in all respects except one—it violates the principle of the boundedness of compositions. Because of the diffusive nature of Eq. (5.53), $f_\phi^*(\psi; t)$ is greater than zero for all values of ψ . Thus if ϕ were a bounded scalar (e.g. $\phi \geq 0$) then the boundedness condition would be violated since the pdf would be positive at values of ψ corresponding to impossible compositions (e.g. $\psi < 0$). (Note that Fig. 5.4a shows regions of negative ϕ^* .) For the simple one-dimen-

sional case considered, the Langevin equation could be modified to guarantee boundedness. But for the general case, such modifications would be prohibitively complicated.

5.2.5. Conclusion

From the preceding examination of deterministic, particle-interaction, and Langevin models, we can draw conclusions about their use in pdf methods.

Because of their simplicity, linear deterministic models (e.g. Eq. 5.30) are appealing, especially from a computational viewpoint. Since they do not cause the pdf shape to relax, they cannot be used alone. But they can be used in conjunction with other models. A linear deterministic model is used to model part of the pressure term (Section 5.4).

For the case considered (scalar dissipation) the Langevin model is, in general, inapplicable because it violates the principle of composition boundedness. Of the models described, only the particle interaction model is satisfactory in all respects. (The simple model described is unsatisfactory in that the pdf shapes obtained are far from Gaussian, but the improved mixing models⁸⁵ are satisfactory.) In the next subsection particle-interaction models for the velocity joint pdf are described.

Although the Langevin model is inapplicable to scalars, it is a good model for the velocities (which are not bounded). A generalized Langevin model for the joint pdf of velocity is presented in Section 5.5.

5.3. Energy Decay and the Return-to-Isotropy

We now turn our attention to the joint pdf of the velocities $f_{\underline{u}}(\underline{V}; t)$ for constant-density homogeneous turbulence with no mean velocity gradients. A good approximation to this flow is the turbulence generated by a uniform stream passing through a grid. In a coordinate system moving with the mean flow velocity, the two principal observations are that the turbulent kinetic energy decays,⁸⁶ and that the Reynolds stresses tend towards isotropy.⁸⁷

The evolution equation for the Reynolds stresses $\langle u_j u_k \rangle$ can be derived from the continuity and momentum equations (Eqs 3.2–3.3). Since the density is constant, the continuity equation (Eq. 3.2) becomes

$$\frac{\partial U_i}{\partial x_i} = 0. \quad (5.57)$$

By decomposing \underline{U} into its mean (in this case zero) and fluctuation \underline{u}

$$\underline{U}(\underline{x}, t) = \langle \underline{U}(\underline{x}, t) \rangle + \underline{u}(\underline{x}, t), \quad (5.58)$$

we obtain

$$\frac{\partial u_i}{\partial x_i} = 0. \quad (5.59)$$

With the assumption of a Newtonian fluid

$$\tau_{ij} = \mu \left(\frac{\partial U_i}{\partial x_j} + \frac{\partial U_j}{\partial x_i} \right), \quad (5.60)$$

the momentum equation (Eq. 3.3) becomes

$$\rho \frac{\partial u_j}{\partial t} + \rho u_i \frac{\partial u_j}{\partial x_i} = \mu \frac{\partial u_j}{\partial x_i \partial x_i} - \frac{\partial p'}{\partial x_j}. \quad (5.61)$$

(The mean pressure is uniform and, since the density is constant, there is no buoyancy effect.) The Reynolds-stress equation is obtained by multiplying Eq. (5.61) by u_k , adding the same equation with j and k commuted, and taking the mean. The result is

$$\rho \frac{\partial \langle u_j u_k \rangle}{\partial t} + \rho \frac{\partial \langle u_i u_j u_k \rangle}{\partial x_i} = \mu \langle u_k \nabla^2 u_j + u_j \nabla^2 u_k \rangle - \left\langle u_k \frac{\partial p'}{\partial x_j} + u_j \frac{\partial p'}{\partial x_k} \right\rangle. \quad (5.62)$$

Finally, making use of the fact that in homogeneous turbulence the spatial gradients of mean quantities ($\langle u_i u_j u_k \rangle$, $\langle u_j u_k \rangle$ and $\langle u_k p' \rangle$) are zero, we can write the Reynolds-stress equation as

$$\rho \frac{d}{dt} \langle u_j u_k \rangle = -\rho \varepsilon_{jk} + P_{jk}, \quad (5.63)$$

where the dissipation tensor is

$$\varepsilon_{jk} \equiv 2 \frac{\mu}{\rho} \left\langle \frac{\partial u_j}{\partial x_i} \frac{\partial u_k}{\partial x_i} \right\rangle, \quad (5.64)$$

and the pressure-rate-of-strain correlation is

$$P_{jk} \equiv \left\langle p' \left(\frac{\partial u_j}{\partial x_k} + \frac{\partial u_k}{\partial x_j} \right) \right\rangle. \quad (5.65)$$

Of course, the Reynolds-stress equation can also be derived from the joint pdf equation. This is achieved by multiplying the equation for $f(\underline{V}, \underline{\psi}; \underline{x}, t)$, Eq. (3.109), by $V_j V_k$, integrating over \underline{V} - $\underline{\psi}$ space and invoking the assumptions of homogeneity, etc.

The decay of the turbulent kinetic energy

$$k \equiv \frac{1}{2} \langle u_i u_i \rangle, \quad (5.66)$$

is due solely to the dissipation: contracting each side of the Reynolds-stress equation yields

$$\frac{dk}{dt} = -\varepsilon, \quad (5.67)$$

where the dissipation rate of turbulent kinetic energy is

$$\varepsilon = \frac{1}{2} \varepsilon_{jj} = \frac{\mu}{\rho} \left\langle \frac{\partial u_j}{\partial x_i} \frac{\partial u_j}{\partial x_i} \right\rangle. \quad (5.68)$$

There is no contribution from the pressure-rate-of-strain because, by virtue of the continuity equation, P_{jj} is zero. It may be noted that ε is a positive quantity.

It is assumed that ε is known, either from a modelled transport equation or through the turbulent time scale $\tau \equiv k/\varepsilon$. In terms of the normalized time ($dt^* \equiv dt/\tau$), the kinetic energy equation is

$$\frac{dk}{dt^*} = -k. \quad (5.69)$$

The net rate of change of the Reynolds stresses is

often expressed as,

$$\frac{d\langle u_j u_k \rangle}{dt} = -\frac{2}{3} \varepsilon \delta_{jk} + R_{jk}, \quad (5.70)$$

where

$$R_{jk} \equiv P_{jk}/\rho - \left[\varepsilon_{jk} - \frac{2}{3} \varepsilon \delta_{jk} \right], \quad (5.71)$$

(Lumley¹¹ and Launder *et al.*²⁰). The isotropic part $(-(2/3)\varepsilon \delta_{jk})$ causes the normal stresses $(\langle u_1 u_1 \rangle, \langle u_2 u_2 \rangle$ and $\langle u_3 u_3 \rangle$) to decay, while the anisotropic part R_{jk} serves to redistribute energy among the Reynolds stresses: the trace R_{jj} is zero. The observed tendency of the Reynolds stresses to become isotropic is due to the term R_{jk} .

Rotta⁸⁸ suggested the model

$$R_{jk} = -C_2 \left(\langle u_j u_k \rangle - \frac{2}{3} k \delta_{jk} \right) / \tau, \quad (5.72)$$

where C_2 is an empirical constant. The Reynolds-stress equation then becomes

$$\frac{d}{dt} \langle u_j u_k \rangle = -\frac{2}{3} \varepsilon \delta_{jk} - C_2 \left(\langle u_j u_k \rangle - \frac{2}{3} k \delta_{jk} \right) / \tau. \quad (5.73)$$

Rotta's model is best understood in terms of the normalized anisotropy tensor

$$b_{jk} \equiv \frac{1}{2} \langle u_j u_k \rangle / k - \frac{1}{3} \delta_{jk}. \quad (5.74)$$

This tensor has zero trace and each component is zero if the Reynolds stresses are isotropic. A scalar measure of the anisotropy is

$$b_{ii}^2 \equiv b_{ij} b_{ji}, \quad (5.75)$$

which is zero for isotropy and positive otherwise. Equations (5.73–75) yield

$$\frac{db_{jk}}{dt^*} = -C'_2 b_{jk}, \quad (5.76)$$

and

$$\frac{db_{ii}^2}{dt^*} = -2C'_2 b_{ii}^2, \quad (5.77)$$

where

$$C'_2 = C_2 - 1. \quad (5.78)$$

It may be seen that for $C_2 < 1$ ($C'_2 < 0$), the anisotropy increases, contrary to experimental observation.⁸⁷ For $C_2 > 1$ ($C'_2 > 0$), the anisotropy decays exponentially with t^* , and for $C_2 = 1$ ($C'_2 = 0$) the anisotropy is constant.

Launder *et al.*²⁰ used Rotta's model with the constant value $C_2 = 1.5$. Lumley¹¹ suggested that Rotta's model (and, hence, Eq. 5.76) accurately describes existing experimental data, although C_2 is not a constant—it is a function of the anisotropy and Reynolds number. Recent experiments and the re-examination of existing data⁸⁷ confirm that C_2 is not a constant and suggest that the return to isotropy may

not be linear in b_{jk} as Rotta's model implies, Eq. (5.76). (This is discussed more in Section 5.5.) Nevertheless, Rotta's model provides a reasonable representation of the experimental results—at least with C_2 being a function of the anisotropy and Reynolds number.

For the flow considered, the evolution equation for the joint pdf of velocity $f_{\underline{u}}(\underline{V}; t)$ is

$$\begin{aligned} \rho \frac{\partial f_{\underline{u}}}{\partial t} &= -\frac{\partial}{\partial V_j} \left[f_{\underline{u}} \left\langle \frac{\partial \tau_{ij}}{\partial x_i} - \frac{\partial p'}{\partial x_j} \right| \underline{V} \right] \\ &= -\frac{\partial}{\partial V_j} \left[f_{\underline{u}} \left\langle \mu \nabla^2 U_j - \frac{\partial p'}{\partial x_j} \right| \underline{V} \right]. \end{aligned} \quad (5.79)$$

(This equation is obtained by integrating the joint pdf equation, Eq. (3.109), over composition space and invoking the assumptions of constant density and homogeneity.) The conditional expectations, which are to be modelled, represent the (conditional) force per unit volume due to viscous stresses and to the fluctuating pressure gradient. A good model causes the pdf to relax to a Gaussian. The mean velocity $\langle \underline{U} \rangle$ does not change, while the second moments evolve (approximately) according to Rotta's model, Eq. (5.73).

A particle interaction model—or, rather two models—produce the required result. The Reynolds-stress equation incorporating Rotta's model, Eq. (5.73), can be rewritten

$$\frac{d}{dt^*} \langle u_j u_k \rangle = -\langle u_j u_k \rangle - C'_2 \left(\langle u_j u_k \rangle - \frac{2}{3} k \delta_{jk} \right). \quad (5.80)$$

The first term on the right-hand side causes the kinetic energy to decay without the anisotropy tensor being affected: the *stochastic mixing model* produces this effect. The second term causes the anisotropy tensor to decay without the kinetic energy being affected: the *stochastic reorientation model* produces this effect.

The stochastic mixing model is directly analogous to that used for the scalar dissipation. The joint pdf $f_{\underline{u}}(\underline{V}; t)$ is represented by the discrete pdf $f_{\underline{u}N}^*$ which is composed of N delta functions:

$$f_{\underline{u}N}^*(\underline{V}; t) \equiv \frac{1}{N} \sum_{n=1}^N \delta(\underline{V} - \underline{U}^{*(n)}(t)). \quad (5.81)$$

The velocities $\underline{U}^{*(n)}$ of the stochastic particles remain constant except at discrete times. In the small interval of time δt , with probability $1 - \delta t/\tau_u$, the velocities $\underline{U}^{*(n)}$ of all the stochastic particles remain constant; where

$$\tau_u \equiv \tau/(NC_u), \quad (5.82)$$

and C_u is a constant to be determined. With probability $\delta t/\tau_u$, a pair of particles mix. The two particles (denoted by p and q) are selected at random without replacement and their velocities are replaced by their common mean velocity:

$$\underline{U}^{*(p)}(t + \delta t) = \underline{U}^{*(q)}(t + \delta t) = \frac{1}{2} [\underline{U}^{*(p)}(t) + \underline{U}^{*(q)}(t)]. \quad (5.83)$$

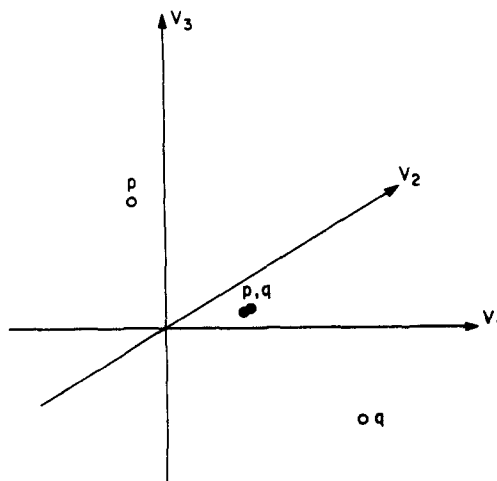


FIG. 5.5. Effect of mixing on the stochastic particles $\underline{U}^{*(p)}$ and $\underline{U}^{*(q)}$: \circ before mixing, \bullet after mixing.

Figure 5.5 shows, in velocity space, the effect of mixing on the stochastic particles p and q , Eq. (5.83). After mixing, both particles lie half-way between their initial locations.

The momentum (per unit mass) $\underline{M}^{(pq)}$ associated with the particles p and q is, simply:

$$\underline{M}^{(pq)} \equiv \underline{U}^{*(p)} + \underline{U}^{*(q)} = 2\underline{U}^{(pq)}, \quad (5.84)$$

where the average velocity $\underline{U}^{(pq)}$ is

$$\underline{U}^{(pq)} \equiv \frac{1}{2} [\underline{U}^{*(p)} + \underline{U}^{*(q)}]. \quad (5.85)$$

Equation (5.83) shows that the average velocity is unaffected by the mixing process

$$\underline{U}^{(pq)}(t + \delta t) = \underline{U}^{(pq)}(t). \quad (5.86)$$

The kinetic energy (per unit mass) associated with the particles is

$$K^{(pq)} \equiv \frac{1}{2} \underline{U}^{*(p)} \cdot \underline{U}^{*(p)} + \frac{1}{2} \underline{U}^{*(q)} \cdot \underline{U}^{*(q)}. \quad (5.87)$$

In terms of the average velocity $\underline{U}^{(pq)}$ and the velocity difference

$$\Delta U^{(pq)} \equiv |\underline{U}^{*(p)} - \underline{U}^{*(q)}|, \quad (5.88)$$

the kinetic energy can be re-expressed as

$$K^{(pq)} = \underline{U}^{(pq)} \cdot \underline{U}^{(pq)} + \frac{1}{4} [\Delta U^{(pq)}]^2. \quad (5.89)$$

Equation (5.83) shows that the change in kinetic energy due to mixing is

$$K^{(pq)}(t + \delta t) - K^{(pq)}(t) = -\frac{1}{4} [\Delta U^{(pq)}(t)]^2. \quad (5.90)$$

Thus, the reduction of the particle separation in velocity space causes a decrease in kinetic energy.

The type of analysis used in Section 5.2.3. can be used to show that the effect of the stochastic mixing model on the Reynolds stresses is

$$\frac{d}{dt^*} \langle u_j u_k \rangle = -C_u \langle u_j u_k \rangle, \quad (5.91)$$

and hence, for compatibility with the first term in Eq. (5.80), C_u is unity.

The stochastic reorientation model differs from the stochastic mixing model only in the definition of the time scale, and in the operation performed on the pair of particles selected. The time scale τ_R is defined by

$$\tau_R \equiv \tau / (C'_2 N). \quad (5.92)$$

In the small time interval δt , with probability $\delta t / \tau_R$, two particles (p and q) are selected at random without replacement. These particles are randomly reorientated in velocity space by

$$\underline{U}^{*(p)}(t + \delta t) = \underline{U}^{(pq)}(t) + \frac{1}{2} \underline{\eta} \Delta U^{(pq)}(t),$$

and

$$\underline{U}^{*(q)}(t + \delta t) = \underline{U}^{(pq)}(t) - \frac{1}{2} \underline{\eta} \Delta U^{(pq)}(t),$$

where $\underline{\eta}$ is a random vector uniformly distributed on the unit sphere (that is, $\underline{\eta}$ is a unit vector of random orientation). In this process, which is illustrated on Fig. 5.6, neither the average velocity $\underline{U}^{(pq)}$ nor the velocity difference $\Delta U^{(pq)}$ is changed. Consequently, neither the momentum nor the kinetic energy is affected.

In Section 5.3.1 the stochastic reorientation model is analyzed to show that its effect on the Reynolds stresses is

$$\frac{d \langle u_j u_k \rangle}{dt^*} = -C'_2 \left\{ \langle u_j u_k \rangle - \frac{2}{3} k \delta_{jk} \right\}. \quad (5.94)$$

When the stochastic mixing model and the stochastic reorientation model are used simultaneously, the net effect is the sum of the two effects (Eqs 5.91 and 5.94). Thus, the stochastic models cause the Reynolds stresses to evolve according to Rotta's model (Eq. 5.80).

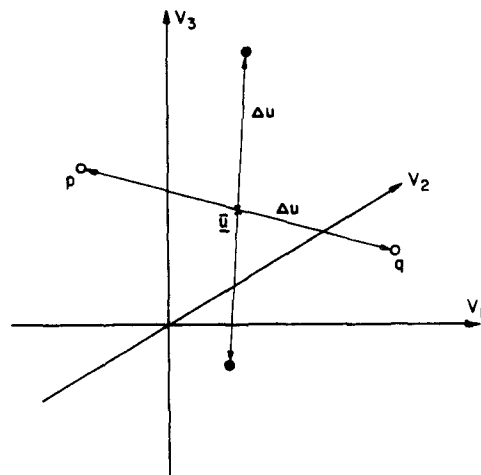


FIG. 5.6. Effect of stochastic reorientation showing that the average velocity \underline{U} and the velocity difference $\Delta \underline{U}$ are unaffected: \circ before reorientation, \bullet after reorientation.

The reorientation process, Eq. (5.93), is directly analogous to a collision between two Maxwellian molecules. Before the collision, the two molecules (p and q) have velocities $\underline{U}^{*(p)}$ and $\underline{U}^{*(q)}$. They collide, and their new velocities $\underline{U}^{*(p)}(t+\delta t)$ and $\underline{U}^{*(q)}(t+\delta t)$ are such that both momentum and energy are conserved. In view of this analogy, it is not surprising that the stochastic reorientation model causes the pdf to relax to a Gaussian (Maxwellian) distribution.

5.3.1. Analysis of the stochastic reorientation model

The effect of the stochastic reorientation model (Eqs 5.92–93) on the Reynolds stresses is determined in this subsection.

In the time interval δt , with probability $\delta t/\tau_R$, the velocities of particles p and q change: otherwise the velocities are constant. Thus the change in $\langle u_j u_k \rangle$ is

$$\begin{aligned} \Delta_{\delta t} \langle u_j u_k \rangle &= \frac{\delta t}{\tau_R} \frac{1}{N} \mathbf{E} \{ U_j^{*(p)}(t+\delta t) U_k^{*(p)}(t+\delta t) \\ &\quad + U_j^{*(q)}(t+\delta t) U_k^{*(q)}(t+\delta t) \\ &\quad - U_j^{*(p)} U_k^{*(p)} - U_j^{*(q)} U_k^{*(q)} \}, \end{aligned} \quad (5.95)$$

where, here and below, $\underline{U}^{*(n)}$ is written for $\underline{U}^{*(n)}(t)$. From the definition of $\underline{U}^{*(p)}(t+\delta t)$ and $\underline{U}^{*(q)}(t+\delta t)$, Eq. (5.93), we obtain

$$\begin{aligned} \mathbf{E} \{ U_j^{*(p)}(t+\delta t) U_k^{*(p)}(t+\delta t) \} &= \mathbf{E} \left\{ \bar{U}_j^{(pq)} \bar{U}_k^{(pq)} + \frac{1}{2} \bar{U}_j^{(pq)} \eta_k \Delta U^{(pq)} \right. \\ &\quad \left. + \frac{1}{2} \bar{U}_k^{(pq)} \eta_j \Delta U^{(pq)} + \frac{1}{4} \eta_j \eta_k [\Delta U^{(pq)}]^2 \right\}. \end{aligned} \quad (5.96)$$

Substituting for $\bar{U}^{(pq)}$ (Eq. 5.85), the first term becomes

$$\begin{aligned} \mathbf{E} \{ \bar{U}_j^{(pq)} \bar{U}_k^{(pq)} \} &= \frac{1}{4} \mathbf{E} \{ U_j^{*(p)} U_k^{*(p)} + U_j^{*(p)} U_k^{*(q)} \\ &\quad + U_j^{*(q)} U_k^{*(p)} + U_j^{*(q)} U_k^{*(q)} \} \\ &= \frac{1}{2} \langle u_j u_k \rangle + \langle U_j \rangle \langle U_k \rangle. \end{aligned} \quad (5.97)$$

The last step follows from

$$\mathbf{E} \{ U_j^{*(p)} U_k^{*(q)} \} = \mathbf{E} \{ U_j^{*(p)} \} \mathbf{E} \{ U_k^{*(q)} \} = \langle U_j \rangle \langle U_k \rangle, \quad (5.98)$$

(since $\underline{U}^{*(p)}$ and $\underline{U}^{*(q)}$ are independent) and from

$$\mathbf{E} \{ U_j^{*(p)} U_k^{*(p)} \} = \langle U_j U_k \rangle = \langle U_j \rangle \langle U_k \rangle + \langle u_j u_k \rangle. \quad (5.99)$$

The remaining terms in Eq. (5.90) depend upon $\underline{\eta}$. Since the orientation of $\underline{\eta}$ is random, each component (η_k , $k = 1, 2, 3$) is symmetrically distributed about zero—for any number z , the events $\eta_k = z$ and $\eta_k = -z$ are equally likely. Consequently the expected value of each component is zero:

$$\mathbf{E}(\eta_k) = 0. \quad (5.100)$$

Similarly, for $j \neq k$, the conditional expectation $\mathbf{E}(\eta_j|\eta_k)$ is zero since, for given η_k ($k \neq j$) and z , the events $\eta_j = z$ and $\eta_j = -z$ are equally likely. Hence,

$$\mathbf{E}(\eta_j \eta_k) = 0, \quad j \neq k. \quad (5.101)$$

By definition, the vector $\underline{\eta}$ has unit length:

$$\eta_j \eta_j = \mathbf{E}(\eta_j \eta_j) = \mathbf{E}(\eta_1 \eta_1 + \eta_2 \eta_2 + \eta_3 \eta_3) = 1. \quad (5.102)$$

And, since by symmetry $\mathbf{E}(\eta_1 \eta_1)$, $\mathbf{E}(\eta_2 \eta_2)$ and $\mathbf{E}(\eta_3 \eta_3)$ are equal, we obtain

$$\mathbf{E}(\eta_j \eta_k) = \frac{1}{3}, \quad j = k. \quad (5.103)$$

Equation (5.101) and (5.103) can be written in the common form

$$\mathbf{E}(\eta_j \eta_k) = \frac{1}{3} \delta_{jk}. \quad (5.104)$$

Returning to Eq. (5.96), since $\underline{\eta}$ is independent of the velocities, the second term on the right-hand side is zero:

$$\mathbf{E} \left\{ \frac{1}{2} \bar{U}_j^{(pq)} \eta_k \Delta U^{(pq)} \right\} = \mathbf{E} \left\{ \frac{1}{2} \bar{U}_j^{(pq)} \Delta U^{(pq)} \right\} \mathbf{E}(\eta_k) = 0. \quad (5.105)$$

Similarly the third term is zero. The final term is

$$\begin{aligned} \mathbf{E} \left\{ \frac{1}{4} \eta_j \eta_k [\Delta U^{(pq)}]^2 \right\} &= \frac{1}{4} \mathbf{E}(\eta_j \eta_k) \mathbf{E} \{ [\Delta U^{(pq)}]^2 \} \\ &= \frac{1}{12} \delta_{jk} \mathbf{E} \{ U_i^{*(p)} U_i^{*(p)} - 2 U_i^{*(p)} U_i^{*(q)} + U_i^{*(q)} U_i^{*(q)} \} \\ &= \frac{1}{6} \delta_{jk} \{ \langle U_i U_i \rangle - \langle U_i \rangle \langle U_i \rangle \} \\ &= \frac{1}{3} k \delta_{jk}. \end{aligned} \quad (5.106)$$

All the terms in Eq. (5.95) have now been evaluated. Using these results, the change in the Reynolds stress is found to be

$$\Delta_{\delta t} \langle u_j u_k \rangle = -\frac{\delta t}{N \tau_R} \{ \langle u_j u_k \rangle - \frac{2}{3} k \delta_{jk} \}. \quad (5.107)$$

Dividing by δt , substituting for τ_R (Eq. 5.92), and taking the limit as δt tends to zero, we obtain the required result:

$$\frac{d \langle u_j u_k \rangle}{dt^*} = -C'_2 \left\{ \langle u_j u_k \rangle - \frac{2}{3} k \delta_{jk} \right\}. \quad (5.108)$$

5.4. Rapid Pressure

While still considering constant-density homogeneous turbulence, we now allow uniform mean velocity gradients $\partial \langle U_i \rangle / \partial x_j$. The interaction of the mean velocity gradients with the turbulence gives rise to “rapid” pressure fluctuations. In this section a

deterministic model for these rapid pressure fluctuations is presented.

For constant-density flows, the continuity equation, (Eq. 3.2), yields

$$\frac{\partial U_i}{\partial x_i} = \frac{\partial \langle U_i \rangle}{\partial x_i} = \frac{\partial u_i}{\partial x_i} = 0. \quad (5.109)$$

An equation for the fluctuating velocity u is obtained by subtracting from Eq. (3.3) its mean. For a constant-density Newtonian fluid, the result is,

$$\begin{aligned} \rho \frac{\partial u_j}{\partial t} + \rho \frac{\partial}{\partial x_i} [\langle U_i \rangle u_j + \langle U_j \rangle u_i + u_i u_j - \langle u_i u_j \rangle] \\ = \mu \nabla^2 u_j - \frac{\partial p'}{\partial x_j}. \end{aligned} \quad (5.110)$$

(For the homogeneous case, the gradients of the Reynolds stresses $\partial \langle u_i u_j \rangle / \partial x_i$ are zero.) A Poisson equation for the fluctuating pressure is obtained by differentiating Eq. (5.110) with respect to x_j :

$$\nabla^2 p' = -2\rho \frac{\partial \langle U_i \rangle}{\partial x_j} \frac{\partial u_j}{\partial x_i} - \rho \frac{\partial^2 u_i u_j}{\partial x_i \partial x_j}. \quad (5.111)$$

This Poisson equation for p' shows that there are two sources of pressure fluctuations; one due to the interaction of turbulence with the mean velocity gradients, and the other solely due to turbulence. These contributions to p' are denoted by $p^{(1)}$ and $p^{(2)}$ respectively. The contribution $p^{(1)}$ is termed the "rapid" pressure since it changes rapidly in response to changes in the mean velocity gradient. The separation of p' into two contributions allows its effect on the joint velocity pdf $f_{\underline{u}}(\underline{V})$ to be separated (cf. Eq. 5.79):

$$\begin{aligned} \rho \frac{\partial f_{\underline{u}}}{\partial t} \dots = \dots \frac{\partial}{\partial V_j} \left[f_{\underline{u}} \left\langle \frac{\partial p'}{\partial x_j} \right| \underline{V} \right] \\ = \dots \frac{\partial}{\partial V_j} \left[f_{\underline{u}} \left\langle \frac{\partial p^{(1)}}{\partial x_j} \right| \underline{V} \right] + \frac{\partial}{\partial V_j} \left[f_{\underline{u}} \left\langle \frac{\partial p^{(2)}}{\partial x_j} \right| \underline{V} \right]. \end{aligned} \quad (5.112)$$

The stochastic mixing and reorientation models have been used to model the term in $p^{(2)}$; a deterministic model for the term in $p^{(1)}$ is now developed.

From Eq. (5.111) we have

$$\nabla^2 p^{(1)} = -2\rho \frac{\partial \langle U_i \rangle}{\partial x_m} \frac{\partial u_m}{\partial x_i}, \quad (5.113)$$

and differentiating with respect to x_j (recalling that the mean velocity gradient is uniform) we obtain

$$\nabla^2 \frac{\partial p^{(1)}}{\partial x_j} = -2\rho \frac{\partial \langle U_i \rangle}{\partial x_m} \frac{\partial^2 u_m}{\partial x_i \partial x_j}. \quad (5.114)$$

This equation can be solved using Green's theorem to yield an expression for the conditional rapid pressure gradient in terms of the two-point conditional expectation of velocity:

$$\left\langle \frac{\partial p^{(1)}}{\partial x_j} \right| \underline{u} = \underline{v} \rangle = -2\rho \frac{\partial \langle U_i \rangle}{\partial x_m} B_{m'j}(\underline{v}), \quad (5.115)$$

where

$$B_{m'j}(\underline{v}) = -\frac{1}{4\pi} \int \frac{1}{|\underline{r}|} \frac{\partial^2}{\partial r_i \partial r_j} \langle u_m(\underline{x} + \underline{r}) | \underline{u}(\underline{x}) = \underline{v} \rangle d\underline{r}. \quad (5.116)$$

A derivation of this equation is presented in Section 5.4.1 where several properties of the tensor $B_{m'j}(\underline{v})$ are deduced.

The task of modelling the rapid pressure term has now been reduced to that of modelling the tensor $B_{m'j}(\underline{v})$. Since \mathbf{B} has dimensions of velocity and is independent of the scale of the turbulence, Pope⁷² suggested modelling it as a function \underline{v} and the Reynolds stresses. It is expedient to assume that \mathbf{B} is a linear function of \underline{v} since this leads to a model that is compatible with Reynolds stress models. Some support for the linearity assumption is provided by the exact result (Eq. 5.146 of Section 5.4.1):

$$B_{m'j} = v_m. \quad (5.117)$$

The general form of the linear model is

$$B_{m'j} = v_q C_{qm'j}, \quad (5.118)$$

where \mathbf{C} is a non-dimensional tensor function of the Reynolds stresses.

Before considering the determination of the tensor \mathbf{C} , let us examine the form of the model. Combining Eqs (5.118) and (5.115) yields

$$\left\langle \frac{\partial p^{(1)}}{\partial x_j} \right| \underline{u} = \underline{v} \rangle = -2\rho \frac{\partial \langle U_i \rangle}{\partial x_m} C_{qm'j} v_q, \quad (5.119)$$

or alternatively

$$\left\langle \frac{\partial p^{(1)}}{\partial x_j} \right| \underline{U} = \underline{V} \rangle = -2\rho \frac{\partial \langle U_i \rangle}{\partial x_m} C_{qm'j} (V_q - \langle U_q \rangle). \quad (5.120)$$

The effect of the rapid pressure on the joint pdf of velocity (Eq. 5.112) is, then,

$$\frac{\partial f_{\underline{u}}}{\partial t} \dots = \dots -2 \frac{\partial \langle U_i \rangle}{\partial x_m} C_{qm'j} \frac{\partial}{\partial V_j} [f_{\underline{u}} (V_q - \langle U_q \rangle)], \quad (5.121)$$

and the corresponding conditional Lagrangian equation is

$$\frac{d \hat{U}_j}{dt} = \dots 2 \frac{\partial \langle U_i \rangle}{\partial x_m} C_{qm'j} (\hat{U}_q - \langle U_q \rangle). \quad (5.122)$$

Thus, the effect of the rapid pressure is to move conditional particles in velocity space at a rate proportional to their distance from the mean velocity ($\hat{U} - \langle U \rangle$) and proportional to the mean velocity gradient. Since the mean velocity is unaffected, the net motion in each direction (in \underline{V} -space) is zero; and, since the kinetic energy is unaffected, the mean-square outward motion from $\underline{V} = \langle \underline{U} \rangle$ is balanced by the mean-square inward motion.

As with the other linear deterministic models, this model does not change the shape of the distribution, only its moments. Thus a joint normal distribution

remains normal and, conversely, any other distribution does not relax to a normal distribution. For the other processes considered, the lack of relaxation was considered to be a defect in the model. But rapid distortion theory⁸⁹ shows that the rapid pressure has a deterministic effect on the turbulence, and hence, does not cause the pdf to become Gaussian.

A completely satisfactory model for the non-dimensional tensor C has yet to be developed. The best available model is obtained by relating C to a fourth-order tensor A that appears in Reynolds-stress models. Multiplying Eq. (5.119) by $(-f_u v_k)$ and integrating we obtain

$$-\left\langle u_k \frac{\partial p^{(1)}}{\partial x_j} \right\rangle = \left\langle p^{(1)} \frac{\partial u_k}{\partial x_j} \right\rangle = 2\rho \frac{\partial \langle U_i \rangle}{\partial x_m} C_{qmj} \langle u_k u_q \rangle. \quad (5.123)$$

Now, the term $\langle p^{(1)} \partial u_k / \partial x_j \rangle$ appears as an unknown in the Reynolds-stress equation and is generally modelled by,

$$\left\langle p^{(1)} \frac{\partial u_k}{\partial x_j} \right\rangle = \rho k \frac{\partial \langle U_i \rangle}{\partial x_m} A_{jk\ell m}, \quad (5.124)$$

where there are several suggestions for the tensor A (Lauder *et al.*,²⁰ Lumley and Khajeh-Nouri⁹⁰ and Lin and Wolfson⁹¹). Comparing these two equations, we see that A and C are related by

$$A_{jk\ell m} = (2/k) C_{qmj} \langle u_k u_q \rangle, \quad (5.125)$$

and

$$C_{qmj} = \frac{1}{2} k \langle u_k u_q \rangle^{-1} A_{jk\ell m}. \quad (5.126)$$

From this last equation, Pope⁷² evaluated the tensor C corresponding to Launder *et al.*'s model for A .

For many flows the quantitative performance of Launder *et al.*'s model may be adequate. But their model—and all the others mentioned—do not guarantee (weak) realizability. In the pdf model, the (weak) realizability principle imposes no conditions on C —except that it be finite. But, if the turbulence becomes two-dimensional, the Reynolds stress tensor becomes singular and then the right-hand side of Eq. (5.126) becomes infinite, unless A satisfies a particular condition. Current models for A do not satisfy this condition and hence are badly behaved when the turbulence becomes two-dimensional. In view of this, it would be preferable to model C directly. The corresponding model for A deduced from Eq. (5.125) would then guarantee realizability.

5.4.1. Solution of the Poisson equation

An exact solution for the conditional rapid pressure gradient is obtained in terms of the two-point conditional expectation, Eqs (5.115–116). The solution follows from a straightforward application of Green's theorem, but some care is needed to ensure proper behavior at the origin and at infinity.

Let \underline{x} and $\underline{y} = \underline{x} + \underline{r}$ be points within a regular region R with bounding surface S , Fig. 5.7. The length of the

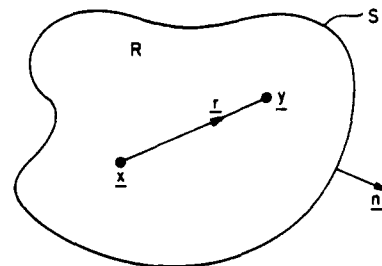


FIG. 5.7. Sketch showing points \underline{x} and \underline{y} in region R .

separation vector \underline{r} is

$$r = (\underline{r} \cdot \underline{r})^{1/2}, \quad (5.127)$$

\underline{n} is the outward-pointing normal vector and $\partial/\partial n$ denotes the derivative in the direction of \underline{n} .

The Poisson equation

$$\nabla^2 \frac{\partial p^{(1)}}{\partial x_j} = -2\rho \frac{\partial \langle U_i \rangle}{\partial x_m} \frac{\partial^2 u_m}{\partial x_i \partial x_j}, \quad (5.128)$$

(where $\partial \langle U_i \rangle / \partial x_m$ is uniform) has the solution

$$\frac{\partial p^{(1)}}{\partial x_j} = -2\rho \frac{\partial \langle U_i \rangle}{\partial x_m} B_{m\ell j}^* + I_j^{(1)} + I_j^{(2)}, \quad (5.129)$$

where

$$B_{m\ell j}^* \equiv -\frac{1}{4\pi} \iint_R \frac{1}{r} \frac{\partial^2 u_m(\underline{y})}{\partial y_\ell \partial y_j} d\underline{y}, \quad (5.130)$$

$$I_j^{(1)} \equiv \frac{1}{4\pi} \iint_S \frac{\partial^2 p^{(1)}(\underline{y})}{\partial y_j \partial n} \frac{1}{r} dS, \quad (5.131)$$

and

$$I_j^{(2)} \equiv -\frac{1}{4\pi} \iint_S \frac{\partial p^{(1)}(\underline{y})}{\partial y_j} \frac{\partial}{\partial n} \left(\frac{1}{r} \right) dS. \quad (5.132)$$

This solution follows directly from Green's second identity (see, for example, Ref. 92).

We now take the expectation of Eq. (5.129) conditional on $\underline{u}(\underline{x}) = \underline{y}$, and then take the limit as R tends to infinity. In this process, both surface integrals vanish. For $I_j^{(2)}$, for example, we have

$$\begin{aligned} \langle I_j^{(2)} | \underline{u}(\underline{x}) = \underline{y} \rangle &= -\frac{1}{4\pi} \iint_S \left\langle \frac{\partial p^{(1)}(\underline{y})}{\partial y_j} \right\rangle | \underline{u}(\underline{x}) = \underline{y} \rangle \frac{\partial r^{-1}}{\partial n} dS \\ &= -\frac{1}{4\pi} \iint_S \frac{\partial}{\partial r_j} \langle p^{(1)}(\underline{x} + \underline{r}) | \underline{u}(\underline{x}) = \underline{y} \rangle \frac{\partial r^{-1}}{\partial n} dS. \end{aligned} \quad (5.133)$$

Now as R , and hence r , becomes infinite, $p^{(1)}(\underline{x} + \underline{r})$ becomes independent of $\underline{u}(\underline{x})$:

$$\lim_{r \rightarrow \infty} \langle p^{(1)}(\underline{x} + \underline{r}) | \underline{u}(\underline{x}) = \underline{y} \rangle = \langle p^{(1)} \rangle = 0. \quad (5.134)$$

Consequently the derivative of $\langle p^{(1)}(\underline{x} + \underline{r}) | \underline{u}(\underline{x}) = \underline{y} \rangle$ also tends to zero, yielding

$$\lim_{R \rightarrow \infty} \langle I_j^{(2)} | \underline{u}(\underline{x}) = \underline{y} \rangle = 0. \quad (5.135)$$

The same argument yields the same result for $I_j^{(1)}$.

The conditional expectation of the volume integral,

Eq. (5.130), is

$$\begin{aligned} \langle B_{m\ell j}^* | \underline{u}(\underline{x}) = \underline{y} \rangle &= -\frac{1}{4\pi} \iint \int_R \frac{1}{r} \left\langle \frac{\partial^2 u_m(\underline{y})}{\partial y_i \partial y_j} \Big| \underline{u}(\underline{x}) = \underline{y} \right\rangle d\underline{y} \\ &= -\frac{1}{4\pi} \iint \int_R \frac{1}{r} \frac{\partial^2}{\partial r_i \partial r_j} \\ &\quad \times \langle u_m(\underline{x} + \underline{r}) | \underline{u}(\underline{x}) = \underline{y} \rangle d\underline{r}. \end{aligned} \quad (5.136)$$

In the limit as R tends to infinity, this equation defines the third-order tensor $B_{m\ell j}(\underline{y})$,

$$\begin{aligned} B_{m\ell j}(\underline{y}) &\equiv \lim_{R \rightarrow \infty} \langle B_{m\ell j}^* | \underline{u}(\underline{x}) = \underline{y} \rangle \\ &= -\frac{1}{4\pi} \int \frac{1}{r} \frac{\partial^2}{\partial r_i \partial r_j} \langle u_m(\underline{x} + \underline{r}) | \underline{u}(\underline{x}) = \underline{y} \rangle d\underline{r}, \end{aligned} \quad (5.137)$$

where $\int d\underline{r}$ represents the volume integral over the whole physical space. The convergence of the integral is not in doubt since, as r tends to infinity, $\langle u_m(\underline{x} + \underline{r}) | \underline{u}(\underline{x}) = \underline{y} \rangle$ tends to zero more rapidly than r^{-1} .

The conditional expectations of all the integrals in Eq. (5.129) have now been evaluated to yield the required solution

$$\left\langle \frac{\partial p^{(1)}}{\partial x_j} \Big| \underline{u}(\underline{x}) = \underline{y} \right\rangle = -2\rho \frac{\partial \langle U_i \rangle}{\partial x_m} B_{m\ell j}(\underline{y}), \quad (5.138)$$

where $B_{m\ell j}$ is given by Eq. (5.137). This solution is useful because it shows explicitly the role of the mean velocity gradient and because several properties of $B_{m\ell j}$ can be deduced. It is evident from Eq. (5.137) that the result is unaffected by reversing the order of differentiation: hence,

$$B_{m\ell j} = B_{mj\ell}. \quad (5.139)$$

The continuity equation, Eq. (5.109), at the point \underline{y} is

$$\frac{\partial u_m(\underline{y})}{\partial y_m} = \frac{\partial u_m(\underline{x} + \underline{r})}{\partial r_m} = 0, \quad (5.140)$$

and hence

$$\frac{\partial}{\partial r_m} \langle u_m(\underline{x} + \underline{r}) | \underline{u}(\underline{x}) = \underline{y} \rangle = 0. \quad (5.141)$$

Thus, in Eq. (5.137) the integrand vanishes if ℓ or j is contracted with m :

$$B_{mmj} = 0, \quad (5.142)$$

and

$$B_{m\ell m} = 0. \quad (5.143)$$

(Eq. 5.143 also follows from Eqs 5.139 and 5.142).

The final property of $B_{m\ell j}$ is slightly more difficult to obtain. Contracting ℓ and j in Eq. (5.136) yields

$$\begin{aligned} \langle B_{m\ell\ell}^* | \underline{u}(\underline{x}) = \underline{y} \rangle &= -\frac{1}{4\pi} \iint \int_R \frac{1}{r} \frac{\partial^2}{\partial r_i \partial r_i} \\ &\quad \times \langle u_m(\underline{x} + \underline{r}) | \underline{u}(\underline{x}) = \underline{y} \rangle d\underline{r}. \end{aligned} \quad (5.144)$$

Now the integrand is the Laplacian multiplied by the Green's function ($1/r$). Hence, from the exact solution

to Poisson's equation⁹² we obtain

$$\begin{aligned} \langle B_{m\ell\ell}^* | \underline{u}(\underline{x}) = \underline{y} \rangle &= \langle u_m(\underline{x}) | \underline{u}(\underline{x}) = \underline{y} \rangle \\ &\quad - \frac{1}{4\pi} \iint \int_S \frac{1}{r} \frac{\partial}{\partial n} \langle u_m(\underline{x} + \underline{r}) | \underline{u}(\underline{x}) = \underline{y} \rangle dS \\ &\quad + \frac{1}{4\pi} \iint \int_S \langle u_m(\underline{x} + \underline{r}) | u(\underline{x}) = \underline{y} \rangle \frac{\partial r^{-1}}{\partial n} dS. \end{aligned} \quad (5.145)$$

The first term on the right-hand side is just v_m , while, as r tends to infinity, the other terms vanish. Hence we obtain

$$B_{m\ell\ell}(\underline{y}) = \lim_{R \rightarrow \infty} \langle B_{m\ell\ell}^* | \underline{u}(\underline{x}) = \underline{y} \rangle = v_m. \quad (5.146)$$

5.5. Langevin Model

In the previous two sections a model for the evolution of the velocity joint pdf f_u is described. The dissipation and return-to-isotropy terms are modelled by the stochastic mixing and reorientation models (Section 5.3), and a linear deterministic model is used for the rapid pressure (Section 5.4). In this section an alternative model for the evolution of f_u is described. This is the generalized Langevin model—a generalization of Eq. (4.91) (see also Eq. 5.52). As in the previous sections, we consider constant-density homogeneous turbulence with uniform mean velocity gradients.

In terms of the velocity increment of a stochastic particle,

$$\Delta_{\delta t} \underline{U}^*(t) \equiv \underline{U}^*(t + \delta t) - \underline{U}^*(t), \quad (5.147)$$

the generalized Langevin model is

$$\begin{aligned} \Delta_{\delta t} U_i^* &= -\frac{\delta t}{\rho} \frac{\partial \langle p \rangle}{\partial x_i} + G_{ij}(U_j^* - \langle U_j \rangle) \delta t \\ &\quad + B^{1/2} \Delta_{\delta t} (W_i)_t, \end{aligned} \quad (5.148)$$

where \underline{W}_t is an isotropic Weiner process:

$$\langle \Delta_{\delta t} (W_i)_t \Delta_{\delta t} (W_j)_t \rangle = \delta t \delta_{ij}. \quad (5.149)$$

The second-order tensor G and the positive scalar B define the particular model, and their determination is discussed below. Both G and B can depend upon time but are independent of \underline{U}^* and \underline{x} (in homogeneous turbulence). The first term on the right-hand side of Eq. (5.148) defines the effect of the mean pressure gradient on the stochastic particle to be the same as that on a fluid particle.

With \underline{U}^* evolving according to the Langevin equation (Eq. 5.148), the Eulerian pdf $f_{\underline{u}}^*(\underline{V}; \underline{x}, t)$ evolves by (cf. Eq. 4.105),

$$\begin{aligned} \frac{\partial f_{\underline{u}}^*}{\partial t} + V_i \frac{\partial f_{\underline{u}}^*}{\partial x_i} &= \frac{1}{\rho} \frac{\partial \langle p \rangle}{\partial x_i} \frac{\partial f_{\underline{u}}^*}{\partial V_i} - G_{ij} \frac{\partial}{\partial V_i} [f_{\underline{u}}^*(V_j - \langle U_j \rangle)] \\ &\quad + \frac{1}{2} B \frac{\partial^2 f_{\underline{u}}^*}{\partial V_i \partial V_i}. \end{aligned} \quad (5.150)$$

Although the fluctuating velocity field is (by assumption) statistically homogeneous, the pdf $f_{\underline{u}}^*(\underline{V}; \underline{x}, t)$ depends upon \underline{x} (because the mean velocity

$\langle \underline{U}(\underline{x}, t) \rangle$ is not uniform). It is useful, therefore, to consider $g(\underline{v}; t)$ —the Eulerian joint pdf of the velocity fluctuations:

$$g(\underline{v}; t) \equiv f_{\underline{u}}^*(\underline{V}; \underline{x}, t), \quad (5.151)$$

where

$$\underline{v} \equiv \underline{V} - \langle \underline{U}(\underline{x}, t) \rangle. \quad (5.152)$$

When the evolution equation for g is derived from Eqs (5.150–152), the spatial derivative and mean pressure terms vanish, leaving

$$\frac{\partial g}{\partial t} = \left\{ \frac{\partial \langle U_i \rangle}{\partial x_j} - G_{ij} \right\} \frac{\partial}{\partial v_i} [gv_j] + \frac{1}{2} B \frac{\partial^2 g}{\partial v_i \partial v_i}. \quad (5.153)$$

This equation is qualitatively correct in that it admits joint normal solutions. And, as noted in Section 5.2.4, the term in B causes arbitrary initial distributions to relax to Gaussians (for $B > 0$).

The coefficient B is determined by requiring that (in a limited sense) the Langevin equation be a direct model of fluid particle behavior. Consider a time interval s that is much less than τ , but much greater than the Kolmogorov time scale τ_η :

$$\tau_\eta \ll s \ll \tau. \quad (5.154)$$

The quantity

$$\Delta_s \underline{U}^+(t) = \underline{U}^+(t+s) - \underline{U}^+(t), \quad (5.155)$$

is the change in the Lagrangian velocity of a fluid particle over the time interval s . According to Kolmogorov's (1941) hypotheses,⁹³ the covariance of $\Delta_s \underline{U}^+(t)$ is (to first order in s):

$$\langle \Delta_s U_i^+(t) \Delta_s U_j^+(t) \rangle = C_0 \varepsilon s \delta_{ij}, \quad (5.156)$$

where C_0 is a universal constant.

From the Langevin model (Eq. 5.148) we obtain (to first order in s):

$$\langle \Delta_s U_i^*(t) \Delta_s U_j^*(t) \rangle = B s \delta_{ij}, \quad (5.157)$$

for

$$0 \leq s \ll \tau. \quad (5.158)$$

By comparing Eqs (5.156) and (5.157), we see that (for $\tau_\eta \ll s \ll \tau$) fluid particles and stochastic particles have the same statistical properties provided that B is chosen to be

$$B = C_0 \varepsilon. \quad (5.159)$$

For time intervals s much less than τ_η , the covariance of $\Delta_s \underline{U}^*(t)$ is of order s (Eq. 5.157), but for fluid particles the covariance of $\Delta_s \underline{U}^+(t)$ is only of order s^2 .⁹³ Thus only in the limited range (5.154) does the Langevin model provide a direct model of fluid particle behavior.

For homogeneous isotropic turbulence (without mean velocity gradients), the tensor G_{ij} can be deduced without further modelling assumptions. The tensor must be isotropic ($G_{ij} \propto \delta_{ij}$), and the coefficient of proportionality is determined by requiring that the

modelled equation yield the correct energy decay rate (Eq. 5.67). Thus, for isotropic turbulence (with $\langle \underline{U} \rangle = 0$), the Langevin equation, (Eq. 5.148), becomes

$$\Delta_{st} U_i^* = - \left(\frac{1}{2} + \frac{3}{4} C_0 \right) (\delta t / \tau) U_i^* + (C_0 \varepsilon)^{1/2} \Delta_{st} (W_i)_t. \quad (5.160)$$

Anand and Pope⁴⁴ used this model equation to calculate the diffusion of heat behind a line source in grid turbulence. Excellent agreement with the available experimental data was obtained for $C_0 \approx 2.1$. Since, according to Kolmogorov's hypotheses, C_0 is a universal constant, we adopt this value for the general model.

We now consider modelling G_{ij} for the more general case of homogeneous anisotropic turbulence with uniform mean velocity gradients. At this level of closure, \mathbf{G} can be a function of τ , $\langle u_i u_j \rangle$ and $\partial \langle U_i \rangle / \partial x_j$. The most general model for \mathbf{G} contains far more scalar coefficients than could possibly be determined with confidence. Haworth and Pope⁹⁴ considered a simpler model for \mathbf{G} that is linear in both the Reynolds stresses and the mean velocity gradients:

$$G_{ij} = (\alpha_1 \delta_{ij} + \alpha_2 b_{ij}) / \tau + H_{ijk\ell} \frac{\partial \langle U_k \rangle}{\partial x_\ell}, \quad (5.161)$$

where

$$H_{ijk\ell} = \beta_1 \delta_{ij} \delta_{k\ell} + \beta_2 \delta_{ik} \delta_{j\ell} + \beta_3 \delta_{i\ell} \delta_{jk} + \gamma_1 \delta_{ij} b_{k\ell} + \gamma_2 \delta_{ik} b_{j\ell} + \gamma_3 \delta_{i\ell} b_{jk} + \gamma_4 b_{ij} \delta_{k\ell} + \gamma_5 b_{ik} \delta_{j\ell} + \gamma_6 b_{i\ell} \delta_{jk}, \quad (5.162)$$

and the eleven coefficients α_m , β_m and γ_m are to be determined. (The anisotropy tensor \mathbf{b} is defined by Eq. 5.74.)

In the alternative model presented in Sections 5.3–4, the stochastic reorientation model (that does not depend upon $\partial \langle U_k \rangle / \partial x_\ell$) simulates the effect of the “slow” pressure $p^{(2)}$, whereas a term linear in $\partial \langle U_k \rangle / \partial x_\ell$ simulates the effect of the “rapid” pressure $p^{(1)}$, Eq. (5.119). Similarly, the terms in α_1 and α_2 in Eq. (5.161) could be identified with the slow pressure, and the term in $\partial \langle U_k \rangle / \partial x_\ell$ with the rapid pressure. Then, it follows that \mathbf{H} and \mathbf{C} (Eq. 5.118) are related by

$$H_{ijk\ell} = 2 C_{j\ell ki}. \quad (5.163)$$

However, the decomposition of Eq. (5.161) into slow and rapid parts contains the implicit assumption that the slow pressure is independent of mean velocity gradients. There being no strong basis for this assumption, we follow Jones and Musonge⁹⁵ in rejecting it. As a consequence, \mathbf{H} is not subject to many of the constraints that otherwise follow from the properties of $B_{mqj}(\underline{v}) = v_q C_{qmfj}$ (see Section 5.4.1).

In the determination of the eleven coefficients in Eqs (5.161–162), several subtleties arise.⁹⁴ Since the coefficients β_1 and γ_4 multiply

$$\delta_{k\ell} \frac{\partial \langle U_k \rangle}{\partial x_\ell} = \frac{\partial \langle U_k \rangle}{\partial x_k} = 0, \quad (5.164)$$

their values are irrelevant and can be set arbitrarily. The requirement that the model yields the correct kinetic energy evolution leads to the condition:

$$\alpha_1 = -\left(\frac{1}{2} + \frac{3}{4}C_0\right) - \alpha_2 b_{ij} b_{ji} - \tau(\gamma_1 + \gamma_2 + \gamma_3 + \frac{1}{3}\gamma^*) b_{kk} \\ \times \frac{\partial \langle U_k \rangle}{\partial x_i} - \tau \gamma^* b_{ki} b_{ii} \frac{\partial \langle U_k \rangle}{\partial x_i}, \quad (5.165)$$

where

$$\gamma^* \equiv \gamma_2 + \gamma_3 + \gamma_5 + \gamma_6.$$

Two other requirements are imposed: that the model produces the correct response for the rapid distortion of isotropic turbulence; and, that the multiplier of $(\partial \langle U_k \rangle / \partial x_i, -\partial \langle U_i \rangle / \partial x_k)$ has the correct form in the limit of two-dimensional turbulence.⁷⁸ These two requirements lead to the conditions

$$\beta_1 = -1/5, \quad \beta_2 = 4/5, \quad \beta_3 = -1/5, \quad (5.166)$$

and

$$\beta_2 - \beta_3 + \frac{2}{3}(\gamma_2 - \gamma_3) + \frac{1}{3}(\gamma_6 - \gamma_5) = 2. \quad (5.167)$$

With the five conditions Eqs (5.165–167), six degrees of freedom remain in the model.

The only other obvious source of information that can be used to determine the coefficients is experimental data on the evolution of Reynolds stresses in homogeneous turbulence. But when the modelled Reynolds stress equation is deduced from Eq. (5.161), the coefficients appear in groups—only four of which are linearly independent of Eqs (5.166–167). Thus two degrees of indeterminacy remain. Haworth and Pope⁹⁴ remove this indeterminacy by setting

$$\gamma_4 = 0, \quad (5.168)$$

and

$$\gamma_1 = -\frac{3}{5} - \frac{1}{3}\gamma^*. \quad (5.169)$$

This last equation simplifies Eq. (5.165) to

$$\alpha_1 = -\left(\frac{1}{2} + \frac{3}{4}C_0\right) - \alpha_2 b_{ij} b_{ji} - \tau \gamma^* b_{ki} b_{ii} \frac{\partial \langle U_k \rangle}{\partial x_i}, \quad (5.170)$$

which is used to determine α_1 . The four remaining coefficients (assumed constant) are determined by a least-squares optimization against the available experimental data. The values obtained are:

$$\alpha_2 = 3.7, \quad \gamma_2 = 3.01, \quad \gamma_3 = -2.18 \quad \text{and} \quad \gamma_5 = 4.29. \quad (5.171)$$

The values of $\gamma_6 = -3.09$ and $\gamma_1 = -1.28$ then follow from Eqs (5.167) and (5.169).

To summarize: for consistency with Kolmogorov's scaling laws, the coefficient B in the Langevin equation, (Eq. 5.148), is determined to be $C_0 \varepsilon$, where

the universal constant C_0 has the value 2.1. A model for the tensor G_{ij} that is linear in both the anisotropy tensor and the mean velocity gradients has been proposed (Eqs 5.161–162). For homogeneous turbulence, the resulting pdf equation yields a joint normal distribution with the Reynolds stress evolution closely matching experimental observations.

5.6. Joint PdF Models

In the previous sub-sections, models for the conditional expectations

$$\langle \Gamma \nabla^2 \phi_a | \underline{\psi} \rangle, \langle \mu \nabla^2 U_j | \underline{V} \rangle \quad \text{and} \quad \left\langle \frac{\partial p'}{\partial x_j} \middle| \underline{V} \right\rangle,$$

have been developed for homogeneous constant-density turbulence, with no mean composition gradients. With these models and a knowledge of the turbulent time scale $\tau(t)$, the evolution of the composition pdf $f_\phi(\underline{\psi}; t)$, and of the velocity pdf $f_v(\underline{V}; t)$ can be calculated. But, in order to calculate the evolution of the velocity–composition joint pdf $f(\underline{V}, \underline{\psi}; t)$ it is necessary to model each quantity conditional on the joint events $\underline{U} = \underline{V}$ and $\underline{\phi} = \underline{\psi}$. Thus, in this sub-section, we re-examine the models to see how they should be modified in order to represent the expectations

$$\langle \Gamma \nabla^2 \phi_a | \underline{V}, \underline{\psi} \rangle, \langle \mu \nabla^2 U_j | \underline{V}, \underline{\psi} \rangle \quad \text{and} \quad \left\langle \frac{\partial p'}{\partial x_j} \middle| \underline{V}, \underline{\psi} \right\rangle. \quad (5.172)$$

For the homogeneous flows considered, the joint pdf $f(\underline{V}, \underline{\psi}; t)$ is found to be a joint normal distribution.⁶² Consequently, it is completely defined by the means $\langle \underline{U} \rangle$ and $\langle \underline{\phi} \rangle$, the Reynolds stresses $\langle u_i u_j \rangle$, the scalar variances $\langle \phi_a' \phi_b' \rangle$, and the scalar fluxes $\langle u_i \phi_a \rangle$. These scalar fluxes contain all the joint information: $f_v(\underline{V})$ can be determined from $\langle \underline{U} \rangle$ and $\langle u_i u_j \rangle$; $f_\phi(\underline{\psi})$ can be determined from $\langle \underline{\phi} \rangle$ and $\langle \phi_a' \phi_b' \rangle$; but the additional information contained in $\langle u_i \phi_a \rangle$ is needed to determine the joint distribution $f(\underline{V}, \underline{\psi})$. (The determination of the joint pdf from the first and second moments is possible only because the pdf is known to be joint-normal.)

The models presented above are modified in such a way that the effect of the models on f_v and f_ϕ is unchanged. The effects of the modifications are revealed in the behavior of the scalar fluxes.

We consider first the decay of the scalar flux for a single scalar ϕ in isotropic turbulence. For this case the models described below yield the decay law

$$\frac{d \langle u_i \phi \rangle}{dt^*} = -C_f \langle u_i \phi \rangle, \quad (5.173)$$

where the positive coefficient C_f depends upon the details of the model.

Since both $\langle \phi'^2 \rangle$ and $\langle u_i u_j \rangle$ decay, it is inevitable that $\langle u_i \phi \rangle$ also decays. It is more informative to study the evolution of the correlation coefficient r .

$$r^2 \equiv \langle u_i \phi \rangle \langle u_i \phi \rangle / \left\{ \frac{2}{3} k \langle \phi'^2 \rangle \right\}. \quad (5.174)$$

This definition can be understood by noting that, if the coordinate system is chosen such that the scalar flux (which is a vector) is in the x_1 -direction, then Eq. (5.174) becomes

$$r^2 = \langle u_1 \phi' \rangle^2 / \{ \langle u_1 u_1 \rangle \langle \phi'^2 \rangle \} \quad (5.175)$$

(cf. Eq. 2.110). If k , $\langle \phi'^2 \rangle$ and $\langle u_i \phi \rangle$ decay according to Eqs (5.69, 5.25 and 5.173), then it follows that r evolves by

$$\frac{dr}{dt^*} = -C_r r, \quad (5.176)$$

where

$$C_r = C_f - \frac{1}{2} (C_\phi + 1). \quad (5.177)$$

Sirivat and Warhaft⁹⁶ provide experimental data for the correlation coefficient r in decaying grid turbulence. The data show that r decays, but a unique decay constant C_r is not evident. Values of C_r in the range 0.35–0.85 are consistent with the data.

More recently, Shih and Lumley⁹⁷ have proposed a nonlinear model which agrees well with a second set of data from Sirivat and Warhaft⁹⁸ obtained in grid turbulence with a uniform mean temperature gradient. If r^4 can be neglected in comparison to unity (which is usually the case) this model reduces to the decay law Eq. (5.176) with

$$C_r = 0.55 C_\phi^2. \quad (5.178)$$

For the flows of Sirivat and Warhaft⁹⁸ the value of C_ϕ is found to be approximately 1.6 which yields $C_r \approx 1.4$. Thus the experimental data do show that r decays, but the value of the decay constant C_r is uncertain—if, indeed, it is a constant.

We now address the problem of combining models for $f_u(\underline{V})$ and $f_\phi(\underline{\psi})$ to form a model for $f(\underline{V}, \underline{\psi})$. The simplest assumptions are that the increment $\Delta_{\delta t} \underline{U}^*$ is independent of $\underline{\phi}^*$, and that $\Delta_{\delta t} \underline{\phi}^*$ is independent of \underline{U}^* . Since we are considering $\underline{\phi}$ to be a set of *passive* scalars, the first of these assumptions is most reasonable. Certainly for fluid particles, $\Delta_{\delta t} \underline{U}^*$ is (deterministically) independent of $\underline{\phi}^+$. We adopt this assumption without reservation or further discussion. The second assumption—that $\Delta_{\delta t} \underline{\phi}^*$ is independent of \underline{U}^* —has no justification. However, we tentatively adopt the assumption in order to explore its consequence.

With the two independence assumptions, the Langevin model for $\Delta_{\delta t} \underline{U}^*$ (Eq. 5.160) can be combined directly with the stochastic mixing model for $\Delta_{\delta t} \underline{\phi}^*$ (Eqs 5.35, 5.48 and 5.49). The resulting joint model is now analyzed to determine its effect on the scalar flux $\langle u_i \phi_x \rangle$.

With $f(\underline{V}, \underline{\psi})$ being represented by N stochastic particles $\underline{U}^{*(n)}$, $\underline{\phi}^{*(n)}$, $n = 1, 2, \dots, N$, the change in $\langle u_i \phi_x \rangle$ in a small time interval δt is (to first order in δt)

$$\begin{aligned} \Delta_{\delta t} \langle u_i \phi_x \rangle &= \mathbf{E} \frac{1}{N} \sum_{n=1}^N \{ (U_i^{*(n)} + \Delta_{\delta t} U_i^{*(n)}) (\phi_x^{*(n)} \\ &\quad + \Delta_{\delta t} \phi_x^{*(n)}) - U_i^{*(n)} \phi_x^{*(n)} \} \\ &= \mathbf{E} \frac{1}{N} \sum_{n=1}^N \{ U_i^{*(n)} \Delta_{\delta t} \phi_x^{*(n)} + \phi_x^{*(n)} \Delta_{\delta t} U_i^{*(n)} \}. \end{aligned} \quad (5.179)$$

Now $\Delta_{\delta t} \phi_x^{*(n)}$ is zero except, with probability $\delta t/\tau_N$, for the two elements p and q . If mixing takes place, then

$$\Delta_{\delta t} \phi_x^{*(p)} = -\frac{1}{2} (\phi_x^{*(p)} - \phi_x^{*(q)}), \quad (5.180)$$

and similarly for $\Delta_{\delta t} \phi_x^{*(q)}$. Thus, using Eq. (5.160) to substitute for $\Delta_{\delta t} U_i^{*(n)}$, Eq. (5.179) becomes

$$\begin{aligned} \Delta_{\delta t} \langle u_i \phi_x \rangle &= -\frac{\delta t}{2N\tau_N} \mathbf{E}[U_i^{*(p)}(\phi_x^{*(p)} - \phi_x^{*(q)}) \\ &\quad + U_i^{*(q)}(\phi_x^{*(q)} - \phi_x^{*(p)})] \\ &\quad + \frac{1}{N} \mathbf{E} \sum_{n=1}^N \left\{ \phi_x^{*(n)} \left[-\left(\frac{1}{2} + \frac{3}{4} C_0 \right) U_i^{*(n)} \frac{\delta t}{\tau} \right. \right. \\ &\quad \left. \left. + (C_0 \varepsilon)^{1/2} \Delta_{\delta t} (W_i^{(n)})_t \right] \right\} \\ &= -\frac{\delta t}{\tau} \left(C_\phi + \frac{1}{2} + \frac{3}{4} C_0 \right) \langle u_i \phi_x \rangle. \end{aligned} \quad (5.181)$$

In the limit as δt tends to zero we obtain the decay law Eq. (5.173) with

$$C_f = C_\phi + \frac{1}{2} + \frac{3}{4} C_0. \quad (5.182)$$

This implies (Eq. 5.177) that the correlation coefficient decay constant is

$$C_r = \frac{3}{4} C_0 + \frac{1}{2} C_\phi. \quad (5.183)$$

Taking $C_0 = 2.1$ and the conservative value $C_\phi = 1.6$, this yields $C_r \approx 2.4$ —a far higher value than is suggested by the data.

The reason that the model yields too large a value of C_r lies in the assumption that $\Delta_{\delta t} \underline{\phi}^*$ is independent of \underline{U}^* . Molecular mixing is a microscale process. When a fluid particle's composition changes, it does so by molecular exchange with neighboring fluid particles. The velocities of neighboring fluid particles—or even of particles separated by the Kolmogorov scale—are strongly correlated. But in the stochastic mixing model, the velocities of the two particles $\underline{U}^{*(p)}$ and $\underline{U}^{*(q)}$ are independent.

The following modified mixing model suggests itself. The first particle to be mixed (denoted by p) is selected at random as before. Its velocity and composition are $\underline{U}^{*(p)}$ and $\underline{\phi}^{*(p)}$. The choice of the second particle (denoted by q) is biased towards those whose velocity $\underline{U}^{*(q)}$ is close to $\underline{U}^{*(p)}$. The mixing operation is then performed as before. Depending on the amount of bias, this model yields decay constants in the range

$$\frac{3}{4}C_0 - \frac{1}{2}C_\phi \leq C_r \leq \frac{3}{4}C_0 + \frac{1}{2}C_\phi, \quad (5.184)$$

or (taking $C_0 = 2.1$, $C_\phi = 2.0$),

$$0.575 \leq C_r \leq 2.575. \quad (5.185)$$

Thus with biased selection, the modified mixing model, in conjunction with the Langevin equation, yields values of C_r in the range of experimental observations. (In the improved mixing model⁸⁵ the same effect can be achieved by biasing the amount of mixing according to the velocity difference between the two particles. This can be done in an efficient algorithm, whereas an efficient algorithm for biased selection is not evident.)

We now consider the use of the stochastic mixing and reorientation models for $\Delta_{\delta t} \underline{U}^*$ (Section 5.3) instead of the Langevin equation. If the stochastic models for $\Delta_{\delta t} \underline{U}^*$ and $\Delta_{\delta t} \underline{\phi}^*$ are combined, and the two independence assumptions are invoked ($\Delta_{\delta t} \underline{U}^*$ is independent of $\underline{\phi}^*$ and $\Delta_{\delta t} \underline{\phi}^*$ is independent of \underline{U}^*), then the correlation coefficient r decays by Eq. (5.176) with

$$C_r = C_2 + \frac{1}{2}C_\phi + \frac{1}{2}C_u. \quad (5.186)$$

The three constants C_2 , C_ϕ and C_u arise from the three stochastic models—stochastic reorientation, stochastic mixing in composition space, and stochastic mixing in velocity space. Taking the values $C_2 = 0.5$ ($C_2 = 1.5$), $C_\phi = 2.0$ and $C_u \equiv 1$, we obtain $C_r = 2.0$ —again, a larger value than is suggested by the data.

Rather than the second independence assumption, an alternative hypothesis is that steep velocity gradients cause steep composition gradients, and hence mixing in $\underline{\phi}$ -space is correlated with mixing in \underline{U} -space. The following stochastic model accounts for this correlated mixing, with the constant $C_{u\phi}$ ($0 \leq C_{u\phi} \leq 1$) defining the degree of correlation.

The joint pdf $f(\underline{U}, \underline{\phi}; t)$ is represented by N stochastic particles $\underline{U}^{*(n)}, \underline{\phi}^{*(n)}$, $n = 1, 2, \dots, N$. In the small time interval δt , the probability of the occurrence of correlated mixing is $\delta t/\tau_{u\phi}$, where

$$\tau_{u\phi} \equiv \tau/(C_{u\phi} N). \quad (5.187)$$

When correlated mixing occurs, two of the N stochastic particles (denoted by p and q) are selected at random without replacement and their properties are replaced by:

$$\begin{aligned} \underline{U}^{*(p)}(t + \delta t) &= \underline{U}^{*(q)}(t + \delta t) = \frac{1}{2}[\underline{U}^{*(p)}(t) + \underline{U}^{*(q)}(t)], \\ \underline{\phi}^{*(p)}(t + \delta t) &= \underline{\phi}^{*(q)}(t + \delta t) = \frac{1}{2}[\underline{\phi}^{*(p)}(t) + \underline{\phi}^{*(q)}(t)]. \end{aligned} \quad (5.188)$$

The effect of this model alone on the Reynolds stresses and scalar variances is:

$$\frac{d\langle u_i u_j \rangle}{dt^*} = -C_{u\phi} \langle u_i u_j \rangle, \quad (5.189)$$

and

$$\frac{d\langle \phi'_a \phi'_b \rangle}{dt^*} = -C_{u\phi} \langle \phi'_a \phi'_b \rangle. \quad (5.190)$$

Thus, in order to obtain the correct amount of mixing (cf. Eqs 5.91 and 5.51), the stochastic mixing model in composition space is used with the constant C_ϕ modified to

$$C'_\phi = C_\phi - C_{u\phi}, \quad (5.191)$$

and the stochastic mixing model in velocity space is used with the constant $C_u (= 1)$ modified to

$$C'_u = C_u - C_{u\phi}. \quad (5.192)$$

In other words, correlated mixings occur with probability $C_{u\phi} N \delta t/\tau$, composition mixing with probability $C'_\phi N \delta t/\tau$, and velocity mixing with probability $C'_u N \delta t/\tau$.

This combination of the three stochastic mixing models and the random reorientation model produces the correct evolution of the Reynolds stresses and scalar variances, independent of the value of $C_{u\phi}$. The effect on the scalar-flux correlation coefficient r is to cause decay according to Eq. (5.176) with

$$C_r = C_2 + \frac{1}{2}C_\phi + \frac{1}{2}C_u - C_{u\phi}. \quad (5.193)$$

Thus a choice of $C_{u\phi}$ between unity and zero yields values of C_r in the range

$$C_2 + \frac{1}{2}C_\phi - \frac{1}{2} \leq C_r \leq C_2 + \frac{1}{2}C_\phi + \frac{1}{2}, \quad (5.194)$$

or (taking $C_2 = 0.5$, $C_\phi = 2.0$)

$$1.0 \leq C_r \leq 2.0, \quad (5.195)$$

which is closer to the observed range than Eq. (5.186).

5.7. General Flows

The models that have been presented are for inert, constant-density homogeneous flows. They are well-understood and tested even though some components have yet to be finalized. But we wish to apply the joint pdf equation to more complicated flows—inhomogeneous, variable-density reactive flows. Indeed, the virtue of the pdf equation is that it facilitates the treatment of these complications. In this section the extension to general flows is discussed. The modelling for these flows is less well established and far more difficult to test. But, it is argued, the exact terms in the joint pdf equation and the processes already modelled account for the principal influences on the joint pdf.

5.7.1. Inhomogeneity

For a constant density Newtonian fluid with unit Prandtl (or Schmidt) number ($\mu = \Gamma$), the joint pdf equation can be re-expressed as

$$\begin{aligned}
& \rho \frac{\partial f}{\partial t} + \rho V_j \frac{\partial f}{\partial x_j} + \left(\rho g_j - \frac{\partial \langle p \rangle}{\partial x_j} \right) \frac{\partial f}{\partial V_j} + \rho \frac{\partial}{\partial \psi_x} [f S_x(\psi)] \\
& = \frac{\partial}{\partial x_i} \left(\mu \frac{\partial f}{\partial x_i} \right) - \frac{\partial^2}{\partial V_j \partial V_k} \left\{ \left[f \left\langle \mu \frac{\partial U_j}{\partial x_i} \frac{\partial U_k}{\partial x_i} \right| \underline{V}, \underline{\psi} \right\rangle \right] \right. \\
& \quad \left. - \frac{1}{2} f \left\langle p' \left(\frac{\partial U_k}{\partial x_j} + \frac{\partial U_j}{\partial x_k} \right) \right| \underline{V}, \underline{\psi} \right\rangle \} \\
& \quad - \frac{\partial^2}{\partial \psi_x \partial \psi_y} \left[f \left\langle \mu \frac{\partial \phi_x}{\partial x_i} \frac{\partial \phi_y}{\partial x_i} \right| \underline{V}, \underline{\psi} \right\rangle \} \\
& \quad - \frac{\partial^2}{\partial V_j \partial \psi_x} \left[f \left\langle \mu \frac{\partial U_j}{\partial x_i} \frac{\partial \phi_x}{\partial x_i} \right| \underline{V}, \underline{\psi} \right\rangle \} \\
& \quad - \frac{\partial}{\partial x_j \partial V_j} [f \langle p' | \underline{V}, \underline{\psi} \rangle]. \tag{5.196}
\end{aligned}$$

The principal influence of inhomogeneity is to cause convective transport in physical space. This effect appears in closed form in the joint pdf equation through the term $V_j \partial f / \partial x_j$. In contrast, in second-order closures, this term gives rise to the correlations $\langle u_i u_j u_k \rangle$, $\langle u_i u_j \phi_x \rangle$ and $\langle u_i \phi_x \phi_y \rangle$ which are generally modelled by gradient diffusion. It is emphasized that, in the joint pdf equation, the convective term is in closed form and therefore no gradient diffusion models are needed.

The first term on the right-hand side of Eq. (5.196) represents transport in physical space due to molecular diffusion, and (at high Reynolds number) is usually negligible. Nevertheless, the term appears in closed form and can be retained without additional modelling being required.

The next three terms represent the effects of dissipation and pressure fluctuations that have been modelled in Sections 5.3–6. Since dissipation and (to a lesser extent) the slow pressure are associated with the smaller turbulent scales, it is reasonable to assume that these processes are unaffected by inhomogeneities.

For flows remote from walls, it is assumed that the rapid-pressure models still apply. An analysis of the rapid pressure rate of strain⁹⁹ shows that, to first order, departures from homogeneity have no effect. Near walls, however, the velocity gradients and Reynolds stresses vary rapidly. Further, the analysis of Section 5.4.1. has to be modified to include surface integrals at the wall. Consequently, the models (Eqs 5.119 and 5.148) (or at least the tensors C and G) have to be modified: this is a subject for future work.

The final term in Eq. (5.196) represents transport due to the fluctuating pressure. Pope⁷² suggested the model

$$\langle p' | \underline{V}, \underline{\psi} \rangle = \frac{1}{5} (\langle u_i u_j \rangle - v_i v_j), \tag{5.197}$$

which is consistent with Lumley's model¹¹ for $\langle p' u_j \rangle$. But this model has not been tested.

5.7.2. Intermittency

Near to the edge of boundary layers and free shear layers the flow is intermittent—sometimes turbulent,

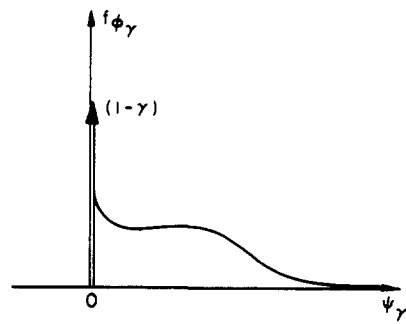


Fig. 5.8. Pdf of indicator ϕ_γ showing a delta function of magnitude $(1 - \gamma)$ at $\psi_\gamma = 0$.

sometimes non-turbulent.¹⁰⁰ Consider a high Reynolds number jet which transports a conserved passive scalar $\phi_\gamma(\underline{x}, t)$, where $\gamma = \sigma + 1$. At the jet exit ϕ_γ is positive, while in the non-turbulent, irrotational fluid remote from the jet ϕ_γ is zero. As the Reynolds number tends to infinity, the condition $\phi_\gamma(\underline{x}, t) > 0$ can be used as an indicator of turbulent fluid. That is, if $\phi_\gamma(\underline{x}, t) > 0$, the fluid is in turbulent motion, if $\phi_\gamma(\underline{x}, t) = 0$, the fluid is in irrotational, non-turbulent motion. The intermittency factor $\gamma(\underline{x}, t)$ is defined as the probability of the fluid at (\underline{x}, t) being turbulent. In terms of the indicator ϕ_γ , the intermittency factor is

$$\gamma(\underline{x}, t) = P(\phi_\gamma(\underline{x}, t) > 0). \tag{5.198}$$

The pdf of ϕ_γ , $f_{\phi_\gamma}(\psi_\gamma; \underline{x}, t)$, is zero for $\psi < 0$, it has a delta function of magnitude $(1 - \gamma(\underline{x}, t))$ at $\psi_\gamma = 0$, and it has a continuous distribution for $\psi > 0$, see Fig. 5.8. Integration over the delta function and over the continuous distribution yields

$$\int_0^{0+} f_{\phi_\gamma}(\psi_\gamma; \underline{x}, t) d\psi_\gamma = 1 - \gamma(\underline{x}, t), \tag{5.199}$$

and

$$\int_{0+}^{\infty} f_{\phi_\gamma}(\psi_\gamma; \underline{x}, t) d\psi_\gamma = \gamma(\underline{x}, t). \tag{5.200}$$

The joint pdf $f(\underline{V}, \underline{\psi}; \underline{x}, t)$ can be decomposed into two parts: the first $f_T(\underline{V}, \underline{\psi}; \underline{x}, t)$ is the joint pdf of \underline{U} and $\underline{\phi}$ conditional upon the fluid being turbulent, the second $f_N(\underline{V}, \underline{\psi}; \underline{x}, t)$ is conditional on the fluid being non-turbulent:

$$f = \gamma f_T + (1 - \gamma) f_N. \tag{5.201}$$

In terms of $f_{\underline{\phi}\phi}(\underline{V}, \underline{\psi}, \psi_\gamma; \underline{x}, t)$ —the joint pdf of \underline{U} , $\underline{\phi}$ and ϕ_γ —these two conditional pdf's are

$$f_T(\underline{V}, \underline{\psi}; \underline{x}, t) = f(\underline{V}, \underline{\psi}; \underline{x}, t | \phi_\gamma > 0)$$

$$= \int_{0+}^{\infty} f_{\underline{\phi}\phi}(\underline{V}, \underline{\psi}, \psi_\gamma; \underline{x}, t) d\psi_\gamma / \gamma(\underline{x}, t), \tag{5.202}$$

and

$$f_N(\underline{V}, \underline{\psi}; \underline{x}, t) = f(\underline{V}, \underline{\psi}; \underline{x}, t | \phi_\gamma = 0)$$

$$= \int_0^{0+} f_{\underline{\phi}\phi}(\underline{V}, \underline{\psi}, \psi_\gamma; \underline{x}, t) d\psi_\gamma / (1 - \gamma(\underline{x}, t)). \tag{5.203}$$

The reason for wanting to discriminate between turbulent and non-turbulent fluids is that their behavior is quite different. Consequently, a gain in accuracy can be expected if different models are used for the different states of the fluid. This can be done in two ways. The first way (that followed by Kollmann and Janicka¹⁰¹) is to derive and model the transport equations for f_T, f_N and γ . The modelling that has been discussed so far is appropriate to the turbulent part f_T , and different modelling can be applied to f_N . The rate at which non-turbulent fluid becomes turbulent is determined by the transport equation for γ .

The second approach—that used by Pope⁴³—is to solve a single transport equation for $f_{u\phi}, (\underline{V}, \underline{\psi}, \psi, \underline{x}, t)$, but to use different modelling depending on the value of ψ . For $\psi > 0$ the modelling appropriate to turbulent fluid is used, while for $\psi = 0$ non-turbulent models are used. The rate of creation of turbulent fluid depends on the flux of $f_{u\phi}$, away from $\psi = 0$. Thus, rather than solving equations for the conditional pdf's f_T and f_N , the equation for $f_{u\phi}$ is solved using *conditional modelling*. Pope⁴³ presented such conditional models and used them to make calculations of a self-similar plane jet. The calculated intermittency factor and conditional statistics agree well with the experimental data. But since several of the conditional model constants were chosen by reference to these experimental data, further calculations are needed to assess the universality of the modelling.

5.7.3. Dissipation rates

In the particle-interaction and Langevin models, rate information enters through the dissipation rate ε and through the turbulent time scale τ ,

$$\tau \equiv k/\varepsilon.$$

(Since the kinetic energy k can be determined from the joint pdf, a knowledge of either τ or ε is sufficient.) In addition, the scalar dissipation rate

$$\varepsilon_{\alpha\beta} \equiv (2\Gamma/\rho) \left\langle \frac{\partial\phi'_\alpha}{\partial x_i} \frac{\partial\phi'_\beta}{\partial x_i} \right\rangle, \quad (5.204)$$

is implicitly modelled by the stochastic mixing model to be

$$\varepsilon_{\alpha\beta} = C_\phi \langle \phi'_\alpha \phi'_\beta \rangle / \tau, \quad (5.205)$$

(cf. Eq. 5.51). This raises the questions: how can τ (or ε) be determined? Is Eq. (5.205) valid? and, if so, is C_ϕ a universal constant? The purpose of this subsection is to outline the problems raised by these questions.

For simple flows, $\tau(\underline{x}, t)$ can be specified. For example, Pope^{42,43} assumed τ to be uniform across a self-similar plane jet. But for most flows, a general means of determining $\tau(\underline{x}, t)$ is required. Since k is known in terms of f , an obvious method is to solve the standard turbulence-model equation for ε .¹⁰ Alternatively a modelled transport equation for τ could be solved.

To solve a modelled transport equation for ε (or τ) is, most likely, the best available method for deter-

mining τ . But there are two problems. First, the representation of turbulence by a single scale most likely limits the validity of the approach to reasonably simple flows.¹⁰² Second, since measurements of ε are scarce and difficult to perform, a modelled transport equation for ε cannot be adequately tested. Thus the one-point joint pdf method (in common with $k-\varepsilon$ and Reynolds-stress models) may suffer from the inaccurate (or at least uncertain) determination of ε .

Scale information can be incorporated by considering multi-point pdf's, or the joint pdf of state variables and their derivatives. Work on these pdf's has been performed by Lundgren,¹⁰³ Levlev,¹⁰⁴ Qian,¹⁰⁵ Meyers and O'Brien¹⁰⁶ and Pope.¹⁰⁷ None of these methods has been applied to inhomogeneous flows. While multipoint pdf methods hold great promise for the future, they lie outside the scope of the present work.

Attention is now turned to the scalar dissipation and the model, Eq. (5.205). For a single, conserved, passive scalar ϕ , C_ϕ can be interpreted as the ratio of velocity-to-composition decay time scales:

$$C_\phi = \tau/\tau_\phi, \quad (5.206)$$

where

$$\tau_\phi \equiv \frac{1}{2} \langle \phi'^2 \rangle / \varepsilon_\phi. \quad (5.207)$$

By measuring the decay of k and $\langle \phi'^2 \rangle$ in grid turbulence, C_ϕ can be deduced. The measurements of Lin and Lin¹⁰⁸ and those of Warhaft and Lumley¹⁰⁹ show that C_ϕ is not a universal constant. For given experimental conditions, C_ϕ remains constant as the turbulence decays: but, depending upon the initial conditions, values of C_ϕ from 0.6 to 2.4 have been observed.

Warhaft¹¹⁰ performed an experiment in which the scalar fluctuations were induced differently than in Refs 108 and 109. In this case C_ϕ is found in the range 1.2–3.1; and, for each of six configurations investigated, C_ϕ decreased by about 40% over the length of the wind tunnel.

In another experiment performed by Warhaft¹¹¹ grid turbulence with scalar fluctuations was passed through an axisymmetric contraction. After the contraction C_ϕ was found to be in the range 1.9–3.1 (depending upon the configuration): C_ϕ then increased significantly, nearly doubling by the end of the tunnel.

It is abundantly clear that, with measured values in the range 0.6–3.1, C_ϕ is not a universal constant. It would appear to be preferable therefore to abandon Eq. (5.205) and instead solve a modelled transport equation for $\varepsilon_{\alpha\beta}$. Such equations have been proposed—by Newman *et al.*,¹¹² for example. At this level of closure, any modelled equation for $\varepsilon_{\alpha\beta}$ implies that (in decaying isotropic turbulence) the time scale ratio C_ϕ has a unique behavior.⁸⁰ Thus, Newman *et al.*'s model causes C_ϕ to remain at its initial value, consistent with the data of Lin and Lin¹⁰⁸ and Warhaft and Lumley.¹⁰⁹ But the model is then incon-

sistent with Warhaft's data.^{110,111} Worse, the principle of linearity and independence of conserved passive scalars constrains the form of the modelled equation for $\varepsilon_{\alpha\beta}$ so that a consistent model is incapable of allowing C_ϕ to remain constant.

The discussion above centers on scalar fluctuations in decaying grid turbulence. But for shear flows in which the scalar and velocity fields share a common history and common boundary conditions, Eq. (5.205) may be less unrealistic. Béguier *et al.*¹¹³ deduced the value of C_ϕ from data of three shear flows: a boundary layer, pipe flow and a plane wake. The value $C_\phi = 2.0$ fits the data to within 20% over nearly all of the flows. Thus, at present, Eq. (5.205) may provide the best model for $\varepsilon_{\alpha\beta}$, but further investigations are clearly needed.

Finally, we draw attention to the fact that none of the models presented depends upon the molecular transport properties. At high Reynolds number it can be assumed¹¹⁴ that the dissipation processes are controlled by the large scales of the turbulence, independent of the viscosity and diffusivity. However, many flows of interest are at moderate Reynolds numbers. It is possible to include a Reynolds number dependence in the modelling (see, for example, Ref. 11), but this has yet to be done in pdf methods.

At moderate Reynolds number, the different molecular diffusivities of different species are known to have a significant effect in some reactive flows.¹¹⁵ Also, when the Prandtl or Schmidt numbers are far from unity—in liquids, for example—the modelling of the mixing terms may not be realistic. Again, this is a topic that has yet to be addressed in pdf methods.

5.7.4. Variable density

In the low Mach number flows considered, the density $\rho(\phi)$ can vary significantly due to variations in composition (and enthalpy). In both inert mixing experiments and combustion experiments, density variations of a factor of five or more are not uncommon. It is clear, therefore, that the density variations have a significant effect on the flow, and that it would be inappropriate to treat them as small fluctuations.

In the joint pdf equation (Eq. 3.109) it is remarkable that the terms pertaining to convection, buoyancy, the mean pressure gradient, and reaction appear in closed form irrespective of variation of density in composition space. The conditional Lagrangian equation (cf. Eq. 4.49) corresponding to these terms is

$$\frac{\partial}{\partial t} \begin{bmatrix} \hat{U} \\ \hat{\phi} \\ \hat{x} \end{bmatrix} = \begin{bmatrix} g - (\nabla \langle p \rangle) / \rho(\hat{\phi}) \\ S(\hat{\phi}) \\ \hat{U} \end{bmatrix}. \quad (5.208)$$

It may be seen that the conditional-particle acceleration due to the mean pressure gradient is inversely proportional to the density—light fluid is accelerated more than heavy fluid. Libby and Bray¹¹⁶ have suggested that this effect is the cause of counter-gradient diffusion in premixed flames. None of the

other terms in Eq. (5.208) contains the density explicitly.

The effect of variable density on the conditional expectations is largely unknown. The major effect is likely to be on the fluctuating pressure p' . The Poisson equation for the pressure becomes

$$-\nabla^2 p = \rho \frac{\partial U_i}{\partial x_j} \frac{\partial U_j}{\partial x_i} + \frac{\partial \rho}{\partial x_j} \left(\frac{DU_j}{Dt} - g_j \right) + \frac{D}{Dt} \left(\frac{\partial U_i}{\partial x_i} \right) - \frac{\partial^2 \tau_{ij}}{\partial x_i \partial x_j}. \quad (5.209)$$

For a constant-density Newtonian fluid, only the first term is non-zero, but, it may be seen, additional terms arise due to density gradients, the velocity divergence and the shear stresses. Not only are there additional influences on p' , but p' also affects the pdf in different ways. For example, the term

$$\left\langle p' \frac{\partial U_i}{\partial x_i} \right\rangle$$

appears as a source in the turbulent kinetic energy equation. (In constant-density flows the divergence of velocity is zero and so pressure fluctuations do not affect the kinetic energy.)

The effect of variable density on the modelled terms is a subject for future work. It is emphasised, however, that even in variable-density flows the terms pertaining to convection, buoyancy, the mean pressure gradient, and reaction appear in closed form in the joint pdf equation.

5.7.5. Laminar flamelets

In the stochastic mixing model for $f_\phi(\psi)$, it is assumed that the rate of mixing is inversely proportional to the turbulent time scale τ . This assumption (modified by the comments of Section 5.7.3) is valid provided that the steepest gradients—which provide the dominant contribution to $\langle \Gamma \nabla^2 \phi | \psi \rangle$ —are caused by turbulent straining. But rapid reactions can also produce steep composition gradients. This effect is studied in more detail for an idealised premixed turbulent flame.

Let the single scalar ϕ be the progress variable (normally denoted by c ⁶⁹) that is zero in the unburnt

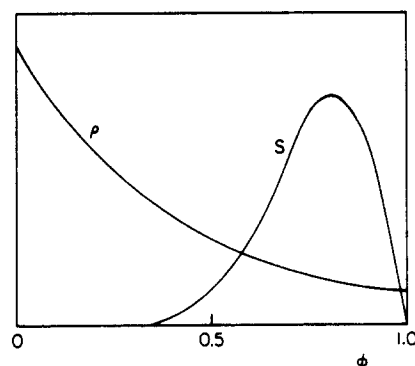


FIG. 5.9. Density ρ and reaction rate S against ϕ (arbitrary scale).

fuel-air mixture and unity in the fully burnt products. Assuming simple gradient diffusion, the transport equation for ϕ is (Eq. 3.20)

$$\rho \frac{D\phi}{Dt} = \frac{\partial}{\partial x_i} \left(\Gamma \frac{\partial \phi}{\partial x_i} \right) + \rho S, \quad (5.210)$$

where the density $\rho(\phi)$, the diffusivity $\Gamma(\phi)$, and the reaction rate $S(\phi)$ are known functions of ϕ . Typical variations of $\rho(\phi)$, and $S(\phi)$ with ϕ are shown in Fig. 5.9. Note that $S(0) = S(1) = 0$, and $S(\phi) \geq 0$.

Equation (5.210) admits a steady one-dimensional solution corresponding to a plane premixed laminar flame. At $x_1 = -\infty$ let the velocity be the laminar flame speed S_f ($U_1 = S_f$, $U_2 = U_3 = 0$) and let the mixture be unburnt, $\phi = 0$. At $x_1 = \infty$ there are pure products $\phi = 1$, and the velocity is $U_1 = S_f \rho(0)/\rho(1)$, $U_2 = U_3 = 0$. With these boundary conditions there is a steady one-dimensional solution to Eq. (5.210):

$$\phi(x_1, t) = \Phi(x_1). \quad (5.211)$$

This solution is sketched in Fig. 5.10. (The origin has been arbitrarily chosen so that $\Phi(0) = 1/2$.) The laminar flame speed S_f is the unique velocity U_1 ($x_1 = -\infty$) for which a stationary solution exists.

From the laminar flame profile $\Phi(x_1)$, any function of the solution can be determined. For example,

$$\frac{\partial \phi}{\partial x_i} \frac{\partial \phi}{\partial x_i} = g_x(x_1), \quad (5.212)$$

where

$$g_x(x_1) \equiv \left[\frac{d\Phi(x_1)}{dx_1} \right]^2. \quad (5.213)$$

Further, since $\Phi(x_1)$ increases monotonically with x_1 , $g_x(x_1)$ is a unique function of Φ :

$$g_x(x_1) = g(\Phi). \quad (5.214)$$

Thus, from the above three equations we obtain

$$\left[\frac{\partial \phi}{\partial x_i} \frac{\partial \phi}{\partial x_i} \right]_{\phi=\Phi} = g(\Phi). \quad (5.215)$$

This result has been obtained for a stationary flame normal to the x_1 coordinate direction with the origin chosen so that $\Phi(0) = 1/2$. But the left-hand side of Eq. (5.215) is a scalar that depends only on gradients of ϕ —it is unaffected by an arbitrary reorientation, shift, or translation of the coordinate system. Conse-

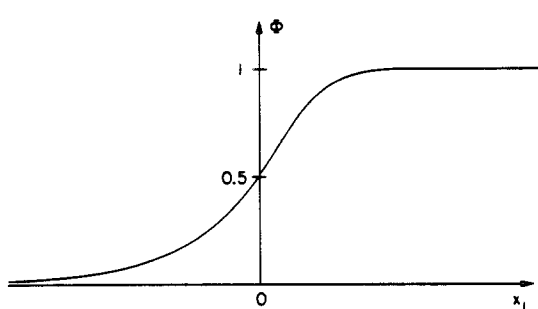


FIG. 5.10. Premixed laminar flame profile $\Phi(x_1)$ against x_1 .

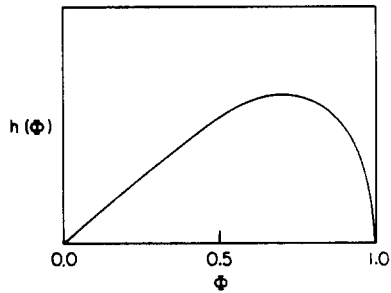


FIG. 5.11. Quantity $h(\Phi)$ against Φ , Eq. (5.216) (arbitrary scale).

quently, Eq. (5.215) holds for any plane premixed laminar flame governed by Eq. (5.210), irrespective of its orientation or of a superimposed uniform fluid velocity.

In the same way, the right-hand side of the conservation equation for ϕ (Eq. 5.210) is known:

$$\left[\frac{\partial}{\partial x_i} \left(\Gamma \frac{\partial \phi}{\partial x_i} \right) + \rho S \right]_{\phi=\Phi} = h(\Phi), \quad (5.216)$$

where

$$h(\Phi) = h_x(x_1) = \frac{d}{dx_1} \left(\Gamma \frac{d\phi}{dx_1} \right) + \rho S = S_f \rho(0) \frac{d\phi}{dx_1}. \quad (5.217)$$

The function $h(\Phi)$ is sketched on Fig. 5.11. It is clear from the last expression in Eq. (5.217) that $h(0) = h(1) = 0$, and $h(\Phi) \geq 0$.

We return now to high Reynolds number turbulent premixed flames and consider two extreme cases. First, when the laminar flame thickness δ_f is much larger than the Kolmogorov scale η ($\delta_f/\eta \gg 1$), the steepest gradients are due to turbulent straining. Then, mixing proceeds at a rate inversely proportional to the turbulence time scale τ in accord with the stochastic mixing model. In the second extreme case ($\delta_f/\eta \ll 1$), the steepest gradients are found within laminar flamelets. Burnt and unburnt mixture are separated by a reaction sheet (which may or may not be simply connected). Turbulence strains this sheet and causes it to wrinkle. But, in the extreme limit considered, the strain rate is small (compared with S_f/δ_f) and the radius of curvature is large (compared with δ_f). Thus, locally, the flame sheet behaves like a plane premixed laminar flame.

In the transport equation for the joint pdf $f(V, \psi)$, the conditional expectation of the right-hand side of Eq. (5.210) appears. With the assumption of laminar flamelet combustion this becomes

$$\left\langle \frac{\partial}{\partial x_i} \left(\Gamma \frac{\partial \phi}{\partial x_i} \right) + \rho S | V, \psi \right\rangle = h(\psi), \quad (5.218)$$

where h is the known function given by Eq. (5.217). We thus reach the remarkable conclusion that for laminar flamelet combustion the reaction and mixing terms appear in closed form.

Using this result (Eq. 5.218), Pope and Anand⁴⁵

have made joint pdf calculations to compare the properties of premixed flames in flamelet and distributed combustion.

6. SOLUTION ALGORITHM

6.1. Introduction

Throughout the development, the ability to solve the modelled joint pdf equation has been a prime consideration. The joint pdf can be represented computationally by the discrete representation, and its evolution can be computed via stochastic models. In this section an algorithm is outlined to solve the modelled joint pdf equation for an unsteady, variable-density, three-dimensional turbulent reactive flow. Variants of the algorithm for simpler flows are outlined in Section 6.8.

In the last section, alternative models are presented. The solution algorithm is described for the velocities being modelled by the Langevin equation, and the scalar dissipation being modelled by the stochastic mixing model. Solution algorithms for other modelled pdf equations follow by analogy. It is assumed that the time scale $\tau(\underline{x}, t)$ is known.

The discrete representation, on which the solution algorithm is based is reviewed briefly in Section 6.2. From a given initial condition at $t = t_0$, the algorithm marches in time with small time steps Δt . In the time interval Δt , several different processes simultaneously affect the evolution of the joint pdf. But the method of fractional steps¹¹⁷ (outlined in Section 6.3) is used so that the effects of some of these processes can be treated sequentially. In the first fractional step (Section 6.4), the pdf evolves under the influence of all processes except stochastic mixing, convection, and the mean pressure gradient. Stochastic mixing takes place during the second fractional step which is described in Section 6.5. In the third fractional step (Section 6.6), the mean pressure is determined by an indirect algorithm. Then the joint pdf evolves under the influence of convection and the mean pressure gradient.

The algorithm described provides the solution in terms of the discrete representation of the joint pdf. But normally, the information sought is mean quantities, such as $\bar{U}(\underline{x}, t)$, $\bar{\phi}(\underline{x}, t)$ or $\bar{S}_a(\phi(\underline{x}, t))$. Furthermore, the mean velocity, the Reynolds stresses, and the mean velocity gradients appear in the modelled pdf equation and must, therefore, be determined from the solution. An obvious way to determine means—that described in Section 3.4—is to divide physical space into cells. Then an ensemble average over the particles in a cell approximates a density-weighted mean at the cell location, Eq.(3.89). But this method—though conceptually useful—has little merit as a computational scheme. As described in Section 6.7, the method of least-squares cubic splines can be used to determine means from the discrete representation of the joint pdf. This is a computationally-efficient method that reduces the statistical error.

6.2. Discrete Representation

We consider the turbulent flow within a three-dimensional volume of physical space—the solution domain. At time t , the mass of fluid within the solution domain is $M(t)$. The mass density function $\mathcal{F}(\underline{V}, \underline{\psi}, \underline{x}; t)$ is represented by $N(t)$ stochastic particles in state space, each particle representing a fixed mass Δm . At time t , the state of the n th stochastic particle is

$$\underline{U}^{*(n)}(t), \underline{\phi}^{*(n)}(t), \underline{x}^{*(n)}(t), n = 1, 2, \dots, N(t). \quad (6.1)$$

As time proceeds, the states of the stochastic particles change—some particles may leave the solution domain and some may enter as prescribed by the boundary conditions. The discrete mass density function, and the discrete pdf of the stochastic particle states are given by

$$\begin{aligned} \mathcal{F}_N^*(\underline{V}, \underline{\psi}, \underline{x}; t) &= \rho(\underline{\psi}) f_N^*(\underline{V}, \underline{\psi}; \underline{x}, t) \\ &= \Delta m \sum_{n=1}^{N(t)} \delta(\underline{V} - \underline{U}^{*(n)}) \delta(\underline{\psi} - \underline{\phi}^{*(n)}) \delta(\underline{x} - \underline{x}^{*(n)}). \end{aligned} \quad (6.2)$$

In the numerical solution, the states of the N stochastic particles are known, but their expected states are not. Nonetheless, the connection between the discrete representation and the joint pdf is best viewed in terms of expectations:

$$\mathcal{F}(\underline{V}, \underline{\psi}, \underline{x}; t) = \langle \mathcal{F}_N^*(\underline{V}, \underline{\psi}, \underline{x}; t) \rangle, \quad (6.3)$$

or

$$\bar{f}(\underline{V}, \underline{\psi}, \underline{x}, t) = \langle f_N^*(\underline{V}, \underline{\psi}; \underline{x}, t) \rangle. \quad (6.4)$$

It follows that \mathcal{F}_N^* must satisfy the consistency condition

$$\begin{aligned} \iint \langle \mathcal{F}_N^*(\underline{V}, \underline{\psi}, \underline{x}; t) \rangle d\underline{V} d\underline{\psi} \\ = \left\langle \Delta m \sum_{n=1}^{N(t)} \delta(\underline{x} - \underline{x}^{*(n)}[t]) \right\rangle = \langle \rho(\underline{x}, t) \rangle, \end{aligned} \quad (6.5)$$

(cf. Eqs 3.82 and 4.107). Equivalently, \mathcal{F}_N^* must satisfy the normalization condition (Eq. 4.108)

$$\begin{aligned} \iint \langle \mathcal{F}_N^*(\underline{V}, \underline{\psi}, \underline{x}; t) \rangle [\rho(\underline{\psi})]^{-1} d\underline{V} d\underline{\psi} \\ = \left\langle \Delta m \sum_{n=1}^{N(t)} \delta(\underline{x} - \underline{x}^{*(n)}[t]) / \rho(\underline{\phi}^{*(n)}[t]) \right\rangle = 1. \end{aligned} \quad (6.6)$$

The pressure algorithm ensures that Eqs (6.5–6) are satisfied.

6.3. Fractional Steps

The modelled equation for $\mathcal{F}(\underline{V}, \underline{\psi}, \underline{x}; t)$ to be solved is

$$\begin{aligned}
& \frac{\partial \mathcal{F}}{\partial t} + V_j \frac{\partial \mathcal{F}}{\partial x_j} + \left(g_j - \frac{1}{\rho(\psi)} \frac{\partial \langle p \rangle}{\partial x_j} \right) \frac{\partial \mathcal{F}}{\partial V_j} + \frac{\partial}{\partial \psi_a} [S_a(\psi) \mathcal{F}] \\
& = -G_{ij} \frac{\partial}{\partial V_i} [(V_j - \tilde{U}_j) \mathcal{F}] + \frac{1}{2} C_0 \epsilon \frac{\partial^2 \mathcal{F}}{\partial V_j \partial V_j} \\
& + 2C_\phi \left\{ 2^\sigma \int \mathcal{F}(\psi + \psi') \mathcal{F}(\psi - \psi') \rho(\psi) / [\rho(\psi + \psi') \right. \\
& \left. \times \rho(\psi - \psi')] d\psi' - \mathcal{F} \right\} / \tau. \tag{6.7}
\end{aligned}$$

The terms on the left-hand side are exact (cf. Eq. 3.109), while the first two terms on the right-hand side are from the Langevin model (cf. Eq. 5.150). The final term is due to the stochastic mixing model. It is a generalization of the right-hand side of Eq. (5.40) to a set of σ compositions in variable-density flow.

Equation (6.7) can be written

$$\frac{\partial \mathcal{F}}{\partial t} = (P_1 + P_2 + P_3) \mathcal{F}, \tag{6.8}$$

where P_1 , P_2 and P_3 are operators corresponding to different processes. We define

$$P_3 \equiv -V_j \frac{\partial}{\partial x_j} + \frac{1}{\rho(\psi)} \frac{\partial \langle p \rangle}{\partial x_j} \frac{\partial}{\partial V_j}, \tag{6.9}$$

to correspond to the effects of convection and the mean pressure gradient. Similarly, P_2 corresponds to the stochastic mixing model and is defined so that $P_2 \mathcal{F}$ is equal to the final term in Eq. (6.7). The remaining processes are contained in P_1 :

$$\begin{aligned}
P_1 \equiv & -g_j \frac{\partial}{\partial V_j} - S_a \frac{\partial}{\partial \psi_a} - \frac{\partial S_a}{\partial \psi_a} I \\
& - G_{ij} (V_j - \tilde{U}_j) \frac{\partial}{\partial V_i} - G_{ii} I + \frac{1}{2} C_0 \epsilon \frac{\partial^2}{\partial V_j \partial V_j}, \tag{6.10}
\end{aligned}$$

where I is the identity operator.

Equation (6.8) shows that all the processes affect the evolution of \mathcal{F} simultaneously. But the method of fractional steps can be used to calculate the evolution of \mathcal{F} by considering the sequential action of each of the processes over sufficiently small time intervals Δt .

Starting from the given initial condition $\mathcal{F}(t_0)$, the method is used to calculate $\hat{\mathcal{F}}(t)$ —a first-order approximation to $\mathcal{F}(t)$ —at successive time steps. For each time step, the method is defined by the three fractional steps:

$$\hat{\mathcal{F}}_1(t) \equiv (I + \Delta t P_1) \hat{\mathcal{F}}(t), \tag{6.11}$$

$$\hat{\mathcal{F}}_2(t) \equiv (I + \Delta t P_2) \hat{\mathcal{F}}_1(t), \tag{6.12}$$

and

$$\hat{\mathcal{F}}(t + \Delta t) \equiv (I + \Delta t P_3) \hat{\mathcal{F}}_2(t). \tag{6.13}$$

Before discussing these steps, we first verify that $\hat{\mathcal{F}}(t)$ is, as claimed, a first-order approximation to $\mathcal{F}(t)$. Using Eqs (6.11–12) to eliminate $\hat{\mathcal{F}}_1$ and $\hat{\mathcal{F}}_2$, Eq. (6.13) becomes

$$\begin{aligned}
\hat{\mathcal{F}}(t + \Delta t) & \equiv (I + \Delta t P_3)(I + \Delta t P_2)(I + \Delta t P_1) \hat{\mathcal{F}}(t), \\
& = (I + \Delta t [P_1 + P_2 + P_3] + \Delta t^2 [P_3 P_2 + P_3 P_1 \\
& + P_2 P_1] + \Delta t^3 P_3 P_2 P_1) \hat{\mathcal{F}}(t) \\
& = \hat{\mathcal{F}}(t) + \Delta t (P_1 + P_2 + P_3) \hat{\mathcal{F}}(t) + \mathcal{O}(\Delta t^2). \tag{6.14}
\end{aligned}$$

A second expression for $\hat{\mathcal{F}}(t + \Delta t)$ is obtained from the Taylor expansion of $\hat{\mathcal{F}}$ about t :

$$\begin{aligned}
\hat{\mathcal{F}}(t + \Delta t) & = \hat{\mathcal{F}}(t) + \frac{\partial \hat{\mathcal{F}}}{\partial t} \Delta t + \frac{\partial^2 \hat{\mathcal{F}}}{\partial t^2} \frac{\Delta t^2}{2!} \dots \\
& = \hat{\mathcal{F}}(t) + \frac{\partial \hat{\mathcal{F}}}{\partial t} \Delta t + \mathcal{O}(\Delta t^2). \tag{6.15}
\end{aligned}$$

Thus, equating the right-hand sides of the last two equations and dividing by Δt we obtain

$$\frac{\partial \hat{\mathcal{F}}}{\partial t} = (P_1 + P_2 + P_3) \hat{\mathcal{F}} + \mathcal{O}(\Delta t), \tag{6.16}$$

which, except for the first-order truncation error, is the same as Eq. (6.8). Consequently $\hat{\mathcal{F}}(t)$ approximates $\mathcal{F}(t)$ with an error of order Δt .

The three fractional steps (6.11–13) are qualitatively the same. We examine the third step since P_3 is the simplest of the operators. In the limit as Δt tends to zero, and if the other two steps are omitted (or if P_1 and P_2 are set to the null operator), then Eq. (6.13) corresponds to the differential equation

$$\begin{aligned}
\frac{\partial \hat{\mathcal{F}}}{\partial t} & = P_3 \hat{\mathcal{F}} \\
& = -V_j \frac{\partial \hat{\mathcal{F}}}{\partial x_j} + \frac{1}{\rho(\psi)} \frac{\partial \langle p \rangle}{\partial x_j} \frac{\partial \hat{\mathcal{F}}}{\partial V_j}. \tag{6.17}
\end{aligned}$$

That is, it corresponds to $\hat{\mathcal{F}}$ evolving under the influence of convection and the mean pressure gradient alone. For finite Δt , Eq. (6.13) corresponds to the approximate solution of this differential equation by the explicit Euler method, from the initial condition $\hat{\mathcal{F}}_2(t)$:

$$\begin{aligned}
\hat{\mathcal{F}}(t + \Delta t) & = \hat{\mathcal{F}}_2(t) + \Delta t P_3 \hat{\mathcal{F}}_2(t) \\
& = \hat{\mathcal{F}}_2(t) - \Delta t V_j \frac{\partial \hat{\mathcal{F}}_2(t)}{\partial x_j} \\
& + \frac{\Delta t}{\rho(\psi)} \frac{\partial \langle p \rangle}{\partial x_j} \frac{\partial \hat{\mathcal{F}}_2(t)}{\partial V_j}. \tag{6.18}
\end{aligned}$$

The details of the implementation of the three fractional steps are described in the next three subsections. While we have defined each step as an explicit Euler step (Eqs 6.11–13), we note that any other scheme (that is at least first-order accurate) yields qualitatively the same result (Eq. 6.16). Having established that $\hat{\mathcal{F}}$ is a first-order approximation to \mathcal{F} , it is no longer necessary to distinguish between the exact and approximate solution to the evolution equation: henceforth both are denoted by \mathcal{F} .

6.4. First Fractional Step

Although the first fractional step contains most of the processes, it is nevertheless the simplest to explain and

implement. The step corresponds to solving the equation

$$\begin{aligned} \frac{\partial \mathcal{F}}{\partial t} + g_j \frac{\partial \mathcal{F}}{\partial V_j} + \frac{\partial}{\partial \psi_\alpha} [S_\alpha(\psi) \mathcal{F}] &= -G_{ij} \frac{\partial}{\partial V_i} [(V_j - \bar{U}_j) \mathcal{F}] \\ &+ \frac{1}{2} C_0 \epsilon \frac{\partial^2 \mathcal{F}}{\partial V_j \partial V_j}, \end{aligned} \quad (6.19)$$

for a time interval Δt , from the initial condition $\mathcal{F}(t)$. This is simply achieved since Eq. (6.19) is the evolution equation corresponding to the stochastic system

$$\begin{aligned} \Delta_{\delta t} U_i^* &= g_i \delta t + G_{ij} [U_j^* - \bar{U}_j] \delta t + (C_0 \epsilon)^{1/2} \Delta_{\delta t} (W_i)_i, \\ \Delta_{\delta t} \phi_\alpha^* &= S_\alpha(\phi^*) \delta t, \end{aligned}$$

$$\Delta_{\delta t} x_i^* = 0, \quad (6.20)$$

(cf. Eqs 4.99–100). Integrating these equations for a time Δt using the explicit Euler method yields (to first-order in Δt):

$$\begin{aligned} U_i^*(t + \Delta t) &= U_i^* + \Delta t \{g_i + G_{ij} [U_j^* - \bar{U}_j]\} \\ &+ (C_0 \epsilon \Delta t)^{1/2} \xi_i, \\ \phi_\alpha^*(t + \Delta t) &= \phi_\alpha^* + \Delta t S_\alpha(\phi^*), \\ x_i^*(t + \Delta t) &= x_i^*, \end{aligned} \quad (6.21)$$

where all quantities on the right-hand side are at time t , and ξ is a standardized joint normal random vector.

Thus in the first fraction step, the states of each of the $N(t)$ stochastic particles change independently according to Eq. (6.21).

The computational work needed to evaluate Eqs (6.21), depends crucially upon the reaction scheme. For each particle in an inert constant-density flow, about forty arithmetic operations are needed to perform the integration. But for a complicated reaction scheme involving many species (for example Westbrook and Dryer⁶⁸) many thousands of operations may be required to evaluate the sources $S_\alpha(\phi^*)$. A computationally efficient algorithm is possible only if the sources S can be evaluated efficiently. If the number of composition variables σ can be reduced to three or less then S can be tabulated (once) and then 4σ operations per particle are required to obtain the values of S from the table. For combustion calculation, the simplified reaction schemes of Westbrook and Dryer¹¹⁹ are well-suited to this purpose.

6.5. Second Fractional Step: Stochastic Mixing Model

In the second fractional step the position \underline{x}^* and velocity \underline{U}^* of the stochastic particles are unaltered, while the compositions may change by mixing.

The stochastic mixing model is described in Section 5.2.3 for the case of homogeneous turbulence. In that case, in the small time interval δt , the probability of a pair of particles mixing is

$$C_\phi N \delta t / \tau.$$

Consequently, the probability of the n th particle being selected is

$$2C_\phi \delta t / \tau,$$

since, if mixing takes place, two out of the N particles are selected. Similarly, for the general inhomogeneous case, in the small time interval Δt the probability of the n th particle being selected is

$$P^{(n)} \equiv 2C_\phi \Delta t / \tau (\underline{x}^{*(n)}[t], t). \quad (6.22)$$

(Clearly Δt should be chosen to be significantly smaller than τ .)

A simple computational algorithm to select particles is to generate N independent random numbers $\omega^{(n)}$, $n = 1, 2, \dots, N$, each uniformly distributed between zero and one. If

$$\omega^{(n)} + P^{(n)} > 1, \quad (6.23)$$

then the n th particle is selected for mixing. (A more efficient, general, and complicated algorithm is given in Ref. 85.)

Mixing takes place locally in physical space, and this is reflected in the pairing of the selected particles. Each particle selected is close (in physical space) to its partner. A simple algorithm to accomplish this local pairing, is to divide physical space into cells, and to pair particles within each cell.[†] This introduces a truncation error of the order of the cell size, but there is little computational penalty in making this size very small (compared to flow length scales).

The pairs of particles mix, as in the homogeneous case, according to Eq. (5.48). This completes the second fractional step.

6.6. Third Fractional Step: Convection and Mean Pressure Gradient

In the third fraction step, the equation

$$\frac{\partial \mathcal{F}}{\partial t} + V_j \frac{\partial \mathcal{F}}{\partial x_j} = \frac{1}{\rho(\psi)} \frac{\partial \langle p \rangle}{\partial x_j} \frac{\partial \mathcal{F}}{\partial V_j}, \quad (6.24)$$

is integrated for a time interval Δt from the initial condition $\mathcal{F}_2(t)$ to yield $\mathcal{F}(t + \Delta t)$. In this subsection we describe both the numerical solution of Eq. (6.24) and the determination of the mean pressure.

Corresponding to Eq. (6.24), the evolution equations for stochastic particle properties are:

$$\frac{d \underline{U}^*}{dt} = \frac{-1}{\rho(\phi^*[t])} [\nabla \langle p \rangle]_{\underline{x}^*(t)}, \quad (6.25)$$

$$\frac{d \phi^*}{dt} = 0, \quad (6.26)$$

and

$$\frac{d \underline{x}^*}{dt} = \underline{U}^*(t). \quad (6.27)$$

The initial conditions—denoted by $\underline{x}^{(2)}$, $\underline{U}^{(2)}$, $\phi^{(2)}$ —are the properties after the second fractional step. Equations (6.25–27) are integrated approximately so that the

[†] There are several solutions to the problem presented by having an odd number of particles in a cell—but this is a computational detail.

properties after the third fractional step— $\underline{\phi}^{(3)}$, $\underline{U}^{(3)}$, $\underline{x}^{(3)}$ —are at least a first-order accurate approximation to the exact solution— $\underline{U}^*(t + \Delta t)$, $\underline{\phi}^*(t + \Delta t)$, $\underline{x}^*(t + \Delta t)$.†

From Eq. (6.26) we obtain

$$\underline{\phi}^{(3)} = \underline{\phi}^{(2)} = \underline{\phi}^*(t + \Delta t). \quad (6.28)$$

Consequently, in this fractional step, the particle's density remains constant. To aid the notation, we define the particle's (constant) specific volume by

$$v^* \equiv 1/\rho(\underline{\phi}^{(2)}). \quad (6.29)$$

The pressure algorithm described below determines the mean pressure field to first order. The gradient of this mean field is denoted by $\underline{P}(\underline{x})$,

$$\underline{P}(\underline{x}) = \nabla \langle p(\underline{x}, t) \rangle + \mathcal{O}(\Delta t), \quad (6.30)$$

and, for the moment, is assumed to be known. Then, Eq. (6.25) is integrated by

$$\begin{aligned} \underline{U}^{(3)} &\equiv \underline{U}^{(2)} - \Delta t v^* \underline{P}(\underline{x}^{(2)}) \\ &= \underline{U}^*(t + \Delta t) + \mathcal{O}(\Delta t^2). \end{aligned} \quad (6.31)$$

Having determined $\underline{U}^*(t + \Delta t)$ to first order, $\underline{x}^*(t + \Delta t)$ can be determined (from Eq. 6.27) to second order:

$$\begin{aligned} \underline{x}^{(3)} &\equiv \underline{x}^{(2)} + \frac{1}{2} \Delta t (\underline{U}^{(2)} + \underline{U}^{(3)}), \\ &= \underline{x}^*(t + \Delta t) + \mathcal{O}(\Delta t^3). \end{aligned} \quad (6.32)$$

It may be seen from Eq. (6.32) that, as with all Lagrangian methods, convection is treated without reference to a grid, and spatial derivatives do not have to be evaluated. Consequently the problems of false diffusion and artificial viscosity encountered in finite-difference schemes¹¹⁸ are avoided.

To summarize, if the mean pressure is known, the third fractional step consists of determining $\underline{\phi}^{(3)}$, $\underline{U}^{(3)}$ and $\underline{x}^{(3)}$ from Eqs (6.28), (6.31) and (6.32).

In principle, the mean pressure can be determined by solving the Poisson equation, Eq. (4.129). But the evaluation of the source terms—especially $\partial^2 \langle \rho \rangle / \partial t^2$ —is computationally impracticable. Instead, an indirect algorithm is used which results in an elliptic equation for $\langle p \rangle$. The algorithm is based on an observation that follows directly from the propositions established in Section 4.7: the normalization condition (Eq. 4.108 or 6.6) is satisfied if, and only if, the mean pressure satisfies the Poisson equation. We deduce, then, the mean pressure field that causes the consistency condition to be satisfied at time $t + \Delta t$.

For simplicity (and without loss of generality) we consider a single particle (i.e. $N = 1$). Then, with a mass M of fluid in the solution domain, the consistency condition at time $t + \Delta t$ is

$$M \langle v^* \delta(\underline{x} - \underline{x}^*[t + \Delta t]) \rangle = 1. \quad (6.33)$$

† The superscripts (2) and (3) refer to the states after the second and third fraction steps, not to the second ($n = 2$) and third ($n = 3$) particles. Below, we write $\underline{x}^{(2,n)}$ to denote the state of the n th particle after the second fraction step.

An elliptic partial differential equation for $\langle p \rangle$ is now obtained by manipulating Eq. (6.33).

If there were no mean pressure gradient, then $\underline{x}^*(t + \Delta t)$ would assume the value

$$\underline{x}' \equiv \underline{x}^{(2)} + \underline{U}^{(2)} \Delta t. \quad (6.34)$$

And in general, from Eqs (6.31–32) it follows

$$\underline{x}^*(t + \Delta t) = \underline{x}' - \frac{1}{2} \Delta t^2 v^* \underline{P}(\underline{x}^{(2)}) + \mathcal{O}(\Delta t^3). \quad (6.35)$$

Substituting this expression for $\underline{x}^*(t + \Delta t)$ in Eq. (6.33), and expanding the delta function as a Taylor series in \underline{x} about \underline{x}' yields

$$\begin{aligned} M^{-1} &= \left\langle v^* \delta(\underline{x} - \underline{x}') + \frac{1}{2} \Delta t^2 (v^*)^2 P_i(\underline{x}^{(2)}) \frac{\partial \delta(\underline{x} - \underline{x}')}{\partial x_i} \right\rangle \\ &\quad + \mathcal{O}(\Delta t^3) \\ &= h(\underline{x}) + \frac{1}{2} \Delta t^2 \frac{\partial}{\partial x_i} \langle (v^*)^2 P_i(\underline{x}^{(2)}) \delta(\underline{x} - \underline{x}') \rangle \\ &\quad + \mathcal{O}(\Delta t^3), \end{aligned} \quad (6.36)$$

where

$$h(\underline{x}) \equiv \langle v^* \delta(\underline{x} - \underline{x}') \rangle. \quad (6.37)$$

Since $\underline{x}^{(2)}$ approximates \underline{x}' with an error of order Δt , the term in \underline{P} can be re-expressed as

$$\begin{aligned} \langle (v^*)^2 P_i(\underline{x}^{(2)}) \delta(\underline{x} - \underline{x}') \rangle &= \langle (v^*)^2 P_i(\underline{x}^{(2)}) \delta(\underline{x} - \underline{x}^{(2)}) \rangle \\ &\quad + \mathcal{O}(\Delta t) \\ &= \langle (v^*)^2 \delta(\underline{x} - \underline{x}^{(2)}) \rangle P_i(\underline{x}) \\ &\quad + \mathcal{O}(\Delta t) \\ &= \gamma(\underline{x}) \frac{\partial \langle p \rangle}{\partial x_i} + \mathcal{O}(\Delta t), \end{aligned} \quad (6.38)$$

where

$$\gamma(\underline{x}) \equiv \langle (v^*)^2 \delta(\underline{x} - \underline{x}^{(2)}) \rangle. \quad (6.39)$$

The last step in Eq. (6.38) simply uses the definitions of \underline{P} (Eq. 6.30) and $\gamma(\underline{x})$. Substituting this result (Eq. 6.38) into Eq. (6.36) yields

$$M^{-1} = h(\underline{x}) + \frac{1}{2} \Delta t^2 \frac{\partial}{\partial x_i} \left\{ \gamma(\underline{x}) \frac{\partial \langle p \rangle}{\partial x_i} \right\} + \mathcal{O}(\Delta t^3), \quad (6.40)$$

and hence the required elliptic equation for $\langle p \rangle$ is

$$\frac{\partial}{\partial x_i} \left\{ \gamma(\underline{x}) \frac{\partial \langle p \rangle}{\partial x_i} \right\} = 2[M^{-1} - h(\underline{x})]/\Delta t^2 + \mathcal{O}(\Delta t). \quad (6.41)$$

The equations derived above are used in a five-step scheme to determine the mean pressure and then to perform the third fractional step:

- (i) the function $\gamma(\underline{x})$ (Eq. 6.39) is determined (or rather approximated) from the initial positions $\underline{x}^{(2,n)}$ and specific volumes $v^{*(n)}$ of the N stochastic particles;
- (ii) for each particle, $\underline{x}^{(n)}$ is determined from Eq. (6.34);

- (iii) the function $h(x)$ (Eq. 6.37) is determined from $x^{(n)}$ and $v^{*(n)}$;
- (iv) Eq. (6.41) is solved to obtain a first-order approximation to $\langle p(x, t) \rangle$; and then
- (v) Eqs (6.31–32) are solved to obtain $\underline{x}^{(3,n)}$ and $\underline{U}^{(3,n)}$ —approximations to $x^{*(n)}(t + \Delta t)$ and $U^{*(n)}(t + \Delta t)$.

6.7. Determination of Means

The algorithm described previously provides a solution to the joint pdf equation in terms of the discrete representation, Eq. (6.2). For this solution to be useful, a method of determining mean quantities from the discrete representation is required. In order to compare theory with experiment, it is desirable to determine all the mean quantities that are measured—the means $\langle \underline{U} \rangle$ and $\langle \phi \rangle$; the second, third and fourth moments; pdf's $f_{u_1}(V_1; \underline{x}, t)$ and $f_{\phi_1}(\psi_1; \underline{x}, t)$; and the joint pdf's of two variables. (Joint pdf's of more than two variables cannot readily be presented graphically.)

Not only are mean quantities required as outputs from the solution, but they are also needed within the solution algorithm. In the first fractional step, \underline{U} , $\partial \underline{U}_i / \partial x_j$ and $\underline{u}_i' \underline{u}_j'$ must be determined in order to evaluate the second-order tensor G_{ij} . And in the third fractional step, the functions $h(x)$ and $\gamma(x)$ (Eqs 6.37 and 6.39) must be determined as part of the pressure algorithm.

In this section, the determination of means is considered by reference to a one-dimensional example. It is shown that the straight-forward method of approximating means by ensemble averages over cells is hopelessly inaccurate, especially for derivatives and pdf's. But the method of least-squares cubic splines provides a more accurate alternative.

The one-dimensional example considered is of a normally-distributed random variable $\phi(x)$ in the interval $0 \leq x \leq 1$. The mean is specified to be

$$\langle \phi(x) \rangle = 3x^2 \sin(\pi x), \quad (6.42)$$

and the uniform standard deviation is

$$\sigma \equiv \langle \phi'^2 \rangle^{1/2} = 1/4. \quad (6.43)$$

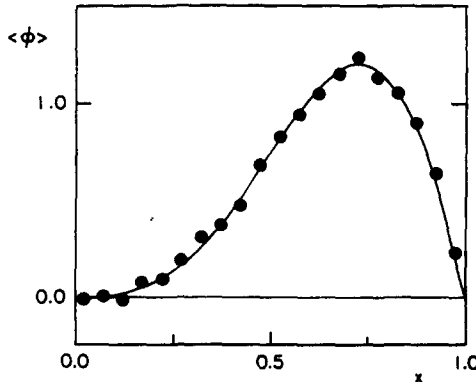


FIG. 6.1. Quantity $\langle \phi(x) \rangle$ against x : ● ensemble average from 1000 samples and 20 cells; — exact result.

The discrete representation of the pdf $f_{\phi}(\psi; x)$ is

$$f_{\phi N}(\psi; x) = \frac{1}{N} \sum_{n=1}^N \delta(\psi - \phi^{(n)}) \delta(x - x^{(n)}), \quad (6.44)$$

where $x^{(n)}$ is the n th sample of a uniformly-distributed random variable ($0 \leq x^{(n)} \leq 1$) and $\phi^{(n)}$ is

$$\phi^{(n)} = \langle \phi(x^{(n)}) \rangle + \sigma \xi^{(n)}, \quad (6.45)$$

where $\xi^{(n)}$ is the n th sample of a standardized normal random variable. The number of samples N is chosen to be 1000.

The x -axis is divided into twenty equal-sized cells ($K = 20$). Figure 6.1 shows the ensemble average of ϕ for each cell compared with the specified mean, Eq. (6.42). Some scatter is evident, but the overall agreement is satisfactory: the r.m.s. error is 0.029. The second derivative $d^2\langle\phi\rangle/dx^2$ is calculated from the cell averages by the three-point central difference. The result, shown on Fig. 6.2, shows erratic behavior, the r.m.s. error being 30.1. Not only is the inaccuracy unacceptable, but also errors of this magnitude in $\partial \bar{U}_i / \partial x_m$, for example, when fed back into the solution algorithm, would inevitably lead to numerical instability.

An alternative method of determining means is least-squares cubic splines (de Boor¹²⁰). A cubic spline is a piecewise cubic polynomial which is continuous and has continuous first and second derivatives. The x -axis is divided into L equal intervals, and within each interval the function (i.e. $\langle \phi \rangle$) is approximated by a cubic polynomial. Thus there are $4L$ polynomial coefficients. At the $(L-1)$ points between the L intervals, the function and its first two derivatives are continuous.

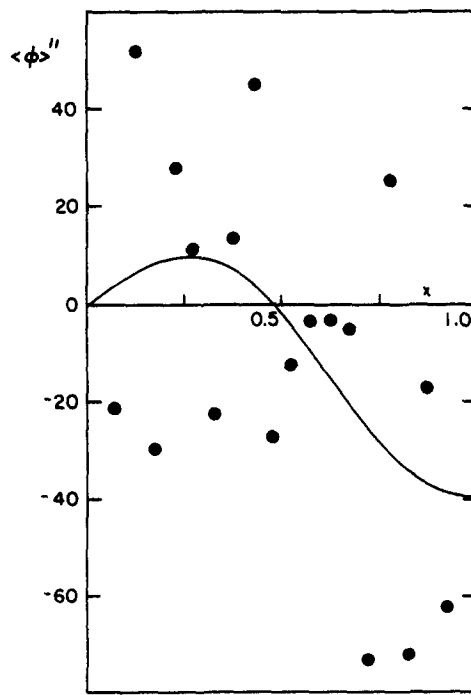


FIG. 6.2. Term $d^2\langle\phi(x)\rangle/dx^2$ against x : ● from central difference of cell averages; — exact result.

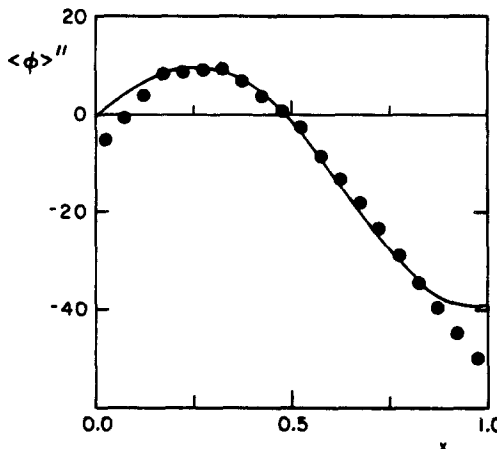


FIG. 6.3. Term $d^2\langle\phi(x)\rangle/dx^2$ against x : ● from least-squares cubic spline; — exact result.

This condition determines $3(L-1)$ of the coefficients, leaving $L+3$ to be determined. These remaining coefficients are determined by requiring that the mean-square error between the spline and the data points $(\phi^{(n)}, x^{(n)})$ be minimized. (An efficient algorithm using B-splines is described by de Boor.¹²⁰)

With six intervals ($L=6$), the least-squares cubic spline approximates $\langle\phi(x)\rangle$ with an r.m.s. error of 0.015—about half that of the cell averages. The approximation to the second derivative shown on Fig. 6.3 shows a more striking improvement. The r.m.s. error is 3.7, a factor of 8 less than that for the cell average. To obtain the same accuracy with cell averages, the number of particles would have to be increased to $N=64,000$, with an increase in storage and computer time of a factor of 64. Clearly then, least-squares cubic splines provide an efficient method of determining mean quantities.

The main reason for the improved accuracy of the least-squares cubic splines is the reduction in the number of degrees of freedom in the approximation from 20 ($K=20$) to 9 ($L+3=9$). But the optimum value of L is not known *a priori*—too large a value

increases the statistical error, while with too small a value, the mean profile cannot be resolved. A more sophisticated technique that overcomes these difficulties is to use smoothing cubic splines,^{120,121} with the smoothing parameter determined by cross-validation.^{122,123} This method has proved successful in several Monte Carlo solutions of the pdf equations.^{27,43,45}

We consider now the determination of pdf's from the discrete representation, taking $f_\phi(\psi; 1/2)$ as our example. A straight-forward method is to form a histogram with interval $\Delta\psi$ from the ensemble of particles in the cell centred at $x=1/2$. Figures 6.4 and 6.5 show the histograms for $\Delta\psi=0.25$ and $\Delta\psi=0.1$ compared with the specified Gaussian pdf. It is immediately apparent that this approximation is inadequate: for large $\Delta\psi$ (Fig. 6.4) the resolution is poor; for small $\Delta\psi$ (Fig. 6.5) the histogram is not smooth.

To estimate the pdf from a finite number of samples is a standard problem for which many algorithms have been proposed, see for example Refs 124–128. (The method of Crump and Seinfeld^{127,128} is particularly interesting in that it is directly analogous to cubic spline smoothing using cross validation.)

All the methods mentioned must compromise between statistical error and truncation error. If the cell (in this case at $x=1/2$) is small, then there are few samples from which to estimate the pdf. But the estimated pdf is an average over the cell, so that if the cell is too large, significant truncation error results.

A method that does not require a compromise between truncation and statistical error is to use least-squares cubic splines (in x) to determine the distribution function $F_\phi(\psi; x)$ for the discrete values of ψ

$$\psi_\ell = \ell \Delta\psi, (\ell \text{ integer}). \quad (6.46)$$

Then, at $x=1/2$, a least-squares cubic spline (in ψ) is used to approximate the continuous distribution function $F_\phi(\psi; 1/2)$. The pdf $f_\phi(\psi; 1/2)$ is then obtained by differentiating $F_\phi(\psi; 1/2)$ with respect to ψ .

Figure 6.6 shows the pdf obtained using this technique with $\Delta\psi=0.05$, 6 splines in x , and 14 splines

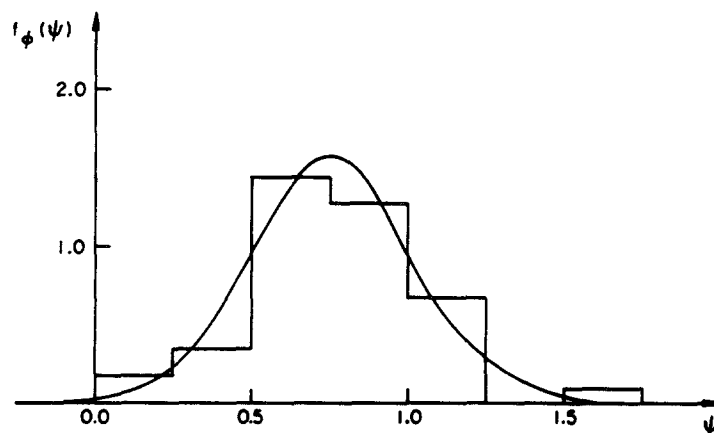


FIG. 6.4. Histogram (with interval $\Delta\psi=0.25$) compared with the pdf $f_\phi(\psi; 1/2)$.

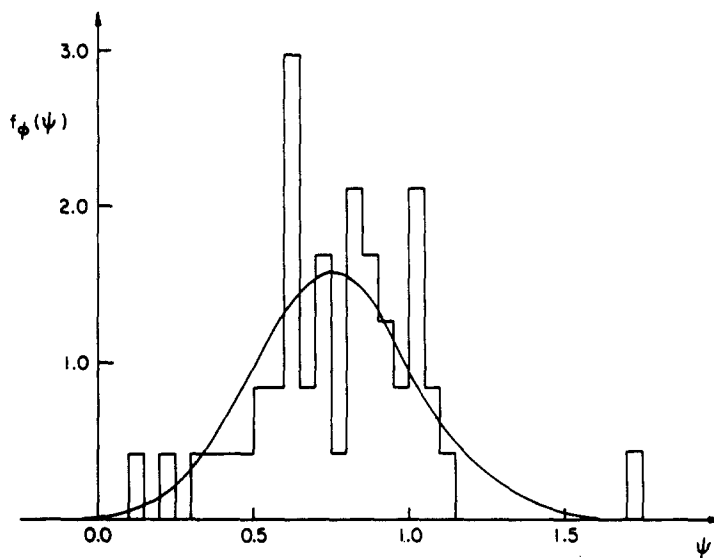


FIG. 6.5. Histogram (with interval $\Delta\psi = 0.1$) compared with the pdf $f_\phi(\psi; 1/2)$.

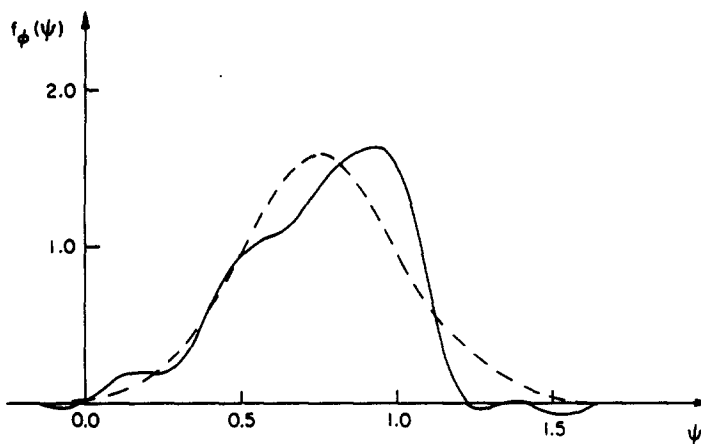


FIG. 6.6. Pdf $f_\phi(\psi; 1/2)$ against ψ : —— Gaussian; —— from least-squares cubic splines with 1000 samples.

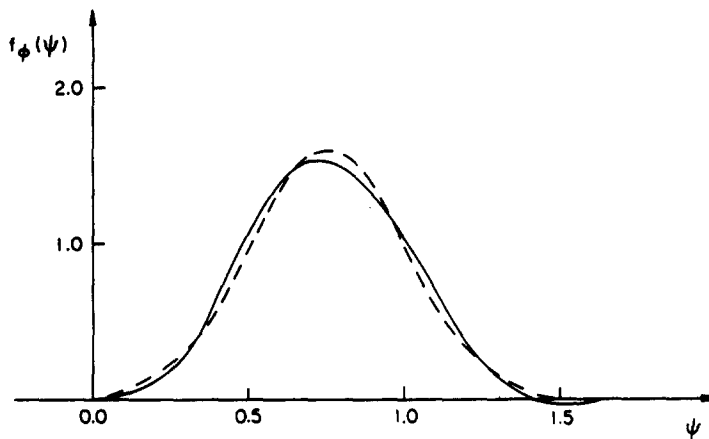


FIG. 6.7. Pdf $f_\phi(\psi; 1/2)$ against ψ : —— Gaussian; —— from least-squares cubic splines with 10,000 samples.

in ψ between $\psi = -1/2$ and $\psi = 2$. It may be seen that the agreement with the Gaussian is better than for the histograms, but it is still not very good. In addition, the approximated pdf contains small negative values, thus violating a fundamental property of pdf's.

Since $f_\phi(\psi; x)$ contains all the one-point statistical information about $\phi(x)$, it is not surprising that it is difficult to obtain an accurate approximation to the pdf from just 1000 data points. Figure 6.7 shows the approximation to $f_\phi(\psi; 1/2)$ obtained by the cubic-spline techniques when the number of data points is increased by a factor of 10 (i.e. $N = 10,000$). It may be seen that the agreement is now satisfactory. Fortunately, satisfactory estimates of simple means (e.g. $\langle \phi \rangle$) can be obtained with far fewer data points.

6.8. Variants

The solution algorithm has been described for a general three-dimensional flow. We consider here the simplifications possible for one and two-dimensional flows, for self-similar flows, and for boundary-layer-type flows.

If, in a given coordinate system, the joint pdf does not vary in one coordinate direction, then the flow is statistically two-dimensional. For example, in polar-cylindrical (r, θ, z) coordinates, the flow is two-dimensional (axisymmetric) if

$$\frac{\partial}{\partial \theta} f(\underline{V}, \underline{\psi}; r, \theta, z, t) = 0. \quad (6.47)$$

In the discrete representation of the joint pdf, the location of the n th particle is $r^{(n)}, \theta^{(n)}, z^{(n)}$. But since (for axisymmetric flows) no mean property depends on θ , the value of $\theta^{(n)}$ is irrelevant and need not be calculated. Thus, the location of the particle is adequately specified by $r^{(n)}$ and $z^{(n)}$.

The simplification afforded by the two-dimensionality is not that $\theta^{(n)}$ need not be calculated, since the integration of the stochastic equation for $\theta^{(n)}$ is trivially simple. Rather, the simplifications are that mean quantities (e.g. $\langle \underline{U} \rangle, \nabla \langle p \rangle$) are determined as functions of only two variables, and that (in the stochastic mixing step) three-dimensional cells are replaced by two-dimensional cells.

In the implementation of the stochastic models, the solution domain is divided into K cells, the k th being centered at $\underline{x}_{(k)}$ and having volume \underline{V}_k . For axisymmetric flows, the cells are two-dimensional areas on the $r-z$ plane, the k th centered at (r_k, z_k) having an area A_k . This cell represents the volume \underline{V}_k of the body of revolution formed by revolving A_k about the axis:

$$\underline{V}_k \approx 2\pi r_k A_k. \quad (6.48)$$

Now with $N_k(t)$ particles in the k th cell, each one representing a mass Δm , the mean density is

$$\langle \rho(r_k, z_k, t) \rangle \approx \Delta m N_k / \underline{V}_k. \quad (6.49)$$

Hence, the particle number density on the $r-z$ plane is

$$N_k / A_k \approx \left(\frac{2\pi}{\Delta m} \right) r_k \langle \rho(r_k, z_k, t) \rangle. \quad (6.50)$$

The accuracy with which means can be determined from the particle properties depends upon the particle number density. It is evident from Eq. (6.50) that near the axis of symmetry (small r_k) the particle number density is relatively low and consequently means cannot be determined accurately. It is desirable to control the particle number density (and hence the accuracy) independently of the coordinates and of the mean fluid density. This can be achieved by a system of adjustable weights: the n th particle with weight $W^{(n)}$ represents a mass $W^{(n)} \Delta m$. The corresponding discrete representation of the joint pdf is

$$\begin{aligned} \mathcal{F}_N^*(\underline{V}, \underline{\psi}, \underline{x}; t) &= \rho(\underline{\psi}) f_N^*(\underline{V}, \underline{\psi}; \underline{x}, t) \\ &= \Delta m \sum_{n=1}^N W^{(n)} \delta(\underline{V} - \underline{U}^{*(n)}) \\ &\quad \times \delta(\underline{\psi} - \underline{\phi}^{*(n)}) \delta(\underline{x} - \underline{x}^{*(n)}), \end{aligned} \quad (6.51)$$

where the mass of fluid in the solution domain is

$$M = \Delta m \sum_{n=1}^N W^{(n)}.$$

From this it follows that for an axisymmetric flow, the particle number density in the $r-z$ plane is

$$N_k / A_k \approx \left(\frac{2\pi}{\Delta m} \right) r_k \langle \rho(r_k, z_k, t) \rangle / \bar{W}_k, \quad (6.52)$$

where \bar{W}_k is the average weight of particles in the k th cell. It may be seen that a uniform particle number density can be achieved by choosing the weights to be proportional to $r \langle \rho \rangle$.

(The implementation of the stochastic models has to be modified to account for particles of different weights.)

For one-dimensional flows, the solution algorithm becomes still simpler. Only one coordinate is needed, and all mean quantities are functions of a single spatial variable.

Self-similar free shear flows—jets, wakes and mixing layers—are two-dimensional. But a transformation of the dependent variables (\underline{U} and ϕ) can be used to make the transport equations for statistical quantities dependent upon a single spatial variable. Thus, for a self-similar plane jet, Pope^{42,43} solved the joint pdf equation for $f(\underline{V}, \underline{\psi}; \eta, t)$, where η is the normalized cross-stream variable.

A simplification is also possible for some free shear flows that are not self-similar. The simplification—which is analogous to the boundary-layer approximation—can be applied when the flow is predominantly in one direction. More precisely, there must be negligible probability of negative velocity in the dominant flow direction. Consider, for example, the statistically two-dimensional turbulent mixing layer formed between two parallel streams, Fig. 6.8. The joint pdf equation is to be solved in the solution domain bounded by the flow surfaces a, b, c and d (that are infinite in the spanwise x_3 -direction). A fluid particle path (in x -space) is sketched on Fig. 6.8. Provided that the velocity U_1 is always positive, all fluid particles within the solution domain entered through the

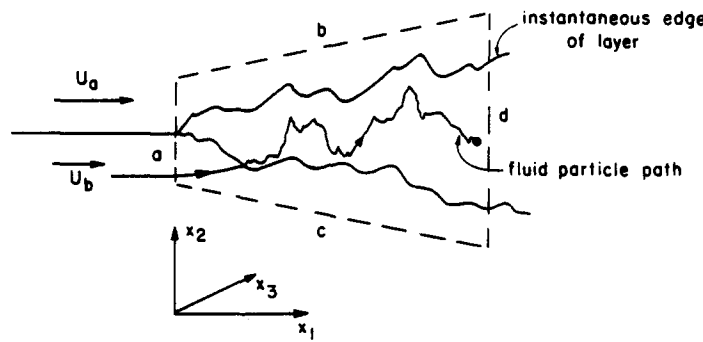


FIG. 6.8. Sketch of a two-dimensional mixing layer showing a fluid particle path.

surfaces a , b and c ; none entered through the downstream surface d . Consequently, in order to solve the joint pdf equation, boundary conditions are required on the surfaces a , b and c , but not on the surface d . An algorithm that exploits these observations is now outlined.

Rather than the mass density function, the dependent variable considered is the axial momentum density function

$$\mathcal{M}(\underline{V}, \underline{\psi}, x_1, x_2) \equiv V_1 \mathcal{F}(\underline{V}, \underline{\psi}, x_1, x_2). \quad (6.53)$$

From the modelled equation for \mathcal{F} (Eq. 6.8) we readily obtain

$$\begin{aligned} \frac{\partial \mathcal{M}}{\partial x_1} &= V_1 \frac{\partial \mathcal{F}}{\partial x_1} \\ &= (P_1 + P_2 + P'_3) \mathcal{F} \\ &= (P_1 + P_2 + P'_3) \mathcal{M} / V_1, \end{aligned} \quad (6.54)$$

where the operators P_1 and P_2 are defined as before (Section 6.3) while the operator P'_3 corresponds to lateral convection and the mean pressure gradient:

$$P_3 \equiv -V_2 \frac{\partial}{\partial x_2} + \frac{1}{\rho(\psi)} \frac{\partial \langle p \rangle}{\partial x_j} \frac{\partial}{\partial V_j}. \quad (6.55)$$

Starting from the given boundary condition at $x_1 = 0$, the method calculates \mathcal{M} at successive axial locations separated by a small distance Δx_1 . We define $\Delta t(V_1)$ to be the time taken for a particle with constant axial velocity V_1 to pass from x_1 to $x_1 + \Delta x_1$:

$$\Delta t(V_1) \equiv \Delta x_1 / V_1. \quad (6.56)$$

Then, from Eq. (6.54) we obtain

$$\begin{aligned} \mathcal{M}(x_1 + \Delta x_1) &= [I + \Delta t(V_1) \{P_1 + P_2 + P'_3\}] \mathcal{M}(x_1) \\ &\quad + \mathcal{O}[\Delta t(V_1)^2] \\ &= [I + \Delta t(V_1) P'_3] [I + \Delta t(V_1) P_2] \\ &\quad \times [I + \Delta t(V_1) P_1] \mathcal{M}(x_1) + \mathcal{O}[\Delta t(V_1)^2], \end{aligned} \quad (6.57)$$

where I is the identity operator.

It may be seen that this equation for $\mathcal{M}(x_1 + \Delta x_1)$ is directly analogous to Eq. (6.14) for $\mathcal{F}(t + \Delta t)$. Consequently an algorithm for \mathcal{M} directly analogous to that for \mathcal{F} described in Sections 6.3–6 is possible. The

algorithm for \mathcal{M} differs in three respects. First, the discrete representation is used to approximate \mathcal{M} rather than \mathcal{F} . Consequently each stochastic particle represents a fixed amount of axial momentum rather than a fixed mass. Second, in each fractional step, the n th particle evolves for a time

$$\Delta t^{(n)} \equiv \Delta x_1 / U_1^{*(n)}, \quad (6.58)$$

rather than for a fixed time Δt . Third, the axial pressure gradient is assumed to be uniform across the flow and is determined from the free-stream conditions. The pressure algorithm described in Section 6.6 is used to determine the lateral pressure gradient.

This algorithm is clearly inapplicable to flows in which U_1 is likely to be zero or negative, since then $\Delta t^{(n)}$ would be infinite or negative, Eq. (6.58). In addition, since the truncation error is of order $\Delta x_1 / U_1^*$, the method is most easily applied to flows in which U_1^* is never very small (compared to a characteristic velocity difference).

7. COMPOSITION JOINT PDF

The velocity–composition joint pdf $f(\underline{V}, \underline{\psi}; \underline{x}, t)$ contains all the one-point statistical information about the velocity and compositions. In order to solve the modelled transport equation for f , the only information required is the turbulent time scale $\tau(\underline{x}, t)$ (and, of course, initial and boundary conditions). An alternative approach that has been used by several authors^{25,27–36} is to treat the velocity field with a conventional turbulence model, and to solve a modelled transport equation for the joint pdf of the compositions. This alternative approach is described in this section.

Most of the composition pdf calculations have been performed in conjunction with the $k-\varepsilon$ turbulence model.¹⁰ Modelled transport equations are solved for the turbulent kinetic energy k and its rate of dissipation ε . The turbulent time scale τ is obtained from

$$\tau = k / \varepsilon, \quad (7.1)$$

and a turbulent viscosity μ_T is defined by

$$\mu_T = \langle \rho \rangle C_\mu k^2 / \varepsilon, \quad (7.2)$$

where the constant C_μ is ascribed the value 0.09. The turbulent viscosity is used to determine the Reynolds

stresses through the isotropic viscosity hypothesis:

$$\langle \rho \rangle \widetilde{u_i'' u_j''} = -\mu_T \left(\frac{\partial \bar{U}_i}{\partial x_j} + \frac{\partial \bar{U}_j}{\partial x_i} \right) + \frac{2}{3} \delta_{ij} \left(\langle \rho \rangle k + \mu_T \frac{\partial \bar{U}_i}{\partial x_i} \right). \quad (7.3)$$

This is the simplest possible consistent gradient-diffusion model for momentum transport. The analogous gradient-diffusion model for composition transport is,

$$\langle \rho \rangle \widetilde{u_i'' \phi_a''} = -\Gamma_T \frac{\partial \tilde{\phi}_a}{\partial x_i}, \quad (7.4)$$

where the turbulent diffusion coefficient is

$$\Gamma_T = \mu_T / \sigma_\phi, \quad (7.5)$$

and the turbulent Schmidt number σ_ϕ is taken to be 0.7.

If the mean density $\langle \rho(\underline{x}, t) \rangle$ is known, then the equations for k, ε and the mean velocities \bar{U} form a closed set. In this approach, the mean density is determined from the solution to the modelled composition joint pdf equation.

7.1. Composition Joint Pdf Equation

The joint pdf of the compositions ϕ is $f_\phi(\underline{\psi}; \underline{x}, t)$. The transport equation for f_ϕ can be derived either from the conservation equation for ϕ_a (following the procedure of Section 3.5), or, more simply, by integrating the equation for $f(\underline{V}, \underline{\psi}; \underline{x}, t)$ (Eq. 3.109) over velocity space. By either method the result is:

$$\begin{aligned} \frac{\partial}{\partial t} [\rho(\underline{\psi}) f_\phi] + \frac{\partial}{\partial x_i} [\rho(\underline{\psi}) \langle U_i | \underline{\psi} \rangle f_\phi] \\ + \frac{\partial}{\partial \psi_a} [\rho(\underline{\psi}) S_a(\underline{\psi}) f_\phi] = \frac{\partial}{\partial \psi_a} \left[\left\langle \frac{\partial J_a}{\partial x_i} \right| \underline{\psi} \right] f_\phi. \end{aligned} \quad (7.6)$$

There is some advantage in considering the density-weighted (Favre) joint pdf \tilde{f}_ϕ , and the composition mass density function \mathcal{F}_ϕ :

$$\mathcal{F}_\phi(\underline{\psi}, \underline{x}; t) = \langle \rho \rangle \tilde{f}_\phi(\underline{\psi}; \underline{x}, t) = \rho(\underline{\psi}) f_\phi(\underline{\psi}; \underline{x}, t). \quad (7.7)$$

The second term in Eq. (7.6) can be re-expressed as

$$\begin{aligned} \rho(\underline{\psi}) \langle U_i | \underline{\psi} \rangle f_\phi &= [\bar{U}_i + \langle u_i'' | \underline{\psi} \rangle] \langle \rho \rangle \tilde{f}_\phi \\ &= [\bar{U}_i + \langle u_i'' | \underline{\psi} \rangle] \mathcal{F}_\phi. \end{aligned} \quad (7.8)$$

Then the joint pdf equation can be written (in terms of the composition mass density function) as

$$\begin{aligned} \frac{\partial \mathcal{F}_\phi}{\partial t} + \frac{\partial [\bar{U}_i \mathcal{F}_\phi]}{\partial x_i} + \frac{\partial}{\partial \psi_a} [S_a(\underline{\psi}) \mathcal{F}_\phi] \\ = \frac{\partial}{\partial \psi_a} \left[\left\langle \frac{1}{\rho} \frac{\partial J_a}{\partial x_i} \right| \underline{\psi} \right] \mathcal{F}_\phi - \frac{\partial}{\partial x_i} [\langle u_i'' | \underline{\psi} \rangle \mathcal{F}_\phi]. \end{aligned} \quad (7.9)$$

The first two terms represent the rate of change of \mathcal{F}_ϕ following a particle moving with the mean velocity \bar{U} ; the third term represents the effect of reaction. Both these terms are in closed form whereas the terms on the

right-hand side of Eq. (7.9) contain conditional expectations that have to be modelled. The first term on the right-hand side represents transport in composition space due to molecular mixing. The stochastic mixing model (Section 5.2.3) accounts for this process.

The final term in Eq. (7.9) represents transport in physical space due to turbulent velocity fluctuations. In the velocity-composition joint pdf equation this process appears in closed form. But the composition pdf \tilde{f}_ϕ contains no information about the velocities and so the conditional expectation $\langle u'' | \underline{\psi} \rangle$ has to be modelled. Most calculations have been performed using the gradient-diffusion model²⁴:

$$\langle \rho \rangle \langle u_i'' | \underline{\psi} \rangle \tilde{f}_\phi = -\Gamma_T \frac{\partial \tilde{f}_\phi}{\partial x_i}. \quad (7.10)$$

The composition pdf approach—in which transport equations are solved for \tilde{f}_ϕ (or \mathcal{F}_ϕ), k, ε and \bar{U} —has two disadvantages compared to the velocity-composition pdf approach—in which transport equations are solved for $\tilde{f}(\underline{V}, \underline{\psi}; \underline{x}, t)$ (or \mathcal{F}) and ε . First, because of the use of the isotropic viscosity hypothesis (Eq. 7.3), the $k-\varepsilon$ model provides a far less accurate closure for the velocity field. Second, the turbulent convection of \tilde{f}_ϕ has to be modelled, whereas that of \tilde{f} appears in closed form. The assumption of gradient-diffusion transport Eq. (7.10) is particularly questionable in variable-density reactive flows. Nevertheless, for simple free shear flows, the $k-\varepsilon$ model and the gradient-diffusion assumption may be reasonably accurate. Then the composition pdf approach has the advantage that the transport equation for \mathcal{F}_ϕ is simpler to solve than that for \mathcal{F} .

While the composition pdf approach is inferior to the velocity-composition pdf approach, it still retains the valuable attribute of being able to treat nonlinear reactions without approximation. Consequently, it avoids the closure problem encountered when mean-flow or second-order models are applied to reactive flows.

7.2. Solution Algorithm

In this section we outline a solution algorithm for the modelled composition joint pdf equation that is analogous to the algorithm for $f(\underline{V}, \underline{\psi}; \underline{x}, t)$ described in Section 6. But first, we mention two different methods that have been used previously. Janicka *et al.*²⁵ used a finite-difference technique to solve a modelled transport equation for $f_\phi(\underline{\psi}; x_1, x_2)$ in a jet diffusion flame. For one, or maybe two, composition variables finite-difference solutions are possible, but, as the number of variables increases, the computational requirements become prohibitive. Pope³² has devised a combined finite-difference/Monte Carlo method in which the computational effort increases only linearly with the number of composition variables. Consequently it can be used²⁷⁻³² to solve the equation for the joint pdf of many compositions.

The algorithm briefly described here (like that of Section 6) does not require a finite-difference grid in physical space, and so the truncation errors associated

with finite-difference approximations are avoided. Consequently this algorithm is to be preferred over that of Pope.³²

The modelled equation for the composition mass density function $\mathcal{F}_\phi(\psi, \underline{x}; t)$ can be written

$$\begin{aligned} \frac{\partial \mathcal{F}_\phi}{\partial t} + \frac{\partial}{\partial x_i} [\bar{U}_i \mathcal{F}_\phi] - \frac{\partial}{\partial x_i} \left[\Gamma_T \frac{\partial}{\partial x_i} (\mathcal{F}_\phi / \langle \rho \rangle) \right] \\ = -\frac{\partial}{\partial \psi} [S_a(\psi) \mathcal{F}_\phi] + P_2 \mathcal{F}_\phi, \quad (7.11) \end{aligned}$$

where the operator P_2 corresponds to the stochastic mixing model. Using the method of fractional steps, reaction and then mixing can be treated in the way described in Sections 6.4–5. In the third and final fractional step, the spatial transport terms are treated; which amounts to solving Eq. (7.11) with the right-hand side set to zero. As is now described, this is readily achieved since the left-hand side of Eq. (7.11) corresponds to a diffusion process in physical space.

With M being the mass in the solution domain, and $\underline{x}^*(t)$ and $\phi^*(t)$ being the position and composition of a stochastic particle, the composition mass density function can be written

$$\mathcal{F}_\phi(\psi, \underline{x}; t) = M \langle \delta(\psi - \phi^*(t)) \delta(\underline{x} - \underline{x}^*(t)) \rangle. \quad (7.12)$$

We consider the diffusion process

$$\Delta_{\delta t} \underline{x}^*(t) = \underline{D}(\underline{x}^*[t], t) \delta t + [\underline{B}(\underline{x}^*[t], t)]^{1/2} \Delta_{\delta t} \underline{W}_t, \quad (7.13)$$

where the coefficients \underline{D} and \underline{B} are to be determined and \underline{W}_t is an isotropic Weiner process. This process is directly analogous to Eq. (4.81). Hence from Eqs (4.88), (4.39) and (7.12) we obtain the corresponding evolution equation for \mathcal{F}_ϕ :

$$\frac{\partial \mathcal{F}_\phi}{\partial t} + \frac{\partial}{\partial x_i} [D_i \mathcal{F}_\phi] - \frac{1}{2} \frac{\partial^2}{\partial x_i \partial x_i} [B \mathcal{F}_\phi] = 0. \quad (7.14)$$

In order for the diffusion process Eq. (7.13) to correspond to the spatial transport in the modelled pdf equation, Eq. (7.14) should be the same as Eq. (7.11) with the right-hand side set to zero. This requirement determines the coefficients to be

$$B = 2\Gamma_T / \langle \rho \rangle, \quad (7.15)$$

and

$$\underline{D} = \bar{\underline{U}} + \frac{1}{\langle \rho \rangle} \nabla \Gamma_T. \quad (7.16)$$

Thus, in the solution procedure, spatial transport (during the time interval Δt) is accounted for by moving each stochastic particle independently by

$$\begin{aligned} \underline{x}^*(t + \Delta t) = \underline{x}^*(t) + \Delta t \left[\bar{\underline{U}} + \frac{1}{\langle \rho \rangle} \nabla \Gamma_T \right]_{\underline{x}^*(t)} \\ + [2\Delta t \Gamma_T / \langle \rho \rangle]_{\underline{x}^*(t)}^{1/2} \xi \quad (7.17) \end{aligned}$$

where ξ is a standardized joint normal random vector.

8. CONCLUSIONS

The aim of this work has been to describe the derivation, modelling, and solution of pdf transport equations for turbulent reactive flows. The main conclusions are now summarized, and the attributes of the velocity–composition joint pdf approach are discussed in Section 8.2.

8.1. Summary

At low Mach number, a turbulent flow of a single-phase mixture of species can be described by the velocity $\underline{U}(\underline{x}, t)$ and by a set of σ scalars $\phi(\underline{x}, t)$. Any thermochemical property of the mixture can be determined from $\phi(\underline{x}, t)$ and a reference pressure p_0 .

The joint pdf $f(\underline{V}, \psi; \underline{x}, t)$ is the probability density of the simultaneous events $\underline{U}(\underline{x}, t) = \underline{V}$ and $\phi(\underline{x}, t) = \psi$. At each point and time (\underline{x}, t) , the velocity–composition joint pdf f contains a complete statistical description of \underline{U} and ϕ , but it contains no two-point information. The mean of any function of \underline{U} and ϕ can be determined from f , Eq. (3.42). In variable-density inhomogeneous flows, rather than the joint pdf f , it is most convenient to consider the mass density function $\mathcal{F}(\underline{V}, \psi; \underline{x}, t) = \rho(\psi) f(\underline{V}, \psi; \underline{x}, t)$.

The three independent velocity variables \underline{V} , the σ composition variables ψ , and the three position variables \underline{x} form a $(6 + \sigma)$ -dimensional sample space called state space (or \underline{V} – ψ – \underline{x} space). Any random vector $(\underline{U}^*, \phi^*, \underline{x}^*)$ has the same joint pdf as $\underline{U}(\underline{x}, t)$ and $\phi(\underline{x}, t)$ provided that:

- (i) the joint pdf of \underline{x}^* is proportional to the mean density $\langle \rho(\underline{x}, t) \rangle$, Eq. (3.82), and
- (ii) the joint pdf of \underline{U}^* and ϕ^* is equal to the density-weighted joint pdf of \underline{U} and ϕ at $\underline{x}^* - \bar{\underline{U}}(\underline{V}, \psi; \underline{x}^*, t)$ —Eq. (3.84).

Consequently, the mass density function can be represented by N samples of such a random vector $(\underline{U}^{*(n)}, \phi^{*(n)}, \underline{x}^{*(n)})$, $n = 1, 2, \dots, N$, Eq. (3.76). Each sample of the random vector corresponds to a point in state space and can be thought of as the state of a notional particle. The expected particle number density in state space is proportional to the mass density function; the expected particle number density in \underline{x} -space is proportional to the mean fluid density; and, at given \underline{x} , the expected particle number density in \underline{V} – ψ space is proportional to the density-weighted joint pdf \bar{f} .

A transport equation, Eq. (3.109) for the velocity–composition joint pdf can be derived without assumption from the transport equations for \underline{U} and ϕ . For a variable-density flow with arbitrarily complex and nonlinear reactions, it is remarkable that in this equation the effects of convection, reaction, body forces and the mean pressure gradient appear exactly and do not have to be modelled. The effects of molecular processes and of the fluctuating pressure gradient appear in the joint pdf equation as conditional expectations that have to be modelled.

The joint pdf equation can also be derived by a Lagrangian approach. The Lagrangian conditional joint pdf $f_L(\underline{V}, \underline{\psi}, \underline{x}; t | \underline{V}_0, \underline{\psi}_0, \underline{x}_0)$ is the joint pdf of the fluid particle state $(\underline{U}^+, \underline{\phi}^+, \underline{x}^+)$ at time t , conditional upon its state being $(\underline{V}_0, \underline{\psi}_0, \underline{x}_0)$ at time t_0 . This is the transition density for turbulent reactive flows: the mass density function at time t is equal to the mass-probability-weighted integral of f_L over all initial states, Eq. (4.24).

Many different systems of particles can evolve with the same pdf as fluid particles. But there is only one such deterministic system. In this system, the N notional particles are called conditional particles and have the states $(\hat{\underline{U}}^{(n)}, \hat{\underline{\phi}}^{(n)}, \hat{\underline{x}}^{(n)}; n = 1, 2, \dots, N)$. The rate of change of state of conditional particles is equal to the conditional expectation of the rate of change of state of fluid particles. The trajectories of conditional particles in the augmented state space ($\underline{V} - \underline{\psi} - \underline{x} - t$ space) are called conditional paths. These conditional paths define a formal solution to the joint pdf transport equation, Eqs (4.52) and (4.56). A physical interpretation of this solution is provided in Section 4.5—loosely, probability is transported along conditional paths.

The essence of the whole approach is to construct a system of stochastic particles whose evolution is simply computed and in which the pdf evolves in the same way as the pdf of fluid particles. Poisson processes and diffusion processes (described in Section 4.6) provide the basis for such a stochastic system.

The modelling is guided primarily by the known behavior of homogeneous turbulent flows. In these simple flows, the joint pdf $f(\underline{V}, \underline{\psi}; t)$ adopts a joint normal distribution. The aim of the modelling is therefore to produce a joint normal distribution whose first and second moments evolve correctly.

For homogeneous turbulence, the joint pdf $f(\underline{V}, \underline{\psi}; t)$ is represented by an ensemble of N stochastic particles with states $(\underline{U}^{*(n)}(t), \underline{\phi}^{*(n)}(t); n = 1, 2, \dots, N)$. The modelling is performed, not directly in the joint pdf equation, but indirectly by prescribing the behavior of the N stochastic particles.

The primary effect of molecular diffusion on the composition variables $\underline{\phi}$ is to decrease the variance $\langle \phi'_i \phi'_j \rangle$ while leaving the mean $\langle \phi_i \rangle$ unchanged, Eqs (5.50–51). The stochastic mixing model is used to produce this effect. Pairs of stochastic particles are randomly selected from the ensemble (at a rate determined by the turbulent time scale τ) and their compositions $\underline{\phi}^*$ adopt their common mean composition, Eq. (5.48).

Alternative models are presented for the effects of the fluctuating pressure gradient and viscous dissipation. The first is based on stochastic particle-interaction models, and the second on the Langevin equation.

With the particle-interaction models, in homogeneous turbulence with no mean-velocity gradients, the decay of turbulence energy and the return to isotropy of the Reynolds stresses is simulated by the

stochastic mixing model and the stochastic reorientation model. In the stochastic mixing model, pairs of particles are randomly selected and their velocities adopt their common mean velocity, Eq. (5.83). In the stochastic reorientation model, pairs of particles are randomly selected and are randomly reorientated in velocity space (Eq. 5.93). Both energy and momentum are conserved in this process. The effect of these two models on the Reynolds stresses (Eq. 5.80) is to cause decay and return to isotropy in accord with Rotta's model. Mean-velocity gradients give rise to rapid-pressure fluctuations. A deterministic model for their effect (to be used in conjunction with the particle-interaction models) is presented in Eq. (5.122) and shown to be consistent with Reynolds-stress models, Eq. (5.126).

In the alternative—Langevin—model, the velocity $\underline{U}^*(t)$ of a stochastic particle evolves according to a diffusion process, Eq. (5.148). In the small time interval δt , $\underline{U}_i^*(t)$ changes deterministically by an amount $\delta t G_{ij} U_j^*$, and randomly by amount $(B \delta t)^{1/2} \xi_i$ (where ξ is a standardized joint normal random vector). For consistency with Kolmogorov's scaling laws, the coefficient B is determined to be $C_0 \varepsilon$, where $C_0 = 2.1$ is a universal constant. A model for the tensor G_{ij} has been proposed (Eqs 5.161–162). For homogeneous turbulence, the resulting pdf equation yields a joint normal distribution with the Reynolds-stress evolution closely matching experimental data.

The extension of these models to inhomogeneous, variable-density reactive flows is discussed in Sections 5.6 and 5.7.

In Section 6, a solution algorithm is described to solve the modelled velocity–composition joint pdf equation for unsteady, three-dimensional, variable-density flows. The velocities are modelled by the Langevin equation, and the scalar dissipation by the stochastic mixing model.

The mass density function is represented by N stochastic particles in state space, Eq. (6.2). Given the states of the particles at time t , the states at time $t + \Delta t$ are calculated through a sequence of three fractional steps. In the first fractional step, the velocities and compositions evolve due to reaction, the Langevin model and buoyancy, Eq. (6.21). In the second fractional step, the particle compositions change according to the stochastic mixing model. And in the third fractional step, the particle positions and velocities change due to convection and the mean pressure gradient.

The determination of the mean pressure field is an integral part of the third fractional step. The indirect algorithm used is based on the observation that the stochastic particle number density in physical space should be proportional to the mean fluid density. The mean pressure is determined—as the solution of an elliptic partial differential equation—by requiring that this condition be satisfied. (Subtle connections between the mean pressure, the mean continuity equation, and consistency conditions are discussed in Section 4.7).

The algorithm provides a solution to the pdf equation in terms of stochastic particle properties. A conceptually simple way to obtain mean quantities is to divide physical space into cells, and then to form ensemble averages over the particles in each cell. In Section 6.7 it is shown that this straightforward method is hopelessly inaccurate, and better methods based on cubic splines are described.

For simpler flows—one and two-dimensional flows, self-similar flows, and boundary-layer-type flows—variants of the solution algorithm are described in Section 6.8.

The composition joint pdf approach is discussed in Section 7. In this approach, the mean velocity and turbulence fields are determined using a standard turbulence model and a modelled transport equation is solved for the joint pdf of the compositions $f_\phi(\psi; \mathbf{x}, t)$. This approach is inferior to the velocity-composition approach in that a turbulence model is required and the turbulent transport of f_ϕ has to be modelled—usually by gradient diffusion. Nevertheless, nonlinear reactions can still be handled without approximation, and the approach may be adequate for simple flows. A solution algorithm for the modelled composition transport equation is described in Section 7.2.

8.2. Discussion

In the following four subsections we discuss: the inherent limitations of one-point closures; the advantages of the pdf approach compared to other one-point closures; aspects of the modelling in need of improvement; and the computational requirements of the solution algorithm.

8.2.1. Limitations of one-point closures

The joint pdf method—in common with most other turbulence models^{10,11}—is a one-point closure. The joint pdf contains no length-scale or time-scale information (see Section 2.9). In modelling the joint pdf equation, the time scale τ has to be specified either directly, or indirectly through a modelled transport equation for ε . The direct specification of scale information is only possible in simple flows, and the validity of the modelled dissipation equation has often been called into question (e.g. Ref. 102). In addition, as discussed in Section 5.7.3, one-point closures are incapable of correctly determining the scalar dissipation rate—at least in grid turbulence.

These inherent problems do not invalidate the approach. For simple shear flows, for example, the use of the modelled dissipation equation is justifiable,¹⁰² and the scalar dissipation time scale appears to be simply proportional to τ .¹¹³ For more complex flows—with rapidly changing scales—the modelling is less secure, but the magnitudes of the errors resulting from the modelling inadequacies have yet to be quantified. (Several multi-point pdf methods have been suggested.)^{103–107}

8.2.2. Advantages of the pdf approach

Since the joint pdf provides a complete one-point statistical description of the flow field, the pdf approach has advantages over other one-point closures. The principal advantages are that reaction and convection transport can be treated without approximation, even in variable density flows.

For constant-density homogeneous flows, the models for the effects of the fluctuating pressure gradient and for molecular mixing are compatible with Reynolds-stress models and hence are equally accurate. For inhomogeneous flows, the joint pdf equation can be expected to be more accurate since additional models are required in the Reynolds-stress equations. Thus even for inert, constant-density flows, joint pdf calculations can be expected to be more accurate than Reynolds-stress calculations. But the pdf approach has the additional advantage of being able to handle, without approximation, nonlinear reactions and the effect of variable density on convection.

8.2.3. Model improvements

Several aspects of the modelling need to be refined, but we identify two areas in particular need of further study.

The treatment of scalar dissipation by the improved stochastic mixing is only partially satisfactory. Prandtl or Schmidt number effects are not accounted for nor can the model be justified when reaction times are of the order of the Kolmogorov time scale (or smaller).

As discussed in Section 5.7.4, the large density variations encountered in flows of interest undoubtedly have a significant influence on the modelled terms. But little is known about the nature and magnitude of variable-density effects.

In addressing these and other modelling questions, we expect that direct numerical simulations of homogeneous turbulence^{129–131} will play a central role. In the past, modelling has been guided by theory and experimental data. But it is now possible to solve the governing flow equations for homogeneous turbulence at Reynolds numbers comparable to those of wind-tunnel experiments. From the computed flow fields, multi-point statistical information can be extracted, and this provides an additional source of guidance to modelling. In the joint pdf equation, the modelling is most naturally viewed in Lagrangian terms. While Lagrangian statistics are extremely difficult to obtain experimentally, it is relatively easy to obtain them from direct numerical simulations.¹³¹

8.2.4. Computational considerations

The usefulness of the pdf approach depends on the existence of a practicable means of solving the modelled equations. Many Monte Carlo calculations have been performed, both for the velocity-composition joint pdf^{42–46} and for the composition joint pdf.^{27–32} Typical computational requirements are

50,000 words of storage, and 5 min of CPU time on a mainframe computer.

None of the calculations referenced above are for the general three-dimensional case for which the solution algorithm has been described (Section 6): the most difficult case treated so far is a jet diffusion flame.⁴⁶ Nevertheless, the modest computer requirements for the calculations performed give every reason to suppose that the Monte Carlo method will prove practicable for more difficult cases.

Acknowledgments—For comments and suggestions on the first version of this paper, I am grateful to Professors W. Kollmann, P. A. Libby and W. C. Reynolds as well as to the editor and reviewers. I am grateful to D. C. Haworth for providing suggestions and corrections on the revised version, and for allowing me to use the unpublished results of our collaborative work (Ref. 94). And I thank Barbara Benedict for her careful and patient typing of the paper.

This work was performed at the Massachusetts Institute of Technology and at Cornell University. It was supported in part by grant numbers CPE8000026 and CPE8212661 from the National Science Foundation (Engineering Energetics Program), and by grant numbers DAAG29-82-K-0017 and DAAG29-84-K-0020 from the U.S. Army Research Office.

REFERENCES

- MURTHY, S. N. B. (Ed.), *Turbulent Mixing in Nonreactive and Reactive Flows*, Plenum Press (1975).
- BRACCO, F. V. (Ed.), *Combust. Sci. Technol.* **13**, 1–275 (1976).
- BRODKEY, R. S. (Ed.), *Turbulence in Mixing Operations*, Academic Press (1975).
- LIBBY, P. A. and WILLIAMS, F. A. (Eds), *Turbulent Reactive Flows*, Springer-Verlag (1980).
- LIBBY, P. A. and WILLIAMS, F. A., *A. Rev. Fluid Mech.* **8**, 351–376 (1976).
- KELLER, J. U. (Ed.), *J. Non-equilib. Thermodyn.* **6**, 321–386 (1981).
- KELLER, J. U. (Ed.), *J. Non-equilib. Thermodyn.* **7**, 1–70 (1982).
- JONES, W. P. and WHITELAW, J. H., *Combust. Flame* **48**, 1 (1982).
- LIEPMANN, H. W., *Am. Sci.* **67**, 221–228 (1979).
- LAUNDER, B. E. and SPALDING, D. B., *Mathematical Models of Turbulence*, Academic Press (1972).
- LUMLEY, J. L., *Adv. appl. Mech.* **18**, 123 (1978).
- HAWTHORNE, W. R., WEDDELL, D. S. and HOTTEL, H. C., *Third Symposium on Combustion, Flame and Explosive Phenomena*, p. 266, Williams and Wilkins (1949).
- BRAY, K. N. C. and MOSS, J. B., University of Southampton Report AASU335 (1974).
- LOCKWOOD, F. C. and NAGUIB, A. S., *Combust. Flame* **24**, 109 (1975).
- RHODES, R. P., in Ref. 1, p. 235.
- POPE, S. B., *J. Non-Equilib. Thermodyn.* **4**, 309 (1979).
- POPE, S. B., *Phil. Trans. R. Soc. Lond.* **A291**, 529 (1979).
- POPE, S. B., *Turbulent Shear Flows 2* (L. J. S. Bradbury et al., Eds), 7–16, Springer-Verlag (1980).
- LUNDGREN, T. S., *Phys. Fluids* **12**, 485 (1969).
- LAUNDER, B. E., REECE, G. J. and RODI, W., *J. Fluid Mech.* **68**, 537 (1975).
- DOPAZO, C. and O'BRIEN, E. E., *Acta astronaut.* **1**, 1239 (1974).
- DOPAZO, C. and O'BRIEN, E. E., *Phys. Fluids* **17**, 1968 (1975).
- DOPAZO, C. and O'BRIEN, E. E., *Combust. Sci. Technol.* **13**, 99 (1976).
- POPE, S. B., *Combust. Flame* **27**, 299 (1976).
- JANICKA, J., KOLBE, W. and KOLLMANN, W., *Proc. Heat Transf. Fluid Mech. Inst.*, 296–312, Stanford University Press (1978).
- JANICKA, J., KOLBE, W. and KOLLMANN, W., *J. Non-equilib. Thermodyn.* **4**, 47 (1978).
- NGUYEN, T. V. and POPE, S. B., *Combust. Sci. Technol.* **42**, 13–45 (1984).
- POPE, S. B., *Eighteenth Symposium (Intl) on Combustion*, 1001–1010, The Combustion Institute (1981).
- MCNUTT, D. G., M.S. Thesis, Massachusetts Institute of Technology (1981).
- SHERIKAR, S. V. and CHEVRAY, R., *Third Symposium on Turbulent Shear Flows*, Davis, CA (1981).
- GIVI, P., SIRIGNANO, W. A. and POPE, S. B., *Combust. Sci. Technol.* **37**, 59–78 (1984).
- POPE, S. B., *Combust. Sci. Technol.* **25**, 159 (1981).
- DOPAZO, C., *Phys. Fluids* **18**, 397 (1975).
- KOLLMANN, W. and JANICKA, J., *Phys. Fluids* **25**, 1755–1769 (1982).
- KOLLMANN, W. and SCHMITT, F., *Seventh Biennial Symposium on Turbulence*, University of Missouri-Rolla (1981).
- WU, M.-Z. and O'BRIEN, E. E., *Combust. Sci. Technol.* **29**, 53 (1982).
- HANDSCOMB, D. C. and HAMMERSLEY, J. M., *Monte Carlo Methods*, Methuen (1965).
- DAHLQUIST, G. and BJÖRCK, A., *Numerical Methods*, Prentice-Hall (1974).
- POPE, S. B., *MIT Report EL-80-012* (1980) (Revised version appeared as Ref. 32).
- SPIELMAN, L. A. and LEVENSPIEL, O., *Chem. Engng Sci.* **20**, 247 (1965).
- FLAGAN, R. C. and APPLETON, J. P., *Combust. Flame* **23**, 249–267 (1974).
- POPE, S. B., *Turbulent Shear Flows 3* (L. J. S. Bradbury et al., Eds), 113–123, Springer-Verlag (1982).
- POPE, S. B., *AIAA J.* **22**, 896 (1984).
- ANAND, M. S. and POPE, S. B., *Turbulent Shear Flows 4* (L. J. S. Bradbury et al., Eds), 46–61, Springer-Verlag (1985).
- POPE, S. B. and ANAND, M. S., *Twentieth Symp. (Intl) on Combustion*, The Combustion Institute (to be published) (1985).
- POPE, S. B. (in preparation) (1985).
- FROST, V. A., *Third All-Union Conference on Combustion*, Press of Acad. Sci. USSR **1** (1960).
- FROST, V. A., *Fluid Mech., Sov. Res.* **4**, 124 (1975).
- CHUNG, P. M., *AIAA J.* **7**, 1982 (1969).
- CHUNG, P. M., *Combust. Sci. Technol.* **13**, 123 (1976).
- LANGEVIN, P., *C. R. Acad. Sci. Paris* **146**, 530 (1908).
- BYWATER, R. J., *AIAA J.* **20**, 824 (1982).
- HINZE, J. O., *Turbulence* (2nd Edn), McGraw-Hill (1975).
- DRAKE, A. W., *Fundamentals of Applied Probability Theory*, McGraw-Hill (1967).
- GNEDENKO, B. V., *The Theory of Probability*, Chelsea (1962).
- LUMLEY, J. L., *Stochastic Tools in Turbulence*, Academic Press (1970).
- PANCHEV, S., *Random Functions and Turbulence*, Pergamon Press (1971).
- BUTKOV, E., *Mathematical Physics*, Addison-Wesley (1968).
- LIGHTHILL, M. J., *Fourier Analysis and Generalized Functions*, Cambridge University Press (1970).
- O'BRIEN, E. E., in Ref. 4, p. 185.
- SPENCER, B. W., Ph.D. Thesis, University of Illinois (1970).
- TAVOURARIS, S. and CORRSIN, S., *J. Fluid Mech.* **104**, 311–347 (1981).
- DRAKE, M. C., PITZ, R. W. and LAPP, M., *AIAA paper no. 84-0544* (1984).
- JEFFREYS, H. and JEFFREYS, B., *Methods of Mathe-*

- mathematical Physics (3rd Edn), pp. 182–187, Cambridge University Press (1972).
65. BIRD, R. B., STEWARD, W. E. and LIGHTFOOT, E. N., *Transport Phenomena*, John Wiley and Sons (1960).
 66. WILLIAMS, F. A., *Combustion Theory*, Addison-Wesley (1965).
 67. STRAHLE, W. C., *Combust. Sci. Technol.* **29**, 243 (1982).
 68. WESTBROOK, C. K. and DRYER, F. L., *Combust. Sci. Technol.* **20**, 125–140 (1979).
 69. BRAY, K. N. C., in Ref. 4, p. 115.
 70. BILGER, R. W., in Ref. 4, p. 65.
 71. DRAKE, M. C., LAPP, M., PENNEY, C. M., WARSHAW, S. and GERHOLD, B. W., *Eighteenth Symposium (Intl) on Combustion*, p. 1521, The Combustion Institute (1981).
 72. POPE, S. B., *Phys. Fluids* **24**, 588–596 (1981).
 73. ARNOLD, L., *Stochastic Differential Equations: Theory and Applications*, Wiley (1974).
 74. DURBIN, P. A., *NASA RP 1103* (1983).
 75. WAX, N., *Noise and Stochastic Processes*, Dover (1954).
 76. VAN KAMPEN, N. G., *Stochastic Processes in Physics and Chemistry*, North-Holland (1981).
 77. SCHUMANN, U., *Phys. Fluids* **20**, 721–725 (1977).
 78. SPEZIALE, C. G., *Geophys. astrophys. Fluid Dyn.* **23**, 62–84 (1983).
 79. SHIH, T.-H., *Refined Modeling of Flows* (J. P. BENEQUE *et al.*, Eds), pp. 239–250, Paris: Presses Pont it Chaussees (1983).
 80. POPE, S. B., *Phys. Fluids* **26**, 400–408 (1983).
 81. SPALDING, D. B., *Chem. Engrg. Sci.* **26**, 95 (1971).
 82. POPE, S. B., *Combust. Flame* **34**, 103–105 (1979).
 83. DOPAZO, C., *Phys. Fluids* **22**, 20 (1979).
 84. CURL, R. L., *A.I.Ch.E.J.* **9**, 175 (1963).
 85. POPE, S. B., *Combust. Sci. Technol.* **28**, 131–145 (1982).
 86. COMTE-BELLOT, G. and CORRSIN, S., *J. Fluid Mech.* **18**, 353–378 (1964).
 87. CHOI, K.-S. and LUMLEY, J. L., *Proc. IUTAM Symp. on Turbulence and Chaotic Phenomena in Fluids*, Kyoto, Japan (1983).
 88. ROTTA, J. C., *Z. Phys.* **129**, 547 (1951).
 89. HUNT, J. R. C., *Fluid Dyn. Trans.* **9**, 121–152 (1977).
 90. LUMLEY, J. L. and KHAJEH-NOURI, B., *Adv. Geophys.* **18A**, 169 (1974).
 91. LIN, A. and WOLFSHTEIN, M., *First Symposium on Turbulent Shear Flows*, p. 437, Pennsylvania State University (1977).
 92. KELLOG, O. D., *Foundations of Potential Theory*, Springer-Verlag (1967).
 93. MONIN, A. S. and YAGLOM, A. M., *Statistical Fluid Mechanics*, Vol. 2, MIT Press, Cambridge (1975).
 94. HAWORTH, D. C. and POPE, S. B., A generalized Langevin model for turbulent flow. Submitted to *Phys. Fluids* (1985).
 95. JONES, W. P. and MUSONGE, P., *Fourth Symposium on Turbulent Shear Flows*, Karlsruhe (1983).
 96. SIRIVAT, A. and WARHAFT, Z., *J. Fluid Mech.* **120**, 475–501 (1982).
 97. SHIH, T.-H. and LUMLEY, J. L., *Report FDA-81-06*, Cornell University (1981).
 98. SIRIVAT, A. and WARHAFT, Z., *J. Fluid Mech.* **128**, 323–346 (1981).
 99. POPE, S. B., Ph.D. Thesis, University of London (1976).
 100. CORRSIN, S. and KISTLER, A. L., *NACA Report 1244* (1955).
 101. KOLLMANN, W. and JANICKA, J., *Phys. Fluids* **25**, 1755–1769 (1982).
 102. POPE, S. B., The Limits of Applicability of Turbulent Scale Equations, *Report FS/77/7*, Imperial College (1977).
 103. LUNDGREN, T. S., *Statistical Models and Turbulence* (M. Rosenblatt and C. Van Atta, Eds), p. 70, Springer-Verlag, Berlin (1971).
 104. IEVLEV, V. M., *Dokl. Akad. Nauk.* **208**, 1044 (1973).
 105. QIAN, J., *Phys. Fluids* **26**, 2098–2104 (1983).
 106. MEYERS, R. E. and O'BRIEN, E. E., *Combust. Sci. Technol.* **26**, 123–134 (1981).
 107. POPE, S. B., *Phys. Fluids* **26**, 3448–3450 (1983).
 108. LIN, S. C. and LIN, S. C., *Phys. Fluids* **16**, 1587–1598 (1973).
 109. WARHAFT, Z. and LUMLEY, J. L., *J. Fluid Mech.* **88**, 659 (1978).
 110. WARHAFT, Z., *J. Fluid Mech.* **104**, 93 (1981).
 111. WARHAFT, Z., *J. Fluid Mech.* **99**, 545 (1980).
 112. NEWMAN, G. R., LAUNDER, B. E. and LUMLEY, J. L., *J. Fluid Mech.* **111**, 217 (1981).
 113. BEGUIER, C., DEKEYSER, I. and LAUNDER, B. E., *Phys. Fluids* **27**, 307–310 (1978).
 114. TENNEKES, H. and LUMLEY, J. L., *A First Course in Turbulence*, MIT Press, Cambridge (1972).
 115. BILGER, R. W., *AIAA J.* **20**, 962 (1982).
 116. LIBBY, P. A. and BRAY, K. N. C., *Combust. Flame* **39**, 33 (1980).
 117. YANENKO, N. N., *The Method of Fractional Steps*, Springer-Verlag (1971).
 118. ROACHE, P. J., *Computational Fluid Dynamics*, Hermosa (1972).
 119. WESTBROOK, C. K. and DRYER, F. L., *Combust. Sci. Technol.* **27**, 31–43 (1981).
 120. DE BOOR, C., *A Practical Guide to Splines*, Springer-Verlag (1978).
 121. REINSCH, C. H., *Num. Math.* **10**, 177–183 (1967).
 122. CRAVEN, P. and WAHBA, G., *Num. Math.* **31**, 377–403 (1979).
 123. DIACONIS, P. and EFFRON, B., *Sci. Am.* **248**, 116–130 (1983).
 124. BEAN, S. J. and TSOKOS, C. P., *Int. statist. Rev.* **48**, 267–287 (1980).
 125. SCOTT, D. W. and FACTOR, L. E., *J. Am. statist. Ass.* **76**, 9–15 (1981).
 126. GOOD, I. J. and GASKINS, R. A., *J. Am. statist. Ass.* **75**, 42–73 (1980).
 127. CRUMP, J. G. and SEINFELD, J. H., *Aerosol Sci. Technol.* **1**, 15–34 (1982).
 128. CRUMP, J. G. and SEINFELD, J. H., *Aerosol Sci. Technol.* **1**, 363–369 (1982).
 129. ROGALLO, R. S. and MOIN, P., *A. Rev. Fluid Mech.* **16**, 99–137 (1984).
 130. ROGALLO, R. S., *NASA TM-81315* (1981).
 131. RILEY, J. J. and PATTERSON, G. S., *Phys. Fluids* **17**, 292 (1974).